#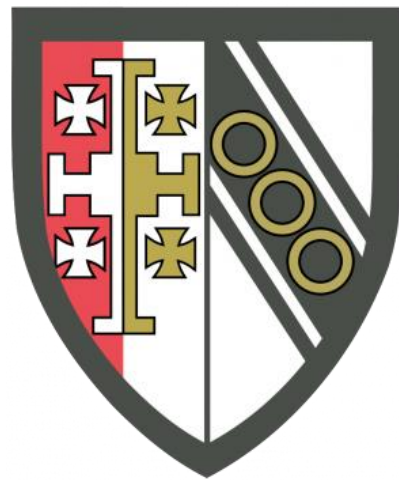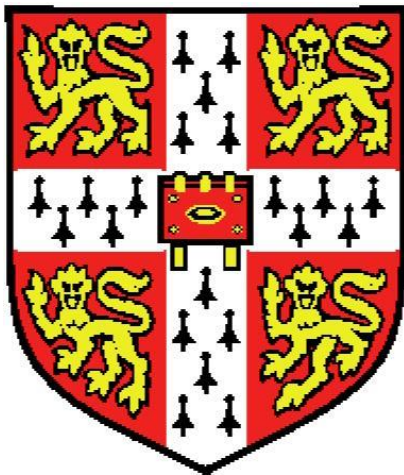 Applying recombinant protein technology to study *Plasmodium falciparum* erythrocyte receptor-ligand interactions and their potential as therapeutic targets

**Zenon Zenonos**

**Selwyn College, University of Cambridge**

**The Wellcome Trust Sanger Institute**

*This dissertation is submitted for the degree of Doctor of Philosophy*

*September 2013*

*This PhD thesis is dedicated to*

*Anna,*

*my dearest friend who passed*

*away in November 2012...*

## DECLARATION

This dissertation is the result of my own work and includes nothing which is the outcome of work done in collaboration except where specifically indicated in the text.

This thesis does not exceed the word limit of 60,000 as set by the Degree Committee for the Faculty of Biology.

## <u>ABSTRACT</u>

*Plasmodium falciparum* is the causative agent of the most severe form of malaria, a serious infection accounting for an estimated one million deaths annually. Currently, there is no licenced malaria vaccine available. Erythrocyte invasion by the blood stage of the parasite, the merozoite, is a critical step in parasite's lifecycle and has long been targeted for the development of therapeutics. However, the development of a highly efficacious blood stage malaria vaccine has been challenged by the highly polymorphic nature of merozoite ligands, as well as by functional redundancy of the receptor-ligand pairs involved in the invasion process. The identification of cell surface receptor-ligand interactions which are essential for erythrocyte invasion by merozoite has been hampered by the difficulties in recombinant expression of *Plasmodium* spp. proteins, and by the technical challenges in systematically identifying interacting partners for cell surface proteins.

In earlier work from our laboratory, BSG and Semaphorin7A were identified as the erythrocyte receptors for merozoite RH5 and MTRAP, respectively. Importantly, the interaction between RH5 and BSG is the only one known so far that is essential and universally required for erythrocyte invasion. Antibodies against either RH5 or BSG could potently inhibit erythrocyte invasion in all *P. falciparum* strains tested; therefore, the blockade of RH5-BSG interaction can be exploited for therapeutic purposes, for the treatment of *P. falciparum* infected individuals.

Most of the work described in this thesis is aimed at the development of a humanised or chimeric anti-BSG antibody as a potential anti-malarial therapeutic. For this purpose, a plasmid system, which enables the recombinant expression of engineered antibodies, was established. By using this versatile plasmid system, two anti-BSG monoclonals, MEM-M6/4 and MEM-M6/8 (obtained from a published report), were successfully humanised by Complementarity Determining Region (CDR) grafting. The therapeutic potential of huMEM6-M/4 and huMEM6-M/8 was hindered by the low affinity of these antibodies for BSG. To obtain a higher potency antibody, a panel of hybridoma lines secreting anti-BSG antibodies was generated by directly immunising animals. A monoclonal antibody, m6D9, secreted by one of the generated hybridoma clones, demonstrated high efficacy in inhibiting erythrocyte invasion in parasite culture, and was selected for chimerisation. The chimeric antibody, ch6D9, retained its high affinity for BSG and blocked erythrocyte invasion

at very low concentrations in all parasite lines tested. Furthermore, ch6D9 displayed reduced binding to FcγRIIA and C1q *in vitro*, suggesting that this antibody may have reduced ability to trigger antibody effector functions. Attempts to fully humanise this antibody were unsuccessful.

In another approach, two anti-RH5 monoclonals (2AC7 and 9AD4; Douglas *et al.*, 2013) were successfully chimerised. Both ch2AC7 and ch9AD4 preserved their high affinity for RH5 and inhibited erythrocyte invasion in parasite culture, but with much higher $IC_{50}$ as compared to ch6D9. The variable regions of ch2AC7 and ch6D9 were combined in an anti-RH5 and anti-BSG bi-specific antibody: 2AC7-6D9 DVD-Ig. 2AC7-6D9 DVD-Ig was capable of simultaneous binding to RH5 and BSG but its affinity for BSG decreased in comparison to ch6D9. When tested in a *P. falciparum* growth inhibition assay, 2AC7-6D9 DVD-Ig was more efficient than ch2AC7, but less than ch6D9 in blocking erythrocyte invasion.

Finally, in a parallel project, I aimed to identify novel receptor-ligand pairs involved in erythrocyte invasion. For this purpose, I expanded an existing *P. falciparum* merozoite recombinant protein library by 26 proteins, which were chosen based on transcription microarray data, and information available in the literature. The new members of the *P. falciparum* protein library were recombinantly expressed and systematically screened against an equivalent library consisting of erythrocyte receptors. The screen identified a putative interaction (PF13_0125 – P4HB). Further characterisation of the identified interaction provided inconclusive results, and more experiments are required to confirm its validity. The recombinant *P. falciparum* merozoite proteins reported in this project should prove to be a useful tool for the deeper understanding of erythrocyte invasion, and *P. falciparum* biology in general.

# Table of Contents

# List of Figures

**CHAPTER 6**

# List of Tables

# CHAPTER 1

**Introduction**

## 1.1 Summary and Aims

The first aim of the work described in this PhD thesis was to investigate the potential of using monoclonal antibodies targeting the RH5-Basigin interaction, as novel anti-malarial therapeutics. To this end, I developed a series of humanised or chimeric monoclonal anti-Basigin and anti-RH5 antibodies, and characterised their ability to interfere with the RH5-Basigin interaction and *P. falciparum* erythrocyte invasion. The second goal was the identification of novel receptor-ligand pairs involved in erythrocyte invasion by *Plasmodium falciparum*. The current chapter provides background information concerning both these projects.

To mirror the twin experimental goals of the PhD thesis, this introductory chapter is split into two sections. In the first section, I discuss the general structure and functions of antibodies, as well as their value in the clinic for the treatment of various diseases. In the second part I describe malaria, focusing particularly on erythrocyte invasion, and on how this critical stage in parasite's lifecycle can be exploited for the development of anti-malarial intervention measures.

## 1.2 General structure and properties of antibodies

In the early 1890s, Emil von Behring together with Kitasato Shibasaburo, with their work in diphtheria and tetanus, were the first to propose that mediators in serum can react with foreign substances (A G N, 1931). These mediators were later termed antibodies (antikörper in German*)* by Paul Ehlirch in 1891, who reported that if two substances give rise to two different "antikörper", then they themselves must be different (Lindenmann, 1984). In 1920s, Michael Heidelberger and Oswald Avery found that antibodies "were made of proteins"(Van Epps, 2006).

Later studies demonstrated that antibodies are large Y-shaped proteins secreted by B-cells, and are responsible for organism's humoral immunity (Abbas *et al.*, 2011). An antibody is a tetrameric molecule consisting of four polypeptide chains; two identical heavy chains (α, δ, ε, γ, μ) pair with each other, as well as with two identical light chains (κ,λ), via disulfide bonds (Fig. 1.1A). The type of heavy chain present, defines the class of antibody (see below). Both heavy and light chains have a globular structure consisting of tandem immunoglobulin (Ig) domains, and are subdivided into constant (C) and variable (V) region. The V region is responsible for antibody specificity and binding to the antigen: within the variable regions of both

heavy (VH) and light (VL) chains, three polypeptide segments show exceptional variability between different antibodies and are known as hypervariable regions. These diverse stretches from both VH and VL chain are brought together to form an antigen-binding surface (Abbas *et al.*, 2011).

Hypervariable regions form a surface that is complementary to the structure of the bound antigen, and hence hypervariable regions are also called complementarity determining regions (CDRs) (Male *et al.*, 2006; Abbas *et al.*, 2011) (Fig. 1.1A). Amino acid residues within the CDRs form multiple contacts with the target antigen. The most extensive contact is with the third hypervariable region of the heavy chain (CDRH3). The latter CDR is also the most variable amongst the CDRs of both VH and VL because it is encoded by a stretch in the genome which is derived from an "error prone" recombination event between three different segments (V,D,J) in the genome (Male *et al.*, 2006; Abbas *et al.*, 2011).

CDRs are surrounded by four less variable sequences, known as framework regions (FRs) which are thought to play supporting role for the CDRs during binding to the antigen (Fig. 1.1A). Some residues within the FRs may directly contact the antigen, but the primary role of FRs is to sterically maintain the CDRs at a position that maximizes interaction with antigen binding sites (Male *et al.*, 2006; Abbas *et al.*, 2011).

## 1.3 Antibody classes

The C region Ig domains are separate from the antigen-binding site and do not participate in antigen recognition. The heavy chain C region interacts with other effector molecules and cells of the immune system and therefore, mediates most of the biological functions of antibodies (section 1.4). Antibodies are divided into five dinstict classes (isotypes) named IgA, IgD, IgE, IgG, and IgM, depending on which heavy chain (α,γ,δ,ε,μ) is present (Fig 1.1B). In humans, IgA and IgG isotypes can be further divided into subclasses called IgA1, IgA2 and IgG1, IgG2, IgG3, IgG4, respectively (Abbas *et al.*, 2011).

**A.**
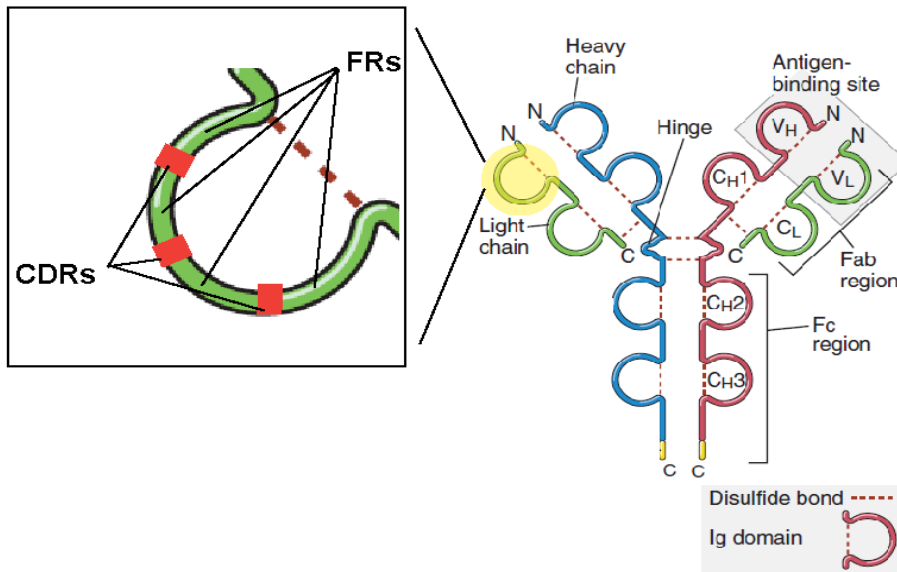


**B.**
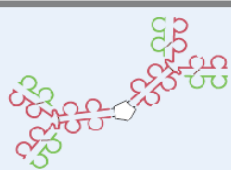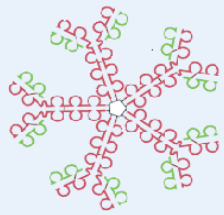
| Isotope of Antibody | Subtypes (H Chain) | Serum Concentration (mg/mL) | Serum Half-life (days) | Secreted Form | |
|---|---|---|---|---|---|
| IgA | IgA1,2 ($\alpha$1 or $\alpha$2) | 3.5 | 6 | IgA (dimer) Monomer, dimer, trimer | |
| IgD | None ($\delta$) | Trace | 3 | None | |
| IgE | None ($\epsilon$) | 0.05 | 2 | IgE Monomer | |
| IgG | IgG1-4 ($\gamma$1, $\gamma$2, $\gamma$3, or $\gamma$4) | 13.5 | 23 | IgG1 Monomer | |
| IgM | None ($\mu$) | 1.5 | 5 | IgM Pentamer | |

**Figure 1.1 Structure and properties of antibodies.**

*A.* The structure of an IgG antibody is shown as representative of all antibody classes. IgG consists of two heavy and two light chains, each of which has a constant (CH1-3 for heavy chain, and CL for light chain) and a variable region (VH for heavy chain, and VL for light chain). The antibody specificity is due to the three Complementarity Determining Regions (CDRs) found in the variable regions of both heavy and light chains. The three CDRs of each heavy and light chain are surrounded by four Framework Regions (FRs). The antibody molecule is subdivided into Fab and Fc region, based on the fragments obtained after proteolytic processing by specific enzymes. Abbreviations: CH1-3, Constant Heavy Immunoglobulin Domains 1-3; CL, Constant Light; VH, Variable Heavy; VL, Variable Light.

*B.* Antibodies are divided into five different classes (IgG, IgE, IgA, IgM and IgD), depending on which heavy chain (α, γ, δ, ε, μ) is present. Subtypes of γ (γ1-4) and α (α1-2) chains further devide IgGs and IgAs in IgG1-4 and IgA1-2 subclasses, respectively. Heavy and light chains are indicated with magenta and green colour, respectively. Pictures adapted and modified from Abbas *et al.*, 2011.

IgG (Fig. 1.1) is the predominant form of antibodies in blood and extracellular fluids. IgGs account for the 70-75% of the total serum immunoglobulin pool, and provide the majority of antibody-based immunity (Male *et al.*, 2006; Abbas *et al.*, 2011). It is the most well studied class of antibodies and due to their high abundance, extended serum half-life and versatility in triggering antibody effector functions (sections 1.4 and 1.5), they have attracted most of the interest towards the development of antibody-based therapeutics for various diseases (section 1.6). Therefore, for the rest of this PhD thesis, I am focusing mainly on the properties and functions of IgGs.

## 1.4 How do antibodies function?

### 1.4.1 Direct neutralisation of microbes and microbial toxins

Antibodies against microbes inhibit the interaction of microbes with cellular components. Many microbes (e.g influenza virus, HIV, *P. falciparum* merozoites) use molecules exposed on their surface to recognise and infect host cells. Antibodies that bind to these microbial structures interfere with their ability to recognise and bind to host cell surface receptors. In this way, antibodies neutralise pathogens and prevent the initiation or continuation of infection (Abbas *et al.*, 2011).

Similarly, many microbial toxins mediate their pathologic effect by binding to host cell surface receptors. For example, diphtheria toxin binds to HB-EGF (Naglich *et al.*, 1992) to enter host cells where it inhibits protein synthesis, and tetanus toxin (tetanospasmin) binds to a cell surface receptor to infect inhibitory neurons and thereby inhibiting the release of neurotransmitters. Antibodies against such toxins hinder the interaction with host cells and therefore, prevent the onset of injury or disease (Abbas *et al.*, 2011).

### 1.4.2 Antibody effector functions

### 1.4.2.1 Antibody effector functions mediated by Fc receptors

Besides antibody direct neutralisation of pathogens and pathogenic toxins, more sophisticated effector systems have co-evolved with antibodies to maximize the protection against microbes: Antibody Dependent Cellular Phagocytosis (ADCP), Antibody Dependent Cellular Cytotoxicity (ADCC), and Complement Dependent Cytotoxicity (CDC) (Hogarth and Pietersz, 2012). ADCP and ADCC (see below) are mediated by a class of cell surface receptors - Fc receptors (FcRs) - which bind

specifically to the Fc portion of antibodies (Fig. 1.1). The engagement of Fc receptors to antibody Fc region initiates intracellular signalling cascades which activate, regulate and modulate immunity (Hogarth and Pietersz, 2012).

The Fc receptors that bind IgGs are called Fcγ receptors (FcγR). FcγRs comprise a diverse family of cell surface receptors consisting of three classes of receptors (FcγRI-III) encoded by six genes: *FCGR1A* (which encodes FcγRI; also known as CD64), *FCGR2A* (which encodes FcγRIIA; also known as CD32A), *FCGR2B* (which encodes FcγRIIB; also known as CD32B), *FCGR2C* (which encodes FcγRIIC; also known as CD32C), *FCGR3A* (which encodes FcγRIIIA; also known as CD16A) and *FCGR3B* (which encodes FcγRIIIB; also known as CD16B) (Hogarth and Pietersz, 2012). FcγRs cellular distribution is shown in Fig. 1.2A.

Within the three classes of FcγRs, several polymorphisms with functional relevance have been described. Position 158, in the amino acid sequence of FcγRIIIA, has been shown to be polymorphic, and either valine or phenylalanine are found in this position. The $V_{158}$ allotype has been shown to be associated with more efficient natural killer (NK) cell activity (Male *et al.*, 2006). Similarly, high- or low-responder forms of FcγRIIA are defined by either Arginine ($R_{131}$) or Histidine ($H_{131}$) residues at position 131, respectively (Hogarth and Pietersz, 2012). Finally, polymorphisms in FcγRIIIB result in three allotypes, FcγRIIIB-NA1 ($R_{36}$, $N_{65}$, $D_{82}$ , $V_{106}$), FcγRIIIB-NA2 ($S_{36}$, $S_{65}$, $N_{82}$, $I_{106}$) and FcγRIIIB-SH ($S_{36}$, $S_{65}$, $D_{78}$, $N_{82,}$ $I_{106}$), which differ in their glycosylation pattern (Bruhns, 2012).

Structurally, each FcγR has a unique Fc-binding α-chain of which the extracellular region consists of two immunoglobulin-like domains (Fig. 1.2B). FcγRI is an exception, since it has three immunoglobulin-like domains (Fig. 1.2B). Of note, is that FcγRI displays the highest affinity for antibody Fc regions, in comparison to the rest FcγRs (Fig. 1.2C) (Woof and Burton, 2004; Hogarth and Pietersz, 2012). The α-chain of FcγRI and FcγRIIIA is incapable of intracellular signal transduction upon receptor engagement. Hence, it is complexed through its transmembrane region with a dimer of the common FcR γ-chain which contains an immunoreceptor tyrosine based activation motif (ITAM), responsible for the initiation of stimulating signals (Fig. 1.2B)

**A.**

| | FcγRI | FcγRIIA | FcγRIIB | FcγRIIC | FcγRIIIA | FcγRIIIB |
|---|---|---|---|---|---|---|
| B cell | - | - | + | - | - | - |
| T cell | - | - | - | - | - | - |
| NK cell | - | - | - | + | + | - |
| Monocyte/Macrophage | + | + | +/- | + | + | - |
| Neutrophil | (+) | + | +/- | + | - | + |
| Dendritic cell | + | + | + | - | - | - |
| Basophil | - | + | + | - | - | +/- |
| Mast cell | (+) | + | - | - | - | - |
| Eosinophil | - | + | - | - | - | - |

**B.**



**C.**

| | FcγRI | FcγRIIA | | FcγRIIB | FcγRIIC | FcγRIIIA | | FcγRIIIB |
|---|---|---|---|---|---|---|---|---|
| | | $H_{131}$ | $R_{131}$ | | | $V_{158}$ | $F_{158}$ | NA1,NA2,SH |
| IgG1 | 650 | 52 | 35 | 1.2 | 1.2 | 20 | 11.7 | 2.0 |
| IgG2 | - | 4.5 | 1.0 | 0.2 | 0.2 | 0.7 | 0.3 | - |
| IgG3 | 610 | 8.9 | 9.1 | 1.7 | 1.7 | 98 | 77 | 10 |
| IgG4 | 340 | 1.7 | 2.1 | 2.0 | 2.0 | 2.5 | 2.0 | - |
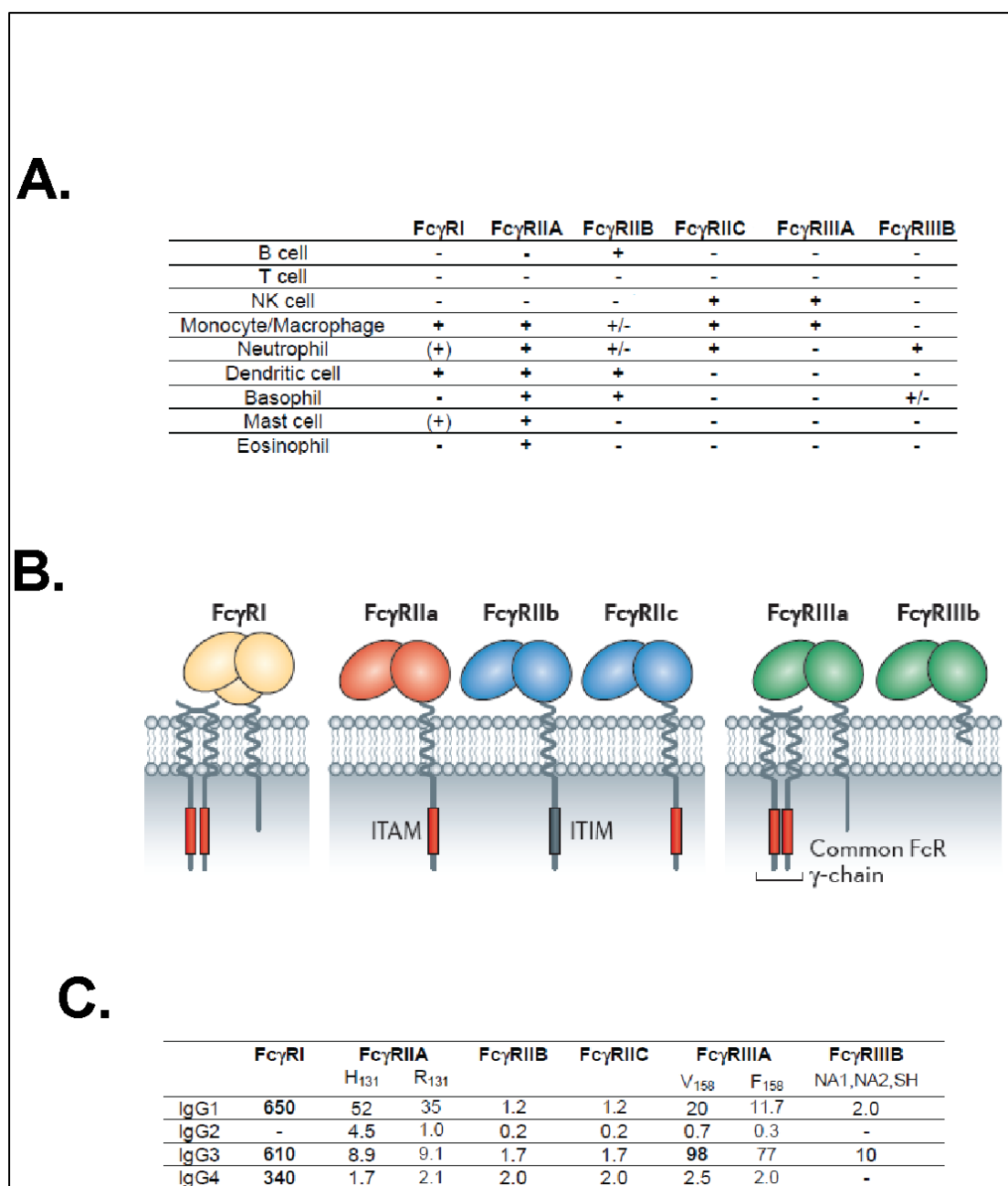
**Figure 1.2 The Fcγ family of receptors.**

*A.* Cellular distribution of human FcγRs. *B.* Diagrammatic representation of the human FcγR general protein structure. Of note, is that the extracellular region of FcγRI has an additional immunoglobulin-like domain in comparison to the other FcγRs. *C.* A table showing the affinity constants ($K_A$) of human FcγRs for human IgG subclasses (x$10^5$ M$^{-1}$). For details see text. Abbreviations: ITAM, immunoreceptor tyrosine-based activation motif; ITIM, immunoreceptor tyrosine-based inhibitory motif; +, constitutive expression; (+), inducible expression; +/-, expression in some cell subsets only. Pictures adapted and modified from Bruhns, 2012 and Hogarth & Pietersz, 2012.

(Woof and Burton, 2004). FcγRIIIA can associate with other signalling molecules as well, such as homodimers of the T cell receptor (TCR) ζ-chain or heterodimers composed of γ and ζ chains in NK cells. FcγRIIA, FcγRIIB and FcγRIIC do not associate with other molecules for signal transduction but they carry their signalling motifs in the cytoplasmic tail of the α-chain. FcγRIIB, instead of an ITAM, contains an immunoreceptor tyrosine based inhibitory motif (ITIM) in its α-chain cytoplasmic region, through which it transduces suppressing signals (Nimmerjahn and Ravetch, 2008). The simultaneous expression of activating and inhibitory molecules on the same cell is the key for the generation of a balanced immune response (Nimmerjahn and Ravetch, 2006).

### 1.4.2.1.1 Antibody Dependent Cellular Phagocytosis (ADCP)

An important biological function of antibodies is the Antibody Dependent Cellular Phagocytosis (ADCP). Phagocytosis of IgG-coated microbes is mediated by the engagement of the Fc portions of antibodies to FcγRs expressed on a phagocyte's cell surface (Abbas *et al.*, 2011). Phagocytes express a combination of FcγRs including FcγRI and FcγRIIA (Desjarlais and Lazar, 2011). Following the binding to the antibody Fc portion, the target foreign particle is internalized by the phagocytes, and is finally destroyed in phagolysosomes. Besides the phagocytosis itself, the binding of IgGs to FcγRs on phagocytes triggers the secretion of lytic enzymes and reactive oxygen species which are directed against microbes that are too large to be phagocytosed (Abbas *et al.*, 2011).

### 1.4.2.1.2 Antibody Dependent Cell mediated Cytotoxicity (ADCC)

In a process called antibody dependent cell mediated cytotoxicity (ADCC), NK-cells recognise and destroy antibody-coated target cells. This process is primarily mediated by the low affinity, NK-cell surface exposed, FcγRIIIA, which binds to the Fc region of antibodies aggregated on target cells. The engagement of FcγRIIIA, activates NK-cell and triggers the discharge of perforins and granzymes which form pores and lyse the foreign cells (Male *et al.*, 2006; Abbas *et al.*, 2011).

### 1.4.2.2 Complement dependent cytotoxicity

Antibodies bound to the surface of target cells can activate the classical pathway of the complement cascade. IgG subtypes have different ability in triggering the classical pathway cascade with IgG3>IgG1>>IgG2>>IgG4 (Woof and Burton,

2004). The first component of this pathway, C1, is a complex between a hexameric recognition unit C1q, and two molecules of each of the proteases C1r and C1s. Once C1q in the C1 complex binds to the Fc region of immobilized antibodies – at least two out of six arms of C1q must be bound - it undergoes conformational changes which trigger autocatalytic activation of C1r. C1r subsequently cleaves and activates C1s. C1s then cleaves C4 into 2 fragments C4a and C4b, of which the latter stays associated with C1 to ensure that the reaction proceeds on the target cell surface (Male *et al.*, 2006).

The pathway continues with a series of enzymatic events and finally results in the formation of the so called membrane attack complex (MAC) which is a pore on the target cell membrane, formed by multiple copies of C9 protein, arranged like barrel staves around a central cavity. The MAC complex allows free flow of solutes and water across the target membrane. The entry of water results in osmotic swelling and rupture of the cells upon whose surface the MAC is deposited (Male *et al.*, 2006).

## 1.5 The interactions between IgG Fc portion and C1q or Fcγ receptors have been characterised

The interactions between IgG Fc region and C1q or FcγRs have been studied extensively, and a number of amino acids within antibody Fc portion have been suggested to participate in the binding to C1q and FcγRs. The latter amino acids are of great therapeutic interest, and provide a means of modulating antibody effector functions *in vivo* when antibodies are used for treatment of various diseases.

Several studies reported that the so called lower hinge region (Fig. 1.1A), is of key importance for the binding of C1q and FcγRs to antibody Fc region. For example Morgan and colleagues demonstrated that changing the leucine 235 to glutamic acid (Eu numbering) abolished FcγRI binding (Morgan *et al.*, 1995). The same group also reported that the mutation of glycine to alanine at position 237 abolished FcγRI binding and reduced complement lysis and FcγRIII-mediated function (Morgan *et al.*, 1995). Chappel and colleagues proposed that the entire sequence spanning residues 234-237 of hIgG1, is required for binding to FcγRI (Chappel *et al.*, 1991). Similarly, Shields and colleagues exchanged the amino acid residues 233-236 of hIgG1 with those found in hIgG2 at the same positions. They showed that the

E233P/L234V/L235A/G236Δ hIgG1 variant binds to all Fcγ receptors with reduced affinity (Shields *et al.*, 2001)

Another area in antibody Fc region that has attracted interest and has been proposed to play important role in driving antibody effector mechanisms, is the area spanning the residues 327–331 from a bend, joining two β-strands close in the tertiary structure to the lower hinge region (Armour *et al.*, 1999). Alanine substitution at positions P329, and P331 significantly reduced the ability of C1q binding to hIgG1 (Idusogie *et al.*, 2000). Moreover, the introduction of P331S mutation in IgG3, as found in IgG4, reduced affinity for FcγRI by a factor of 10 (Canfield and Morrison, 1991). Lysine at position 322, which is located N-terminally to the 327–331 region, has also been implicated in the stimulation of antibody effector functions. Armour and colleagues in two elegant studies combined mutations in the two Fc regions mentioned above and demonstrated that the E233P/L234V/L235A/G236Δ/A327G/A330S/P331S mutant has impaired binding to FcγRI, FcγRIIA$_{H131}$, FcγRIIA$_{R131}$ and FcγRIIB (Armour *et al.*, 1999, 2003). A number of other amino acid residues in the Fc region have also been implicated in the modulation of antibody effector functions (Idusogie *et al.*, 2000; Hezareh *et al.*, 2001; Shields *et al.*, 2001).

Finally, the presence of oligosaccharides attached to the asparagine at position 297, has been shown to be important for most antibody effector functions (Idusogie *et al.*, 2000). Previous studies provided evidence that that interaction sites on IgG Fc for FcγRI, FcγRII, FcγRIII and C1q are comprised principally of only the protein moiety (Jefferis, 2009). Nevertheless, the generation of the interaction sites for these ligands appears to be dependent on IgG Fc protein – carbohydrate interactions. Indeed, it has been shown that effector mechanisms mediated through FcγRI, FcγRII, FcγRIII and C1q are severely affected for aglycosylated forms of IgG (Jefferis, 2009).

## 1.6 The discovery of hybridoma technology and the emergence of antibody therapeutics

In 1975 Kohler and Milstein were the first to introduce the hybridoma technology (Köhler and Milstein, 1975). They demonstrated that cell lines (hybridomas) derived from the fusion of myeloma and mouse spleen cells from an immunised donor can grow indefinitely in culture, and have the ability to secrete

antibodies. Each hybridoma clone produces antibodies of a single specificity (monoclonal antibodies) and therefore, if the spleen cell donor is immunised with an antigen of interest, it is possible to isolate clones which secrete antibodies of the desired specificity. Hybridoma technology provided an unlimited source of monoclonal antibodies, and enabled of the possibility that monoclonal antibodies could be used as putative therapeutics.

Monoclonal antibodies have rapidly emerged as a clinically important class of biological drugs. Their fine specificity, long serum half-lives (Fig. 1.1B) and the ability they offer to modulate antibody effector functions simply by mutating amino acids within antibody Fc region (section 1.5), have established antibody based therapies as one of the most successful therapeutic strategies (Beck *et al.*, 2010). The first antibody that was approved for clinical therapy in 1986 was OKT3, a mouse anti-CD3 monoclonal, used for the treatment of acute allograft rejection in renal transplantation (Smith, 1996; Chan and Carter, 2010). Since then, more than 30 antibodies have been approved by FDA for human therapy (Beck *et al.*, 2010) and more than 240 antibodies are currently under clinical trials for a variety of diseases, ranging from cancer and organ transplantation, to autoimmunity and infectious diseases (Chan and Carter, 2010; Reichert, 2010).

Alemtuzumab (marketed as Campath) was amongst the first antibodies to be used in clinic (Riechmann *et al.*, 1988; Gorman and Clark, 1990). It is an anti-CD52 humanised antibody (for the humanisation technology see Chapter 4), and it was originally intended for the treatment of leukemias (Gorman and Clark, 1990; Magliocca and Knechtle, 2006; Coles, 2013). Because of its ability to transiently deplete peripheral lymphocytes, it is now also being considered for the treatment of multiple sclerosis (Coles, 2013). Alemtuzumab has also been used as an induction agent during organ transplantations (Magliocca and Knechtle, 2006).

Trastuzumab (Herceptin) is another well-known therapeutic antibody. It is directed against Human Epidermal growth factor Receptor 2 (HER2) and has been used to treat HER2 positive metastatic breast cancer, in patients who had received one or more chemotherapy regimens (Reichert, 2010). In 2012, FDA approved trastuzumab to be used in combination with pertuzumab – another anti-HER2 antibody which inhibits HER2 dimerization- and docetaxel, for the treatment of patients with HER2-positive metastatic breast cancer who have not previously

received anti-HER2 therapy or chemotherapy for metastatic disease (Baselga *et al.*, 2012; Blumenthal *et al.*, 2013).

## 1.7 Malaria is a significant global health problem

The parasitic protozoon of the genus *Plasmodium* is the causative agent of malaria, a serious infection which accounted for 219 million clinical cases and 1.2 million deaths in 2010 alone (Murray *et al.*, 2012; World Health Organization, 2012)*.* Malaria is transmitted to humans through the bites of female *Anopheline* mosquitoes (section 1.9), and is strongly associated with poverty as mortality rates are highest in developing countries with lower gross national income (GNI) per capita (World Health Organization, 2012). The vast majority of malaria fatalities (85–90%) occur in sub-Saharan Africa, mainly in the vulnerable populations of children under the age of five and pregnant women (Geels *et al.*, 2011; World Health Organization, 2012). Globally, an estimated 3.3 billion people (nearly half the world's population) were at risk of malaria in 2011, and today there is on-going malaria transmission in 99 countries (World Health Organization, 2012).

## 1.8 Five species of *Plasmodium* are infective to humans

Historically, it was thought that four species *of Plasmodium* naturally infect humans: *P. falciparum, P. vivax, P. ovale* (recently subdivided into two closely related species, *P. ovale curtisi* and *P. ovale wallikeri*; Sutherland *et al.*, 2010)*,* and *P. malariae.* The number of *Plasmodium* species that infect humans has recently been increased by the observation that *P. knowlesi,* a simian malaria parasite which primarily infects macaques, causes a substantial number of naturally-acquired infections in human populations in South East Asia (Singh *et al.*, 2004; Antinori *et al.*, 2013). It has yet to be established whether *P. knowlesi* has switched hosts and transmission is between humans or whether all infections are zoonotic (Singh *et al.*, 2004; Antinori *et al.*, 2013).

The work described in this thesis focuses primarily on *P. falciparum*, the most virulent amongst human *Plasmodium* spp., and a major cause of mortality in children below five years of age, globally (Elliott and Beeson, 2008; Richards and Beeson, 2009).

**1.9 *P. falciparum* has a complex lifecycle**

The lifecycle of *P. falciparum* is complex, and the parasite alternates between the human host and a mosquito vector (Fig. 1.3) (Bannister and Sherman, 2009). Malaria infection is initiated when the transmissive form of *P. falciparum*, the sporozoites, enter the skin of the human host through the bite of an infected female *Anopheline* mosquito (Prudêncio *et al.*, 2006; Bannister and Sherman, 2009). Sporozoites migrate to the liver where they invade hepatocytes, and subsequently replicate and differentiate to form thousands of invasive merozoites (the exo-erythrocytic form of the parasite). After about nine days, merozoites enter the blood stream and invade erythrocytes initiating an asexual replication cycle that has a duration of 48 hours. This cycle ends with the release of new merozoites from the mature infected erythrocyte (schizont), which can, in turn, infect new erythrocytes (Bannister and Sherman, 2009). In the blood, some intra-erythrocytic stages develop into the sexual parasite stages, the male and female gametocytes, which, during transmission, are ingested by mosquitoes as part of their blood meal (Cowman and Crabb, 2006; Prudêncio et al., 2006). Once within the mosquito gut, the gametocytes develop into mature gametes, and undergo fertilization to form a zygote. The zygote then develops into a motile ookinete which penetrates the mosquito midgut wall, and transforms into an oocyst. The parasite replicates within the oocyst to form mature sporozoites which are finally released and migrate to mosquito salivary glands, ready to be transmitted to human again.

The asexual erythrocytic stages of the parasite are responsible for the clinical manifestations of the disease (Miller *et al.*, 2002a). The synchronised release of merozoites into the blood stream due to erythrocyte rupture at the end of each 48-hour asexual blood cycle, is accompanied by recurrent attacks of chills and fever (Chen *et al.*, 2000). Moreover, sequestration of infected erythrocytes injures endothelial cells and disrupts blood flow, causing tissue hypoxia and lactic acidosis. When sequestration occurs in the brain or placenta, it can lead to life threatening conditions known as cerebral malaria and placental malaria, respectively (Miller *et al.*, 2013).
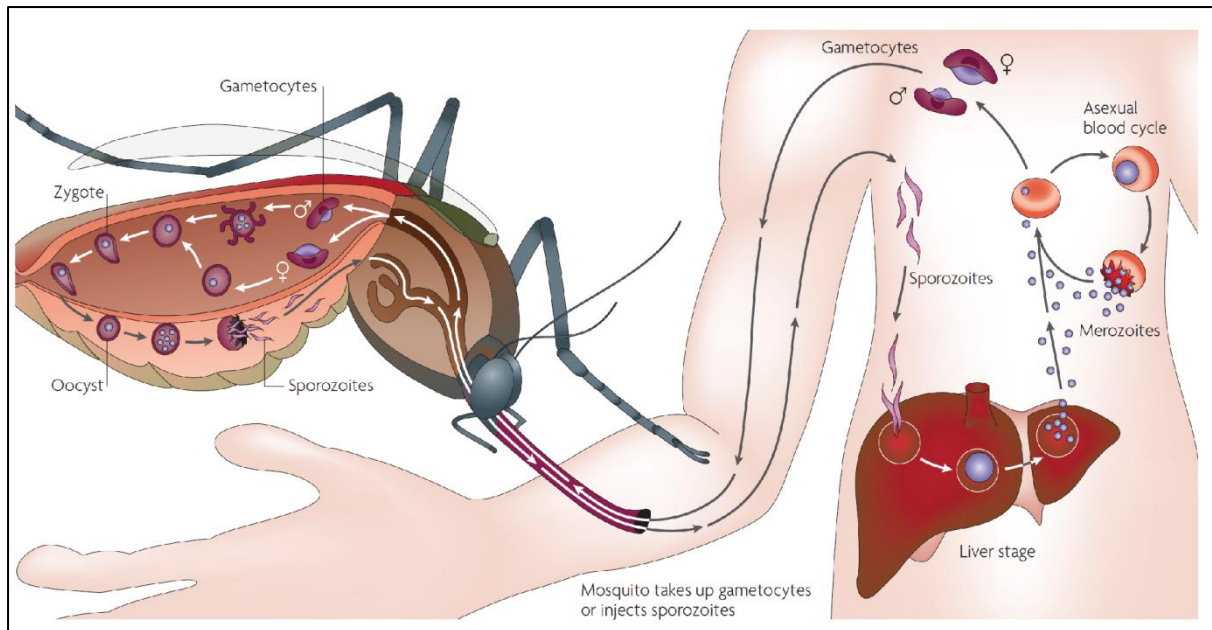
**Figure 1.3 The lifecycle of *Plasmodium falciparum*.** The lifecycle begins when sporozoites enter human host body, after a bite from a *P. falciparum* infected female *Anopheline* mosquito. Sporozoites migrate to the liver and invade hepatocytes, where they grow and replicate. After about nine days, thousands of merozoites are released into the bloodstream (Bannister and Sherman, 2009), where they rapidly invade host erythrocytes. Erythrocyte invasion marks the initiation of a new proliferation cycle which ends up with the release of new merozoites from matured infected erythrocytes (schizonts). The free merozoites are then able to invade new erythrocytes to continue the asexual blood-stage lifecycle. During blood stages, a number of parasites develop into male or female gametocytes which can then be ingested by a mosquito during a blood meal. Gametocytes mature in mosquito gut, and fuse to form a zygote. The zygote develops into a motile ookinete which transverses the midgut epithelium and transforms into an oocyst. The parasite replicates within the oocyst to form mature sporozoites, which are finally released and migrate to mosquito salivary glands, ready to transmitted to be human again (Cowman and Crabb, 2006; Prudêncio et al., 2006). Picture adapted from Su *et al.*, 2007.

## 1.10 Erythrocyte recognition and invasion are critical steps in the *P. falciparum* lifecycle

Erythrocyte host entry is an obligatory step in the *P. falciparum* lifecycle (Cowman and Crabb, 2006). On lysis of infected erythrocytes, 16-32 daughter merozoites – the only extracellular form of the parasite during blood stages - are released into the bloodstream, and are capable of rapidly invading (within 30 to 40 seconds) new erythrocytes (Dvorak *et al.*, 1975; Gilson and Crabb, 2009). Merozoites have evolved to carry a full complement of organelles (see below) needed to invade erythrocytes in a rapid and efficient manner (Garcia *et al.*, 2008). Nevertheless, the brief extracellular exposure of merozoites outside their intra-erythrocytic niche, render them vulnerable to host immune defences. Indeed, a significant arm of naturally-acquired immunity to malaria is directed against merozoite antigens (Cohen *et al.*, 1969). Therefore, erythrocyte invasion has long been considered to be an exploitable target for therapeutic intevention; consequently, a deep understanding of the molecular processes that underpin erythrocyte invasion may aid the efforts to control malaria globally.

Below, I describe what is known about the structure of merozoite and the molecular events that drive erythrocyte invasion. Particular emphasis is given to the structure and function of proteins exposed on merozoite cell surface. Such proteins are directly accessible to human host humoral system and thus, they are of fundamental importance for the development of anti-malarial therapeutics.

### 1.10.1 Merozoite structure

*P. falciparum* merozoites are ovoid-shaped cells, ~1.2µm in length, and have a distinct structural organization of organelles within their apical protuberance (Bannister and Mitchell, 2003) (Fig. 1.4). A nucleus, a mitochondrion, and a plastid called apicoplast, are responsible for genetic and metabolic processes, and are located basally. Trafficking organelles such as the rough endoplasmic reticulum and Golgi complex are absent or residual in the mature merozoite (Garcia *et al.*, 2008). Underlying the plasma membrane, two additional membranes form a closed flat cisterna called the inner membrane complex (IMC) (Cowman *et al.*, 2012). The IMC together with the plasma membrane form the merozoite pellicle that lines the whole cell apart from the apical end (Bannister and Mitchell, 2003; Garcia *et al.*, 2008).
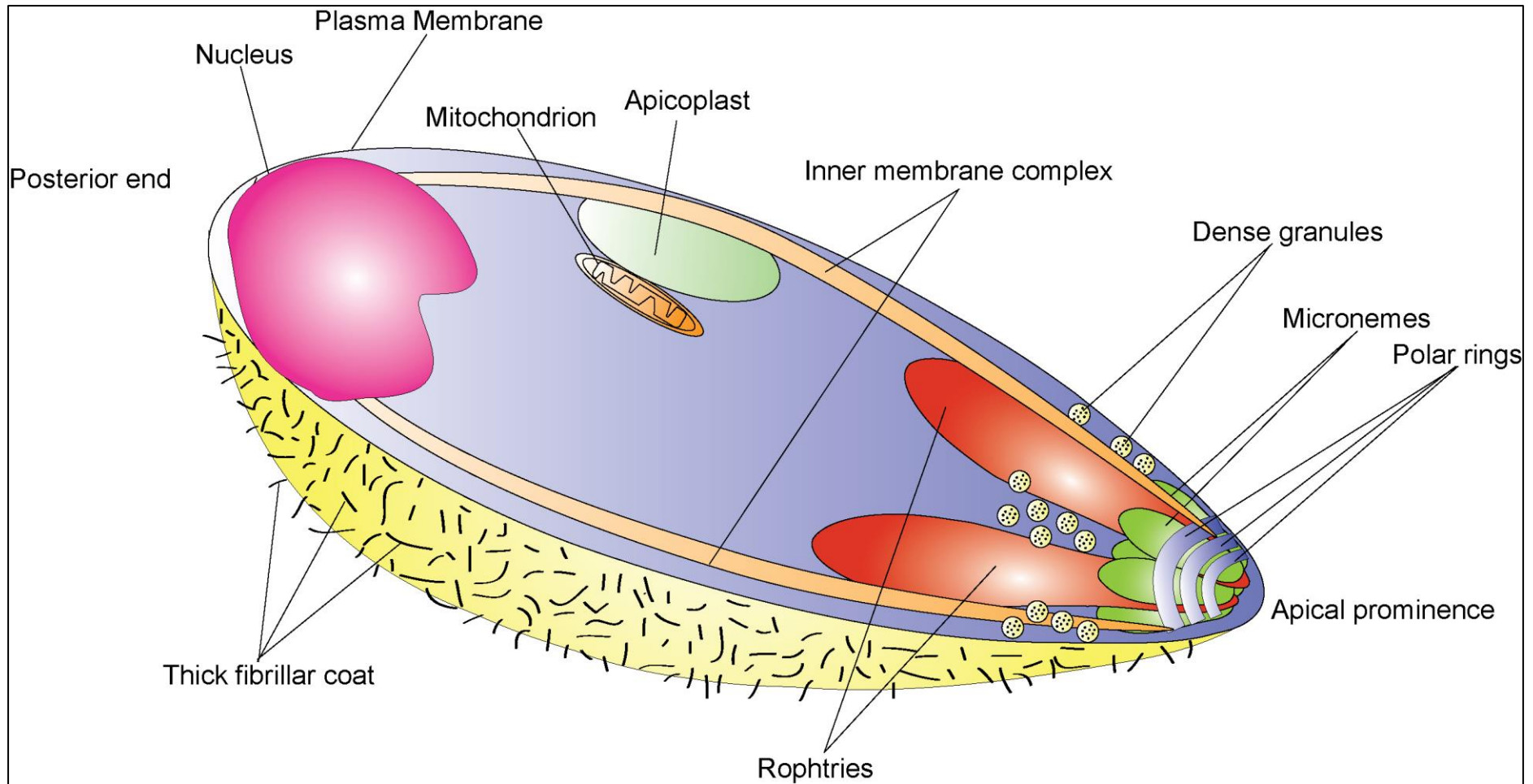
**Figure 1.4 Merozoite structure**. Merozoite has a polarised morphology and is covered by a proteinaceous fibrillar coat (~15nm thick) (Garcia *et al.*, 2008). Merozoite carries a nucleus, an apicoplast and a single mitochondrion. The secretory organelles (rhoptries, micronemes and dense granules) are located apically and play key role in erythrocyte invasion. The three polar rings are located at the apical end of merozoite. The inner membrane complex is necessary for anchoring the actin-myosin motor, which generates the force required during invasion.

The IMC appears to provide anchorage to several accessory proteins (e.g *Pf*GAP45, *Pf*GAP50) which support the actin-myosin motor within the merozoite, during erythrocyte invasion (Farrow *et al.*, 2011)

Two (or sometimes three) subpellicular microtubules (omitted for clarity in Fig. 1.4) line up in parallel along the side of the merozoite (Garcia *et al.*, 2008). This structure is called the *P. falciparum* merozoite assemblage of subpellicular microtubules (*f*-MAST) (Pinder *et al.*, 2000), and has been proposed to provide mechanical support for the merozoite (Garcia *et al.*, 2008). A possible role of *f*-MAST in invasion was proposed, due to the inhibitory effects of microtubule disrupting drugs in erythrocyte invasion (Pinder *et al.*, 2000). Consistent with this, evidence from electron microscopy also implicates microtubules in microneme targeting to the merozoite apex (see below) (Bannister and Mitchell, 2009). Another cytoskeletal structure is the three polar rings which are located at the apical end of merozoite, and define the site for rhoptry and microneme secretion during invasion (see below; Garcia *et al.*, 2008).

The merozoite is exquisitely adapted for invading host erythrocytes, and contains a set of secretory organelles (micronemes, rhoptries, dense granules, mononeme, exoneme) within which the molecules necessary for erythrocyte invasion are stored. Micronemes are elongated, densely staining vesicles that are clustered apically (Garcia *et al.*, 2008) (Fig. 1.4). It is likely that more than one subpopulation of micronemes exist, allowing sequential secretion of different micronemal contents in different phases of invasion (Singh *et al.*, 2007; Cowman *et al.*, 2012). Rhoptries are two pear-shaped organelles, much larger than micronemes, with their apical ends converging on the centre of the merozoite prominence (Kats *et al.*, 2006). Rhoptries can be subdivided into two functional domains, the bulb and the neck, which are not physically separated; however, their contents are distinct, and are thought to be released at different time points during erythrocyte invasion (see below; Kats *et al.*, 2006; Cowman *et al.*, 2012; Zuccala *et al.*, 2012). Rhoptry neck proteins are thought to be released on the merozoite cell surface before their counterparts located in rhoptry bulb (Kats *et al.*, 2006). Rhoptry secretion is thought to follow microneme, though the exact sequence of the molecular events that drive erythrocyte invasion, is not yet fully understood (Harvey *et al.*, 2012).

Dense granules are small, spheroidal vesicles scattered in the apical half of the merozoite (Garcia *et al.*, 2008) (Fig. 1.4). In *P. falciparum* is thought that the contents of dense granules are discharged by exocytosis onto the merozoite surface after invasion, and these proteins decorate the parasitophorus vacuolar membrane (PVM) to enable exchange of molecules between the parasite and the host erythrocyte (Kats *et al.*, 2006). Mononemes and a type of vesicle called exonemes are two secretory organelles that have only recently been described, and both contain proteases with pivotal roles in merozoite invasion(Singh *et al.*, 2007; Yeoh *et al.*, 2007).

## 1.10.2 Erythrocyte invasion is a multistep process

The cellular steps of erythrocyte invasion have been well studied by microscopy (Dvorak *et al.*, 1975; Gilson and Crabb, 2009). Mature merozoites are released from the bursting schizont, and disperse among surrounding red blood cells (Harvey *et al.*, 2012). Merozoites then contact, probably at random, uninfected erythrocytes and loosely adhere on their cell surface (Cowman and Crabb, 2006) (Fig 1.5A). Primary merozoite contact is associated with an obvious warping of erythrocyte cell membrane during which, the merozoite reorients itself to orient its apical end in direct apposition with the erythrocyte cell membrane (Gilson and Crabb, 2009). Merozoite reorientation is followed by the establishment of additional protein-protein contacts between the two juxtaposed cell membranes, probably committing the merozoite to invasion (Riglar *et al.*, 2011; Cowman *et al.*, 2012; Harvey *et al.*, 2012). These contacts are followed by the formation of a so called tight or moving junction (section 1.10.5) which is finally transformed into to a migrating ring that moves towards the basal end of merozoite, encircling merozoite within the erythrocyte (Aikawa *et al.*, 1978) (Fig 1.5).

## 1.10.3 The initial attachment to erythrocytes is primarily mediated by proteins displayed on the merozoite cell surface

Once released from the erythrocyte, the merozoite surface is observed to be covered by a coat of proteins (Fig 1.4). These proteins are synthesised and transported to the merozoite cell surface during merozoite maturation within the
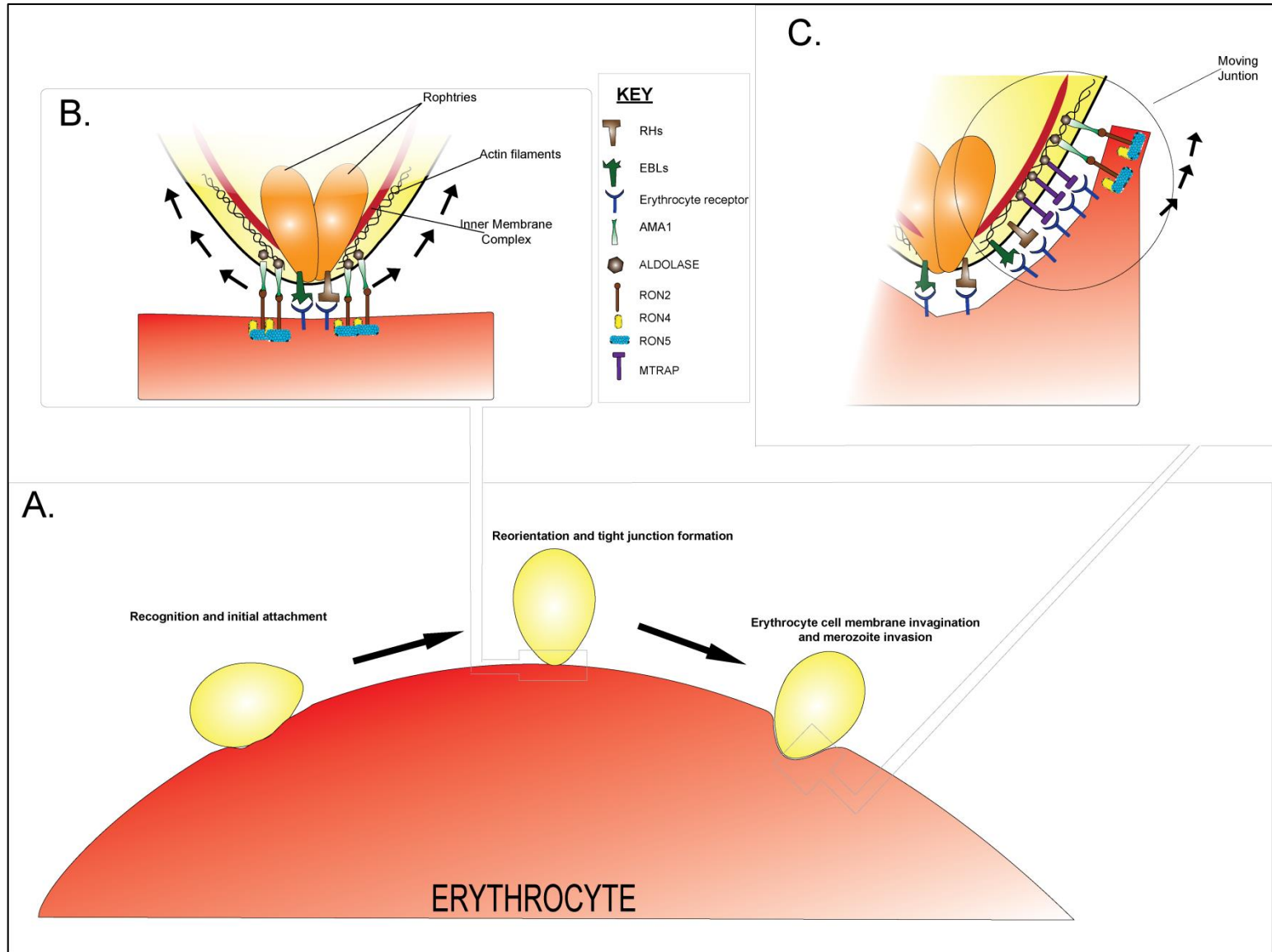
**Figure 1.5 Erythrocyte invasion is a multistep process.**

*A.* **Sequence of events leading to erythrocyte invasion**. First, merozoite recognises and loosely adheres to erythrocyte cell surface. Then, it reorients itself, putting its apical end facing the erythrocyte cell membrane. At this point a so called tight or moving junction is formed. During erythrocyte invasion, the tight junction starts moving towards the basal end of the merozoite, encircling merozoite within the erythrocyte.

*B.* **The formation of the tight junction**. The RON complex (RON2, RON4 and RON5) is embedded into erythrocyte's plasma membrane, marking the initiation of an irreversible series of events which end by the completion of erythrocyte invasion. Amongst RON complex proteins, RON2 is thought to directly interact with the microneme protein AMA-1 which is secreted on parasite's cell surface (Besteiro *et al.*, 2011). There is some evidence that AMA-1 cytoplasmic region is bound to aldolase which in turn is associated with parasite's actin myosin-motor (see text). Around the time of the tight junction formation, members of the reticulocyte binding protein homologues (RHs) and erythrocyte binding ligands (EBLs) families of proteins are secreted on parasite's cell surface, and bind to specific erythrocyte receptors.

*C.* **Moving junction migration**. During the invasion process, the moving junction migrates from the apical to the basal end of the merozoite (direction of arrows; also see *B.*). MTRAP is thought to bridge the gap between parasite actin-myosin motor and host erythrocyte plasma membrane: its cytoplasmic tail binds to aldolase which is associated with parasite's actin-myosin motor, and MTRAP ectodomain binds to receptors on erythrocyte cell surface.

schizont and are thought to mediate the initial attachment of the merozoites to erythrocytes (Garcia *et al.*, 2008). Studies have demonstrated that more than 20 proteins are associated with the merozoite cell surface prior to egress (Sanders et al., 2005; Cowman and Crabb, 2006; Cowman et al., 2012). These are divided into proteins that are directly anchored to the merozoite plasma membrane (usually through a Glycophosphatidylinositol (GPI anchor)) and peripheral proteins which are associated by interactions with surface-tethered proteins (Sanders *et al.*, 2005; Cowman *et al.*, 2012).

Several merozoite cell surface proteins contain domains that have been implicated in mediating protein–protein interactions. These include Duffy binding–like (DBL) or erythrocyte binding–like (EBL) domains (carried by MSPDBL-1 and MSPDBL-2; Wickramarachchi *et al.*, 2009; Hodder *et al.*, 2012; Sakamoto *et al.*, 2012) that are specific to *Plasmodium* spp. and are present in many proteins with diverse functions, ranging from erythrocyte invasion (section 1.10.4) to erythrocyte remodelling and cytoadherence (e.g. *Pf*EMP-1; Cowman *et al.*, 2012). Other proteins which carry six-cysteine (6-cys) domains (e.g. Pf12, Pf38, Pf41) are again likely to be involved in protein–protein interactions (Cowman *et al.*, 2012).

Structural studies have demonstrated that the structure of the 6-cys proteins is similar to that of the surface antigen (SAG) related sequence (SRS) superfamily found in *Toxoplasma gondii*, a parasite which, like *Plasmodium,* belongs to the Apicomplexa phylum (Gerloff *et al.*, 2005). The cysteine rich domains in the prototype protein *Tg*SAG1, dimerise to form a receptor binding site at the tip of the molecule (Cowman *et al.*, 2012). Initial experiments suggested that the structural similarity between the *P. falciparum* 6-cys proteins and the *Tg*SAG1 is very unlikely to extend to their molecular functions (Gerloff *et al.*, 2005). More recent studies demonstrated that at least two members of *P. falciparum* 6-cys family of proteins, P12 and P41, are able to form a heterodimer on the infective merozoite surface, but the complex ,however, does not appear to have a major role in erythrocyte invasion (Taechalertpaisarn *et al.*, 2012). Another protein motif that is carried by proteins associated with merozoite cell surface is the EGF-like domain, which has also been implicated in protein-protein binding (Cowman and Crabb, 2006).

## 1.10.3.1 Merozoite Surface Proteins (MSPs) are important components of merozoite cell surface

Proteins belonging to the Merozoite Surface Protein (MSP) family (e.g. MSP-1, MSP-2, MSP-3, MSP-6, MSP-7, MSP-9, MSP-10) have been shown to be components of the protein coat that covers the mature merozoite (Sanders *et al.*, 2005). Among all the merozoite cell surface proteins, MSP-1 is most likely to be the most abundant (Cowman *et al.*, 2012). The *msp-1* gene is refractory to genetic deletion suggesting that it is essential for blood stage growth. Structurally, MSP-1 is a GPI-anchored, 195 kDa protein which translocates to the merozoite cell surface during schizogony (Koussis *et al.*, 2009; Kadekoppala and Holder, 2010). Just prior to erythrocyte egress, a serine protease, *Pf*SUB1, is discharged from the exonemes (Yeoh *et al.*, 2007) (section 1.10.1) into the parasitophorous vacuole (PV) and processes the 195kDa MSP-1 precursor into four fragments: an N-terminus MSP-1$_{83}$, two central fragments MSP-1$_{30}$ and MSP-1$_{38}$, and a C-terminal MSP-1$_{42}$ , all remain associated with each other (Koussis *et al.*, 2009; Kadekoppala and Holder, 2010). Two polypeptides (MSP-6$_{36}$ and MSP-7$_{22}$), derived from proteolytic processing, by *Pf*SUB1, of another two merozoite surface proteins, MSP-6 and MSP-7, are non-covalently associated with the four MSP-1 fragments to form the MSP1/6/7 complex (Koussis *et al.*, 2009). The latter protein complex is attached to the merozoite cell surface via the GPI-anchor of MSP-1$_{42}$, and is likely to be implicated in the primary attachment of the merozoite to the erythrocyte cell surface (Perkins and Rocco, 1988; Nikodem and Davidson, 2000; Kadekoppala *et al.*, 2008; Koussis *et al.*, 2009; Boyle *et al.*, 2010; Kadekoppala and Holder, 2010). Interestingly, Band 3 has been proposed to be the host erythrocyte receptor for MSP-1 (Goel *et al.*, 2003); however, this remains controversial and antibodies against Rhesus Band 3 did not inhibit *P. knowlesi* merozoite initial binding to erythrocytes, but they did abolish erythrocyte invasion (Miller *et al.*, 1983).

During the invasion process, and while the moving junction migrates towards the basal end of the merozoite (section 10.1.5), the proteinaceous coat that covers the merozoite cell surface is shed into the supernatant by the activity of proteases (Harvey *et al.*, 2012). As part of the merozoite protein coat, the MSP1/6/7 complex is also shed by *Pf*SUB2 cleavage (Harris *et al.*, 2005). *Pf*SUB2 cleaves MSP-1$_{42}$ into two fragments: an N-terminal 33kDa (MSP-1$_{33}$) fragment, which is released into the supernatant together with the other components of the MSP1/6/7 complex, and a 19kDa peptide (MSP-1$_{19}$) that remains bound to the merozoite cell surface

(Kadekoppala and Holder, 2010). MSP-1$_{19}$ contains two epidermal growth factor (EGF)-like domains and following invasion is transferred to the developing food vacuole, where it remains until the end of the next intracellular cycle. MSP-1$_{19}$ is the first marker of the biogenesis of the food vacuole and it is likely that the protein has an important role in this location (Blackman *et al.*, 1994; Kadekoppala and Holder, 2010). Antibodies that inhibit the processing of MSP-1$_{42}$ by *Pf*SUB2 have been shown to prevent erythrocyte invasion (Blackman *et al.*, 1994).

### 1.10.3.2 Members of the Serine Rich Antigen (SERA) family of proteins are exposed on the merozoite cell surface

Besides MSPs, members of the SERA family of proteins are also components of merozoite cell surface. SERA is a protein family which consists of nine members (SERA1-9; Blackman, 2008). All SERAs were found to carry a centrally conserved papain-like domain (Miller *et al.*, 2002b). Interestingly, SERA1–5 and 9 have a cysteine to serine substitution within the active site (Miller *et al.*, 2002b). Among SERA family members, SERA5 and SERA6 are the most abundant during parasite blood stages and the genes encoding for both these proteins cannot be disrupted, suggesting that they are essential in this lifecycle stage (Miller *et al.*, 2002b; McCoubrie *et al.*, 2007). SERA5 is translocated in the PV as a 126kDa precursor, and similar to MSP-1, is processed by *Pf*SUB1, into an N-terminal 47kDa fragment (P47), a central 56kDa polypeptide which carries the papain-like domain (P56), and a small 18kDa C-terminal fragment (P18) (Yeoh *et al.*, 2007; Blackman, 2008). P56 is further processed by a C-terminal truncation to result a P50 peptide which eventually accumulates in culture supernatants. On the contrary, the N- and C-terminal fragments, P47 and P18, remain associated in via disulfide bonds and appear to bind to the surface of the released merozoites. Intriguingly, antibodies against P47 but not against P50, block erythrocyte invasion (Blackman, 2008).

SERA6 is also released in PV and is processed by *Pf*SUB1 (Yeoh *et al.*, 2007). Cleavage of SERA6 by *Pf*SUB1 converts it to an active cysteine protease (Ruecker *et al.*, 2012). Intriguingly, pharmacological blockade of *Pf*SUB1, inhibits egress and ablates the invasive capacity of released merozoites (Yeoh *et al.*, 2007). Moreover, mutations that replace the predicted catalytic cysteine of SERA6 could not be stably introduced into the parasite SERA6 encoding gene, indicating that SERA6 is an essential enzyme (Ruecker *et al.*, 2012).

## 1.10.4 EBL and RH are two protein families with major roles in erythrocyte invasion

Erythrocyte Binding Ligands (EBLs) and Reticulocyte binding-protein Homologues (RHs) are two protein families which play a pivotal role in erythrocyte invasion (Iyer *et al.*, 2007) (Fig. 1.6). The *Pf*EBL family is comprised of five proteins, EBA-175, EBA-140 (BAEBL), EBA-181 (JESEBL), EBL1 and EBA-165 (PAEBL) (Iyer *et al.*, 2007). However, only three *Pf*EBL proteins are likely expressed in most *P. falciparum* strains. In the 3D7 reference genome *eba-165* is a pseudogene, containing two frameshift mutations which result in premature termination of protein translation (Triglia *et al.*, 2001; Rayner *et al.*, 2004; Stubbs *et al.*, 2005). Similarly, *ebl-1* is likely to be a pseudogene in a number of *P. falciparum* strains (Drummond and Peterson, 2005; Githui *et al.*, 2010), although an erythrocyte receptor for a truncated form of EBL-1 has been identified (see below; Mayer *et al.*, 2009). EBLs are stored in the micronemes from where they are then released at the apical merozoite cell surface. Structurally, EBLs are type I transmembrane proteins (Fig.1.6), divided into six regions. Region II (RII) carries two tandem cysteine rich DBL domains (F1 and F2; Fig. 1.6), which are responsible for receptor binding. Region III-V links RII to RVI, which also consists of a small cysteine-rich domain (Tham *et al.*, 2012).

The *Pf*RH family consists of six proteins, RH1, RH2a, RH2b, RH3, RH4 and RH5 (Fig 1.6) (Tham *et al.*, 2012). RH2a and RH2b are identical over 80% of the protein sequence, differing only at the C-terminus (Tham *et al.*, 2012). With the exception of RH5 (section 1.10.6.1) which lacks a transmembrane domain, all *Pf*RH members are predicted to be type I transmembrane proteins, localised in the rhoptry neck from where they are secreted at the merozoite apex, during invasion (Tham *et al.*, 2012). Similar to *ebl-1* and *eba-165, rh3* is transcribed but it appears not to be translated, probably due to two reading frameshifts at the 5' end of the gene (Taylor *et al.*, 2001).

As mentioned in section 1.10.1, the exact sequence of the molecular events mediating erythrocyte invasion, is not yet completely clear. The EBLs and RHs are thought to bind to specific erythrocyte receptors at some point between the initial merozoite attachment and the formation of the tight junction (Harvey *et al.*, 2012). A model suggests that upon schizont rupture, merozoites are exposed to the low
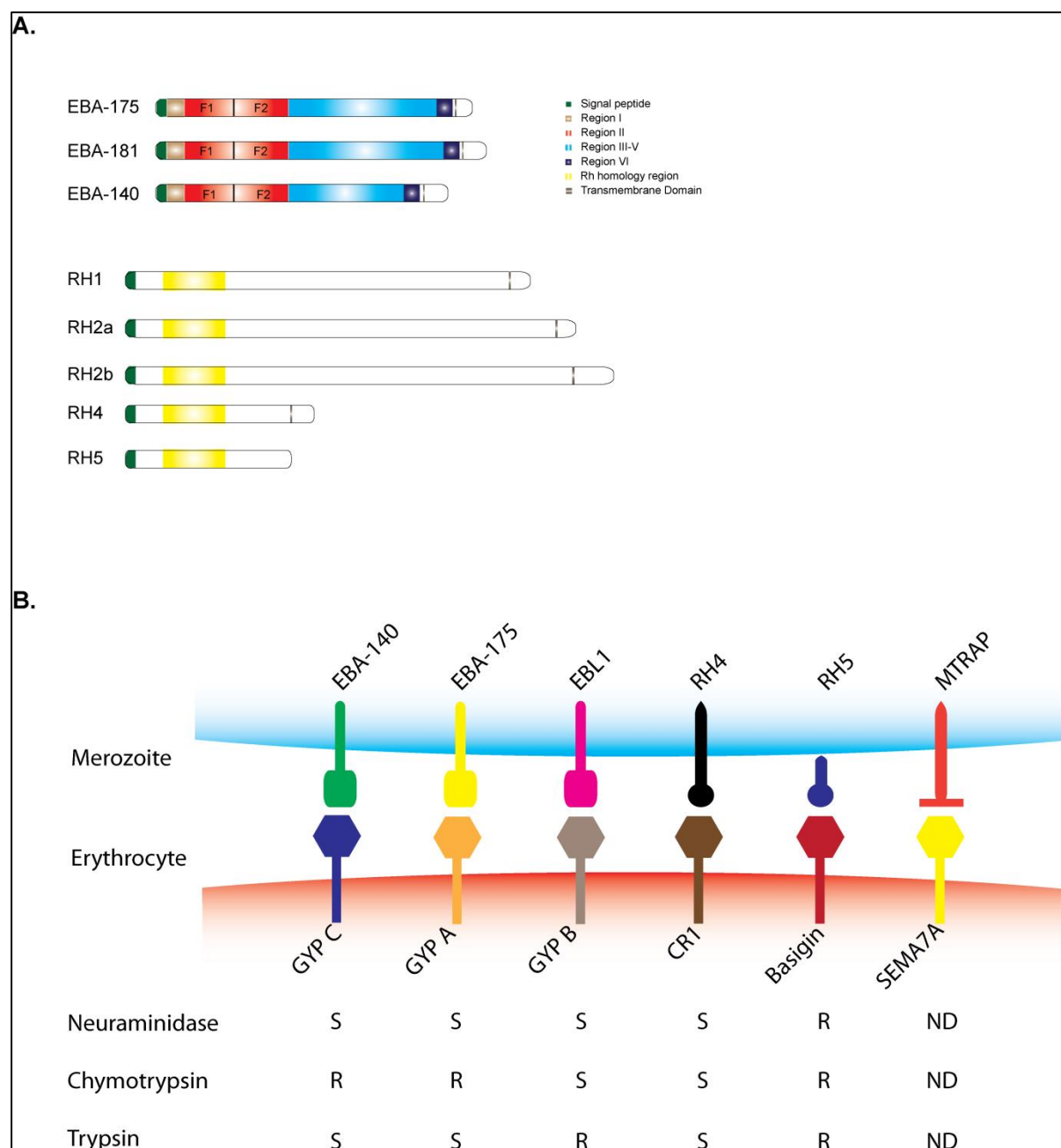
**Figure 1.6 Cell surface Proteins involved in erythrocyte invasion.**

*A.* A schematic representation of the structure of Erythrocyte Binding Ligands (EBLs) (top) and Reticulocyte binding Homologues (RHs) (bottom) families of invasion ligands. Apart from RH5 which is secreted, all the members of both protein families are type I integral membrane proteins. EBL Region II is cysteine rich, and contains 2 Duffy Binding Like domains (F1 and F2) which are known to mediate binding of EBLs to erythrocytes. Region VI is also cysteine rich and it was suggested to control the subcellular localisation of the protein prior to secretion (Culleton and Kaneko, 2010). The region of homology between RHs is indicated in yellow.

**B.** Known receptor-ligand pairs between merozoite and erythrocytes, during erythrocyte invasion. Abbreviations: GYPA, Glycophorin A; GYPB, Glycophorin B; GYPC, Glycophorin C; SEMA7A, Semaphorin7A; CR1, Complement Receptor 1; S, Sensitive; R, Resistant; ND, Not Determined.

potassium levels of the plasma, which triggers calcium release from the endoplasmic reticulum (Singh *et al.*, 2010). The rise in cytosolic calcium induces secretion of microneme contents onto the merozoite cell surface (Singh *et al.*, 2010). Following the primary contact of the merozoite with the erythrocyte, EBLs and RHs are engaged with their receptors, likely committing the merozoite to invasion by activating subsequent events which lead to erythrocyte entry (Cowman *et al.*, 2012; Harvey *et al.*, 2012) .

The erythrocyte receptors for EBA-175, EBL-1, EBA-140, RH4 and RH5 have been identified to be Glycophorin A (GYPA; Sim *et al.*, 1994), GYPB (Mayer *et al.*, 2009), GYPC (Lobo *et al.*, 2003; Maier *et al.*, 2003), Complement Receptor 1 (CR1;Tham *et al.*, 2010) and Basigin respectively (Crosnier *et al.*, 2011) (Fig. 1.6). EBA-181 binds to an unknown sialylated, trypsin-resistant red blood cell receptor which is cleaved after chymotrypsin treatment (Gilberger *et al.*, 2003). RH2a and RH2b appear to bind a yet unidentified trypsin-resistant, chymotrypsin- and neuraminidase-sensitive cell surface receptor (Triglia *et al.*, 2011). On the other hand, RH1 binds to a trypsin resistant receptor, in a sialic acid dependent manner (Rayner *et al.*, 2001).

### 1.10.4.1 EBLs and RHs mediate alternative invasion pathways

Several studies have highlighted that there is a remarkable functional redundancy between EBLs and RHs across different *P. falciparum* strains, but also within the same parasite strain (Tham *et al.*, 2012). EBLs and RHs have been shown to define a series of alternative invasion pathways where distinct ligand-receptor combinations can operate independently to mediate invasion with equal efficiency (Harvey *et al.*, 2012). For example, genetic disruption of *eba-175* in the W2mef strain - which primarily invades erythrocytes in a sialic acid dependent manner - results in up-regulation of the normally silenced *rh4*. As a result, the parasite switches to a sialic acid independent invasion pathway, concomitantly suggesting that the parasite is capable of accessing different invasion pathways by using different invasion ligands (Stubbs *et al.*, 2005).

Moreover, the targeted deletion of *rh2a* and *rh2b* in the 3D7 parasite line resulted in no detectable reduction in erythrocyte invasion efficiency (Duraisingh *et al.*, 2003). Nevertheless, 3D7 parasite lines lacking RH2b expression invaded both

neuraminidase- and trypsin-treated erythrocytes at significantly lower efficiency than the 3D7 parental line, suggesting a switch in invasion pathway. No alternation in the invasion phenotype was observed for 3D7Δ*rh2a* (Duraisingh *et al.*, 2003). Interestingly, the expression pattern of RH2b varies significantly among *P. falciparum* parasite strains with some strains completely lacking expression. The latter suggests that RH2b is of different functional significance among *P. falciparum* strains (Duraisingh *et al.*, 2003).

Similarly, experiments show that RH1 presents a differential expression pattern among different parasite strains (Triglia *et al.*, 2005). Gene deletion of *rh1* in Tak994 *P. falciparum* line, resulted in an unchanged growth rate (Triglia *et al.*, 2005). However, T994Δ*rh1* parasites demonstrated increased ability to invade both trypsin and neuraminidase-treated erythrocytes, reflecting a shift in these parasites towards the utilization of receptors that are more neuraminidase- and trypsin-resistant compared to the Tak994 parent line (Triglia *et al.*, 2005).

Other studies suggested that polymorphisms which result in amino acid changes in the protein sequence may represent another mechanism through which the parasite accesses alternative invasion pathways. Polymorphisms within the receptor-binding regions of EBA-140 and EBA-181 changed the erythrocyte binding profile of these proteins in a way that suggested an alteration in erythrocyte receptor binding specificity (Mayer *et al.*, 2002, 2004). However, later studies argued that these polymorphisms affected the affinity of EBA-140 and EBA-181 binding to receptors, but not the receptor specificities of these proteins (Maier *et al.*, 2009).

Individual EBLs and RHs appear to have overlapping functions which renders them individually dispensible for erythrocyte invasion. Other studies, however, have underscored the collective indispensability of EBLs and RHs, and highlight the requirement for a minimal complement of these proteins, necessary for erythrocyte invasion in each parasite strain (Harvey *et al.*, 2012; Tham *et al.*, 2012). For example, whereas *eba-181* and *rh4* can be deleted in the W2mef strain, genetic disruption of the same genes cannot be achieved in 3D7 suggesting that, at least in the 3D7 strain, these genes are essentially required for erythrocyte invasion (Gilberger *et al.*, 2003; Stubbs *et al.*, 2005). Furthermore, addition of anti-RH2b antibodies into parasite growth assays demonstrated a higher growth inhibitory effect in parasite lines in which different *ebl* genes were disrupted, suggesting that RH2b

complements the function of EBLs (Lopaticki *et al.*, 2011). In support of the notion of synergy between the EBLs and RHs, a combination of anti-EBA-175, RH2a/b, and RH4 antibodies were much more efficient in erythrocyte invasion, than individual antibodies alone (Lopaticki *et al.,* 2011).

Taken together, the functional redundancy between EBLs and RHs is believed to enable the parasite to switch between different invasion pathways, and enables different strains of *P. falciparum* to invade using different host receptors (Cowman and Crabb, 2006; Harvey et al., 2012). This phenotypic variation of invasion pathways has major implications for the parasite survival within the human host. It most likely guarantees that the parasite will gain access to erythrocytes even in the case where the availability of certain erythrocyte receptors is limited (Cowman and Crabb, 2006). For example, the expression of GYPA – the host receptor of EBA-175 - is significantly reduced in aged erythrocytes (Sparrow *et al.*, 2006). Moreover, this phenotypic variation provides the parasite with a mechanism to evade host humoral immune responses targeting a subset of ligands that would block invasion, and with the means to counteract the extremely polymorphic nature of the erythrocyte surface receptors in terms of their primary sequence and levels of expression (Tham *et al.*, 2012).

### 1.10.5 The formation of the tight junction and the role of AMA1, MTRAP and RON proteins in mediating erythrocyte invasion

Once the apex of the merozoite is apposed directly towards the erythrocyte membrane, the discharge of rhoptry neck contents is triggered (Richard *et al.*, 2010; Riglar *et al.*, 2011; Cowman *et al.*, 2012). Among the proteins secreted from the rhoptry are three rhoptry neck proteins (RONs), RON2, RON4 and RON5. These three proteins appear to form a complex that is embedded in the erythrocyte plasma membrane (Fig. 1.5) (Richard *et al.*, 2010; Srinivasan *et al.*, 2011; Harvey *et al.*, 2012). RON4 and RON5 are predicted to be peripheral proteins located entirely within the erythrocyte cytosol, whereas RON2 localises to the erythrocyte membrane such that an exposed C-terminal loop protrudes to the extracellular space (Srinivasan *et al.*, 2011; Harvey *et al.*, 2012). The extracellular part of RON2 directly interacts with the Apical Membrane Antigen 1 (AMA1), a micronemal protein which - together with other microneme proteins - is secreted on merozoite apical cell surface following merozoite egress (Srinivasan *et al.*, 2011). This remarkable process where

the parasite provides both the receptor and ligand leads to the formation of the tight junction (Fig. 1.5), that the nexus bridging both host and parasite cell membranes (Farrow *et al.*, 2011) and appears as an electron dense thickening (by electron microscopy) below the erythrocyte membrane (Aikawa *et al.*, 1978).

AMA1 is a key component of the tight junction and is essential for parasite invasion. It is synthesised during schizogony as an 83kDa precursor and is proteolytically cleaved within the micronemes to yield a 66kDa protein. It is a type I integral membrane protein with a large extracellular domain and a short cytoplasmic tail (Harvey *et al.*, 2012). Similar to MSP-1, AMA-1 is processed by *Pf*SUB2 during the late stages of erythrocyte invasion resulting into two alternative fragments, 44kDa and 48kDa, which are released into the supernatant (Howell *et al.*, 2001; Harris *et al.*, 2005).

The engagement of AMA-1 with RON2 appears to initiate downstream signalling cascades that eventually result in the release of the rhoptry bulb contents (Riglar *et al.*, 2011; Srinivasan *et al.*, 2011; Cowman *et al.*, 2012). The cytoplasmic domain of AMA1 is not required for correct trafficking and surface translocation, but is essential for AMA1 function (Treeck *et al.*, 2009). Indeed, the cytoplasmic tail *of P. falciparum* AMA1 is phosphorylated at serine 610. It was suggested that the enzyme responsible for serine 610 phosphorylation is the cAMP regulated protein kinase A (*Pf*PKA). Importantly, mutation of AMA1 serine 610 to alanine abrogates phosphorylation of AMA1 *in vivo* and impedes erythrocyte invasion (Leykauf *et al.*, 2010).

Following the binding of AMA1 to RON2, the tight junction is transformed into a circumferential ring of contacts between the erythrocyte and merozoite, which migrates towards the basal end of merozoite (Aikawa *et al.*, 1978) (Fig. 1.5). The migrating ring is called moving junction and is thought to be powered by an actin myosin motor. Studies show that the cytoplasmic tail domain (CTD) of AMA-1 binds to the actin binding protein aldolase *in vitro* (Fig. 1.5) and thus, likely links parasite surface ligands with the intracellular actin–myosin motor (Srinivasan *et al.*, 2011). Phosphorylation of serine 610 does not appear to be required for aldolase binding (Srinivasan *et al.*, 2011). Other studies, however, report that the localisation RON4, which is also part of the moving junction, does not overlap with the localisation of actin filaments, suggesting that other proteins – besides the already known

components of the moving junction - are involved in the engagement of the actin-myosin motor with the moving junction (Angrisano *et al.*, 2012).

Merozoite Thrombospondin-Related Anonymous Protein (MTRAP) is another micronemal protein which is thought to be an important constituent of the moving junction (Baum *et al.*, 2006). Similar to AMA-1, MTRAP has been proposed to be involved in bridging the gap between parasite ligands and the actin-myosin motor (Baum *et al.*, 2006; Morahan *et al.*, 2008). Indeed, the MTRAP CTD has been shown to bind to aldolase *in vitro* and this interaction was reduced when a conserved tryptophan residue was mutated to alanine (Baum *et al.*, 2006). A receptor for MTRAP has recently been recently identified to be Semaphorin7A (Bartholdson *et al.*, 2012) (Fig. 1.6). Despite MTRAP being essential for erythrocyte invasion, attempts to block the interaction between MTRAP and Semaphorin7A during *in vitro* invasion assays, using recombinant proteins and antibodies, showed no significant inhibitory effect and thus, the functional relevance of this interaction is still unclear (Bartholdson *et al.*, 2012).

## 1.10.6 The interaction between RH5 and Basigin is essential and universally required for erythrocyte invasion

RH5 is exceptional across EBLs and RHs, since it is indispensable for erythrocyte invasion in all *P. falciparum* strains tested to date (Douglas *et al.*, 2011; Bustamante *et al.*, 2013). Basigin has been identified as the erythrocyte receptor for RH5 (Crosnier *et al.*, 2011) and antibodies against either RH5 or Basigin can potently block erythrocyte invasion in *P. falciparum* parasite culture (Crosnier *et al.*, 2011; Douglas *et al.*, 2011; Bustamante *et al.*, 2013)

### 1.10.6.1 RH5 is a merozoite ligand, required for erythrocyte invasion

RH5 is structurally different from the other RH family members, as it is much smaller and lacks an obvious transmembrane and cytoplasmic domain and is therefore predicted to be secreted (Fig. 1.6). Unlike the redundancy displayed by the EBLs and RHs, *rh5* is broadly refractory to genetic deletion (Hayton *et al.*, 2008; Baum *et al.*, 2009), suggesting that is essential for parasite survival during the blood stages. RH5 is expressed as a 63kDa protein and in mature merozoites it localises to the rhoptry body (Rodriguez *et al.*, 2008; Baum *et al.*, 2009). During erythrocyte invasion, RH5 is located at the tight junction (Baum *et al.*, 2009). Interestingly,

polymorphisms in RH5 have been implicated in the determination of species-specific pathways of *P. falciparum* erythrocyte invasion (Hayton *et al.*, 2008).

A recent study identified a binding partner for RH5, the RH5-interacting protein (RIPR), which is localised in the micronemes of mature merozoites (Chen *et al.*, 2011). RIPR complexes with RH5 on the surface of the free merozoite, and the complex is located at the leading edge of the moving junction during erythrocyte invasion. Similar to *rh5*, *ripr* is refractory to genetic disruption and polyclonal antibodies raised against RIPR inhibit erythrocyte invasion consistent with an essential role in this process (Chen *et al.*, 2011). Nevertheless, no direct binding of RIPR to erythrocytes could be detected and thus, the precise functional role of the RH5/RIPR complex remains elusive (Chen *et al.*, 2011). Interestingly, RIPR also lacks a transmembrane domain (Chen *et al.*, 2011) suggesting that additional proteins are likely to be required if RH5 and RIPR function at the merozoite surface.

### 1.10.6.2 Basigin is a multifunctional transmembrane glycoprotein

Basigin, "*bas*ic *i*mmuno*g*lobul*in* superfamily" (BSG in human; Bsg in mouse), is a widely expressed transmembrane glycoprotein belonging to the immunoglobulin superfamily (Muramatsu and Miyauchi, 2003; Liao *et al.*, 2011a). Studies showed that Basigin is likely to become differentially glycosylated in different tissues (Kanekura *et al.*, 1991; Fadool and Linser, 1993). Four protein isoforms (Basigin-1, -2, -3, -4) derived from alternative splicing and the use of an alternative promoter, have been described (Fig 1.7). Basigin-2, which carries two immunoglobulin-like domains, is thought to be the major isoform expressed on erythrocytes and corresponds to the Ok$^a$ blood group antigen (Crosnier *et al.*, 2011).

### 1.10.6.2.1 Physiological functions of Basigin

Basigin has been assigned with a number of physiological functions. *Bsg* null mouse embryos developed normally during pre-implantation stages but the majority of mutant embryos died around the time of implantation (Igakura *et al.*, 1998). Bsg is strongly expressed in both the embryo trophectoderm and the uterine endometrium, suggesting that Bsg is likely to be involved in intercellular recognition processes required for implantation (Igakura *et al.*, 1998; Muramatsu and Miyauchi, 2003). Male *bsg* deficient mice are sterile due to an arrest of spermatogenesis at the metaphase of the first meiosis. Female mice lacking Bsg expression are also sterile, probably
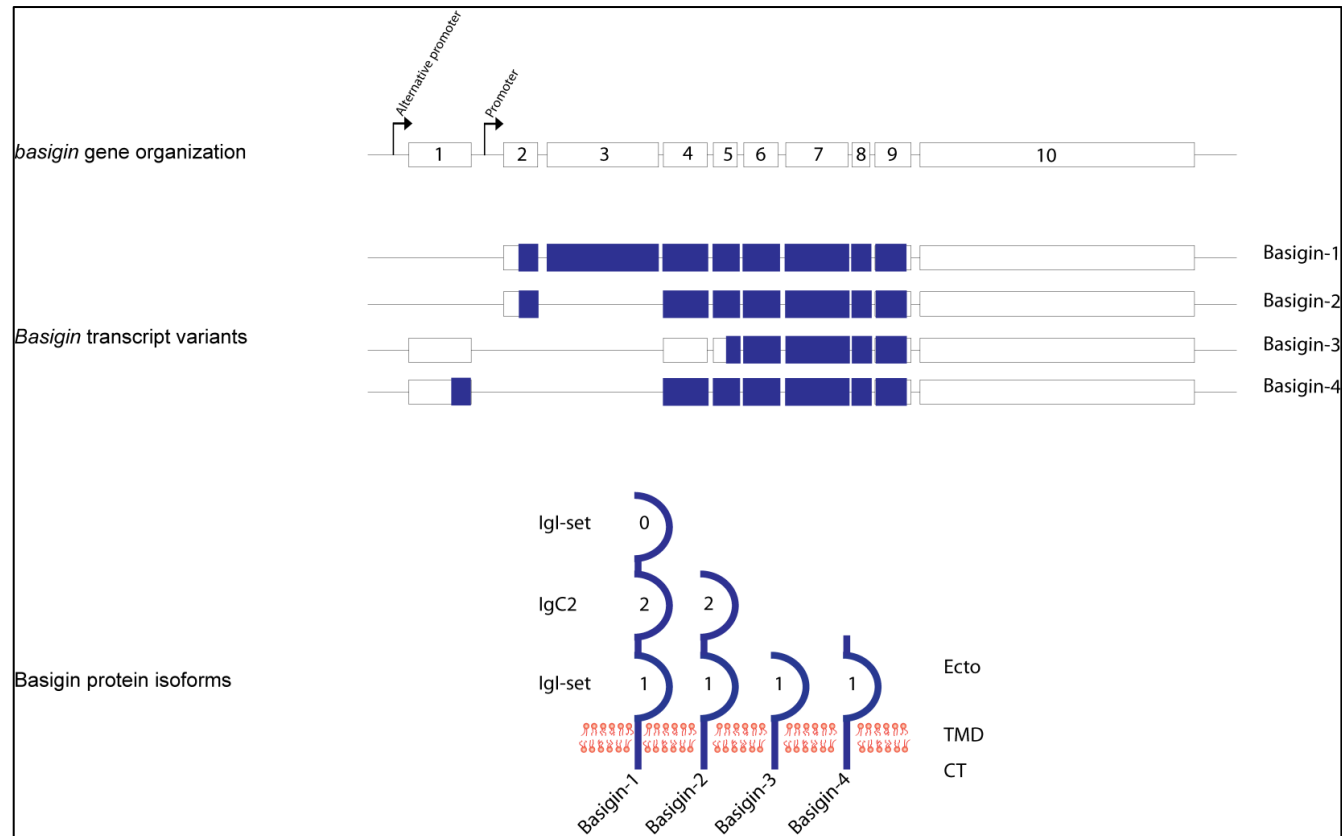
**Figure 1.7 Structure of Basigin gene and protein isoforms.** The top a diagram shows the *basigin* gene organization in human. The gene consists of 10 exons (1-10) and is regulated by 2 promoters. Alternative splicing events and the use of an alternative promoter, result into transcript variants which are translated into the four Basigin isoforms which are shown at the bottom of the figure. Zero and 1 are IgI-set domains whereas domain 2 is an Ig-C2 domain. Blue shaded boxes represent coding sequence. White boxes represent non-coding sequence. Abbreviations: Ecto, Ectodomain; TMD, Transmembrane Domain; CT, Cytoplasmic Tail.

due to defects in embryo implantation (Igakura *et al.*, 1998; Muramatsu and Miyauchi, 2003).

*Bsg* deficient mice also exhibit various disorders related to defects of the neural system. They have defects in learning, and in memory and water finding tasks, and are more sensitive to painful stimuli such as electric shock (Muramatsu and Miyauchi, 2003). *Bsg* null mice are also less sensitive to irritating odors and are virtually blind (Muramatsu and Miyauchi, 2003). The loss of vision has been associated with the function of Basigin as a molecular chaperone for monocarboxylate transporters (MCT) MCT1, MCT3 and MCT4 (Muramatsu and Miyauchi, 2003; Iacono *et al.*, 2007). The association of Basigin with MTCs facilitates the cell surface targeting of the MCTs thereby acting as a chaperone for correct localisation. In mice lacking Basigin expression, the cell surface localisation of MCT1, MCT3 and MCT4 is either lost or greatly reduced in both the retinal pigment epithelium and the retina (Muramatsu and Miyauchi, 2003). Of great importance is the loss of MCT1 and MCT4 at the surface of the Müller glial cells and the photoreceptor cells themselves. The loss of MCT activity blocks the transport of lactate from Müller glia to the photoreceptor cells, depriving them of a crucial energy source (Muramatsu and Miyauchi, 2003). Interactions of Basigin with Cyclophilin A, integrins and caveolin-1 have also been described (Muramatsu and Miyauchi, 2003; Iacono *et al.*, 2007).

The role of Basigin in human erythrocytes is not fully understood. MCT1 is also expressed in human erythrocytes where it functions as an L-lactate-protein transporter (Bartholdson *et al.*, 2013). Therefore, Basigin it is likely to act as chaperone, escorting MCT1 to erythrocyte plasma membrane. Moreover, studies demonstrated that blockade of Basigin by using an anti-Basigin F(ab)$_2$ fragment, interferes with the migration of erythrocytes out of the spleen (Coste, 2001). Thus, erythrocyte Basigin is likely act as an adhesion molecule, which plays a critical role in the recirculation of mature erythrocytes from the spleen into the blood stream (Coste, 2001).

## 1.10.6.2.2 Basigin based anti-cancer therapies

Basigin has attracted a great deal of interest as a cancer biomarker (Weidle *et al.*, 2010). It has been shown that Basigin is shed from tumor cells and stimulates

matrix metalloprotease (MMPs) synthesis and release in peritumorial cells, and the tumor cells themselves (Gabison *et al.*, 2005; Iacono *et al.*, 2007). Homophilic interactions between secreted and membrane tethered Basigin have been proposed to be important for the induction of MMP expression and secretion (Belton *et al.*, 2008). Various studies showed that Basigin is capable of inducing expression of MMP1-3, MMP9 and MMP11 (Muramatsu and Miyauchi, 2003; Iacono *et al.*, 2007), and thereby facilitates tumor invasion during metastasis. Apart from stimulating MMP expression in neighbouring cells, evidence suggests that Basigin induces its own expression through a positive feedback mechanism and also induces the production of vascular endothelial growth factor (VEGF) though which tumor metastasis is promoted (Iacono *et al.*, 2007).

The critical role of Basigin in tumor progression has led to the evaluation of anti-Basigin monoclonal antibodies as anti-cancer agents. In 2005, the Chinese Food and Drug Administration licenced the use of an anti-BSG iodine-131-labeled F(ab)$_2$ fragment under the brand name Licartin (also known as metuximab), for the treatment of patients suffering from hepatocellular carcinoma (HCC) (Yu *et al.*, 2008; He *et al.*, 2013). Licartin has been proved to be safe and effective for targeted treatment in clinical trials, and has been approved as a new radioimmunotherapeutical drug for clinical therapy of primary HCC (Yu *et al.*, 2008). This suggests that despite the fact that Basigin is broadly expressed on a number of cell types, anti-Basigin monoclonal antibodies do not have intrinsic safety issues when used as therapeutics.

### 1.10.6.2.3 The value of Basigin as a target for the treatment of Graft versus host disease

Besides erythrocytes, other circulating blood cells, like activated T and B lymphocytes, dendritic cells, monocytes and macrophage also express Basigin (Iacono *et al.*, 2007). Basigin was identified as an activation associated antigen on phytohemaglutinin (PHA) activated T cells (Koch *et al.*, 1999) and has been implicated in T cell chemotaxis at areas of inflammation (Iacono *et al.*, 2007). The important role of Basigin on activated T cells has been exploited for the development of therapeutics in the treatment of steroid-refractory acute graft-versus-host disease (GVHD).

GVHD is a T cell driven disease where donor lymphocytes recognise host tissues as foreign and initiate immune responses against them. As a result, acute GVHD is an important complication following hematopoietic stem cell transplantation. (Iacono *et al.*, 2007). Because Basigin is highly expressed on activated T cell populations, those cells that would mediate GVHD can be selectively depleted without affecting the entire T cell repertoire (Iacono *et al.*, 2007). Indeed, treatment of patients with steroid refractory, acute GVHD with an anti-Basigin antibody (a mouse IgM; known as CBL-1 or ABX-CBL) was shown to be very effective, in part due to decreased leukocyte activation (Heslop *et al.*, 1995; Deeg *et al.*, 2001; Macmillan *et al.*, 2007).

## 1.11 The importance of antibodies in malaria immunity

The role of antibodies in immunity against malaria became clear from the very early days. Initial studies which involved passive transfer of malaria immunity to animals and human provided solid evidence for the critical role of naturally occurring antibodies in protection against the blood stages of the disease. In 1937, Coggeshall and colleagues demonstrated that the transfer of serum from *Macacus rhesus* monkeys with chronic *P. knowlesi* infection to non-infected monkeys, confer partial or full protection against a subsequent parasite challenge, even after inoculation with large numbers of parasites (500 millions; Coggeshall & Kumm, 1937).

Later, in 1961, Cohen and colleagues were the first to recapitulate these experiments in man (Cohen *et al.*, 1961). Twelve Gambian children aged four months to 2.5 years old (weight 5.4-12.6 Kg) who had been diagnosed with clinical malaria were injected with gamma-globulin prepared from pooled serum obtained from apparently malaria immune adults living in Gambia, a malaria hyperendemic area. The total dose of immunoglobulin was 1.2-2.5 grams per child and it was administered over three days. After the initiation of gamma-globulin therapy, parasitemia levels dramatically decreased with concomitant disappearance of clinical symptoms. By the fourth day after inception of treatment, parasite levels dropped to less than 1% of the initial value and by day nine there was no detectable parasitemia in eight out of 12 cases. The gamma-globulin treatment appeared to be effective both against *P. falciparum* and *P. malariae* blood stage parasites but with no obvious action against gametocytes. Due to the absence of morphological abnormalities in the intra-erythrocytic forms of the parasite in peripheral blood, it was suggested that

the protective antibodies acted either on mature intracellular forms of the parasite or on merozoites liberated from infected erythrocytes (Cohen *et al.*, 1961).

Around the same time, Edozien and colleagues performed a similar study which involved the injection of gamma-globulin purified from peripheral or cord blood of malaria immune adult Nigerians, to six Nigerian children who suffered from *P. falciparum* or *P. malariae* malaria (Edozien *et al.*, 1962). The gamma-globulin was administered by intramuscular route at intervals of 8-24h for three days with a total dose of 1.2-2.8 grams per child. The group of children treated with adult gamma-globulin there was displayed a constant decrease in parasite-counts by the fourth day, and by day eight there was no detectable parasitemia in four out of five children. Concurrently, clinical symptoms were eliminated. Similar results were obtained in another case where a 12 months old child was treated with cord blood gamma-globulin. It was not however clear whether immune gamma-globulin is equally effective when administered to patients living in a different hyperedemic area, where possibly different *P. falciparum* strains are transmitted.

To address this question, McGregor and colleagues tested the therapeutic effect of West African immune gamma-globulin in malaria *P. falciparum* infected East African children (McGregor *et al.*, 1963). For this purpose gamma-globulin purified from pooled immune adult serum of healthy Gambia residents was administered via intramuscular route to nine children aged 6-20 months old who belonged to the M'bondei or M'samba tribes living in the area around Magila, Tanzania, and all showed clinical signs of malaria infection. Gamma-globulin therapy was associated with alleviation of pyrexia and clinical illness and by day four, the average parasite count was less than 1% of the mean initial count. However, in four cases parasite density relapsed on day seven to nine, probably representing rapid multiplication of a serologically distinct strain of *P. falciparum* which was resistant to antibody present in West African gamma-globulin. Collectively, these results suggested that gamma globulin from West African immune adults contained antibodies which, at least in part, are effective against *P. falciparum* malaria in people living in East Africa.

More recently, Sabchareon and colleagues used IgGs purified from immune serum obtained from 178 young African adults (age range 19-23) living in Cote d'Ivoire, which were then administered intravenously to eight *P. falciparum* infected Thai children, aged 5-12 years old, originated from Prachiburi province, and who

previously failed to be treated with quinine (Sabchareon *et al.*, 1991). While gametocyte counts fluctuated during the study, the asexual parasitemia fall significantly. In certain cases, parasitemia remitted by day nine to 12, but following a second round of gamma-globulin injection it decreased again, without however achieving a sterilizing effect. Nevertheless, these data established the critical role of antibodies in immunity against *P. falciparum* malaria, and simultaneously confirmed McGregor and colleagues' observations that the transferred antibodies conferred, at least in part, immunity against *P.falciparum* malaria to people living in different geographical region that the antibody donors.

## 1.11.1 Merozoite cell surface proteins are targets of protective antibodies of the naturally acquired malaria immunity.

The studies involving passive transfer of immunity clearly demonstrated that serum contained antibodies significantly contribute to protective immunity against malaria. However, the targets of protective antibodies had been unclear until Cohen and colleagues provided evidence that at least a fraction of antibodies is directed against erythrocyte invasion ligands (Cohen *et al.*, 1969). Cohen's group demonstrated that while immune serum antibodies had little effect on the *in vitro* intra-erythrocytic growth of *P. knowlesi* they severely affected re-invasion of red blood cells (Cohen *et al.*, 1969), suggesting that merozoite cell surface proteins are targets of protective antibodies.

Subsequent studies demonstrated that the presence of antibodies in serum directed against specific merozoite cell surface proteins is correlated with protection against severe disease. In 1993 Dziegiel and colleagues showed that asymptomatically infected Gambian children, aged five to eight years old, had significantly higher levels of IgG antibodies against the carboxy terminal domain of GLURP than clinically ill children of the same age, suggesting that antibodies targeting GLURP c-terminal domain may contribute to immunity against *P. falciparum* malaria (Dziegiel *et al.*, 1993). The role of GLURP as a target of protective immunity was also investigated by Dodoo and colleagues in two subsequent studies where they showed that the presence of IgGs targeting the non-repeat region of GLURP were significantly correlated with clinical protection from *P. falciparum* malaria in Ghanian children (Dodoo *et al.*, 2000, 2008). In the latest of Dodoo's studies, it was also reported that higher levels of IgG targeting $MSP1_{19}$,

MSP3 and IgM against $MSP1_{19}$, MSP3 and AMA1 were associated with decreased malaria incidence (Dodoo *et al.*, 2008).

In another report Conway and colleagues showed that serum IgG antibodies against MSP1 block 2 were strongly associated with protection from *P. falciparum* malaria in Gambian children (Conway *et al.*, 2000). Similarly, the presence of serum anti-RH5 antibodies has been shown to predict protection to malaria in Malian children (Tran *et al.*, 2013). Finally, a number of other studies have reported that the presence of circulating antibodies against the erythrocyte invasion ligands AMA1, MSP2, MSP3, EBA-175 and SERA5 is correlated with reduced malaria risk (Okech *et al.*, 2006; Fowkes *et al.*, 2010). Together, all the aforementioned publications clearly demonstrated that at least a fraction of malaria protective antibodies is directed against merozoite adhesins and invasins

## 1.12 Malaria prevention and control

Several intervention measures have been applied to control malaria. Tactics used to prevent the spread of disease, or to protect individuals from getting infected, include prophylactic drugs (e.g. quinacrine, chloroquine, primaquine), mosquito eradication by using insecticides, and prevention of mosquito bites by using insecticide-treated bed nets (ITNs) (Crompton *et al.*, 2010; Geels *et al.*, 2011; Greenwood and Targett, 2011; World Health Organization, 2012). Moreover, artemisinin-based combination therapy (ACT) is currently being used for malaria treatment (Miller *et al.*, 2013).

The general increases in funding during the last decade, enabled a wider application of anti-malarial intervention measures, which in turn resulted in a decrease in malaria deaths by 32%, between the years 2004-2010 (Murray *et al.*, 2012). However, there are still serious problems towards the goal of efficient malaria control worldwide. The emergence of parasite drug resistance is a major impediment for malaria control (Verdrager, 1986; Phyo *et al.*, 2012). Mosquito insecticide resistance is another important problem that is emerging (Riley and Stewart, 2013). From a financial point of view, the global funding requirement for malaria control was estimated by the Global Malaria Action Plan (GMAP) in 2008, to exceed US$ 5.1 billion annually between the years 2011 and 2020, with Africa alone needing US$ 2.3 billion each year. However, the total international and domestic resources directed

towards malaria control was estimated to be US$ 2.3 billion in 2011, less than half the total amount needed to reach the global goals (World Health Organization, 2012).

Taken all together, the development of a cost effective (US$ 1-2 per dose) (Moorthy *et al.*, 2012) and highly efficacious malaria vaccine is clearly imperative for the control, elimination, or even possible eradication of malaria (Crompton *et al.*, 2010).

## 1.13 The development of an effective malaria vaccine is a challenging problem

The development of a highly efficient malaria vaccine has been a long standing goal for the global control of malaria. The key fact underpinning the efforts for the development of a malaria vaccine is that adults in malaria endemic areas can naturally become immune to malaria after repeated exposure to the parasite (Marsh and Kinyanjui, 2006). This immunity affords protection against symptomatic disease, high-density parasitemia and death (Richards and Beeson, 2009). Nevertheless, even in adults who have had decades of exposure to *P. falciparum*, sterile immunity to blood-stage infection is infrequently observed, and an occasional episode of fever can occur (Crompton *et al.*, 2010). Infants and young children who have never been exposed to *P. falciparum* are more vulnerable in developing severe malaria and therefore, it is these age groups that particularly require the development of a vaccine that protects against malaria (Crompton *et al.*, 2010; Greenwood and Targett, 2011).

The completion of the *P. falciparum* genome project in 2002 (Gardner *et al.*, 2002) identified thousands of novel proteins, providing new opportunities for vaccine development. However, the function of the vast majority of these proteins is still unclear and therefore, targeting proteins essential for parasite survival becomes a challenging task (Richards and Beeson, 2009). Vaccine development is further complicated by the functional redundancy of several *P. falciparum* proteins, especially the proteins involved in erythrocyte invasion (Drew *et al.*, 2008; Bannister and Mitchell, 2009) (section 1.10.4.1). The latter suggests that multiple antigens should be targeted at the same time to induce an effective response. Additionally, the extensive naturally occurring antigenic polymorphisms between different parasite

strains is a major obstacle for the formulation of a cross-protective vaccine (Richards and Beeson, 2009).

The problems faced with recombinant expression of *P. falciparum* proteins is another important impediment (Richards and Beeson, 2009). Such recombinant protein expression is invaluable for the construction of a protein based, subunit malaria vaccine but also as tools to address fundamental biological questions. The technical challenges that prevent the high level expression of *P. falciparum* proteins in a recombinant form and in their native conformation have been attributed to the unusually high (~80%) A+T content of the parasite genome with the consequent non-optimal codon bias in heterologous expression systems. Also, *Plasmodium* proteins are typified by the prevalence of repetitive amino acid stretches (Tsuboi *et al.*, 2008). Moreover, the high molecular weight (> 56 kDa) and presence of export motifs and atypical signal peptides are all protein characteristics that were associated with the problematic recombinant expression of *P. flaciparum* proteins (Birkholtz *et al.*, 2008).

Malaria vaccine approaches can be grouped as pre-erythrocytic, transmission blocking and blood stage (Richards and Beeson, 2009). All three approaches are analysed below.

### 1.13.1 Transmission blocking vaccines

The principle of transmission blocking vaccines is to immunise people with *P. falciparum* antigens that are expressed while the parasite is in mosquito, before the formation of oocyst. Antibodies against such antigens would be taken up by the mosquito during a blood meal and would prevent parasite development in the mosquito midgut thereby preventing malaria transmission (Crompton *et al.*, 2010).

Vaccines based on the gamete surface antigens, P230, P48/45 and HAP2, abolish fertilization in the mosquito midgut, whereas those based on the ookinete antigens, P25 and P28, elicit antibodies that prevent ookinetes from traversing the wall of the mosquito midgut (Greenwood and Targett, 2011). To the best of my knowledge, there is only one reported clinical trial of a transmission blocking vaccine: vaccination with Pfs25 generated significant transmission-blocking activity in vaccinated individuals, even though the trial was not completed because of the high reactogenicity of the adjuvant that was used (Wu *et al.*, 2008).

The idea of developing a transmission blocking vaccine has been questioned. It has been characterised as an altruistic vaccination strategy because there is no direct benefit for the immunised individuals (no protection against disease) but there is benefit for the whole community instead (Hill, 2011; Vaughan and Kappe, 2012). Hence, it might be difficult to convince governments, health care workers or communities to implement such vaccination programmes. Moreover, because all age groups of a population can potentially transmit malaria, this strategy would require mass vaccinations and this could be logistically challenging (Hill, 2011; Vaughan and Kappe, 2012).

Another problem associated the development of vaccines against parasite antigens which are exclusively expressed during mosquito stages, is that there will be no natural boosting by malaria infection and thus, unless boosting injections are provided, the antibody responses in immunised individuals might be short lived (Carter *et al.*, 2000; Vaughan and Kappe, 2012). Others argue that if the complete blockade of parasite development in the mosquito is not achieved, transmission blocking vaccines are likely to paradoxically increase transmission because of the decrease in parasite load within the mosquito, which will reduce the impact of the parasite on mosquito mortality. Therefore, the competence of the mosquito as a vector will be enhanced (Sinden, 2010).

During the last few years the concept of developing a transmission blocking vaccine has regained ground. Recently, there has been a renewed call for global malaria eradication (World Health Organization, 2008). An effective transmission blocking vaccine will probably be needed to achieve eradication, in addition to other existing measures (Richards and Beeson, 2009). The combination of a pre-erythrocytic or blood stage vaccine, to prevent infection (see below), and a transmission blocking vaccine, may be an ideal vaccine strategy because, if effective, it would reduce transmission and provide some protection to vaccinated individuals (Crompton *et al.*, 2010).

## 1.13.2 Pre-erythrocytic vaccines

It is currently unclear whether protective immunity to the pre-erythrocytic stages of the parasite can be naturally acquired (Marsh and Kinyanjui, 2006). However, it is possible to evoke, by vaccination, pre-erythrocytic immune responses which might

be in place to prevent the blood-stage infection from occurring (Crompton *et al.*, 2010). The idea of a pre-erythrocytic vaccine took shape with the work of Nussenzweig and colleagues, who demonstrated that vaccination of mice with irradiated sporozoites resulted in protection against *P. berghei* malaria (Nussenzweig *et al.*, 1967; Crompton *et al.*, 2010).

Early trials in humans confirmed the initial observations of Nussenzweig. In 1973 Clyde and colleagues showed that immunisation of human volunteers with the bites of *P. falciparum* infected, irradiated mosquitoes could protect humans against later challenge with fully infectious *P. falciparum* sporozoites (Clyde *et al.*, 1973). Later studies demonstrated that ~92% protective efficacy, in the form of sterilizing immunity, can be achieved in humans, after immunisation with >1000 bites of mosquitoes carrying live, radiation attenuated *P. falciparum* sporozoites (Hoffman *et al.*, 2002). A more recent study reported that 100% of subjects exposed on three occasions to bites of 12 to 15 *P. falciparum* infected mosquitoes and concomitantly treated with a chloroquine prophylactic regiment, were protected from later challenge (Roestenberg *et al.*, 2009).

Despite the previously reported high efficacies of immunisation regimes which utilize whole live sporozoites, this approach has raised several concerns regarding the practicalities of its implementation. The requirement of manufacturing and scaling up the product, as well as the cost and feasibility of delivering a vaccine that is cryopreserved, are major logistic challenges (Schwartz *et al.*, 2012). On the other hand, such a vaccination approach is likely to require intravenous administration which could prove clinically impractical on a large scale (Hoffman *et al.*, 2002). Indeed, vaccination with cryopreserved, live attenuated sporozoites, using the intradermal route, conferred protection to only the 5% of vaccinees (Epstein *et al.*, 2011). In contrast, in a similar study where sporozoites were administered intravenously, all subjects (100%) who received five doses of the vaccine were protected against later challenge (Seder *et al.*, 2013).

Besides immunising with sporozoites, other vaccination strategies have been examined for their ability to elicit immune responses to pre-erythrocytic *P.falciparum* stages. One such strategy utilizes vectored vaccines, aiming mainly to induce cellular immunity against the parasite liver-stage (Hill, 2011). The ME (multiepitope) – TRAP (thrombospondin – related protein) vaccine is an example of a

multicomponent viral vectored vaccine (Hill, 2011). The ME-TRAP construct, encodes for a fusion antigen consisting of 17 B-cell, CD4 and CD8 T cell epitopes from six *P. falciparum* antigens (LSA1, CSP, STARP, LSA3, Exp1, TRAP) fused to the T9/96 allele of TRAP. It also includes a single *Plasmodium berghei* CD8+ T cell epitope (Pb9) for potency studies in mice, and a T-helper epitope (FTTp) from tetanus toxoid protein (McConkey *et al.*, 2003; Graves and Gelband, 2006; Draper and Heeney, 2010; Schwartz *et al.*, 2012). In a Phase Ib clinical trial, priming humans with a construct of chimpanzee (Ch) adenovirus 63 encoding ME-TRAP (AdCh63- ME-TRAP), followed by a boost with a modified vaccinia Ankara (MVA) construct, MVA–ME-TRAP, induced strong CD8 T cell responses (Ogwang *et al.*, 2013).

Proteins in adjuvant, is another vaccine platform that has been investigated for immunisation against pre-erythrocytic *P. falciparum* stages (Duffy *et al.*, 2012). In general, this approach involves the administration of recombinantly expressed pre-erythrocytic antigens as a mixture with adjuvants which can robustly activate the immune responses (Duffy *et al.*, 2012). RTS,S is a recombinant protein based vaccine against parasite pre-erythrocytic stages and is currently in a multicenter Phase III clinical trial in sub- Saharan Africa.

## 1.13.2.1 The RTS,S vaccine

The initial observation of Nussenzweig that immunisation of mice with the bites of radiation-attenuated, parasite infected mosquitoes, conferred protection against challenge with infectious sporozoites (Nussenzweig *et al.*, 1967), led to the identification of the immunodominant cell surface antigen, the circumsporozoite protein (CSP), which is expressed on sporozoites and liver stage schizonts (Enea *et al.*, 1984; Casares *et al.*, 2010). *Pf*CSP is a 58kDa, GPI-anchored cell surface protein, composed of an N-terminal region (RI) that binds heparin sulfate proteoglycans, a central region containing approximately 41 repeats (range 37–49) of NANP (N, asparagine; A, alanine; P, proline) amino acid sequences and a smaller number of NVDP (V, valine; D, aspartic acid) sequences, and a C-terminal thrombospondin-like domain (RII) (Casares *et al.*, 2010; Crompton *et al.*, 2010). The central repeat region contains immunodominant B cell epitopes whereas the C-terminal region contains both B and T cell epitopes (Plassmeyer *et al.*, 2009).

Initial studies demonstrated that the recombinantly expressed central region of *Pf*CSP was immunogenic to humans (Regules *et al.*, 2011). However, there was little or no protection against sporozoite challenge (Regules *et al.*, 2011). To boost antibody responses, a construct was designed that encodes for a fusion protein consisting of 16 *Pf*CSP NANP repeats fused at the N-terminus with the S antigen from hepatitis B virus (HBsAg) (Casares *et al.*, 2010). The fusion protein, designated R16HBsAg, was expressed in yeast cells and it was capable of self-assembling into virus-like particles similar to native HBsAg (Regules *et al.*, 2011). R16HBsAg elicited high antibody titers in experiments involving immunisation of both animals and humans (Regules *et al.*, 2011).

There was, however, the concern that R16HBsAg was still lacking the T cell epitopes located at the C-terminal region of CSP, which would be required for the induction of T cell responses (Casares *et al.*, 2010). Therefore, the construct encoding for R16HBsAg was redesigned to include 19 NANP repeats from the central region (R), the entire C-terminal region of *Pf*CSP which contains the T cell epitopes (T), and the HBsAg (S). To stabililize the recombinant viral particles, the fusion protein was co-expressed in yeast together with free HBsAg (S). The result is a viral particle, RTS,S, containing RTS and HBsAg in 1:4 ratio (Gordon *et al.*, 1995).

Currently, RTS,S (formulated with AS01 adjuvant) is under a Phase III randomized clinical trial which takes place in 11 centres, in seven African countries (Agnandji *et al.*, 2012). In 2011, it was reported that RTS,S/AS01 had an efficacy of 55.8% and 47.3% against clinical and severe malaria respectively, among children 5 to 17 months of age (Agnandji *et al.*, 2011). The latest data from the currently on-going clinical trial demonstrate that the efficacy of RTS,S in infants 6-12 weeks old, during one year of follow-up, is ~31% against clinical malaria and ~26% against severe malaria (Agnandji *et al.*, 2012). The mechanism, by which a vaccine that targets the liver stages protects against severe malaria, which is caused by blood-stage infection, is still elusive. It is possible that RTS,S induces protection against clinical malaria by reducing the number of merozoites released from the liver. This may lead to prolonged exposure to subclinical levels of asexual blood-stage parasites, which in turn enables the acquisition of blood-stage immunity (Crompton *et al.*, 2010) .

**1.13.3 Blood stage vaccines**

There is strong rationale for the development of a vaccine targeting the asexual blood stages of the parasite. Parasite blood stages have a central role in disease pathology (Cowman *et al.*, 2012) and naturally acquired immunity is principally directed against asexual blood stage antigens (Richards and Beeson, 2009). Early studies demonstrated that transfer of IgGs from malaria-immune adults to malaria infected children, rapidly reduced parasitemia and fever (section 1.11), suggesting that antibodies directed against blood stage antigens is a key component of the naturally acquired immunity (Richards and Beeson, 2009). Hence, the development of a vaccine, able to elicit in children the antibodies that protect against disease in adults, is likely to have a major impact on malaria morbidity and mortality world-wide. The latter is also supported by the belief that one of the mechanisms by which RTS,S (section 1.13.2.1) confers protection to severe malaria, may be the leaky pre-erythrocytic protection, which results in the continued exposure of the organism to blood stage parasites which in turn induces blood stage immunity (Crompton *et al.*, 2010; Ellis *et al.*, 2010).

The efforts for the development of an asexual blood stage vaccine have been primarily focused on erythrocyte invasion (section 1.10). It is an obligatory step in the *Plasmodium* lifecycle and is essential for survival of the parasite within the human host (Cowman and Crabb, 2006). During invasion, the merozoite is – albeit briefly – directly exposed to the host humoral immune system immune system, and therefore, its cell surface proteins are tractable vaccine candidates (Bartholdson *et al.*, 2013). Indeed, out of the eight blood stage antigens that are under clinical development, seven (all but RESA) are merozoite cell surface exposed: apical membrane antigen 1 (AMA1), merozoite surface protein (MSP) -1, MSP-2, MSP-3, glutamate rich protein (GLURP), ring-infected erythrocyte surface antigen (RESA), serine repeat antigen 5 (SERA5), and erythrocyte-binding antigen 175 (EBA-175) (Ellis *et al.*, 2010).

The immunity against the blood stages of the parasite is thought to primarily be mediated by protective antibodies (section 1.11). Therefore, most candidate vaccines against *P. falciparum* blood stages, are recombinant proteins, but peptides, DNA and viral vectored approaches have also been used (Ellis *et al.*, 2010). As mentioned in section 1.13, one major problem that arises from the use of

recombinant proteins for the formulation of blood stage vaccines, is the technical difficulties in expressing *Plasmodium* proteins in a biochemically active recombinant form that are capable of eliciting high antibody titers, and at levels adequate to allow large-scale manufacturing (Hill, 2011; Bartholdson *et al.*, 2013).

Another important challenge towards the development of highly efficient blood stage malaria vaccine, is the functional redundancy observed between the merozoite ligands, which are involved in erythrocyte invasion (section 1.10.4.1; Cowman *et al.*, 2012). Merozoites are believed to express on their surface a set of ligands with overlapping roles, that enables the parasite to access alternative invasion pathways (Duraisingh *et al.*, 2003; Baum *et al.*, 2005; Stubbs *et al.*, 2005). Therefore, it is thought that an efficient blood stage vaccine should simultaneously target multiple merozoite antigens to block a broad array of invasion pathways (Lopaticki *et al.*, 2011).

Besides the ability of the parasite to access alternative invasion pathways, another important obstacle for the development of an effective blood stage malaria vaccine, is the vast allelic polymorphism found across different *Plasmodium* strains (Manske *et al.*, 2012). Vaccine approaches need to account for this, such that they cover the majority of *P. falciparum* antigenic polymorphisms (Richards and Beeson, 2009). The antigenic variation, was the main reason why the two leading blood stage vaccine candidates AMA1 and MSP1$_{42}$ did not demonstrate protective efficacy in African children (Ogutu *et al.*, 2009; Thera *et al.*, 2011). Despite eliciting good antibody titers, there was insufficient cross-protection against diverse malaria strains (Ogutu *et al.*, 2009; Thera *et al.*, 2011).

Recently, however, the identification of the interaction between RH5 and Basigin (section 1.10.6) which has been shown to be essential and universally required for erythrocyte invasion, allowed new hopes for the formulation of a highly efficacious blood stage vaccine (Crosnier *et al.*, 2011). Erythrocyte invasion can be completely blocked using low concentrations of anti-Basigin monoclonal antibodies and this effect was observed in multiple *P. falciparum* laboratory-adapted lines and field isolates (Crosnier *et al.*, 2011). Conversely, polyclonal antibodies raised against the 3D7 variant of RH5 were able to block erythrocyte invasion in nine different *P. falciparum* strains, which, between them, included all of the five most common RH5 polymorphisms (Bustamante *et al.*, 2013). Moreover, virally delivered RH5 can

induce antibodies that inhibit erythrocyte invasion of a wide range of parasite genetic variants (Douglas *et al.*, 2011). Thus, it is likely that the identification of the interaction between RH5 and Basigin will lead to the development of efficient therapeutic interventions targeting the blood stages of the parasite.

## 1.14 Host oriented approaches for treatment of various infectious diseases

As mentioned in section 1.13.3 the development of highly efficacious interventions targeting merozoite-erythrocyte interactions, has been hampered by the highly polymorphic nature of merozoite ligands, as well as by functional redundancy of the receptor-ligand pairs involved in the invasion process (Cowman and Crabb, 2006). Another fundamental problem towards the development of effective anti-malarial therapeutics targeting merozoite cell surface proteins, is the short timing window during which merozoite antigens are available for binding to a therapeutic agent (e.g an antibody), as merozoites are only extracellular for 1-2 minutes following schizont rupture (Dvorak *et al.*, 1975; Mason and Williams, 1980; Saul, 1987).

One possible strategy to overcome the obstacles is the development of approaches directed against the human host, instead of the parasite. In contrast to *Plasmodium* spp. and pathogens in general, humans have a much longer generation time and therefore, they are not evolving as rapidly as the parasite, minimizing the problems arising from sequence variability (Baillie and Digard, 2013). Furthermore, the development of a therapeutic agent targeting host cell surface molecules overcomes the problem of a restrictive time-window, as unlike merozoite ligands, erythrocyte receptors are constantly exposed on the cell surface and hence, are continuously available for binding. Moreover, the targeting of host factors that are essential for the survival of different *Plasmodium* species and strains, may allow the development of more broad spectrum interventions (Prussia *et al.*, 2011). In addition, it is unlikely that individual point mutations in parasite components could compensate for the loss of essential host factors and thus, the potential for the development of resistance or escape mutants is diminished (Prussia *et al.*, 2011).

While perhaps at fist counter-intuitive, host-oriented intervention strategies have been successfully applied for the treatment of a number of viral infections, and particularly HIV. For example, ibalizumab, a humanised monoclonal antibody against

human CD4 –the receptor required for HIV entry in human T helper cells-demonstrated high anti-HIV efficacy and was well tolerated by subjects (Bruno and Jacobson, 2010; Fessel *et al.*, 2011). Similarly, PRO 140, a humanised anti-CCR5 antibody, has been shown to be safe for administration, with potent and prolonged antiretroviral activity (Jacobson *et al.*, 2010). Importantly, a CCR5 antagonist (maraviroc) has recently been approved by the US Food and Drug Administration for the same purpose (Tan *et al.*, 2007; Lieberman-Blum *et al.*, 2008). Other examples of host-oriented anti-viral approaches are those proposed against poxvirus (Reeves *et al.*, 2005), West Nile virus (Hirsch *et al.*, 2005) and influenza virus (Pleschka *et al.*, 2001; Morita *et al.*, 2013).

Host-targeted therapeutics have shown considerable promise in the context of other infectious diseases but have not been to date developed for malaria. Previously, we showed that the RH5-Basigin interaction is essential and universally required for erythrocyte invasion by *P. falciparum*, and low concentrations of anti-Basigin monoclonal antibodies were able to potently block erythrocyte invasion *in vitro* (Crosnier *et al.*, 2011). While vaccine targeting the parasite component of this interaction are under active development (Douglas *et al.*, 2011; Bustamante *et al.*, 2013; Reddy *et al.*, 2013), the potent invasion-blocking effect of anti-Basigin monoclonal antibodies also raises the possibility that these could be used as therapeutics to treat *P. falciparum* infected individuals. The previous safe use of anti-Basigin monoclonal antibodies in the clinic (section 1.10.6.2.2 and 1.10.6.2.3) is encouraging that antibodies against Basigin would be safe and very efficient in when administered to treat malaria patients.

In this PhD thesis, I aimed at the development of a recombinant anti-Basigin humanised chimeric monoclonal antibody, as a potential anti-malarial therapeutic. In a parallel project I aimed at the identification of novel erythrocyte-merozoite cell surface protein interactions which are critical for erythrocyte invasion.

## 1.15 Aims of this thesis

### 1.15.1 Development of a humanised or chimeric anti-BSG monoclonal antibody as a potential anti-malarial therapeutic

One of the goals of this PhD project was to exploit the essential nature of the RH5-Basigin interaction as a therapy, based on humanised or chimeric anti-BSG

monoclonal antibodies. In pursuit of this aim, I established a versatile plasmid vector system which enables the rapid and efficient recombinant expression of engineered antibodies (Chapter 3). By using this plasmid system, two anti-BSG monoclonal antibodies, MEM-M6/4 and MEM-M6/8 (Koch *et al.*, 1999) were successfully humanised by Complementarity Determining Region (CDR) grafting. The therapeutic potential of huMEM6-M/4 and huMEM6-M/8 was hampered by their low affinity for BSG. To obtain a higher potency antibody, a panel of hybridoma lines secreting anti-BSG antibodies was generated by directly immunising animals. A monoclonal antibody, m6D9, secreted by one of the generated hybridoma clones, demonstrated high efficacy in inhibiting erythrocyte invasion in parasite culture, and was selected for chimerisation. The chimeric antibody, ch6D9, retained its high affinity for BSG and blocked erythrocyte invasion with very low $IC_{50}$ in all parasite lines tested. Furthermore, ch6D9 displayed reduced binding to FcγRIIA and C1q *in vitro*, suggesting that this antibody may have reduced ability to trigger antibody effector functions. Attempts to fully humanise this antibody were unsuccessful.

To directly compare the efficacy between anti-BSG and anti-RH5 antibodies in inhibiting erythrocyte invasion, two anti-RH5 monoclonals (2AC7 and 9AD4;Douglas *et al.*, 2013) were successfully chimerised. Both ch2AC7 and ch9AD4 preserved their high affinity for RH5 and inhibited erythrocyte invasion in parasite culture, but with much higher $IC_{50}$ as compared to ch6D9. Finally, the variable regions of ch2AC7 and ch6D9 were combined in an anti-RH5 and anti-BSG bi-specific antibody: 2AC7-6D9 DVD-Ig. 2AC7-6D9 DVD-Ig was capable of simultaneous binding to RH5 and BSG but its affinity for BSG decreased in comparison to ch6D9. When tested in *P. falciparum* growth inhibition assay, 2AC7-6D9 DVD-Ig was more efficient than ch2AC7, but less than ch6D9 in blocking erythrocyte invasion.

## 1.15.2 Identification of novel receptor-ligand pairs involved in erythrocyte invasion

During erythrocyte invasion, the merozoite is directly exposed to the host humoral system, and therefore, merozoite cell surface proteins they are of fundamental importance for the development of anti-malarial therapeutics. Merozoites, however, are known to use a functionally redundant set of ligands that enable the parasite to access alternative invasion pathways complicating the development of highly effective therapeutic interventions. To date, only a handful of

receptor-ligand interactions implicated in invasion have been identified, and of those, only the interaction between RH5 and BSG has been shown to be essential and universally required for merozoite invasion.

A goal of this PhD project was the identification of novel receptor-ligand pairs involved in erythrocyte invasion. For this purpose, an existing *P. falciparum* merozoite recombinant protein library was expanded by 26 proteins. The new members of the *P. falciparum* protein library were expressed recombinantly and systematically screened against an equivalent library consisting of erythrocyte receptors. The screen identified a putative interaction (PF13_0125 – P4HB). Further characterisation of the identified interaction provided inconclusive results, and more experiments are required to confirm its validity. The recombinant *P. falciparum* merozoite proteins reported in this project will also be useful for further studies towards the understanding of erythrocyte invasion and *P. falciparum* merozoite biology.                                                                                          .

# CHAPTER 2

**Materials and Methods**

## 2.1 Production of recombinant cell surface and secreted *P. falciparum* and erythrocyte proteins

Secreted proteins, and the full-length ectodomains of membrane embedded proteins were produced in soluble recombinant form, by using an established system based on transient transfection of the HEK293E (Human Embryonic Kidney-293-EBNA1 variant) human cell line (Durocher *et al.*, 2002). The cells, adapted for suspension culture, were maintained in Freestyle media (*Invitrogen*) supplemented with 1% fetal bovine serum, 50 µg/ml of geneticin (*Sigma*), 100 units/ml penicillin (*Invitrogen*) and 100 µg/ml streptomycin (*Invitrogen*), incubated at 37°C, 5% $CO_2$ and 70% humidity with orbital shaking at 120 r. p. m.

### 2.1.1 Design and construction of protein expression plasmids

Transmembrane protein coding sequences were truncated for removal of the transmembrane and cytoplasmic regions (as predicted by TMHMM Server; http://www.cbs.dtu.dk/services/TMHMM/) enabling recombinant expression in a soluble, secreted form. The sequences encoding for the full-length secreted proteins or for the ectodomains of cell surface proteins (from 3D7 reference genome), were codon optimised for expression in mammalian cells, using the *GeneArt* gene synthesis service (*Invitrogen).* The optimised sequences were provided already sub-cloned into a pTT3-based expression vector (Durocher *et al.*, 2002) containing a region coding for the immunoglobulin-like domains 3 and 4 of rat Cd4 (Brown and Barclay, 1994) together with either

i. A 17-amino acid peptide substrate for the *Escherichia coli* biotin ligase BirA (Brown and Barclay, 1994; Bushell *et al.*, 2008), and a hexa-His tag (BLH; Fig. 2.1), or

ii. The pentamerisation domain of the rat cartilage oligomeric matrix protein (COMP) (Tomschy *et al.*, 1996), an ampicillin resistance protein β-lactamase (Bushell *et al.*, 2008), a Flag tag and a hexa-His tag (BLFH; Fig. 2.1)

Endogenous signal peptides were included for erythrocyte cell surface/secreted proteins (Crosnier *et al.*, 2011), however those of *Plasmodium* proteins (as predicted by using SignalP; http://www.cbs.dtu.dk/services/ SignalP/)were replaced by the leader sequence of the mouse variable κ light chain 7-33 (Crosnier *et al.*, 2010) during gene synthesis.
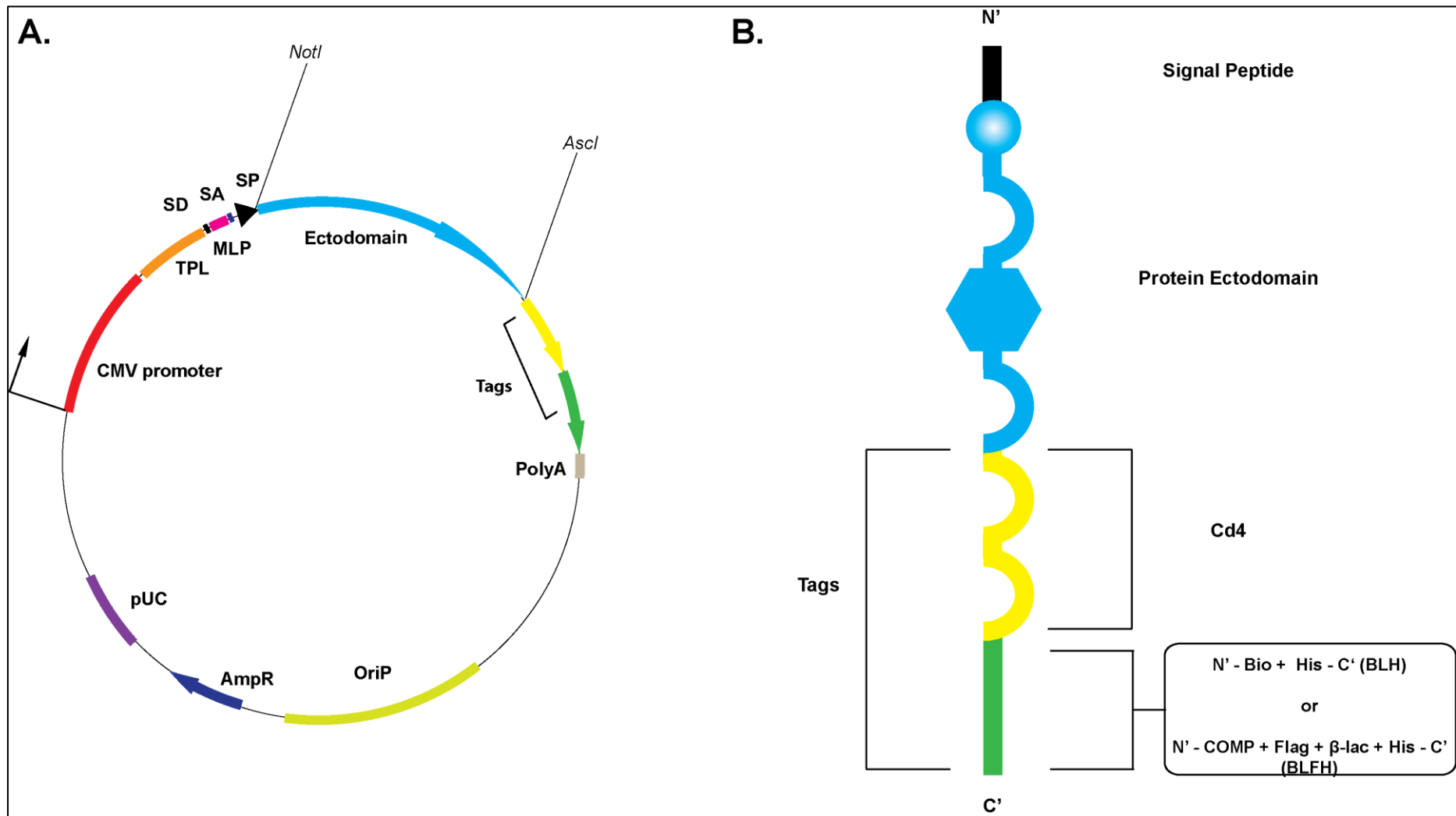
**Figure 2.1 Design of recombinant protein expression vectors**

**A.** The transfection vector which was used for recombinant protein expression.

**B**. A simplified cartoon of a typical recombinant protein as expressed from the transfection vector. The protein is tagged either with the Cd4, Bio and His or with the Cd4, COMP, β-lac, Flag and His tags.

Abbreviations: CMV promoter, Cytomegalovirus promoter; TPL, Tripartite Leader Sequence; SD, Splicing Donor; SA, Splicing Acceptor; MLP, Adenovirus Major Late Promoter enhancer; SP, Signal Peptide; NotI, NotI resctriction enzyme recognition site; AscI, AscI restriction enzyme recognition site; polyA, SV40 polyadenylation sequence; OriP, Epstein Barr virus origin of replication; AmpR, β-lactamase gene; pUC origin, bacterial origin of replication; Cd4, domains 3 and 4 of rat Cd4 ; Bio, Biotinylation signal for BirA; Flag, Flag tag ; His, hexa-histidine; COMP, coiled-coil sequence from the rat Cartilage Oligomeric Matrix Protein; β-lac, β-lactamase.

Evidence suggests that *Plasmodium* proteins are not N-linked glycosylated *in vivo* (Dieckmann-Schuppert *et al.*, 1992; Gowda and Davidson, 1999, 2000; Kimura *et al.*, 2000). To prevent spurious addition of glycans in the human cell secretory pathway the potential N-linked glycosylation sites (N-XS/T, with X≠proline) of *Plasmodium* proteins (as predicted by using NetNGlyc; http://www.cbs.dtu.dk/services/NetNGlyc/) were also systematically removed by substituting alanine for serine/threonine at these sites.

During gene assembly, flanking unique *NotI* (5') and *AscI* (3') restriction endonuclease recognition sites were introduced to all sequences encoding for recombinant proteins; these restriction sites were used for the subcloning of protein coding sequences, into expression vectors carrying different tags (Fig. 2.1). Briefly, after digestion with *NotI* (*New England BioLabs*, *NEB*) and *AscI* (*NEB*) for 2h at 37°C, both the vectors and inserts were resolved by agarose gel electrophoresis (section 2.8) and purified using the *QIA*quick Gel Extraction kit (*QIAGEN*) as per manufacturer's instructions. Ligations were performed for 1h at room temperature with T4 DNA Ligase (*NEB*) in ligation buffer (50 mM Tris-HCl, 10 mM MgCl$_2$, 1 mM ATP, 10 mM dithiothreitol, pH 7.5). Chemically-competent *E.coli* TOP10 cells (*Invitrogen*) were transformed with the ligation products and positive clones were selected on LB-agar plates containing 100 µg/ml of ampicillin.

Plasmids were then purified using the *QIA*prep Miniprep Spin kit (*QIAGEN*) according to manufacturer's instructions, tested for the correct insert via *NotI* and *AscI* digestion and sequenced with primers 462, 463, 497, 498, 3732, 3381, 3811, 3397, 3851 (Table 2.1 at the end of this chapter). Sequence-verified expression plasmids were transformed into TOP10 competent cells. Single positive clones were then inoculated into 100 ml cultures of LB broth supplemented with 100 µg/ml of ampicillin and grown overnight at 37°C with shaking at 200 r.p.m. Plasmids were purified from pelleted bacterial cultures using the PureLinkTM HiPure Plasmid Maxiprep kit (*Invitrogen*). The purified plasmid DNA was assessed for quantity and quality by measuring the absorbance at 260 nm (A260) and 280 nm (A280) using Nanodrop (*Thermo Scientific*). In terms of purity, A260/A280 ratios between 1.8-1.95 were considered to be acceptable. All plasmid DNA preparations were diluted to 1 mg/ml in EB buffer (10 mM Tris-Cl, pH 8.5) for use in transfections.

## 2.1.2 Recombinant protein expression by transient transfection of protein expression plasmids

The recombinant protein expression plasmids (Fig. 2.1) were transiently transfected into HEK293E cells by using the cationic reagent polyethylenimine (PEI; Tom *et al.*, 2008). Cells were split into 50 ml of fresh media at a density of $2.5 \times 10^5$ cells/ml and allowed to recover for 24 hours prior to transfection. For recombinant erythrocyte or *Plasmodium* protein expression each culture was inoculated with the following transfection mixture: 25 µl of the expression plasmid (at 1 mg/ml), 50 µl of linear PEI (at 1 mg/ml) and 2 ml of non-supplemented Freestyle media. The transfection mixture was incubated for 10 min at room temperature before it was added to the cell culture. Six days after transfection cells and cell debris were removed by centrifugation at 3220*g* for 20 min, supernatants were then filtered (0.2-µm filter) and stored at 4°C until use. When producing biotinylated proteins, the culture media was supplemented with 100 µM D-biotin (*Sigma*) and 2.5 µl of a plasmid (at 1 mg/ml) coding for a secreted form of BirA (Bushell *et al.*, 2008) was included in the transfection mix. After harvesting, filtered culture supernatants containing biotinylated proteins were dialysed against 5 L of Hepes Buffered Saline (HBS; 0.14 M NaCl, 5 mM KCl, 2 mM CaCl$_2$, 1 mM MgCl$_2$, 10 mM HEPES) over 2 days (7 changes of buffer) in Snakeskin dialysis tubing (10 kDa MWCO, *Thermo Scientific*) to remove excess D-biotin.

## 2.1.3 Purification of His-tagged recombinant proteins by using ÄKTAxpress purification system

His-tagged proteins were purified from harvested culture supernatants on nickel-charged Sepharose columns (HisTrap HP 1 ml; *GE Healthcare*) using the ÄKTAxpress purification system (*GE Healthcare*). In each case, the column was pre-equilibrated with binding buffer (20 mM sodium phosphate, 40 mM imidazole, 0.5 M NaCl, pH 7.4) at a flow rate of 1 ml/min. The harvested supernatant (> 200 ml) was supplemented with imidazole (10 mM) and NaCl (100 mM), before passed through the column at 1 ml/min. When loading was complete, the column was washed with 15 column volumes (15 CV) of binding buffer to remove non-specific adherents and with 10 CV of elution buffer (20 mM sodium phosphate, 0.4 M imidazole, 0.5 M NaCl, pH 7.4) to recover specifically-bound protein. The elutant was monitored at 280 nm in real-time and collected in 0.5 ml fractions. The two/three fractions with the highest

concentration of purified protein (as estimated by measuring the absorbance at 280 nm) were analysed by SDS-PAGE and pooled for downstream applications.

His-tagged proteins recovered from nickel column purification were further purified by gel filtration prior to use in surface plasmon resonance experiments (section 2.12). This step was necessary for removing protein aggregates. The gel filtration column (Superdex Tricorn 200 10/600 GL, *GE Healthcare*) connected to *Ä*KTAxpress was pre-equilibrated with ~100ml (~2CV) of the running buffer, HBS-EP (10 mM HEPES, 150 mM NaCl, 30 mM EDTA, 0.05% polyoxyethylenesorbitan 20, pH 7.4) before injecting each protein sample. One millilitre fractions were collected once 22 ml of running buffer (equivalent to the void volume of the column) had passed through the column. Absorbance at 280 nm and *in silico* predicted extinction coefficients were used to estimate the concentrations of peak fractions. The actual sizes of proteins and their conformational states (i.e. monomer, dimer or oligomer) were deduced from the elution volumes of the peak fractions, by comparison against a standard curve generated using well-defined protein standards from the low molecular weight and high molecular weight gel filtration calibration kits (*GE Healthcare*).

## 2.1.4 Purification of His-tagged recombinant proteins by using the Protein Press

His-tagged merozoite cell surface and secreted proteins were purified from harvested culture supernatants on a 96-well, nickel-charged Sepharose column plate (*His Multitrap HP; GE Healthcare*), using the protein press. Protein press is a device designed and developed in our laboratory (by Dr Yi Sun) which allows high throughput protein purification in a 96-well plate format. The column plate was pre-equilibrated with binding buffer (20 mM sodium phosphate, 40 mM imidazole, 0.5 M NaCl, pH 7.4) at a flow rate of 1 ml/min. The harvested supernatants (~200 ml for each protein) were supplemented with imidazole (10 mM) and NaCl (100 mM), before passed through the column plate (1 well per sample) at 1 ml/min. When loading was completed, each well was washed with 1.6ml (2CV) of binding buffer to remove non-specific adherents and with 0.2ml of elution buffer (20 mM sodium phosphate, 0.4 M imidazole, 0.5 M NaCl, pH 7.4) to recover specifically-bound protein.

## 2.2 Production of humanised or chimeric recombinant antibodies and DVD-Igs

### 2.2.1 Immunisation of animals

Six-week-old male BALB/c mice were immunised subcutaneously - three times with four weeks interval in between immunisations - with 10µg purified His-tagged Basigin in Titermax Gold adjuvant (*Sigma)*. Mice selected for hybridoma production were boosted intraperitoneally (without adjuvant) 3 days before dissecting the spleen.

### 2.2.2 Cell culture and hybridoma generation

The SP2/0 myeloma and SP2/mIL6 cell lines were grown in advanced DMEM medium (*GIBCO*) supplemented with 20% fetal bovine serum, penicillin (100 U/mL), streptomycin (100 µg/mL) and L-glutamine (2 mM). SP2/mIL6 conditioned medium was harvested every 3 days. Hybridomas were generated as described previously (Crosnier *et al.*, 2010). Briefly, following spleen dissection and dissociation, $10^8$ splenocytes were fused to $10^7$ SP2/0 myeloma cells in 50% PEG (PEG 1500; *Roche*). The resulting hybridomas were plated over ten 96-well plates (*COSTAR*) and initially grown in advanced DMEM medium (*GIBCO*) supplemented with 20% fetal bovine serum, 20% SP2/mIL6 conditioned medium, penicillin (100 U/mL), streptomycin (100 µg/mL) and L-glutamine (2 mM) before addition of Hypoxanthine Aminopterin Thymidine (HAT) selection medium 24 h after the fusion; after a regular exchange of selection medium for ten days, hybridoma supernatants were harvested for screening (section 2.2.3). Positive clones were re-plated in 48-well plate and grown for a further five days before further cloning by limiting dilution

### 2.2.3 Antibody screening

Hybridoma supernatants were screened using an ELISA-based assay as previously described (Crosnier *et al.*, 2010). Briefly, the biotinylated ectodomain of Basigin was bound to streptavidin-coated plates (*NUNC*) and incubated for 1 h with 50 µL hybridoma supernatant diluted 1:2 in phosphate buffered saline (PBS; 135 mM NaCl, 1.3 mM KCl, 3.2 mM Na2HPO4, 0.5 mM KH2PO4, pH 7.4) containing 2% w/v bovine serum albumin (BSA). The plates were washed in PBS/0.1% Tween20 (PBST) before incubation with an anti-mouse immunoglobulin (anti-mIgG) antibody coupled to alkaline phosphatase (*Sigma*) for 1 h at room temperature. After washes

in PBST and PBS positive wells were detected with *p*-nitrophenyl phosphate (Substrate 104; *Sigma*) at 1 mg/ml (100 µl/well).

## 2.2.4 RNA preparation and amplification of antibody variable regions

Amplification of antibody variable regions was performed as previously described (Crosnier *et al.*, 2010). Total RNAs were prepared from selected hybridoma using the RNeasy mini kit (*QIAGEN*) and the reverse transcription was performed with a polydT primer, using SuperscriptIII (*Invitrogen*). The functionally rearranged light variable region of a selected hybridoma was amplified without its signal peptide sequence, using a set of 17 degenerate forward primers (primers 3 to 19; Table 2.1) and one unique reverse primer corresponding to the constant region of the κ light chain (primer 20; Table 2.1). Similarly, the functionally rearranged heavy variable region was amplified without its signal peptide sequence, using a set of 18 degenerate forward primers (primers 27 to 44; Table 2.1) and four reverse primers (primers 45 to 48; Table 2.1). In total, the primers can recognise 97 and 98% of functional heavy and kappa (κ) light chain variable regions, respectively (Crosnier *et al.*, 2010). Lambda light chains only constitute 5% of those used in mouse immunoglobulins and primers were, therefore, not designed to this light chain (Crosnier *et al.*, 2010).

Both heavy and light chain variable region sequences were amplified with *Pfu*Ultra II Fusion HS DNA polymerase (*Agilent*) using the PCR conditions: 95°C for 2 min; ten cycles at 95°C for 45 s, 62°C for 30 s, 72°C for 1 min; 20 cycles at 95°C for 45 s, 61°C to 57 °C for 30 s with 1°C decrement every five cycles, 72°C for 1 min; ten cycles at 95°C for 45 s, 56 °C for 30 s, 72°C for 1 min, and one cycle 72°C for 10 min.

## 2.2.5 Identification of Complemetarity Determining Regions (CDRs) and antibody humanisation by CDR grafting

PCR-amplified antibody variable regions were analysed by gel electrophoresis (section 2.8) and gel extracted by using *QIA*quick Gel Extraction kit (*QIAGEN*) as per manufacturer's instructions. Gel extracted DNA was cloned by blunt end ligation in pCR®-Blunt II-TOPO® vector (*Invitrogen)* according to manufacturer's instructions. Chemically-competent *E.coli* TOP10 cells (*Invitrogen*) were transformed with the ligation products and positive clones were selected on LB-agar plates containing 50

µg/ml of kanamycin. Forty eight clones for each antibody heavy and light chain were sequenced by using T7, SP6, M13F and M13R primers (Table 2.1).

Sequencing results were analysed by using Seqman Pro (*DNAStar Lasergene Core Suite 11)*, and assembled sequences were subjected to variable region identification as well as to CDR and FR assignment by using IMGT/V-Quest (www.imgt.org). The sequences identified to correspond to the aberrantly rearranged κ chain (IGKV3-12) which is transcribed from SP2/0 myeloma genome (Strohal *et al.*, 1987) were excluded from further analysis. For the identification of the closest human variable regions, the verified mouse variable region sequences were blasted against the complete human variable region repertoire by using IMGT/DomainGapAlign (www.imgt.org). The human variable region sequence with the highest similarity in FRs was chosen to serve as CDR acceptor during antibody humanisation. If two or more human sequences were equally similar, the human sequence classified as I (genomic and rearranged evidence) on Vbase2 database (www.vbase2.org; Dr Mike Clark, personal communication) and/or had evidence of existence on protein level (www.imgt.org) was preferred. The latter provided evidence that the chosen CDR acceptor human variable region sequence is naturally expressed, increasing the probabilities of the engineered-humanised sequence to be functional.

For antibody humanisation, the human CDRs of the chosen human variable regions were replaced *in silico* by their mouse counterparts.

## 2.2.6 Design and construction of antibody and DVD-Ig expression vectors

## 2.2.6.1 Design and generation of anti-Basigin antibody expression vectors

For the construction of anti-Basigin chimeric and humanised antibody expression vectors the coding sequences of human Immunoglobulin kappa constant *(hIgCκ;* ENST00000390237*)* and a modified version *(*E233P / L234V / L235A / G236Δ / A327G / A330S / P331S / K214T / D356E / L358M; Greenwood and Clark, 1993; Armour *et al.*, 1999, 2003, 2006; Ghevaert *et al.*, 2008) of human Immunoglobulin heavy constant gamma 1 *(hIgG1;* ENST00000390549), each flanked by unique (5') *NotI* and (3') *EcoRI* restriction sites were synthesised by gene synthesis (*GeneArt).* The synthesised sequences were cloned into the pTT3 vector vector by using the *NotI-EcoRI* restriction sites.

The engineered or mouse antibody variable heavy or light chain sequences, were fused (*in silico*) downstream to the stated signal peptides which carry a *NotI* restriction site to their 5' end. The oligonucleotide GCTAGC was incorporated to the 3' end of each heavy chain variable region sequence. The latter sequence is in fact an *NheI* site and corresponds to the 5' end sequence of hIgG1. Similarly the oligonucleotide CGGACCGTGGCCGCTCCCAGCGTGTTCATCTTCCCACCCAG-CGACGAGCAGCTGAAG*TCCGGA* was incorporated to the 3' end of light chain variable region sequences. The latter sequence corresponds to the 5' end of *hIgCκ* and includes a *BspEI* cutting site (underlined).

The sequences consisting of the signal peptide, antibody (heavy or light) variable region and 3' oligonucleotide were synthesised by gene synthesis (*GeneArt).* The synthesised sequences carrying the heavy variable regions were cloned in pTT3 vector (by using the *NotI-NheI* restriction sites) in which the modified hIgG1 had been previously incorporated. Similarly the sequences encoding for light variable regions were cloned in pTT3 vector carrying the hIgCκ, by using the *NotI-BspEI* restriction sites. Chemically-competent *E.coli* TOP10 cells (*Invitrogen*) were transformed with the ligation products and positive clones were selected on LB-agar plates containing 100μg/ml ampicillin. Correct clones were verified by sequencing, using the primers V022F, V022R and hIgG1Rnew for heavy chain expression vector and V022F, V022R and hIgCκR for light chain expression vector (Table 2.1).

### 2.2.6.2 Design and construction of anti-RH5 expression vectors

For the construction of anti-RH5 chimeric antibody expression vectors, ch6D9 heavy and light variable regions were deleted from ch6D9 heavy and light chain encoding vectors, respectively, by inverted PCR by using the primer pairs LeaderHR-hIgG1F and LeaderLR-hIgCκF respectively (Table 2.1.). For the PCR reactions the Phusion High Fidelity DNA Polymerase (*Thermo Scientific*) was used under the following conditions: (1) 98$^{o}$C for 30s; (2) 98$^{o}$C for 10s; (3) 65$^{o}$C for 30s; (4) 72$^{o}$C for 1min and 45s; repeat steps 2-4 for 34 times; 72$^{o}$C for 10min. PCR products were analysed by agarose gel electrophoresis (section 2.8) and the bands corresponding to linear ch6D9 heavy and light chain expression vectors lacking the variable regions (~7 and ~6kb respectively) were extracted from the gel by using the *QIA*quick Gel Extraction kit (*QIAGEN*) as per manufacturer's instructions.

The variable heavy and light chain sequences of 9AD4 and 2AC7 anti-RH5 antibodies were cloned and verified as described in sections 2.2.4 and 2.2.5. 9AD4 and 2AC7 variable heavy chain sequences were amplified from pCR®-Blunt II-TOPO® vector (*Invitrogen)* by using the primer pairs 7H27F-4H12R and 7H27F-7H27R respectively (Table 2.1). Similarly, TOPO-cloned 9AD4 and 2AC7 variable light chain sequences were amplified by using the primer pairs LL2F-2L1R and 2L1F-2L1R respectively (Table 2.1). For the PCR reactions the *Pfu*Ultra II Fusion HS DNA polymerase (*Agilent*) was used under the following conditions: (1) 95$^{\circ}$C for 2min; (2) 95$^{\circ}$C for 20s; (3) 60$^{\circ}$C for 20s; (4) 72$^{\circ}$C for 15s; (5) repeat steps 2-4 for 34 times; (6) 72$^{\circ}$C for 3min

PCR products were analysed by agarose gel electrophoresis (section 2.8) and the bands corresponding to variable heavy and light sequences were extracted from the gel by using the *QIA*quick Gel Extraction kit (*QIAGEN*) as per manufacturer's instructions. Gel extracted DNA encoding for antibody variable heavy and light chain, was cloned by blunt end ligation (*T4 ligase, NEB*; room temperature, overnight) to the empty linear ch6D9 heavy and light chain respectively. Chemically-competent *E.coli* TOP10 cells (*Invitrogen*) were transformed with the ligation products and positive clones were selected on LB-agar plates containing 100µg/ml ampicillin. Correct clones were verified by sequencing, using the primers V022F, V022R and hIgG1Rnew for heavy chain expression vectors, and V022F, V022R and hIgCκR for light chain expression vectors (Table 2.1)

### 2.2.6.3 Design and generation of 2AC7-6D9 DVD-Ig expression vectors

Ch6D9 heavy and light chain encoding vectors were linearised by inverted PCR by using the primer pairs 6D9HF-LeaderHR and 6D9LF-LeaderLR respectively (Table 2.1). The PCR conditions for the linearisation of ch6D9 heavy chain expression vector are as follows: (1) 98$^{\circ}$C for 30s; (2) 98$^{\circ}$C for 10s; (3) 60$^{\circ}$C for 30s; (4) 72$^{\circ}$C for 1 min and 50 sec; (5) repeat steps 2-4 for 34 times; (6) 72$^{\circ}$C for 10min. The same PCR conditions were used for the amplification and linearisation of ch6D9 light chain encoding vector, with the difference of using 1min and 40s extension time in step 4.

For the construction of 2AC7-6D9 DVD-Ig long, 2AC7 variable heavy and light chain encoding sequences were PCR amplified from ch2AC7 heavy and light chain

expression vectors by using the primer pairs 7H27F-LG1Linker and 2L1F-LCkLinker, respectively (Table 2.1). Likewise, for the generation of the short version of 2AC7-6D9 DVD-Ig, 2AC7 variable heavy and light chains were amplified by using the primer pairs 7H27F-SG1Linker and 2L1F- SCkLinker (Table 2.1). The conditions used for all PCR reactions are as follows: (1) $98^{o}$C for 30s; (2) $98^{o}$C for 10s; (3) $60^{o}$C for 30s; (4) $72^{o}$C for 10 sec; (5) repeat steps 2-4 for 34 times; (6) $72^{o}$C for 10min.

PCR products were analysed by agarose gel electrophoresis (section 2.8) and the bands corresponding to the 2AC7 variable heavy and light sequences were gel extracted by using the *QIA*quick Gel Extraction kit (*QIAGEN*) as per manufacturer's instructions. Gel extracted DNA, encoding for 2AC7 variable heavy and light chain was cloned by blunt ligation (*T4 ligase, NEB*; room temperature overnight) to the linearised ch6D9 heavy and light chain respectively. Chemically-competent *E.coli* TOP10 cells (*Invitrogen*) were transformed with the ligation products and positive clones were selected on LB-agar plates containing 100µg/ml ampicillin. Correct clones were verified by sequencing, using the V022F, V022R, 7H27F, 7H27R for heavy chain expression vectors, and V022F, V022R, 2L1F and 2L1R for light chain expression vectors (Table 2.1)

For all PCR reactions the Phusion High Fidelity DNA Polymerase (*Thermo Scientific*) was used.

### 2.2.7 Site directed mutagenesis of hu6D9

Hu6D9 mutants were generated by using the QuikChange® XL Site-Directed Mutagenesis Kit (*Agilent*) according to manufacturer's instructions. For the generation of C58P and R80V the primer pairs CYS58PROF-CYS58PROR and ARG80VALF-ARG80VALR were used respectively. C58P/R80V double mutant was developed by introducing the R80V mutation in hu6D9VHC58P mutant.

### 2.2.8 Recombinant antibody and DVD-Ig expression by transient transfection of expression plasmids

Recombinant antibodies and DVD-Igs were produced by using the HEK-293F (Human Embryonic Kidney-293-Fast growing variant) protein expression system. The cells, adapted for suspension culture, were maintained in non-supplemented Freestyle media (*Invitrogen*) incubated at 37°C, 5% CO2 and 70% humidity with orbital shaking at 120 r. p. m. Expression plasmids for recombinant antibodies were

transiently transfected into HEK293F by using the cationic reagent polyethylenimine (PEI; Tom *et al.,* 2008). Cells were split into 50 ml of fresh media at a density of $2.5 \times 10^5$ cells/ml and allowed to recover for 24 hours prior to transfection. For recombinant antibody or DVD-Ig expression a transfection mixture consisting of 12.5 µl (at 1 mg/ml) heavy chain expression vector mixed with 12.5 µl (at 1 mg/ml) light chain expression vector, 2 ml of non-supplemented Freestyle medium and 50 µl of linear PEI (at 1 mg/ml) was added to the cell culture. Five to six days after transfection cells and cell debris were removed by centrifugation at 3220*g* for 20 min, supernatants were then filtered (0.2-µm filter) and stored at 4°C until use.

## 2.2.9 Purification of antibodies by affinity chromatography on protein G loaded column

Antibodies were purified from harvested culture supernatants on protein G Sepharose columns (HiTrap Protein G HP, 1 ml; *GE Healthcare*) using the ÄKTAxpress purification system (*GE Healthcare*). In each case, the column was pre-equilibrated with binding buffer (20 mM sodium phosphate, pH 7) at a flow rate of 1 ml/min, before loading of the harvested supernatant. When loading was complete, the column was washed with 15 column volumes (15 CV) of binding buffer to remove non-specific adherents and with 10 CV of elution buffer (0.1 M glycine HCl, pH 2.7) to recover specifically-bound protein. The elutant was monitored at 280 nm in real-time and collected in 0.5 ml fractions. The two/three fractions with the highest concentration of purified antibody (as estimated by measuring the absorbance at 280 nm) were pooled and dialysed (by using Slide-A-Lyzer Dialysis cassettes; *Thermo Scientific*) against HBS or PBS for the removal of glycine and to restore the pH to neutral. In several cases were antibodies were used in *P. falciparum* erythrocyte invasion assays, antibodies were also dialysed against RPMI 1640 (*GIBCO)* after dialysis against HBS or PBS.

## 2.2.10 Purification of antibodies with ammonium sulfate

Precipitation by ammonium sulfate is one of the oldest and widely used approaches for partial antibody purification. The principle is simple: at a specific concentration of ammonium sulfate, the number of water molecules that are available to keep a given protein moiety in solution is insufficient, resulting in protein

precipitation. The purity is not high because proteins with similar chemical properties to antibodies are salted out of the solution.

A saturated solution of ammonium sulfate was gradually added to harvested hybridoma supernatant with concomitant stirring, until the mixture became cloudy. Then, the stirring was stopped and the solution was left in 4$^o$C until the cloud completely precipitated. After the supernatant was discarded, the pellet (containing IgG) was dissolved in PBS, followed by dialysis against PBS (by using Slide-A-Lyzer Dialysis cassettes; *Thermo Scientific*) before use.

## 2.2.11 Antibody isotyping

Antibody isotyping was performed by using IsoQuick Strips (*Sigma*). Fifty microliters of 1µg/ml of m6D9 were loaded to the isotyping strip and incubated in room temperature for 20 minutes, before the results were detected.

## 2.3 Enzyme-linked-immunosorbent assays (ELISAs)

ELISAs were performed as previously described in (Bushell *et al.*, 2008). For quantitation of recombinant proteins from merozoite cell surface and secreted protein library, serially diluted biotinylated proteins were immobilised on streptavidin-coated 96-well plates (*NUNC*) for 1 h before incubation with 100µl of the mouse anti-rCd4 monoclonal OX68 (1µg/ml in HBS containing 0.1% Tween-20 and 2% BSA; HBST-BSA) for another hour. The plates were then washed in HBST before incubation with an anti-mIgG (*Sigma*) secondary antibody conjugated to alkaline phosphatase, for 1h. Plates were then washed three times in HBST and once in HBS before the addition of *p*-nitrophenyl phosphate (Substrate 104; *Sigma*) at 1 mg/ml (100 µl/well).

Similarly, for the assessment of mouse, humanised or chimeric antibody binding, biotinylated RH5 or Basigin were immobilised on streptavidin-coated 96-well plates (*NUNC*) for 1h, at concentrations sufficient for complete saturation of the available binding surface, followed by incubation with 100µl of serially diluted purified or tissue culture supernatant contained antibody. The plates were then washed in HBST before incubation with an anti-mIgG (*Sigma*) or anti-hIgG (*Sigma*) secondary antibody conjugated to alkaline phosphatase for 1h. Plates were then washed three times in HBST and once in HBS before the addition of *p*-nitrophenyl phosphate (Substrate 104; *Sigma*) at 1 mg/ml (100 µl/well).

In all ELISAS, absorbance was measured at 405 nm on a PHERAstar plus *(BMG Labtech)* plate reader after 10-15 mins. All the steps in the procedure were carried out at room temperature.

## 2.4 Immunoreactivity of recombinant merozoite proteins

In addition to quantifying biotinylated proteins and assessing antibody binding, ELISAs were used for testing the conformational state of merozoite cell surface and secreted proteins by means of specific antibodies present in immune sera, that recognise non-linear, heat-labile epitopes. For the latter analysis, proteins were heat-treated for 10 min at 80°C and then incubated on ice for a further 10 min, prior to use in ELISAs with untreated controls. Heat treated or untreated proteins were immobilised on streptavidin-coated 96-well plates (*NUNC*), at concentrations sufficient for complete saturation of the available binding surface/well (as determined by ELISA). In the cases where the concentration of biotinylated proteins was below saturating levels, 200µl of protein were used for protein immobilisation.

After washing the plates three times in HBST immobilised proteins were incubated for 2h, in the presence of 100µl of purified IgGs (provided by Dr Faith Osier; used at dilution 1:1000 in PBST, 2% BSA) from pooled immune sera obtained from previously malaria infected Malawian adults, or IgG purified from pooled non-immune sera from people who had never been exposed to malaria (provided by Dr Faith Osier; used at dilution 1:1000 in PBST, 2% BSA; negative control). The anti-rCd4 monoclonal OX68 (at concentration 1µg/ml) was used to confirm immobilisation of proteins. The plates were then washed in PBST before incubation with an anti-mIgG (*Sigma*) or anti-hIgG (*Sigma*) secondary antibody conjugated to alkaline phosphatase for 1h. Plates were then washed three times in PBST and once in PBS before the addition of *p*-nitrophenyl phosphate (Substrate 104; *Sigma*) at 1 mg/ml (100 µl/well). Absorbance was measured at 405 nm on a PHERAstar plus *(BMG Labtech)* plate reader after 10-15 mins. All the steps were carried out at room temperature.

## 2.5 Normalisation of β-lactamase tagged membrane protein ectodomains

Beta-lactamase tagged pentameric proteins were normalised as described by Bushell *et al.*, 2008, by monitoring their enzymatic activity over time, in a nitrocefin (*Calbiochem*) turnover assay. Twenty microliters of harvested culture supernatants

were incubated with 60 µl of nitrocefin (at 250 µg/ml) for a period of 20 mins at room temperature, during which nitrocefin turnover was quantified by monitoring the absorbance at 485 nm on a PHERAstar plus *(BMG Labtech)* plate reader. Prey activity was considered sufficient for AVEXIS if the available nitrocefin was completely turned over within 5-10 mins (Bushell *et al.*, 2008). Normalisation of proteins was achieved either by concentrating with 20 kDa MWCO spin concentrators (*Vivascience*) or diluting as required in HBST, 2% BSA.

## 2.6 Avidity-based extracellular interactions screen (AVEXIS)

This protocol was adapted from Bushell *et al.*, 2008. Streptavidin-coated 96-well plates (*NUNC*) were blocked with HBST, 2%BSA (100µl/well) for 1h. Biotinylated proteins (the baits) were diluted in HBST, 2% BSA and immobilised on the pre-blocked streptavidin-coated 96-well plates at concentrations sufficient for complete saturation of the available binding surface/well (as determined by ELISA). In the cases where the concentration of biotinylated proteins was below saturating levels, 200µl of purified protein (unknown concentration) were used for protein immobilisation. The plates were then washed three times in HBST before addition of normalised β-lactamase tagged pentameric proteins (the preys) and incubation for 2h. The plates were then washed three times in HBST and once in HBS. Nitrocefin (250 µg/ml; 60 µl per well) was added and developed for ~3h, before absorbance was measured at 485 nm on a PHERAstar plus *(BMG Labtech)* plate reader. All steps were performed at room temperature.

The binding events in the AVEXIS screen were analysed as follows: the binding of each prey to Cd4 bait was subtracted from the binding to a specific bait (actual binding). The average actual binding of a prey across the whole merozoite bait panel was then subtracted from the actual binding to a specific bait. The latter value was finally divided to the standard deviation of the binding of the prey under investigation to the whole panel of merozoite baits, to obtain a z-score for each interaction. A z-score represents the number of standard deviations, a given interaction is above or below the mean binding of a prey to the whole panel of merozoite baits.

## 2.7 High-throughput screen for the identification of glycan binding specificities of merozoite membrane and secreted proteins

Mono-biotinylated synthetic carbohydrate probes (*GlycoTech*) were immobilised at 50 µg/ml (100 µl/well) on pre-blocked (HBST, 2%BSA; 100µl/well; 1h) streptavidin-coated 96-well plates (*NUNC*) for 1 h at room temperature. The plates were then washed twice in HBST and blocked with HBS-BSA (100 µl per well) for 30 mins before addition of normalised β-lactamase tagged pentameric proteins and incubation for 2 h at room temperature. The plates were then washed three times in HBST and once in HBS before detection of the prey proteins by using nitrocefin as described before in section 2.6.

## 2.8 Agarose gel electrophoresis

DNA samples diluted in loading buffer (30% glycerol, 0.25% bromophenol blue, 0.25% xylene cyanol FF) were loaded onto 1% agarose, TAE-buffered (40 mM tris, 20 mM acetic acid, 1 mM EDTA) gels containing 0.1 µg/ml ethidium bromide. After electrophoresis at a constant voltage of 80V, DNA was visualised using a UV transilluminator (*BIORAD*).

## 2.9 SDS-polyacrylamide gel electrophoresis (SDS-PAGE)

Proteins were analysed by SDS-PAGE using Novex NuPage 4-12% Bis-Tris pre-cast gels (*Invitrogen*), as per manufacturer's instructions. Electrophoresis was performed at a constant voltage of 200 V for 50 mins and proteins were visualized using Coomassie brilliant blue (G250) staining solution (*Thermo Scientific*) according to the manufacturers' protocols.

## 2.10 Western blotting

Western blotting was used to confirm the size of recombinant antibodies or biotinylated proteins. Tissue culture supernatant or two micrograms of each protein or antibody were separated by SDS-PAGE (section 2.9), before transferring to PVDF membrane using a XCell II blotting module (*Novex*), at a constant voltage of 30 V, for 1 hour, at room temperature, in NuPage transfer buffer (25 mM Bicine, 25 mM Bis-Tris, 1 mM EDTA, 0.05 mM Chlorobutanol) (*Invitrogen*), supplemented with 10% methanol. The blots were incubated for 2h in room temperature, in PBST containing 5% milk to block non-specific binding sites. Biotinylated proteins or recombinant antibodies were then probed with horseradish peroxidase (HRP)-conjugated

streptavidin (1:37 000 dilution in PBST, 2% milk; *Jackson Immunoresearch Laboratories*) or anti-human-HRP (1:20 000 in PBST, 2% milk; *Sigma*) respectively, and detected by SuperSignal® West Pico Chemiluminescent Substrate (*Thermo Scientific*) after exposure to Hyperfilm (*GE Healthcare*).

## 2.11 *In vitro* biotinylation of antibodies and DVD-Igs

Purified mouse or recombinant antibodies and DVD-Igs were diluted at 2µg/ml in PBS at a final volume of ~150µl. Diluted antibodies and DVD-Igs were biotinylated *in vitro* using a 20-fold molar excess of EZ-link sulfo-NHS-biotin (*Thermo Scientific*) for 1h at room temperature. The biotinylated antibody and DVD-Ig preparations were then dialysed against 5 L HBS overnight (5 changes of buffer) by using Slide-A-Lyzer Dialysis cassettes (*Thermo Scientific*) to remove free, unconjugated biotin.

## 2.12 Surface plasmon resonance (SPR)

Surface plasmon resonance was used to derive affinity and kinetic parameters for protein-protein (including antibody-antigen) interactions. All SPR experiments were performed on a Biacore T100 instrument (*GE Healthcare*) using HBS-EP as the running buffer at 25°C.

### 2.12.1 Regeneration scouting by using SA chip

For the regeneration scouting experiment the Series S Sensor Chip SA (*GE Healthcare*) was used. The sensor chip surface was activated with three 1 min injections of 1 M NaCl and 50 mM NaOH at a flow rate of 30 µl/min. Regeneration scouting experiment was performed by using the Regeneration Scouting setup of Biacore T100 Control software (*GE Healthcare*), according to manufacturer's instructions. Briefly biotinylated MEM-M6/4 was captured on the activated chip surface, at about 400 response units (RU). Basigin contained in tissue culture supernatant was injected over immobilised antibody at a flow rate of 20µl/min for 30s, followed by injection of the stated regeneration solution at a flow rate of 30µl/min for 30s. Five consecutive analyte (Basigin) binding and regeneration cycles were tested for each regeneration solution before the results were analysed by using the Biacore T100 Control software (*GE Healthcare*) and Graphpad Prism 5 (*Graphpad Software Inc.*).

### 2.12.2 Analysis of protein-protein interactions by using CAP chip

SPR analysis of protein-protein (including antibody antigen) interactions were performed by using Biotin CAPture Kit (*GE Healthcare*), according to manufacturer's instructions. Briefly, Sensor CAP Chip was docked on Biacore T100 instrument and left on standby for at least 24h, in order to become rehydrated. Sensor CAP Chip surface was then conditioned by 3 one minute injections of regeneration buffer (3 parts of 8M guanide-HCl mixed with 1 part of 1M NaOH) at a flow rate of 20µl/min. After conditioning, the Biotin CAPture Reagent was immobilised on chip surface at 3800-4300 RU, followed by immobilisation of the stated ligand (biotinylated protein or antibody) and relevant control. The stated concentrations of analytes were then injected over sensor-surface captured ligands (at the indicated flow rates and for the stated times). Results were analysed by using the BIAevaluation software (*GE Healthcare*), and kinetic parameters were obtained by fitting a 1:1 binding model to the reference subtracted sensorgrams.

### 2.13 Erythrocyte binding assay

The binding of anti-Basigin antibodies to human red blood cells was investigated by a flow cytometric based method. In round-bottom 96-well plates (*COSTAR*) $5 \times 10^5$ human $O^+$ erythrocytes were incubated with each anti-Basigin antibody at a final concentration of 10µg/ml (at a final volume of 100µl) for 2h at $4^o$C. Mouse IgG or hIgG isotype controls (*Abcam*) and the anti-Basigin monoclonal MEM-M6/6 (*Abcam*) were used as negative and positive controls, respectively. After three washes in PBS, red blood cells were incubated for 2h at $4^o$C with goat anti-mIgG (at dilution 1:500; *Abcam)* or goat anti-hIgG (at dilution1:200; *Abcam)* FITC conjugated secondary polyclonals. Erythrocytes were washed twice in PBS, and antibody binding was examined by counting the FITC positive antibody-cell complexes by flow cytometry (BD LSRII flow cytometer; *BD Biosciences*). The data collected were then further analyzed with FlowJo (*Tree Star*).

### 2.14 C1q binding assay

The binding of C1q to ch6D9 was examined by using an ELISA based assay. One hundred microliters of 1.5µg/ml of ch6D9 or hIgG1 isotype (*SouthernBiotech)* were used to coat overnight at $4^o$C the binding surface of a 96-well maxisorb plate (*NUNC).* The plate was washed three times in PBST and blocked with PBST, 2%

BSA for 1h at room temperature, followed by incubation with a 2-fold dilution series of complement component C1q from human serum (*Sigma*) for 2h. The plate was then washed again three times in PBST followed by 1h serial incubations with goat anti-hC1q polyclonal (at dilution 1:1000; *Calbiochem*) and rabbit anti-goat IgG conjugated with alkaline phosphatase. The plate was finally washed three times in PBST and once in PBS before the addition of *p*-nitrophenyl phosphate (Substrate 104; *Sigma*) at 1 mg/ml (100 μl/well). Absorbance was measured at 405 nm on a PHERAstar plus *(BMG Labtech)* plate reader after 10-15 mins

## 2.15 FcγRIIA binding assay

The binding of FcγRIIA$_{131His}$ (α-chain) to ch6D9 was assessed by using an ELISA based assay. Recombinant monomeric biotinylated FcγRIIA was expressed as described in section 2.1.2. Biotinylated FcγRIIA was immobilised on a pre-blocked (with HBST, 2%BSA) streptavidin-coated 96-well plate (*NUNC*) at concentrations sufficient for complete saturation of the available binding surface (as determined by ELISA). The plate was washed with HBST and incubated for 2h at room temperature with a dilution series of ch6D9 or hIgG1 isotype (*SouthernBiotech*). The plate was then washed again three times in PBST followed with 1h incubation with a donkey anti hIgG F(ab)$_2$ polyclonal, conjugated to alkaline phosphatase (*Abcam*). The plate was finally washed three times in PBST and once in PBS before the addition of *p*-nitrophenyl phosphate (Substrate 104; *Sigma*) at 1 mg/ml (100 μl/well). Absorbance was measured at 405 nm on a PHERAstar plus *(BMG Labtech)* plate reader after 10-15 mins.

## 2.16 *P. falciparum* culture, and invasion assays

All *P. falciparum* parasite strains were routinely cultured in human O$^+$ erythrocytes at 5% haematocrit in complete medium (RPMI-1640 supplemented with 10% human serum), under an atmosphere of 1% O$_2$, 3% CO$_2$ and 96% N$_2$. Invasion assays were carried out in round-bottom 96-well plates (*COSTAR*), with a culture volume of 100 μl per well at 2% haematocrit and 0.75% parasitemia, as previously described (Theron *et al.*, 2010; Bustamante *et al.*, 2013). *P. falciparum* cultures were synchronised on early stages by treatment with 5% w/v D-sorbitol solution (*Sigma*). Parasites in trophozoite stage were mixed with monoclonal antibodies (or DVD-Igs) and incubated overnight at 37 °C inside a static incubator culture chamber (VWR),

gassed with 1% $O_2$, 3% $CO_2$ and 96% $N_2$. At the end of the incubation period, red blood cells were collected, fixed with a fixative solution (2% paraformaldehyde, 0.2% glutaraldehyde) and permeabilized with 0.3% Triton-X 100 (*Sigma*). Erythrocytes were then treated with 0.5mg/ml RNAse (Ribonuclease A; *MP Biomedicals)* before staining with SYBR Green I (at dilution 1:5000; *Invitrogen).* Parasitized RBC (pRBC) were counted as SYBR Green I positive cells by using flow cytometry (BD LSRII flow cytometer; *BD Biosciences*). The data collected were then further analyzed with FlowJo (*Tree Star*).

**Table 2.1** **The primers that were used in this study.**

| Primer Name | Sequence |
| --- | --- |
| 462 | CCACTTTGCCTTTCTCTCCA |
| 463 | ATGTCCTTCCGAGTGAGAGA |
| 497 | TGAGATCCAGCTGTTGGGGT |
| 498 | AGAAGGGGCAGAGATGTCGT |
| 3732 | TTTAGGGAGAAGGTGATCCAGG |
| 3381 | TAGAGATCTCCGAGGGATCTCGACC |
| 3811 | AGAAGGGGCAGAGATGTCGTAG |
| 3397 | AGGAAGTGAACCTGGTGGTG |
| 3851 | AGAAGGGGCAGAGATGTCGTAG |
| 3 | TCAATAGTTGAACATAGCGGCCGCASAAAWTGTKCTCACCCAGTC |
| 4 | TCAATAGTTGAACATAGCGGCCGCAGAWATTGTGCTMACTCAGTC |
| 5 | TCAATAGTTGAACATAGCGGCCGCAGACATTGTGCTRACACAGTC |
| 6 | TCAATAGTTGAACATAGCGGCCGCAGACATTGTGATGACMCAGTC |
| 7 | TCAATAGTTGAACATAGCGGCCGCAGAYATCMAGATRAMCCAGTC |
| 8 | TCAATAGTTGAACATAGCGGCCGCAGAYATCCAGATGAYTCAGTC |
| 9 | TCAATAGTTGAACATAGCGGCCGCAGATATCCAGATGACACAGAC |
| 10 | TCAATAGTTGAACATAGCGGCCGCAGACATTGTGCTGACCCAATC |
| 11 | TCAATAGTTGAACATAGCGGCCGCAGACATYSTRATGACCCARTC |
| 12 | TCAATAGTTGAACATAGCGGCCGCAGATRTTKTGATGACYCARAC |
| 13 | TCAATAGTTGAACATAGCGGCCGCAGAYATTGTGATGACBCAGKC |
| 14 | TCAATAGTTGAACATAGCGGCCGCAGATATTGTGATAACCCAGGA |
| 15 | TCAATAGTTGAACATAGCGGCCGCAGACATCYTGCTGACYCAGTC |
| 16 | TCAATAGTTGAACATAGCGGCCGCAGAAAWTGTGYTGACCCAGTC |
| 17 | TCAATAGTTGAACATAGCGGCCGCAGAAACAACTGTGACCCAGTC |
| 18 | TCAATAGTTGAACATAGCGGCCGCAGACATTRTGATGWCACAGTC |
| 19 | TCAATAGTTGAACATAGCGGCCGCAGACATCCAGMTGACMCARTC |
| 20 | GGATACAGTTGGTGCAGCATCAGCCC |
| 27 | TTCACGAGTCCAGCCTCAAGCAGTGAKRTRCAGCTTMAGGAGTC |
| 28 | TTCACGAGTCCAGCCTCAAGCAGTGAGKTYCAGCTBCAGCAGTC |
| 29 | TTCACGAGTCCAGCCTCAAGCAGTCAGGTGCAGMTGAAGSAGTC |
| 30 | TTCACGAGTCCAGCCTCAAGCAGTGAGRTCCAGCTGCAACARTC |
| 31 | TTCACGAGTCCAGCCTCAAGCAGTCAGGTYVAGCTGCAGCAGTC |
| 32 | TTCACGAGTCCAGCCTCAAGCAGTCAGGTYCARCTGCAGCAGTC |

| 33 | TTCACGAGTCCAGCCTCAAGCAGTGAGGTGMAGCTGGTGGAATC |
|---|---|
| 34 | TTCACGAGTCCAGCCTCAAGCAGTGAVGTGMWGCTSGTGGAGTC |
| 35 | TTCACGAGTCCAGCCTCAAGCAGTGARGTGCAGCTGKTGGAGWC |
| 36 | TTCACGAGTCCAGCCTCAAGCAGTGAGGTGAAGCTGATGGAATC |
| 37 | TTCACGAGTCCAGCCTCAAGCAGTGAGGTGCAGCTTGTTGAGTC |
| 38 | TTCACGAGTCCAGCCTCAAGCAGTGAGGTGAAGCTTCTCRAGTC |
| 39 | TTCACGAGTCCAGCCTCAAGCAGTGAAGTGAARMTTGAGGAGTC |
| 40 | TTCACGAGTCCAGCCTCAAGCAGTCAGGTTACTCWGAAAGWGTCTG |
| 41 | TTCACGAGTCCAGCCTCAAGCAGTCAGGTCCAACTGCAGCAGCC |
| 42 | TTCACGAGTCCAGCCTCAAGCAGTGATGTGAACCTGGAAGTGTC |
| 43 | TTCACGAGTCCAGCCTCAAGCAGTCAGATCCAGTTSGTRCAGTC |
| 44 | TTCACGAGTCCAGCCTCAAGCAGTGAGGTRCAGCTKGTAGAGAC |
| 45 | CTATTCTAGCTAATCTAGGCGCGCCGAGGAGACGGTGACCGTGGTCC |
| 46 | CTATTCTAGCTAATCTAGGCGCGCCGAGGAGACTGTGAGAGTGGTGC |
| 47 | CTATTCTAGCTAATCTAGGCGCGCCGCAGAGACAGTGACCAGAGTCC |
| 48 | CTATTCTAGCTAATCTAGGCGCGCCGAGGAGACGGTGACTGAGGTTC |
| M13F | TGTAAAACGACGGCCAGT |
| M13R | CAGGAAACAGCTATGACC |
| T7 | TAATACGACTCACTATAGGG |
| SP6 | ATTTAGGTGACACTATAG |
| LeaderHR | GCTGTGCACGCCAGCTGTGCC |
| hIgG1F | GCTAGCACCAAGGGCCCCAGCG |
| LeaderLR | GCCTCTGCTGGCGGGGATCCAG |
| hIgCκF | CGGACCGTGGCCGCTCCCAG |
| 7H27F | GAGGTGAAGCTGGTGGAGTCTGGGGG |
| 7H27R | CGAGGAGACGGTGACCGTGGCCC |
| 4H12R | CGAGGAGACGGTGACCGTGGTCC |
| 2L1F | GACATTGTGCTGACCCAATCTCCAACTTCTTT |
| 2L1R | TTTGATTTCCAGCTTGGTGCCTCCACC |
| LL2F | GACATTGTTCTCACCCAATCTCCAGCTTCTTTG |
| V022F | TCTCTCCACAGGTGTCCACT |
| hIgG1Rnew | GGGGAAGTAGTCCTTGACCA |
| V022R | TTATTAGCCAGAGGTCGAGG |
| hIgCκR | TTGTCCACCTTCCACTGCAC |
| 6D9HF | GAAGTGCAGCTGCAGCAGAGCGG |

| | |
|---|---|
| 6D9LF | GACATCGTGCTGACCCAGAGCCCC |
| LG1Linker | GGGGGCCAGAGGGAACACGC |
| LCkLinker | GGGTGGGAAGATGAACACGCTGGG |
| CYS58PROF | TGGGCTGGATCAGCCCCTACAACGGCGTGCC |
| CYS58PROR | GGCACGCCGTTGTAGGGGCTGATCCAGCCCA |
| ARG80VALF | GAGTGACCATCACCGTGGACACAAGCGCCAG |
| ARG80VALR | CTGGCGCTTGTGTCCACGGTGATGGTCACTC |

Degenerate base code: M = A+C; R = A+G; W = A+T; S = C+G; Y = C+T; K = G+T; V = A+C+G; B = C+G+T

# CHAPTER 3

**Establishment of a plasmid vector system for recombinant antibody expression**

## 3.1 Summary and Aims

To develop an anti-malarial that targets a host protein, I sought to develop an anti-Basigin therapeutic monoclonal antibody that could prevent *P. falciparum* invasion of erythrocytes by blocking the RH5-Basigin interaction. To achieve this, it was first necessary to establish a rapid and cost effective method of expressing functional monoclonal antibodies in a recombinant form within the laboratory. In this Chapter, I describe the successful adoption and establishment of a versatile plasmid system which enables recombinant expression of engineered antibodies in HEK293 cells. I use two anti-Basigin monoclonal antibodies that will be described in detail in Chapter 4 (huMEM-6/4 and huMEM-M6/8), as exemplar recombinant antibodies to show that the recombinant antibodies are successfully expressed at high levels, and retain their ability to bind their target antigens. This antibody expression system may prove useful for the rapid cloning and expression of recombinant monoclonal antibodies for functional studies outside of malaria research.

## 3.2 Introduction

### 3.2.1 The recombinant antibody technology has revolutionised the application of antibodies

Traditionally, monoclonal antibodies have been produced by immunising animals and then establishing hybridoma clones which express the antibody of the desired specificity (Köhler and Milstein, 1975). Hybridoma technology, despite providing the advantage of infinite supply of the antibody of interests, is labour intensive and inflexible in terms of antibody engineering. The discovery of recombinant DNA technologies has enabled the engineering of antibodies, and has revolutionised their application extending them beyond research and diagnostics, into the clinic for the treatment of various diseases (Peterson, 2005). Based on these technologies, elegant approaches have been devised to reduce the antibody size to its functional minimum (Holliger and Hudson, 2005), make bi-specific agents (Marvin and Zhu, 2005; Morrison, 2007; Chames and Baty, 2009), increase antibody affinity by developing and screening large antibody libraries (Hoogenboom, 2005), or modulate antibody pharmacokinetics (Vaccaro *et al.*, 2005) and effector functions (Shields *et al.*, 2001; Carter, 2006; Yan *et al.*, 2011). Indeed, recombinant monoclonal antibodies have emerged as a very successful group of biological drugs,

used either alone or in combination with other therapies (Nelson *et al.*, 2010; Rasmussen *et al.*, 2012).

The widespread application of recombinant antibody technology (and recombinant protein technology in general) has led to the development of a variety of antibody expression systems. The choice of the expression system depends on the structure of the antibody variant to be expressed, the intended use of the antibody, as well as the antibody yield derived from each system (Chadd and Chamow, 2001). For example, bacterial systems are not generally good for expressing large proteins and lack glycosylation machinery, and are therefore more suitable for the expression of smaller antibody fragments like scFvs (single chain variable fragment) and F(ab)s (Fragment antigen binding; Holliger and Hudson, 2005) which are not naturally glycosylated. On the other hand, mammalian expression systems offer the advantage of expression of soluble fully-folded proteins which carry most of the naturally-occurring post translational modifications (e.g. glycosylation of antibody Fc region), and are therefore more appropriate for expressing full-length antibody molecules (Birch and Racher, 2006).

In this Chapter, a variant of the HEK293 (Human Embryonic Kidney cells) mammalian cell line that is grown at high densities in suspension, was used for recombinant antibody expression. The HEK293 line was first established in the late 70s (Graham *et al.*, 1977), and since then, because it is readily transfected by exogenous DNA, has emerged as a widely used expression system for recombinant protein and antibody production (Meissner *et al.*, 2001; Thomas and Smart, 2005; Clarke *et al.*, 2010; Yu *et al.*, 2010).

### 3.3 Results

### 3.3.1 Design of a vector system for recombinant antibody expression in HEK293 cells

To easily engineer and recombinantly express antibodies, I adopted and established a previously used two plasmid vector system (Clarke *et al.*, 2010; Yu *et al.*, 2010), that rapidly enables rearranged antibody light and heavy chains to be expressed recombinantly in the mammalian HEK293 expression system. For this purpose, I designed two plasmids, one for the light and one for the heavy chain that

could be co-transfected (Fig. 3.1), both based on a modified pTT3-plasmid backbone (Durocher *et al.*, 2002).

PTT3 is a plasmid used for transient transfection of mammalian cells and has several features that facilitate high-level protein expression. Because pTT3 harbours the OriP origin of replication (Fig. 3.1) that binds the Epstein-Barr nuclear antigen 1 (EBNA1) protein, it is capable of replicating in HEK293E cells in which the gene encoding for *ebna1* has been stably introduced. Moreover, the transgene expression is driven by an optimised human cytomegalovirus promoter (CMV), which is particularly active in HEK293 cells, and it was described to provide expression levels reaching up to 20% of total cellular proteins (Massie *et al.*, 1998; Durocher *et al.*, 2002).

In the first vector (heavy chain encoding vector) the sequence encoding for a modified hIgG1 (ENST00000390549 carrying the mutations E233P / L234V / L235A / G236Δ / A327G / A330S / P331S / K214T / D356E / L358M) was synthesised by gene synthesis and inserted upstream of the SV40 polyA coding sequence, leaving convenient restriction enzyme cutting sites (*NotI-NheI*) for the in-frame sub-cloning of any amplified antibody variable heavy chain of interest (Fig. 3.1B). The mutations introduced into the constant heavy chain are to alter antibody effector functions and are therefore useful for therapeutic applications, as described in more detail in Chapter 4. Similarly, in the second plasmid (light chain encoding plasmid), the sequence encoding for hIgCκ (ENST00000390237) was ligated into the pTT3 backbone (Fig. 3.1B). The equivalent antibody variable region of interest can be sub-cloned between the *NotI* and *BsPEI* restriction sites.

### 3.3.2 Functional expression of two exemplar recombinant antibodies

The functionality of the plasmid system described above was tested by the recombinant expression of two exemplar recombinant antibodies. In this case, I am using two humanised monoclonal anti-Basigin antibodies (huMEM-M6/4 and huMEM-M6/8) that will be described in detail in Chapter 4. Briefly, plasmids encoding huMEM-M6/4 and huMEM-M6/8 were made by amplifying rearranged antibody variable regions from the anti-Basigin hybridomas MEM-M6/4 and MEM-M6/8 by RT-PCR, sequencing them, and synthesising the humanised V-regions by gene synthesis. These regions were cloned into the heavy and light chain encoding
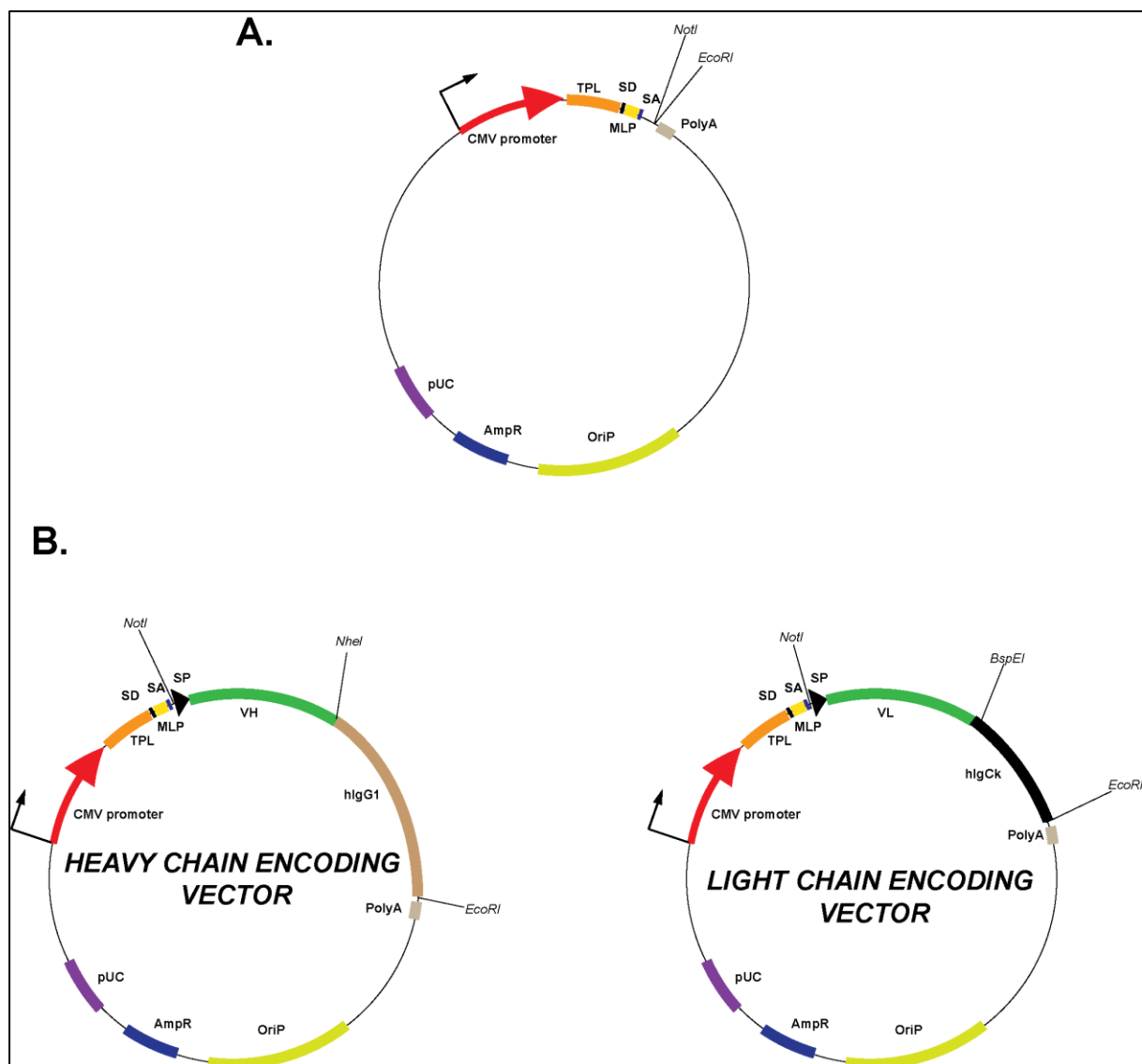
**Figure 3.1 The episomal vectors which were developed for recombinant antibody expression**.

Genetic map of the modified empty pTT3 vector backbone (*A.)* and antibody heavy and light chain encoding vectors *(B.).* Abbreviations: VH, Variable heavy; VL, Variable Light; hIgG1, human Ig γ1 coding sequence; hIgCκ, human Ig costant κ coding sequence; CMV promoter, cytomegalovirus promoter; TPL, Tripartite Leader Sequence; SD, Splicing Donor; SA, Splicing Acceptor; MLP, Adenovirus Major Late Promoter enhancer; SP, Signal Peptide; NotI, NotI resctriction enzyme recognition site; NheI, NheI restriction enzyme recognition site; BspEI, BspEI resctriction enzyme recognition site; polyA, SV40 polyadenylation sequence; OriP, Epstein Barr virus origin of replication; AmpR, β-lactamase gene; pUC origin, bacterial origin of replication.

vectors respectively (Fig. 3.1). To test the functionality of the recombinant antibody expression system, both heavy and light chain encoding plasmids (Fig 3.3B) were co-transfected into HEK293F cells. Six days later, spent tissue culture supernatant was harvested and analysed for the presence of secreted antibody by western blot (Fig. 3.2A). Two bands at 55 and 28kDa, corresponding to antibody heavy and light chain were detected, confirming antibody expression and secretion at approximately stoichiometric amounts. Tissue culture supernatant containing the exemplar anti-basigin antibodies was then tested for their ability to bind BSG by ELISA. The entire ectodomain of the human BSG target was expressed as a soluble recombinant biotinylated protein by transient transfection of HEK293E cells (Fig. 3.2B) and quantitated by ELISA by using the anti-Cd4 antibody OX68 (Fig. 3.2C). Saturating amounts of the biotinylated BSG protein were immobilised on a streptavidin-coated microtitre plate and both exemplar antibodies, huMEM-M6/4 and huMEM-M6/8, demonstrated clear binding to Basigin relative to an anti-BSG positive control and isotype-matched negative control as determined by ELISA (Fig. 3.2D).

These data indicate that the plasmid system I established can be used for the rapid and cost effective recombinant expression of monoclonal antibodies. Antibody heavy and light chains can be readily detected in the tissue culture supernatant of transfected cells, and recombinant antibodies retain their capability of binding to the antigen they normally recognise.

## 3.4 Discussion

To achieve the aim of developing an anti-malarial therapeutic antibody targeting host proteins, we have selected the RH5 erythrocyte receptor Basigin as our target. Because these antibodies, if they are to be useful therapeutically, must be humanised (see Chapter 4) we need to develop a system of expressing functional recombinant antibodies. While there are several examples of similar expression systems that have been developed to produce functional recombinant antibodies (Karu *et al.*, 1995; Chadd and Chamow, 2001), we required one that could be used within the infrastructures of our available laboratory environment and, most importantly, be both rapid and cost-efficient to facilitate the testing of several different antibody sequences within a short timeframe.
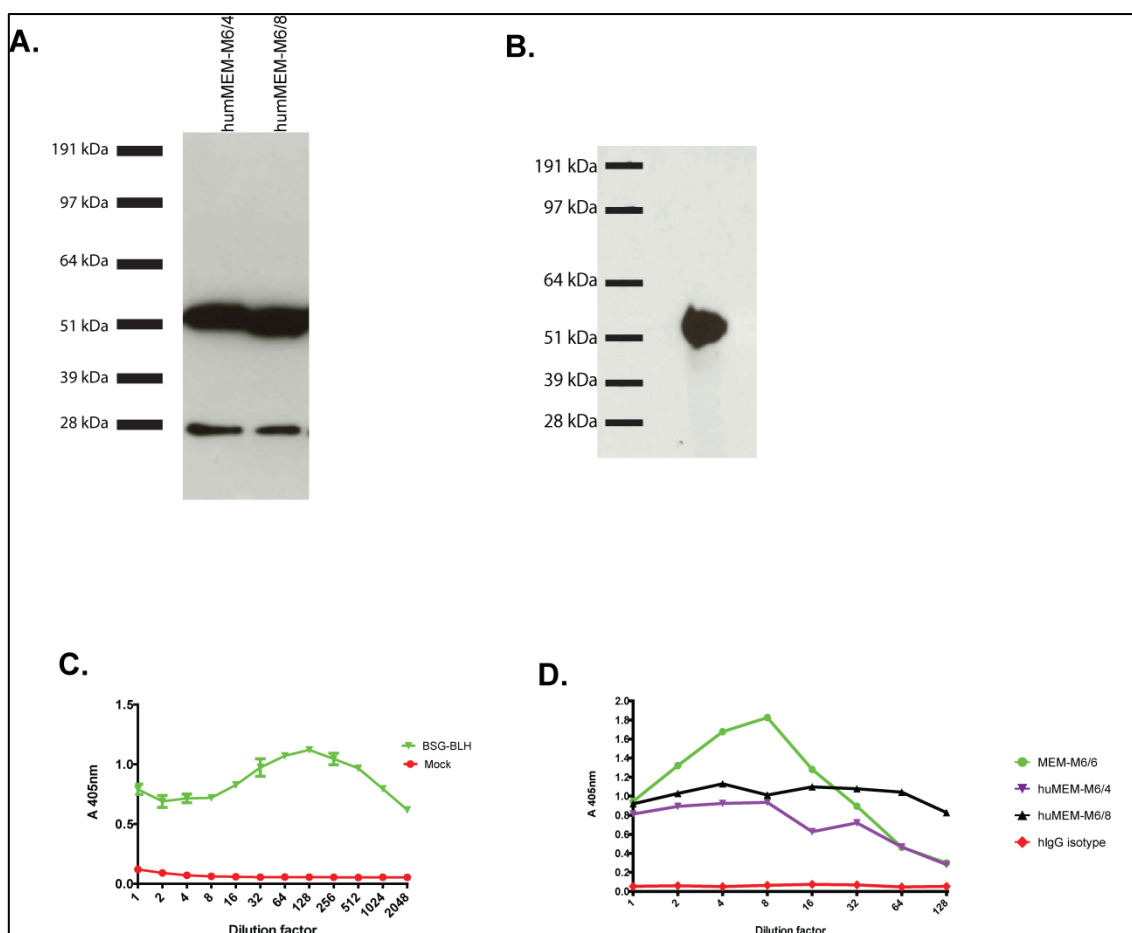
**Figure 3.2 Recombinant expression and functional assessment of two exemplar recombinant monoclonal antibodies.**

*A.* Recombinant antibody heavy and light chains were readily detected in approximately stoichiometric amounts in tissue culture supernatants, by western blot. Tissue culture supernatant containing either of the exemplar recombinant antibodies (huMEM-M6/4 or huMEM-M6/8) was analysed by denaturing SDS-PAGE, blotted and probed by using an anti-hIgG conjugated with Horseradish Peroxidase (HRP). Two bands at 55 and 28 kDa were obtained corresponding to antibody heavy and light chain, respectively.

*B.* BSG-BLH (Bio-Linker-His) was expressed at the correct size as determined by Western blot (a representative blot is shown). Tissue culture supernatant containing BSG-BLH was resolved under reducing conditions by SDS-PAGE, blotted, and probed using streptavidin-HRP. The expected molecular weight for BSG-BLH (including tags) was 56.3kDa.

*C.* Quantitation of recombinant monomeric BSG-BLH by ELISA (a representative graph is shown). Biotinylated BSG-BLH from tissue culture supernatant was serially diluted and immobilised on a streptavidin-coated plate. The wells of the plate were estimated to be saturated at a dilution of ~ 1:128. The anti-Cd4 mouse monoclonal OX68, was used as the primary antibody and an alkaline phosphatase-conjugated anti-mIgG as the secondary.

***D.*** Basigin was bound by unpurified exemplar anti-BSG antibodies. BSG-BLH was immobilised on a streptavidin coated plate at concentrations sufficient for complete saturation of the available binding surface and incubated with a 2-fold dilution series of tissue culture supernatant containing each antibody. An alkaline phosphatase conjugated anti-hIgG was used as secondary. The anti-Basigin monoclonal MEM-M6/6 and a hIgG isotype (both at starting concentration 1µg/ml) were used as positive and negative control, respectively.

Using an expression system based on HEK293 cells grown at high density in suspension and the pTT3 plasmid (Durocher *et al.*, 2002), I designed expression vectors for both antibody heavy and light chains. A key design feature is the ability to use simple restriction enzymes to clone antibody variable regions that have been either amplified directly from hybridoma cDNA or (and which adds a great deal of flexibility) using gene synthesised fragments. This latter point enables antibody regions to be humanised by CDR grafting onto closely-matched human variable regions very rapidly. I estimate that an experienced researcher familiar with this plasmid and expression system could obtain large amounts (>30mg/L) of purified antibody within 15 days for direct cloning, and 30 days for a humanised antibody from successfully amplifying the heavy and light chain V-regions. Similarly, the cost of this system is not prohibitive, enabling a researcher to humanise an antibody for less than 400GBP, depending on the cost of gene synthesis. The expression plasmid system described herein may have various applications, like the rapid screening of antibody functions for infectious diseases (Liao *et al.*, 2011b) as well as the production of recombinant antibodies for structural studies (Liao *et al.*, 2013).

In conclusion, in this Chapter, I have described the successful development of a plasmid system which allows the recombinant expression of antibodies in a rapid and efficient manner. The functionality of this system was confirmed by the recombinant expression of two exemplar antibodies that will be described in more detail in Chapter 4, but that were both able to bind their target antigen. I envisage that this plasmid system will be a useful tool for the rapid expression of functional antibodies and will have many uses both within the laboratory itself and other laboratories that have already adopted the HEK293 expression system.

# CHAPTER 4

**Development and characterisation of an anti-Basigin chimeric antibody, as a putative anti-malarial therapeutic**

## 4.1 Summary and Aims

The interaction between *P. falciparum* RH5 and BSG has been shown to be essential and universally required for erythrocyte invasion (Crosnier *et al.*, 2011). Antibodies against either RH5 or BSG could potently inhibit merozoite invasion in parasite culture, in all *P. falciparum* strains that have been examined (Crosnier *et al.*, 2011; Douglas *et al.*, 2011; Bustamante *et al.*, 2013). Therefore, the blockade of RH5-BSG interaction can be exploited for therapeutic purposes, for the treatment of *P. falciparum* infected individuals.

Most of the work described in this Chapter, was aimed at the development of a humanised or chimeric anti-BSG antibody as a potential anti-malarial therapeutic. By employing the versatile plasmid system which was developed in Chapter 3, two anti-BSG antibodies, MEM-M6/4 and MEM-M6/8 (gift from Prof. Vaclav Horejsi; Koch *et al.*, 1999), were humanised (hu) by Complementarity Determining Region (CDR) grafting, and expressed recombinantly. Despite preserving their ability to bind BSG *in vitro*, huMEM-M6/4 and huMEM-M6/8 could not block erythrocyte invasion when tested in *P. falciparum* erythrocyte invasion assays. This result was found to be due to the low affinity for BSG, of both mouse and humanised antibodies.

To obtain an anti-BSG monoclonal that would be effective for this application, I immunised mice to select several new hybridoma lines secreting anti-BSG monoclonal antibodies. An anti-BSG antibody that I named m6D9, was secreted by one of the generated hybridoma clones, and was prioritised for further study since it demonstrated very high efficacy in blocking the RH5-BSG interaction *in vitro*, and in preventing erythrocyte invasion in *P. falciparum* parasite culture. While attempts to fully humanise m6D9 were unsuccessful, a chimerised antibody, ch6D9 retained its high affinity for BSG and demonstrated high potency in blocking erythrocyte invasion in all parasite lines tested. Furthermore, ch6D9 displayed reduced binding to FcγRIIA and C1q *in vitro*, suggesting that this antibody may have reduced ability to trigger antibody effector functions.

In a parallel approach, two anti-RH5 monoclonals (2AC7 and 9AD4; Douglas *et al.*, 2013) were successfully chimerised. Both ch2AC7 and ch9AD4 preserved their high affinity for RH5 and inhibited erythrocyte invasion in parasite culture, but with much higher $IC_{50}$ as compared to ch6D9. In an attempt to increase the potency and

selectivity of the antibodies, the variable regions of ch2AC7 and ch6D9 were combined in an anti-RH5 and anti-BSG bi-specific antibody: 2AC7-6D9 DVD-Ig. 2AC7-6D9 DVD-Ig was capable of simultaneous binding to RH5 and BSG, but its affinity for BSG decreased in comparison to ch6D9. When tested in a *P. falciparum* growth inhibition assay, 2AC7-6D9 DVD-Ig was more effective than ch2AC7, but less than ch6D9 in blocking erythrocyte invasion. These results suggest that the anti-BSG ch6D9 has higher potency in inhibiting erythrocyte invasion, than the anti-RH5 ch2AC7 or the bi-specific anti-RH5/BSG 2AC7-6D9 DVD-Ig.

## 4.2 Introduction

### 4.2.1 Surface Plasmon Resonance-A valuable tool for measuring the affinity of antibodies and other molecules to their targets

One of the key parameters of antibodies is their affinities for their target. In this Chapter as well as in Chapter 5, I used Surface Plasmon Resonance (SPR) to biophysically characterise the interaction between two proteins; and in this Chapter, between an antibody and its antigen. While increasingly becoming a mainstream research tool, a brief description of this method and its applications is perhaps warranted. SPR optical biosensors exploit the evanescent wave phenomenon to derive information about the physical interactions between an immobilised ligand and a soluble analyte, in real time (Fig 4.1A). When plane-polarised light is shone through a prism - at an angle that leads to total internal reflection - on a conducting film placed at the interface between two media of different refractive index, surface plasmons (coherent oscillating electrons) are generated (Schasfoort and Tudos, 2008). Plasmon excitation is caused by resonance conditions that are established when the frequency of the photons constituting the incident light, matches the natural oscillation frequency of surface electrons. The energy transfer from incident photons to the surface electrons leads to a drop in the intensity of the reflected light at a characteristic angle known as the SPR angle. The SPR angle is dependent upon the relative refractive indices between a glass slide and the region close to the interface, which, in the case of an SPR machine used for protein interaction research, is a small flow cell contained within a disposable chip. The changes in refractive index within the flow cell caused by the accumulation of mass (e.g. proteins) leads to a change in the SPR angle that can be measured in real time and provides information

**A.**
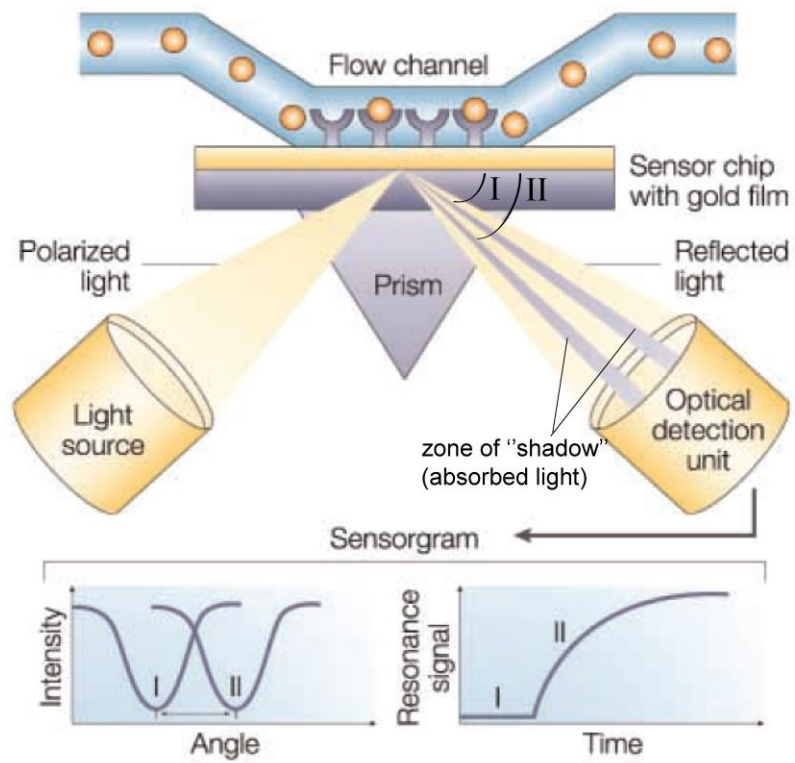


**B.**
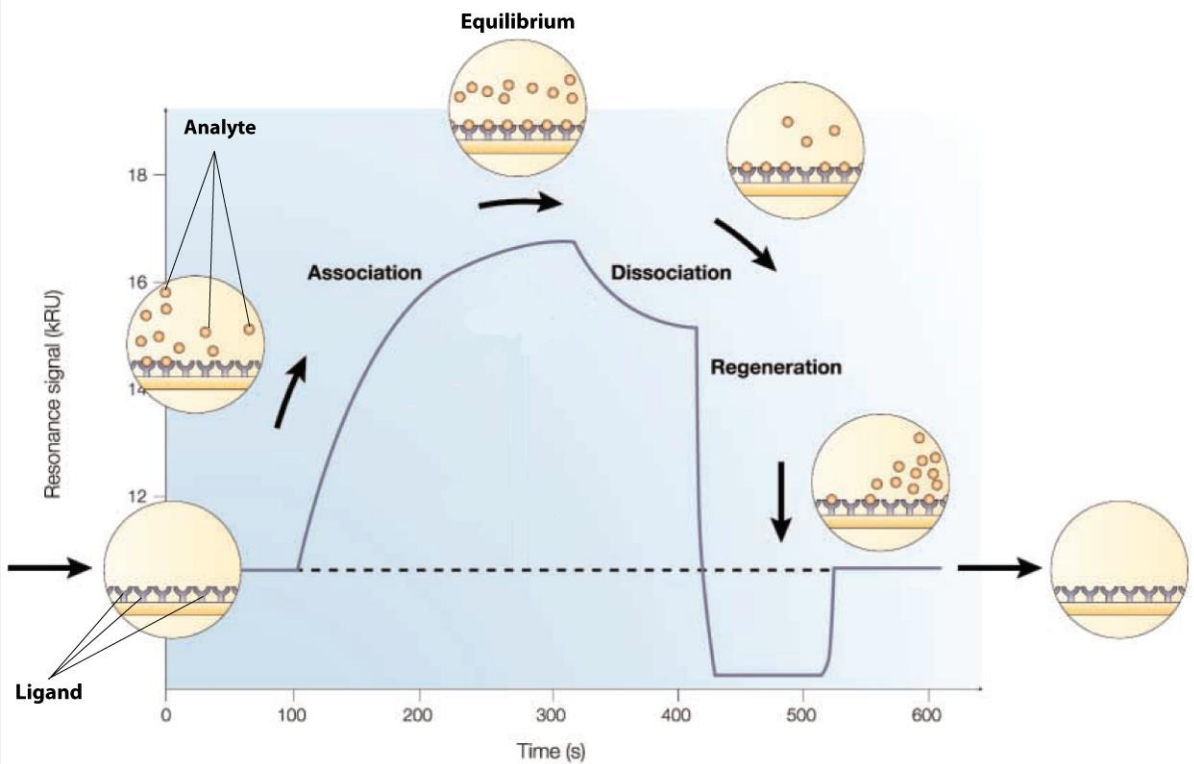
**Figure 4.1 Surface Plasmon Resonance.**

*A*. A typical biosensor setup. Polarized light is shone through a prism on a sensor chip, under conditions of total internal reflection. The absorbance of photon energy by surface electrons results in the loss of intensity of the reflected light at a particular reflection angle (SPR angle; angle I). The binding of molecules on a thin layer in the close vicinity of the gold surface on the chip, results in changes in the refractive index which in turn alters the SPR angle (angle II). These changes in resonance angle can be monitored in real time, and the resonance signal can be plotted against time (graph on the bottom right).

*B.* A typical sensogram obtained during a Surface Plasmon Resonance experiment. The ligand is immobilised in a flow cell by using appropriate chemistry ($t$=0). At $t$=100s, the analyte is injected into the flow cell where the ligand is immobilised. As the analyte binds to the ligand, the refractive index adjacent to the sensor surface increases, leading to an increase in the resonance signal. The association rate constant ($k_a$) can be determined by mathematical analysis of this part of the binding curve (Cooper, 2002). Continuation of analyte flow over the ligand will lead to equilibrium, where the association and dissociation rates are equal. The response level at equilibrium is related to the concentration of active analyte in the sample. At $t$ = 320s, the analyte injection is ceased and the receptor–analyte complex is left to dissociate. Analysis of these data gives the dissociation rate constant ($k_d$) for the interaction. Many biological interactions have extensive half-lives, and therefore a pulse of a regeneration solution (normally high salt or low pH) is required ($t$ = 420s) to disrupt binding and regenerate the free ligand. The entire binding cycle is normally repeated several times with a concentration series of analyte to generate a reliable data set which can then be used for global fitting to an appropriate binding algorithm. The affinity of the interaction can be calculated from the ratio of the rate constants ($K_D = k_d / k_a$) or by a linear or nonlinear fitting of the response at equilibrium ($R_{maximum}$) at varying concentrations of analyte. Pictures adapted and modified from Cooper, 2002

on the affinity and kinetics of a particular interaction (Fig 4.1) (Cooper, 2002; Schasfoort and Tudos, 2008).

Biacore technology, which is the one that was employed for the purposes of my experiments, utilizes sensor chips containing a thin film of gold built on a glass surface over which a solution containing the sample is passed (Fig. 4.1). Normally, a Biacore experiment starts by immobilising the ligand on the chip surface by using the appropriate coupling chemistry. The analyte is then injected over the immobilised ligand and the changes in SPR angle are monitored in real time and obtained in the form of sensorgrams (Fig. 4.1B). By adjusting the flow rate and duration of analyte injection, and by using the appropriate mathematical analysis, binding affinities and kinetics can be determined (Cooper, 2002).

### 4.2.2 Antibody humanisation approaches

Monoclonal antibodies (mAbs) have been an invaluable tool towards the treatment of serious diseases affecting mankind, like cancer, autoimmunity and viral infections (Reichert *et al.*, 2005; Carter, 2006). The utility of mAbs as therapeutics was recognised shortly after the introduction of hybridoma technology by Köhler and Milstein in 1975 (Köhler and Milstein, 1975). Their high affinity and exquisite specificity has rapidly put mAbs to a central position in the class of biological drugs (Beck *et al.*, 2010). However, it was soon realised that mAbs derived from hybridoma technology, are strongly immunogenic when injected in humans. Several studies reported that human-anti-mouse antibody (HAMA) responses were apparent in about 50% of patients after a single injection of murine mAbs, and in more than 90% of patients following two or three repeated injections (Qu *et al.*, 2005). A more extensive survey study, covering the period between January 1984 to December 2003, reported that 84% of murine mAbs surveyed, elicited marked HAMA reactions (more than 15% of the patients developed HAMA), 7% stimulated tolerable HAMA responses (2-15% of the patients developed HAMA), while 9% had negligible HAMA (<2% of the patients developed HAMA) (Hwang and Foote, 2005). As a result, murine mAbs are cleared rapidly in the human body and therefore, they have poor pharmacokinetics with short half-lives. Additionally, mouse mAbs are unable to trigger antibody effector functions such as complement activation or T cell stimulation, when injected into patients (Qu *et al.*, 2005; Tsurushita *et al.*, 2005).

The first attempts to reduce mAb immunogenicity led to the development of mouse-human chimeric mAbs which were generated simply by replacing the constant heavy and light chains of the mouse antibody under investigation, with the respective sequences found in human antibodies (Morrison *et al.*, 1984). The advantage of this approach is that the antibody specificity and affinity is retained because the entire variable regions are transplanted, without altering their amino acid composition which might affect the binding to the antigen. Approximately 60-70% of chimeric antibody (chAb) sequence is of human origin (Gonzales *et al.*, 2005; Qu *et al.*, 2005). Nevertheless, chAbs are still significantly immunogenic since 40% of the chAbs tested between January 1984 and December 2003 elicited marked anti-antibody responses (see above) (Hwang and Foote, 2005).

Since those first trials, more sophisticated approaches have been devised to reduce the murine amino acid content of therapeutic antibodies. In the mid-1980s Dr. Greg Winter and colleagues at the MRC Cambridge, introduced the Complimentarity Determining Region (CDR) grafting technology (Jones *et al.*, 1986; Riechmann *et al.*, 1988). This approach exploits the fine structure of immunoglobulin variable regions which consists of four framework regions (FRs) separated by three CDRs (section 1.2). The antigen-binding specificity of a murine antibody is transferred to a human antibody by replacing the CDR loops (Jones *et al.*, 1986; Riechmann *et al.*, 1988; Gorman and Clark, 1990; Lo, 2004).

In the CDR grafting approach, it is of great importance that key residues in murine FRs are identified and incorporated into the humanised antibody. Nevertheless, it is a common phenomenon that the affinity of a humanised antibody for its antigen, is greatly reduced as compared to the parental mouse one (Lo, 2004; Almagro and Fransson, 2008). The decrease in antibody affinity is likely to be due to incompatibilities between human FRs and murine CDRs. Antibody affinity can potentially be restored by mutating certain amino acids in the FRs of the humanised antibody back to those found at the same position in the murine parental antibody (Lo, 2004; Almagro and Fransson, 2008). The identification of the residues to be mutated is not trivial, and requires expertise in three dimensional modelling (Lo, 2004; Almagro and Fransson, 2008).

With regards to immunogenicity, the non-human sequence composition of a CDR-grafted antibody is typically only 5–10% compared to about 30% for a chimeric

antibody, and it was predicted to be minimally immunogenic (Lo, 2004; Gonzales *et al.*, 2005). Indeed, humanised antibodies were well tolerated, and several clinical trials reported undetectable or minimal anti-immunoglobulin responses (Sharkey *et al.*, 1995; Cobleigh *et al.*, 1999; Kalunian *et al.*, 2002; Crombet *et al.*, 2004). Another study, however, reported that a considerable amount of patients developed anti-antibody responses (Herold *et al.*, 2005), indicative that there was still space for improvement in terms of the "extent" of humanisation.

Padlan and colleagues further refined the antigen binding site within the CDRs: they identified that only 20–33% of the CDR residues participate in antigen-binding (Padlan, 1994), and these residues have been designated as specificity determining residues (SDRs) (Padlan *et al.*, 1995). Tamura and colleagues were the first to successfully humanise an antibody (the CC49 anti-TAG72 mAb) by grafting only the SDRs of the murine antibody into the human antibody FRs (Tamura *et al.*, 2000). This antibody showed reduced immunogenicity in comparison to the CDR grafted CC49 (Tamura *et al.*, 2000). However, similar to humanisation by CDR grafting, the SDR grafting approach entails the risk of significant loss of antigen-binding affinity (Kashmiri *et al.*, 2005; Kim and Hong, 2012).

Finally, antibodies having their entire amino acid content of human origin have been developed by using transgenic animals. Transgenic mice have been genetically engineered, and the genes encoding for the human antibody repertoire have been inserted into the mouse genome, functionally replacing the endogenous mouse loci (Lonberg, 2005; Jakobovits *et al.*, 2007). Therefore, immunisation of these mouse models with the antigen of interest results in the generation of human monoclonal antibodies. A number of different transgenic mouse platforms for antibody discovery exist, but the wide adoption of this technology has been hampered by complications with regards to the commercial rights (Moran, 2013).

### 4.2.3 Combination therapies and the value of bi-specific agents

Combination therapy is a widely acknowledged tactic to confront a range of diseases. By definition, in combination therapy two or more drugs are used together to treat a single disease. Simultaneous blockade of more than one molecules implicated in the same disease pathway is likely to provide better clinical efficacy (Wu *et al.*, 2007). Another major benefit of combination therapy is the reduced risk of

drug resistance development: it is less likely for the disease factor to simultaneously develop resistance to multiple defences, than to one alone. Conditions that are currently being treated with combination therapy include, tuberculosis (Diacon *et al.*, 2012), HIV (Bartlett, 1996; Hirsch *et al.*, 2003) and malaria (Miller *et al.*, 2013). Specifically for malaria, artemisinin-based combination therapies, comprise the first line of defence (Miller *et al.*, 2013).

Combination therapies have also been considered in the case of antibodies. Importantly, in June 2012 an antibody based combination therapy has been approved by FDA, for the treatment of patients with HER2-positive metastatic breast cancer who have not received prior anti-HER2 therapy or chemotherapy for metastatic disease (Blumenthal *et al.*, 2013). However, the co-administration of two or more antibodies to patients, requires complex pharmacokinetics and safety studies which complicates their routine use in clinic (Wu *et al.*, 2007). To avoid this problem, antibody based agents with multiple specificities have been developed. The first attempts to develop bi-specific antibodies were based on a "mix and match" approach where two hybridoma lines producing antibodies of the desired specificities, were fused to form a quadroma (Milstein and Cuello, 1983). Although the resulting hybrid did produce bi-specific antibodies the yields were very low, and only a small fraction of the secreted antibodies had dual specificity.

With the advent of recombinant DNA technology, more sophisticated approaches have been devised to force hetero-dimerization of two antibody arms of different specificity, and thereby resulting in a bi-specific antibody (Davis *et al.*, 2010; Schaefer *et al.*, 2011; Wranik *et al.*, 2012; Labrijn *et al.*, 2013). Other approaches utilize antibody fragments which are fused together in a multi-specific agent (Holliger and Hudson, 2005; Morrison, 2007; Chames and Baty, 2009). Because of their small size, such agents are very versatile and especially when used against solid tumors they demonstrate high penetration and uniform bio-distribution (Holliger and Hudson, 2005; Chames and Baty, 2009). However, most of these engineered antibody fragments have poor pharmacokinetics, because they lack the antibody Fc region which is responsible for antibody recycling. Wu and colleagues described a new methodology to produce full-sized bi-specific antibody molecules, which they named dual–variable domain immunoglobulin or DVD-Ig (Wu *et al.*, 2007). Each heavy and light chain contains two tandem variable domains, joined between each other by a

linker peptide (Fig. 4.19A). As a result each arm of the derived tetravalent molecule is capable of binding to two different antigens at the same time.

## 4.3 Results

### 4.3.1 Characterisation of MEM-M6/4 and MEM-M6/8 anti-BSG monoclonal antibodies

In Chapter 3, I described the establishment of a plasmid system which enables the recombinant expression of engineered antibodies. This system was a necessary tool for the subsequent development of an anti-BSG humanised mAb. Nevertheless, the development of a humanised anti-BSG antibody by CDR grafting, also required the availability of an anti-BSG mAb raised in animals, to serve as CDR donor. For this purpose, I would ideally choose one of the five anti-BSG antibodies (MEM-M6/6, MEM-M6/1, TRA-1-85, 8J251 and P2C2-1-D11) which were previously tested in our laboratory and demonstrated high efficacy in blocking erythrocyte invasion in parasite culture (Crosnier *et al.*, 2011; Bustamante L., unpublished; Theron M., unpublished). However, all of these antibodies were commercially available and therefore, I had no access to the respective hybridoma lines producing them, from where I would be able to amplify and sequence the antibody variable regions (see below). Therefore, we sought such hybridoma lines from the literature and we got access to two of them, namely MEM-M6/4 and MEM-M6/8 (Koch *et al.*, 1999). Both these lines originated from the same panel of mouse hybridoma lines as MEM-M6/6 and MEM-M6/1, two of the five high efficacy mAbs previously tested in our laboratory (see above). Considering that all five anti-BSG antibodies tested in earlier experiments were able to block erythrocyte invasion, it was expected that MEM-M6/4 and MEM-M6/8 would also be able to do so.

To biochemically characterise MEM-M6/4 and MEM-M6/8 mAbs, the respective hybridoma lines were grown in culture, and MEM-M6/4 and MEM-M6/8 mAbs were purified from tissue culture supernatant by affinity chromatography on a protein G column (Fig. 4.2A). To ensure that antibody heavy and light chains were assembled and secreted as a functional antibody, the purified antibodies were analysed by denaturing or native SDS-PAGE (Fig. 4.2B). Antibody heavy and light chains were stoichiometrically balanced in their expression level and capable of association (Fig. 4.2B). Unpurified antibodies from tissue culture supernatant as well as protein G
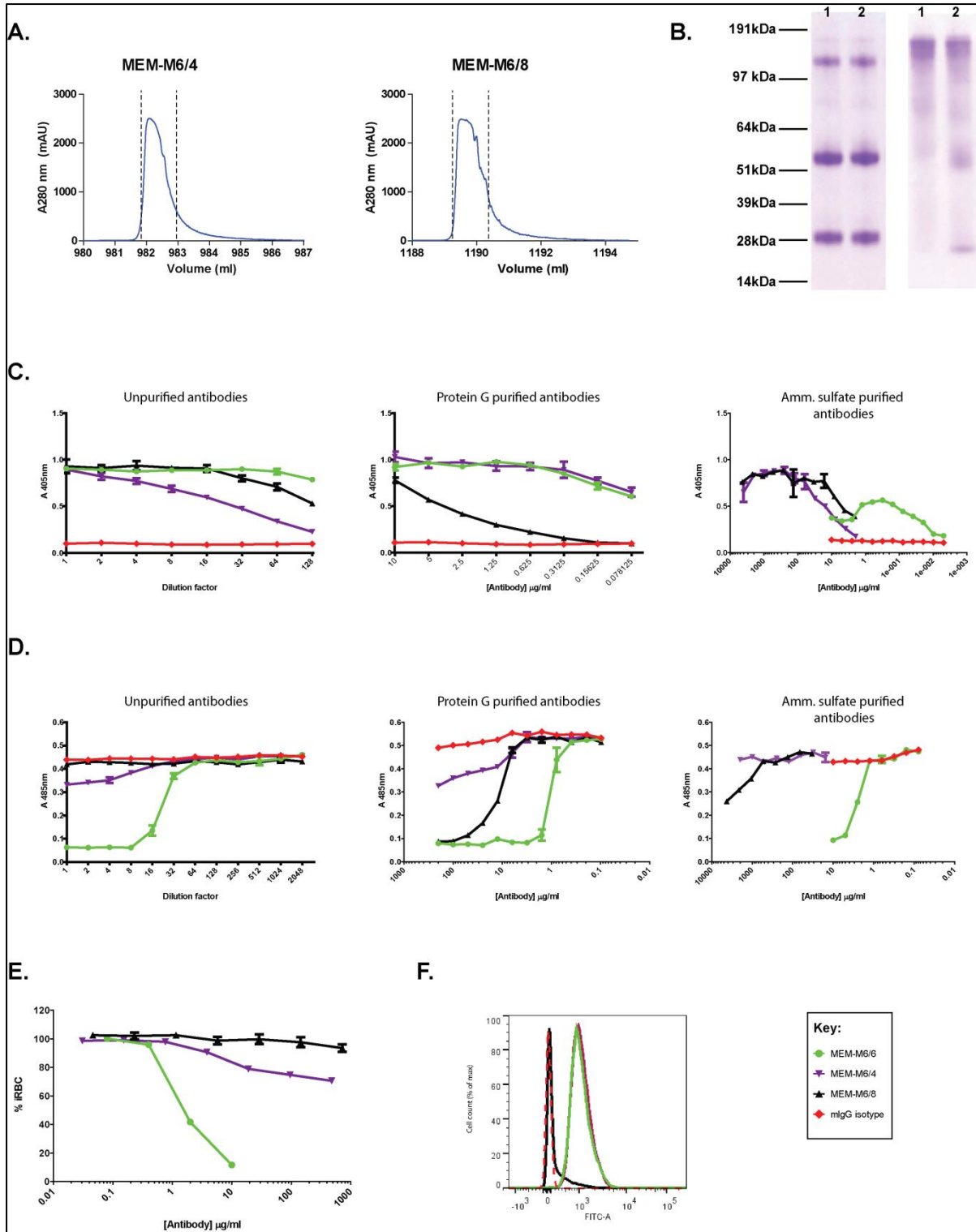
**Figure 4.2 Characterisation of MEM-M6/4 and MEM-M6/8 anti-BSG, mouse monoclonal antibodies.**

*A.* MEM-M6/4 and MEM-MEM-6/8 were affinity purified from tissue culture supernatant on protein G column. The eluate in each experiment was monitored at 280 nm in real-time and the peak fractions containing recombinant antibodies (between dashed lines) were pooled.

*B.* Protein G purified MEM-M6/4 (lane 1) and MEM-MEM-6/8 (lane 2) were analysed by SDS-PAGE under reducing (left) or non-reducing (right) conditions, and visualized by Coomassie brilliant blue. Under reducing conditions (left), two bands were observed for each antibody, at 55 and 28 kDa, representing antibody heavy and light chain respectively. The band at about 100kDa likely represents non-completely reduced antibody molecules. Under native conditions (right), most of the signal was concentrated to a single band at 150kDa, which is characteristic of fully assembled antibody.

*C.* Unpurified (left), protein G purified (middle) or ammonium sulfate purified (right) MEM-M6/4 and MEM-M6/8 were able to bind BSG, in an ELISA assay. BSG-BLH from tissue culture supernatant was immobilised on a streptavidin-coated plate at concentrations sufficient for complete saturation of the available binding surface, followed by incubation with a dilution series of each antibody. The binding of each antibody to BSG was determined by using an anti-mIgG secondary, conjugated with alkaline phosphatase.

*D.* The inhibitory effect of unpurified (left), protein G purified (middle) or ammonium sulfate purified (right) MEM-M6/4 and MEM-M6/8 on RH5-BSG interaction, as assessed by AVEXIS (for details see text). RH5 was used as bait, and pentameric BSG as prey. Pentameric BSG prey was pre-incubated with a dilution series of each antibody prior to probing RH5-BLH which was pre-immobilised on a streptavidin-coated plate.

*E.* Protein G purified MEM-M6/4 and MEM-M6/8 antibodies did not block erythrocyte invasion in parasite culture. Synchonised schizonts were incubated overnight with a dilution series of each antibody, before fixed and stained with SYBR Green I. The graph shows the percentage of infected red blood cells (iRBC) as a function of antibody concentration.

*F.* Binding of protein G purified MEM-M6/4 and MEM-M6/8 to human erythrocytes. Red blood cells were incubated with each antibody, followed by incubation with a FITC-conjugated anti-mIgG secondary and analysis by flow cytometry. The histogram shows the normalised cell count as a function fluorescence intensity at the FITC emission wavelength.

Data in *C*, *D* and *E* are shown as mean ± standard error; *n*=3. In all experiments the anti-BSG antibody MEM-M6/6 was used as positive control, and a mIgG isotype as negative. Where tissue culture supernatant was used for experiments, the starting concentration for MEM-M6/6 or mIgG isotype control was 10µg/ml.

purified MEM-M6/4 or MEM-M6/8, were then tested for binding to BSG by ELISA. Both MEM-M6/4 and MEM-M6/8 demonstrated binding to BSG (Fig. 4.2C). These data suggest that MEM-M6/4 and MEM-M6/8 were secreted from hybridoma lines in a biochemically active form, and were capable of binding to BSG *in vitro.*

### 4.3.2 MEM-M6/4 and MEM-M6/8 inhibit the RH5-BSG interaction *in vitro,* in AVEXIS assay, when used at high concentrations

To test whether MEM-M6/4 and MEM-M6/8 were able to block the RH5-BSG interaction *in vitro,* I employed the AVEXIS assay (Bushell *et al.*, 2008). Firstly, recombinant biotinylated RH5 bait was expressed and quantitated by ELISA (Fig. 4.3A). Immunoblot using a streptavidin-HRP probe, detected a protein band at 88 kDa, corresponded to the 63kDa full length RH5 obtained in previous studies, but containing C-terminal tags (Cd4-Biolinker-His) (Rodriguez *et al.*, 2008; Baum *et al.*, 2009) (Fig 4.3B). A smaller product at 70kDa, likely corresponds to the native 45kDa processed fragment of RH5 which was reported previously, was also observed (Baum *et al.*, 2009). A smaller sized fragment, about 28kDa, was also detectable. This band was observed in previous experiments in our laboratory and represents the protein tags (Cd4-Biolinker-His). The latter protein fragment appears to be the result of a cleavage event within a presumed proteolytically prone area, nearby the C-terminus of the RH5 protein ectodomain sequence (section 5.4.1).

Pentameric, soluble, β-lactamase tagged BSG prey was also expressed recombinantly, and the level of expression was estimated by monitoring the turnover of the β-lactamase substrate, nitrocefin, in a time-course assay (Fig 4.3C). The BSG expression level was above the threshold level required for the AVEXIS assay (section 2.5). The RH5 bait was then immobilised on a streptavidin-coated plate and probed against pentameric BSG prey, which was pre-incubated with a dilution series of hybridoma tissue culture supernatant or purified MEM-M6/4 and MEM-M6/8. Purified MEM-M6/4 mAb as well as MEM-M6/4 tissue culture supernatant showed a moderate inhibitory effect at very high concentrations (Fig 4.2D). MEM6-M/8 blocked the interaction at concentrations greater than 100μg/ml, whereas the equivalent tissue culture supernatant had no inhibitory effect (Fig 4.2D).

Considering the published affinity constants of MEM-M6/4 ($K_D$ =6.69x10$^{-11}$ M) and MEM-M6/8 ($K_D$ =5.38x10$^{-10}$ M; Koch *et al.*, 1999) these results were unexpected,
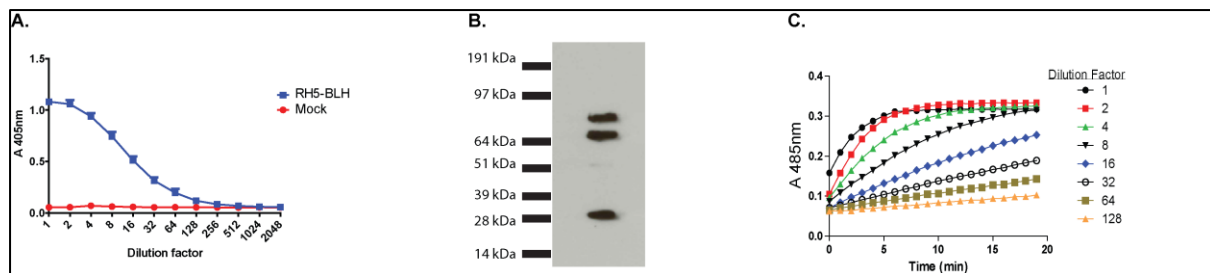
**Figure 4.3 Expression of recombinant RH5-BLH and BSG-BLFH.**

*A.* Quantitation of recombinant monomeric RH5-BLH by ELISA (a representative graph is shown). Biotinylated RH5-BLH from tissue culture supernatant was serially diluted and immobilised on a streptavidin-coated plate. The anti-Cd4 mouse monoclonal OX68, was used as the primary antibody and an alkaline phosphatase-conjugated anti-mIgG as the secondary antibody.

*B.* Immunoblot of recombinant RH5-BLH (a representative blot is shown). Tissue culture supernatant containing RH5-BLH, was resolved under reducing conditions by SDS-PAGE, blotted, and probed using streptavidin-HRP. The two higher molecular weight bands (88kDa and 70kDa) likely correspond to the previously observed 63kDa and 45kDa RH5 products (Baum *et al.*, 2009). The fragment at 28kDa represents the Cd4-BioLinker-His tag which likely derived from proteolytical processing of the RH5-BLH.

*C.* Quantitation of recombinant pentameric BSG-BLFH (Beta-Lac – Flag – His) by monitoring nitrocefin turnover over time (a representative graph is shown). A dilution series of tissue culture supernatant containing BSG-BLFH was tested in this manner.

raising the possibility that the antibodies had lost a fraction of their activity during the low pH elution stage of protein G purification (section 2.2.9). To exclude such a case, I sought to re-purify the antibodies by a method that avoids the use of low pH, such as precipitation by ammonium sulfate. Therefore, I re-grew the two hybridoma cell lines and collected fresh tissue culture supernatant from where antibodies were salted out of solution using a saturated solution of ammonium sulfate. Ammonium sulfate precipitated antibodies were able to bind BSG *in vitro,* as assessed by ELISA (Fig 4.2C). However, their potency to block the RH5-BSG interaction in AVEXIS did not improve in comparison to protein G purified antibodies (Fig 4.2D). These results suggest that the weak inhibitory effect of protein G purified MEM-M6/4 and MEM-M6/8 on RH5-BSG interaction, was not due to loss of antibody activity, after exposure to low pH.

### 4.3.3 MEM-M6/4 is able to stain human erythrocytes *in vitro* and to inhibit erythrocyte invasion in parasite culture

To test whether the *in vitro* results could be recapitulated in another system, MEM-M6/4 and MEM-M6/8 were assessed for their ability to block erythrocyte invasion in parasite culture. To this end, a *P. falciparum* culture was sorbitol synchronised and at the late trophozoite to early schizont stage (36-40h post invasion), a dilution series of each antibody was added to the culture and incubated overnight. Consistent with the *in vitro* data (Fig 4.2D), MEM6-M/4 showed a weak blocking effect at high concentrations (Fig 4.2E). MEM6-M/8 did not affect erythrocyte invasion, even when used at high concentrations (Fig 4.2E). It was not, however, clear whether these results were due to the weak or lack of MEM-M6/4 and MEM-M6/8 binding to surface-exposed BSG on human erythrocytes.

To address this question, the binding of MEM-M6/4 and MEM-M6/8 to human erythrocytes was examined. MEM6-M/4 was previously shown to bind to BSG expressed on both resting and activated T-cells whereas MEM-M6/8 was only able to do so, on activated T cells where BSG is up-regulated (Koch *et al*., 1999). However, none of these antibodies was tested before for their capacity to bind BSG expressed on erythrocytes. Thus, red blood cells were incubated with MEM-M6/4 and MEM-M6/8 followed by incubation with a FITC conjugated anti-mIgG and analysis by flow cytometry. MEM6-M/4 stained human erythrocytes at similar levels

to MEM-M6/6 (positive control) whereas no binding was observed for MEM-M6/8 (Fig 4.2F).

These results suggest that despite the fact that MEM6-M/4 can associate with BSG on human erythrocytes, it is not able to block erythrocyte invasion. It is likely that MEM-M6/4 binds an epitope on BSG which is nearby the RH5 binding site, causing a steric effect to the RH5-BSG interaction which in turn reduces invasion efficiency to a certain level. MEM-M6/8, however, appears unable to bind BSG on the erythrocyte cell surface, most likely due to its low binding affinity (see below) and hence, it has no effect in erythrocyte invasion.

MEM6-M/4 and MEM6-M/8 could not block the RH5-BSG interaction to the level required for the complete abolishment of erythrocyte invasion. Nevertheless, to test whether antibody humanisation by CDR grafting works in my hands, and while the time-consuming work described from section 4.3.7 onwards was ongoing, I decided to humanise and recombinantly express both MEM6-M/4 and MEM6-M/8.

## 4.3.4 Development of humanised MEM-M6/4 and MEM-M6/8 anti-BSG monoclonal antibodies

An antibody humanisation strategy was designed (shown in Fig 4.4), based on CDR (Complementarity Determining Region) grafting methodology (Jones *et al.*, 1986; Riechmann *et al.*, 1988). Briefly, the protocol is as follows: antibody variable heavy and light chain sequences are amplified and sequenced from the hybridoma line secreting the antibody of interest, followed by CDR sequence identification (Fig. 4.4). The identified CDR sequences are then used to replace the CDRs of the human antibody variable region which is most similar (in the framework region sequences) to the murine CDR donor antibody. The engineered antibody variable region sequences are synthesised by gene synthesis and sub-cloned into the antibody expression plasmid system as described in Chapter 3. Humanised antibodies are then recombinantly expressed in HEK293F cells as described in Chapter 3.

To humanise MEM-M6/4 and MEM-M6/8 it was therefore necessary to sequence and verify the rearranged variable heavy and light chains of each antibody. For this purpose, mRNA was isolated from each hybridoma line, followed by reverse transcription for cDNA synthesis. To amplify antibody variable region
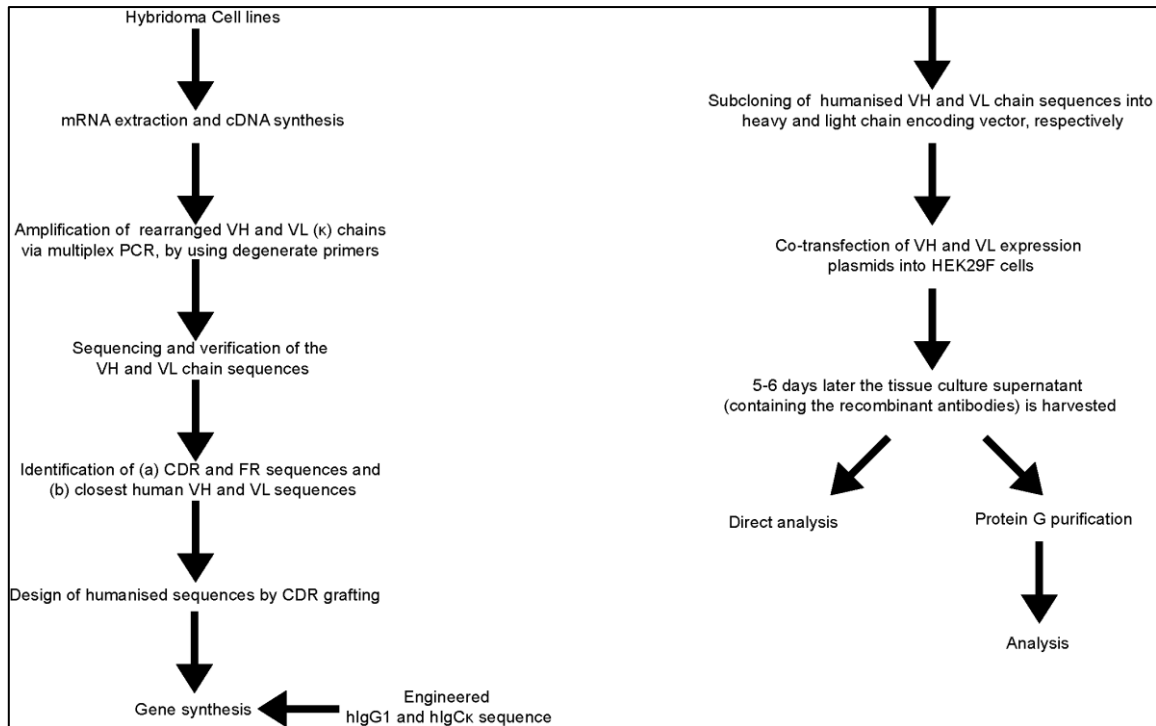
**Figure 4.4      A flow chart summarising the strategy that was devised for recombinant humanised antibody development.** Abbreviations: VH, Variable Heavy; VL, Variable Light; CDR, Complementarity Determining Region; FR, Framework Region.

sequences, the cDNA was used as substrate in a touchdown multiplex PCR which uses degenerate primers (Crosnier *et al.*, 2010). PCR amplicons were analysed by agarose gel electrophoresis and the DNA contained in the ~400bp bands (Fig 4.5A) was gel extracted, cloned, and sequenced.

The DNA sequencing results were assembled *in silico* and analysed using the IMGT/V-QUEST tool of IMGT database (www.imgt.org). About 80% of the light chain clones sequenced contained the transcribed aberrantly-rearranged light chain of SP2/0 myeloma (Strohal *et al.*, 1987), one of the fusion partners used for the generation of MEM-M6/4 and MEM-M6/8 hybridoma lines (Koch *et al.*, 1999). CDRs and FRs for both MEM-M6/4 and MEM-M6/8 were identified from the other sequences (Fig. 4.5B).

To identify the human variable regions that would serve as acceptors of the mouse CDR sequences, the amino acid sequences of MEM-M6/4 and MEM-M6/8 variable heavy and light chains, were blasted against the human antibody variable region repertoire by using the IMGT/DomainGapAlign tool (www.imgt.org). IGVH3-21*02 and IGHV1-69*04 were identified as the human variable segments having the highest similarity (in the FRs) to MEM-M6/4 and MEM-M6/8 variable heavy chain sequences, respectively. Likewise, IGK1-16*01 and IGK1-39*01 were identified as the closest human variable light chain sequences, for MEM-M6/4 and MEM-M6/8, respectively (Fig. 4.5C). Based on the FR-CDR boundaries set by the IMGT database, murine CDR sequences were engrafted into the chosen human variable region acceptor sequences, replacing the pre-existing CDRs (Fig. 4.5C). The engineered DNA sequences were incorporated downstream of the signal peptide sequence of the respective CDR acceptor chain sequence (Fig. 4.5D), codon optimised for expression in human cells and synthesised by gene synthesis.

### 4.3.5 Expression and characterisation of humanised MEM-M6/4 and MEM-M6/8 monoclonal antibodies

For recombinant expression of humanised MEM-M6/4 (huMEM-M6/4) and MEM-M6/8 (huMEM-M6/8), synthesised huMEM-M6/4 and huMEM-M6/8 variable heavy and light chain sequences were sub-cloned into the antibody heavy and light chain expression plasmids developed in Chapter 3, followed by transfection in HEK293F cells. Six days post-transfection, tissue culture supernatant was harvested

**A.** Variable Heavy / Variable Light gel: MEM-M6/4, MEM-M6/8. Ladder markings: 500 bp, 400 bp, 300 bp, 200 bp, 100 bp.

**B.**

| Variable region | FR1 | CDR1 | FR2 | CDR2 | FR3 | CDR3 | FR4 |
|---|---|---|---|---|---|---|---|
| H4 | EVQLVESGGGLVKPGGSLKLSCAAS | GFTFSSNA | MSWVRQTPDKRLEWVAT | ISSGSSYN | YYPDNVKGRFTISRDNAKNTLYLQMSSLRSEDTAMYYC | SSRGDNFLFAY | WGQGTLVTVSA |
| H8 | QVQLQQSGAELVRPGASVKLSCKAS | GYTLTDYY | VNWVRQRPGQGLEWIAR | INPGSGNT | YYTENFKGRATLTAEKSSNTAYMQLTSLASEDSAVYFC | ARSELLRYGFDV | WGTGTTVTVSS |
| L4 | DIQMTQSPSSMYASLGERVTITCKAS | QDINSY | LSWFQQKPGKSPKTLIY | RAN | RLVDGVPSRFSGSGSGQDYSLTISSLEFEDLGIYYC | LQFDEFPWT | FGGGTKLEIK |
| L8 | DIQMTQTTSSLSASLGDRVTISCRAS | QDITNY | LNWYQQKPDGTVKLLIY | YTS | RLHSGVPSRFSGSGSGTDFSLTISHLDQEDIATYFC | QQAHTLPPT | FGGGTKLEIK |

**C.**

| Variable region | Closest human V region | FR1 | CDR1 | FR2 | CDR2 | FR3 | CDR3 | FR4 |
|---|---|---|---|---|---|---|---|---|
| H4 | IGHV3-21*02 | EVQLVESGGGLVKPGGSLRLSCAAS | GFTFSSNA | MNWVRQAPGKGLEWVSS | ISSGSSYN | YYADSVKGRFTISRDNAKNSLYLQMNSLRAEDTAVYYC | SSRGDNFLFAY | WGQGTLVTVSS |
| H8 | IGHV1-69*04 | QVQLVQSGAEVKKPGSSVKVSCKAS | GYTLTDYY | ISWVRQAPGQGLEWMGR | INPGSGNT | NYAQKFQGRVTITADKSTSTAYMELSSLRSEDTAVYYC | ARSELLRYGFDV | WGQGTTVTVSS |
| L4 | IGKV1-16*01 | DIQMTQSPSSLSASVGDRVTITCRAS | QDINSY | LAWFQQKPGKAPKSLIY | RAN | SLQSGVPSRFSGSGSGTDFTLTISSLQPEDFATYYC | LQFDEFPWT | FGQGTKVEIK |
| L8 | IGKV1-39*01 | DIQMTQSPSSLSASVGDRVTITCRAS | QDITNY | LNWYQQKPGKAPKLLIY | YTS | SLQSGVPSRFSGSGSGTDFTLTISSLQPEDFATYYC | QQAHTLPPT | FGGGTKVEIK |

**D.**

| Variable region | Closest human V region | Signal peptide sequence |
|---|---|---|
| H4 | IGHV3-21*02 | MELGLRWVFLVAILEGVQC |
| H8 | IGHV1-69*04 | MDWTWRFLFVVAAATGVQS |
| L4 | IGKV1-16*01 | MDMRVLAQLLGLLLLCFPGARC |
| L8 | IGKV1-39*01 | MDMRVPAQLLGLLLLWLRGARC |

**Figure 4.5 Sequence analysis and humanisation of MEM-M6/4 and MEM-M6/8 variable regions.**

*A.* MEM6-M/4 and MEM6-M/8 variable heavy and light chain sequences were amplified from hybridoma cDNA by multiplex PCR, and analysed by agarose gel electrophoresis. A single band at about 400bp corresponds to the amplified variable heavy or light chain sequences.

*B.* The amino acid sequences of MEM-M6/4 and MEM-M6/8 mouse rearranged variable regions as derived from sequence analysis of the amplified cDNA sequences.

*C.* The amino acid sequences of the humanised MEM-M6/4 and MEM-M6/8 variable heavy and light chains after CDR grafting. The amino acid sequences of mouse variable regions were blasted against the human antibody variable region repertoire in IMGT database. Based on the similarity in the framework regions the closest human variable heavy and light regions were identified and served as acceptors of the mouse CDRs.

*D.* The amino acid sequences of the signal peptides that were incorporated upstream the engineered variable regions.

Abbreviations: CDR, Complementarity Determining Region; FR, Framework Region; H4 and H8, Variable Heavy chains of (hu)MEM-M6/4 and (hu)MEM-M6/8, respectively; L4 and L8, Variable Light chains of (hu)MEM-M6/4 and (hu)MEM-M6/8, respectively.

and analysed for the presence of antibody by western blot (Fig 4.6A). Two bands at 55 and 28kDa, corresponding to antibody heavy and light chain were detected, confirming antibody expression and secretion. Then, the ability of huMEM-M6/4 and huMEM-M6/8 to bind BSG *in vitro* was tested by ELISA. Both unpurified and protein G purified huMEM-M6/4 and huMEM-M6/8 demonstrated binding to BSG in an ELISA assay (Fig. 4.6 B,C).

The capacity of huMEM-M6/4 and huMEM-M6/8 to inhibit the RH5-BSG interaction *in vitro* was also examined in an AVEXIS assay. Pre-incubation of pentameric BSG with a dilution series of either unpurified or protein G purified huMEM-M6/4 and huMEM-M6/8, was insufficient to completely prevent the binding of BSG to RH5 (Fig 4.6D). These data show that MEM-M6/4 and MEM-M6/8 were successfully humanised; recombinantly expressed humanised antibodies retained their capacity to bind BSG *in vitro*. However, similar to the mouse parental antibodies, huMEM-M6/4 and huMEM-M6/8 could not completely inhibit the interaction between RH5 and BSG *in vitro.*

The efficacy of huMEM-M6/4 and huMEM-M6/8 in blocking merozoite invasion was assessed in an erythrocyte invasion assay. HuMEM-M6/4 and huMEM-M6/8 were not able to abolish erythrocyte invasion when included into the culture medium of parasite infected erythrocytes (Fig 4.6E). To further investigate the latter observation, huMEM-M6/4 and huMEM-M6/8 were tested for their binding capacity to human erythrocytes. Both humanised antibodies lacked the ability of staining human erythrocytes *in vitro* as assessed by flow cytometry (Fig 4.6F). These data show that despite retaining their binding specificity, neither huMEM-M6/4 or huMEM-M6/8 could prevent erythrocyte invasion in *P. falciparum* culture, probably due to their inability to bind to erythrocyte exposed BSG.

## 4.3.6 Biophysical characterisation of mouse and humanised MEM-M6/4 and MEM-M6/8 anti-BSG monoclonal antibodies

As demonstrated earlier in this Chapter, MEM-M6/4 and MEM-M6/8 did not inhibit the RH5-BSG interaction to the level required to prevent erythrocyte invasion. Considering the published affinity constants of both antibodies which are on the same range as the highly efficacious MEM-M6/6 (Koch *et al.*, 1999), these results were surprising. Therefore, I sought to measure the affinities of MEM-M6/4 and
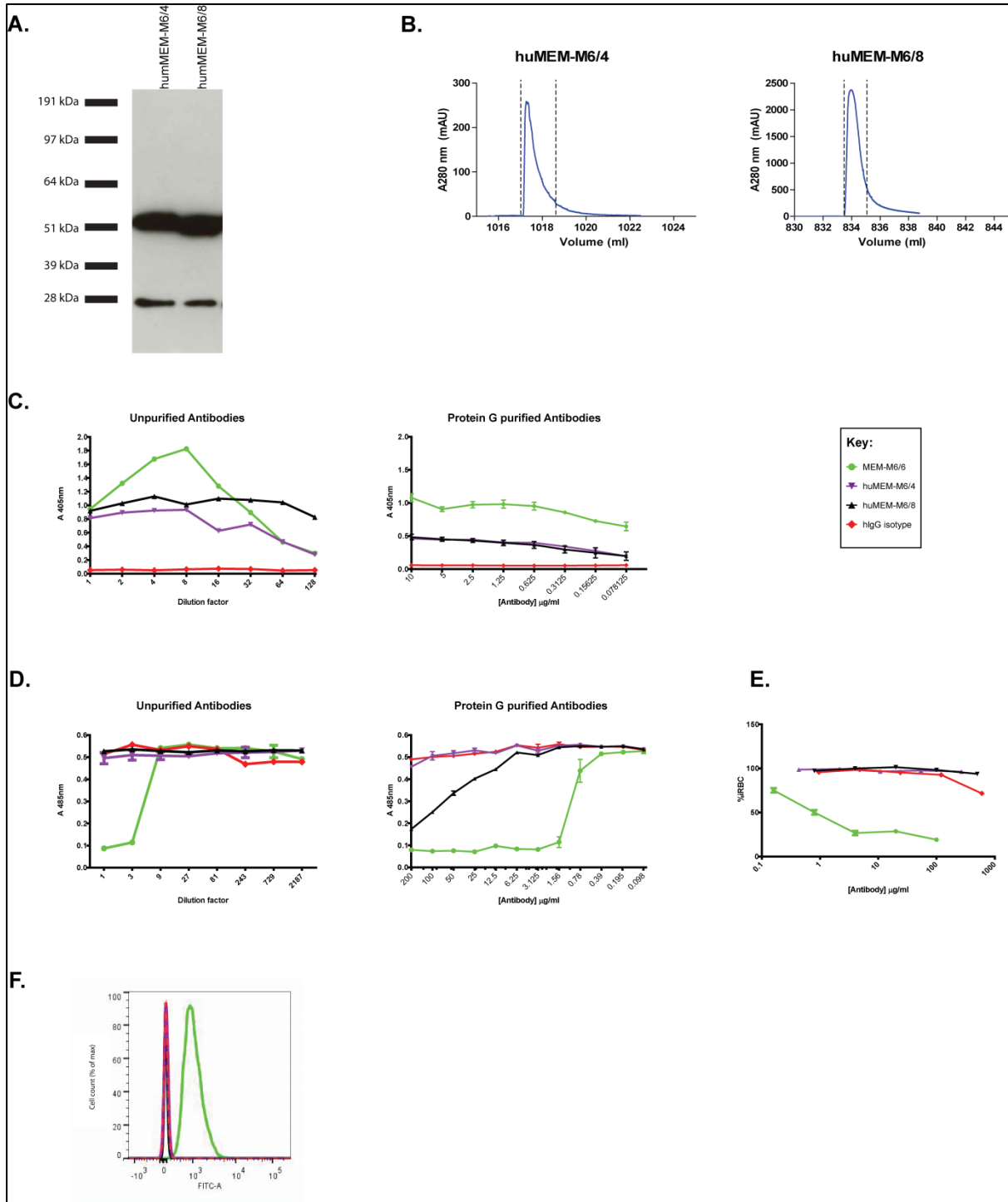
**Figure 4.6 Characterisation of humanised MEM-M6/4 and MEM-M6/8 antibodies.**

*A.* Humanised heavy and light antibody chains were readily detected in tissue culture supernatant, by western blot. Tissue culture supernatant containing huMEM-M6/4 or huMEM-M6/8 was analysed by denaturing SDS-PAGE, blotted and probed by using a Horseradish Peroxidase conjugated anti-hIgG. Two bands at 55 and 28 kDa were obtained corresponding to antibody heavy and light chain, respectively.

*B.* HuMEM-M6/4 and huMEM-MEM-6/8 were affinity purified from tissue culture supernatant on protein G column. The eluate in each experiment was monitored at 280 nm in real-time and the peak fractions containing antibodies (between dashed lines) were pooled.

*C.* BSG was bound by unpurified (left) or protein G purified (right) huMEM-M6/4 and huMEM-M6/8 antibodies, in an ELISA assay. BSG-BLH from tissue culture supernatant was immobilised on a streptavidin-coated plate at concentrations sufficient for complete saturation of the available binding surface, followed by incubated with a 2-fold dilution series of each humanised antibody. An alkaline phosphatase conjugated anti-hIgG was used as secondary.

*D.* Tissue culture supernatant containing huMEM-M6/4 or huMEM-M6/8 (left) or protein G purified antibodies (right) did not block the interaction between RH5 and BSG, in an AVEXIS assay. RH5-BLH from tissue culture supernatant was immobilised on a streptavidin-coated plate at concentrations sufficient for complete saturation of the available binding surface. Immobilised RH5-BLH was then probed against pentameric β-lactamase tagged BSG-BLFH which was pre-incubated with a dilution series of each antibody.

*E.* HuMEM-M6/4 and huMEM-M6/8 had no effect in erythrocyte invasion. A synchronised *P.falciparum* culture*,* at the schizont stage, was incubated overnight with a dilution series of each of the humanised antibodies. The infected erythrocytes were then fixed, stained with SYBR Green I and analysed by flow cytometry. The graph shows the percentage of infected red blood cells (iRBC) as a function of antibody concentration.

*F.* HuMEM-M6/4 and huMEM-M6/8 antibodies did not stain human erythrocytes. Human erythrocytes were incubated with 10µg/ml of each antibody, followed by 1h incubation with a FITC-conjugated anti-hIgG. The binding of huMEM-M6/4 and huMEM-M6/8 to red blood cells was then analysed by flow cytometry. The histogram shows the normalised cell count as a function fluorescence intensity at the FITC emission wavelength.

Data in *C, D* and *E* are shown as mean ± standard error; *n*=3. In all experiments the anti-BSG antibody MEM-M6/6 was used as positive control, and a hIgG isotype as negative.

For clarity reasons *A.* and *C.* (left) are reproduced here from Fig. 3.2.

MEM-M6/8 for BSG by SPR, and compare them with the already published ones as well as with those of the humanised antibody versions.

In the SPR experiments described below, antibodies were immobilised on the sensor chip surface and used as ligands, whereas purified monomeric BSG was used as the analyte. IgG antibodies are dimeric, carrying two antigen binding sites which bind independently to the antigen when the experiment is setup in this orientation (antibody as ligand and BSG as analyte). Using this method, I was able to calculate the kinetic and equilibrium binding parameters based on a simple 1:1 binding model. If the reverse orientation (BSG as ligand and antibody as analyte) was used, the engagement of the two antibody binding sites would not be independent of each other (two state reaction), and this would require the utilization of more complicated mathematical models for the calculation of kinetic and affinity parameters. Therefore, the orientation antibody-ligand and BSG-analyte was preferred.

### 4.3.6.1 Identifying the appropriate condition for regenerating the sensor chip surface

The interaction between an antibody and its target is normally of high affinity, typically in the nM range, and once the antibody-antigen complex is formed, spontaneous dissociation occurs at slow rates that could take several hours for complete dissociation. In SPR experiments, once the desired measurements are taken, antibody-antigen complexes can be disrupted by using a buffer (regeneration solution) that dissociates the complexes and thereby enabling repeated analyses on the same surface. Such a regeneration solution can vary between different antibody-antigen complexes and the identification of a single condition appropriate for all complexes under investigation is not trivial (Andersson *et al.*, 1999; Hoffman *et al.*, 2000).

By definition, regeneration is the process of removing bound analyte from the surface after an analysis cycle without damaging the ligand, in preparation for a new cycle. Incomplete regeneration or loss of the binding activity from the surface will impair the performance of the assay, and influence the final results (www.gehealthcare.com). Therefore, the ideal regeneration condition would result in consistent analyte responses in repeated cycles (differing less than 5% between

each other), and at the end of each regeneration step, the response should return to the baseline. To identify the ideal regeneration condition capable of dissociating the antibody-antigen complex without affecting the immobilised antibody, a regeneration solution scouting strategy was followed.

First, protein G-purified MEM-M6/4 (Fig. 4.2 A, B) was *in vitro* biotinylated, and immobilised on the surface of a streptavidin-coated (SA) sensor chip. BSG contained in tissue culture supernatant was injected over immobilised MEM-M6/4 and the analyte response was taken. This was followed by the injection of the regeneration solution under investigation, and the recording of the baseline response. To get the overall trend, this cycle was repeated five times for each regeneration condition, and a trend plot was drawn (Fig. 4.7). Two concentrations of NaCl, a single concentration of ethylene glycol, 10mM glycine at pH 2.2 or 2.5 and 100mM $H_3PO_4$, all proved to be too mild for disrupting the antibody-antigen complex: the baseline never returned to the reference levels and as a consequence the analyte response in the next cycles was reduced. In contrast 10mM glycine at pH 2 and 0.05%SDS were detrimental for the immobilised ligand (Fig. 4.7). Overall, none of the regeneration conditions tested provided acceptable results.

Therefore, I sought to use an alternative sensor chip of which the principle for regenerating the surface would be different from the SA chip. I chose to employ the CAP chip which I felt it would be ideal for the purposes of my experiments. CAP chip uses a ligand-independent regeneration protocol, removing the need of establishing appropriate regeneration conditions (Fig. 4.8A). It is based on a concept that allows for the reversible capture of biotinylated molecules. CAP chip is built on a carboxymethylated dextran matrix to which a single stranded DNA molecule is pre-immobilised. Biotin CAPture Reagent consists of streptavidin conjugated with the complementary single stranded DNA molecule which can hybridize on the sensor chip surface (gehealthcare.com). The biotinylated ligand under investigation can be then immobilised on the CAPture Reagent, followed by the required analysis with the appropriate analyte. Finally, the sensor chip surface is fully regenerated allowing re-immobilisation of fresh ligand for the next experimental cycle (Fig. 4.8A).

To test the reliability of the CAP chip, BSG contained in tissue culture supernatant was injected over biotinylated MEM-M6/4, immobilised on Biotin CAPture reagent. CAP chip demonstrated satisfactory repeatability as three
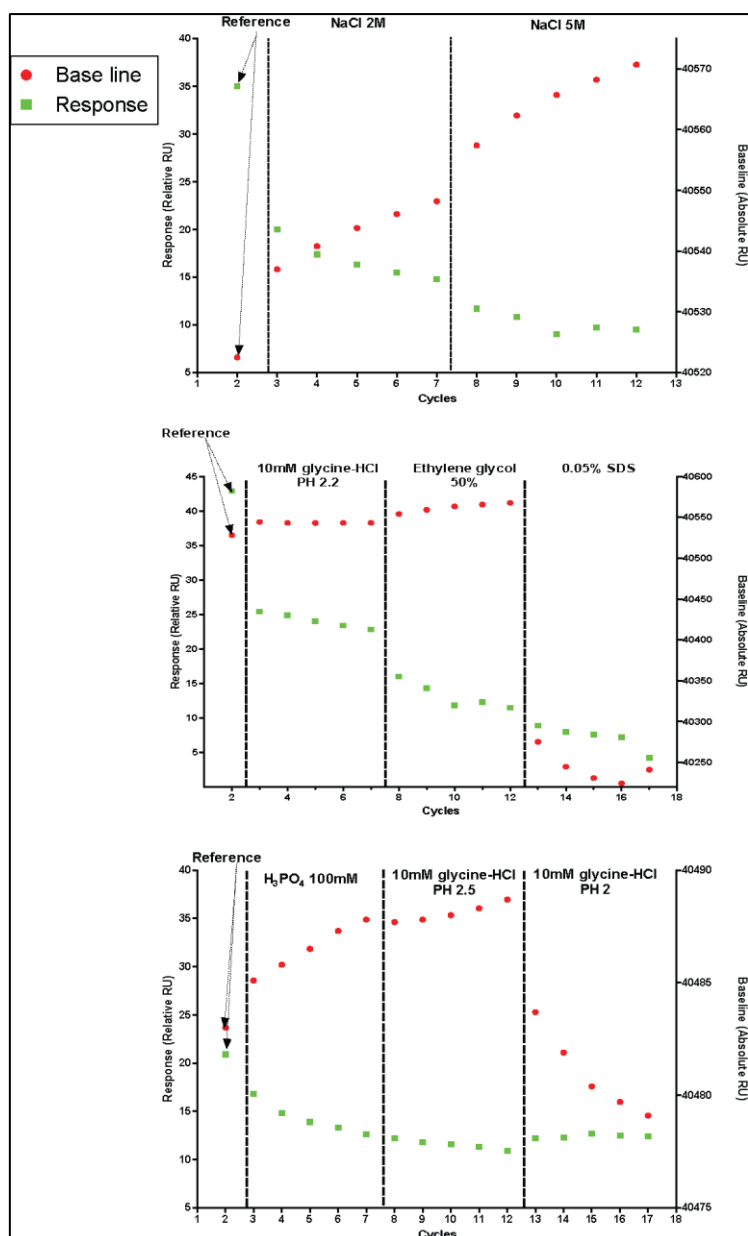
**Figure 4.7 Regeneration scouting of SA chip.**

Trend plots of regeneration scouting experiment by using an SA chip. MEM-M6/4 was *in vitro* biotinylated and captured on the surface of an SA sensor chip at about 400 response units. Five repeated analyte (BSG) binding and regeneration cycles were tested for each regeneration solution. Report points were set shortly before analyte injection for baseline (red dots) and shortly after sample injection for analyte response (green dots). The points of the second cycle indicate the starting values while each of the subsequent points demonstrates the effects of the previous cycle. Analyte responses were obtained after injecting tissue culture supernatant containing BSG over immobilised antibody, at a flow rate of 20μl/min for 30s. For each injection, the analyte response was plotted relative to the baseline of the previous regeneration cycle. Each graph represents a set of experiments, tested on the same flowcell.
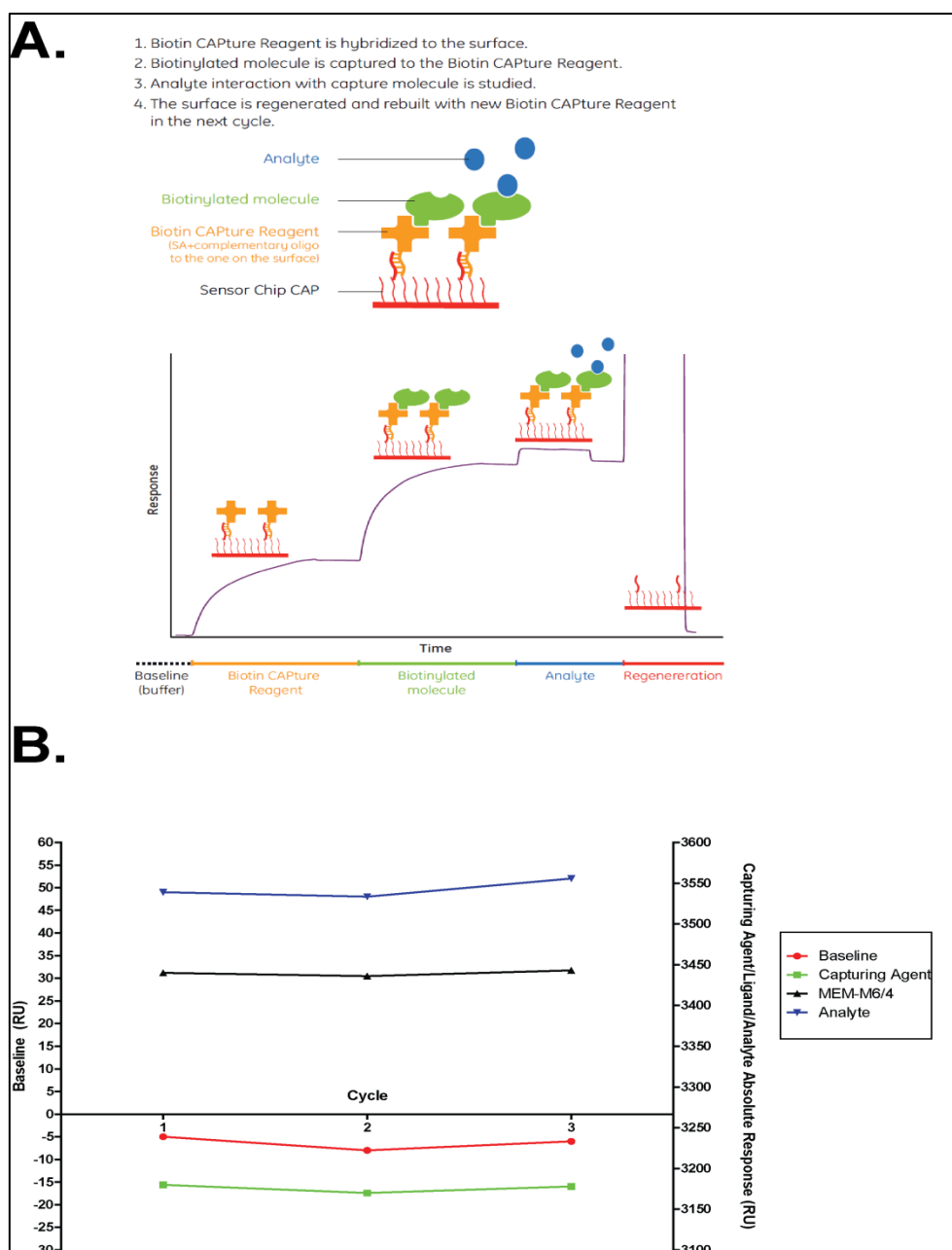
**Figure 4.8 CAP chip provides consistent responses after repeated analyte binding and regeneration cycles.**

*A.* A schematic diagram showing the principle on which CAP chip is based (picture adapted from www.gehealthcare.com)

*B.* Testing the repeatability of CAP chip after three analyte binding and regeneration cycles. The capture reagent was immobilised on the surface of a CAP chip at about 3150 response units followed by capturing of *in vitro* biotinylated MEM-M6/4 at about 300 response units. Analyte responses were obtained after injecting unpurified BSG contained in tissue culture supernatant, over immobilised antibody, at a flow rate of 20µl/min for 30s. The surface was regenerated by using the regeneration solution provided by the manufacturer.

repeated cycles of analyte binding and surface regeneration, gave consistent analyte responses and a steady baseline trend (Fig. 4.8B). Therefore CAP chip was chosen for the subsequent SPR experiments.

## 4.3.6.2 Measurement of affinity and kinetic parameters of mouse and humanised MEM-M6/4 and MEM-M6/8 antibodies

MEM-M6/4 and MEM-M6/8 as well as their humanised versions, were subjected to biophysical analysis. For this purpose, BSG was recombinantly expressed and purified from tissue culture supernatant by affinity chromatography on a nickel-charged Sepharose column (Fig. 4.9A). The purified protein was then subjected to gel filtration to separate any aggregates that can confound SPR measurements and to exchange the protein into the SPR buffer. The protein eluted from the gel filtration column as a monodisperse peak (Fig. 4.9A). The expected elution volume for BSG monomer was 34.6ml, corresponding to an estimated size of 56.3kDa. The gel filtrated protein was analysed by SDS-PAGE under reducing conditions to confirm its purity and presence at the correct size (Fig. 4.9B).

For the measurement of (hu)MEM-M6/4 and (hu)MEM-M6/8 kinetic parameters, *in vitro* biotinylated antibodies were immobilised on the surface of a CAP chip followed by injection of a dilution series of monomeric BSG across the SPR sensor chip. Each group of sensorgrams was obtained after subtracting the signal of the reference flow cell where the appropriate antibody isotype control was captured (Fig. 4.9C).

A 1:1 Langmuir binding model was separately fitted to the association and dissociation parts of the binding curves, allowing the calculation of association and dissociation rate constants, $k_a$ and $k_d$ respectively (Fig. 4.9C, D). The equilibrium dissociation constant ($K_D$) *was* calculated after plotting the reference-subtracted maximum responses of each experiment as a function of analyte concentration (Fig. 4.9C, D). The Chi$^2$ (also known as coefficient of determination or R$^2$), a measure of the difference between the experimental data and the fitted curve, was taken into account as an indication of the goodness of the fit.

The estimated $K_{Ds}$ for MEM-M6/4 and MEM-M6/8 ($3.93 \times 10^{-8}$M and $1.35 \times 10^{-6}$M respectively) vastly differ to those reported previously ($6.69 \times 10^{-11}$ M and $5.38 \times 10^{-10}$ M respectively; Koch *et al.*, 1999), by 3 to 4 orders of magnitude (Fig. 4.9D).

A.

B.

C.

D.

| Antibody | $k_a$ (M$^{-1}$s$^{-1}$) | Association Fitting Chi$^2$ (RU$^2$) | $k_d$(s$^{-1}$) | Dissociation Fitting Chi$^2$ (RU$^2$) | $K_D$(M) | Steady state Fitting Chi$^2$ (RU$^2$) |
|---|---|---|---|---|---|---|
| MEM-M6/4 | $(9.67\pm0.14)\times10^4$ | 4.90 | $(4.292\pm0.004)\times10^{-3}$ | 0.327 | $(3.9\pm0.7)\times10^{-8}$ | 7.78 |
| huMEM-M6/4 | $(1.93\pm0.05)\times10^5$ | 0.120 | $1.167\pm0.009$ | 0.05 | $(3.8\pm0.2)\times10^{-6}$ | 0.0576 |
| MEM-M6/8 | $(5.09\pm0.01)\times10^5$ | 8.02 | $0.1341\pm0.0005$ | 0.604 | $(1.4\pm0.1)\times10^{-6}$ | 10.2 |
| huMEM-M6/8 | $(1.3\pm0.1)\times10^5$ | 0.523 | $1.058\pm0.006$ | 0.04 | $(1.1\pm0.2)\times10^{-6}$ | 0.205 |
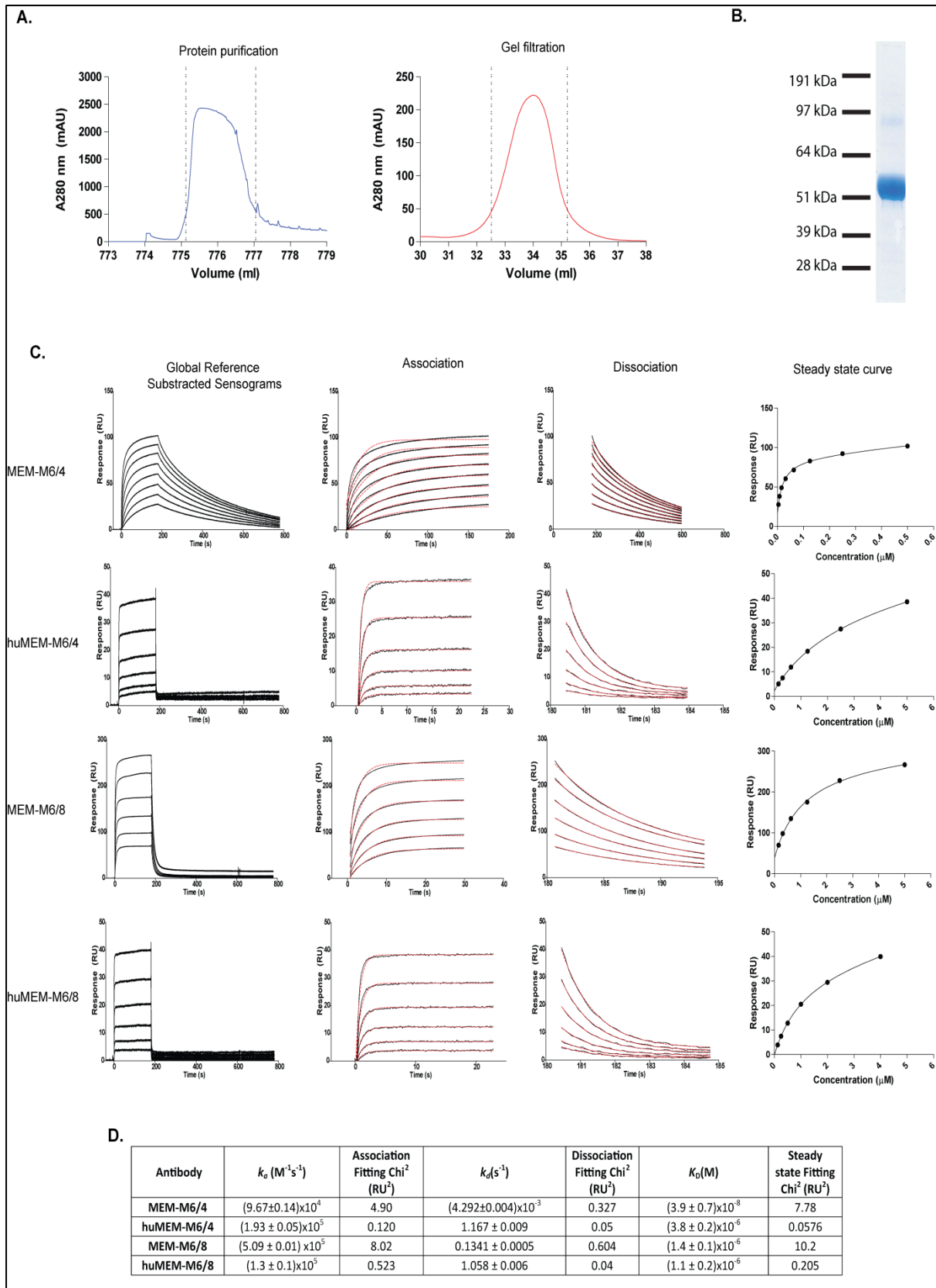
**Figure 4.9 Biophysical analysis of the binding of mouse and humanised MEM-M6/4 and MEM-M6/8 to BSG, by using Surface Plasmon Resonance.**

***A.*** BSG-BLH was affinity purified from tissue culture supernatant, on a nickel column (left), followed by gel filtration (right) to separate monomeric BSG from other forms. The eluate in each of the experiments was monitored at 280 nm in real-time and the peak fractions containing protein (between dashed lines) were pooled. The expected gel filtration elution volume was ~34.6ml.

***B.*** Denaturing SDS-PAGE analysis of gel filtrated BSG. The protein was visualised using Coomassie brilliant blue. The expected band size was 56.3 kDa.

***C.*** Reference subtracted sensorgrams (black lines) from the injection of a 2-fold dilution series of BSG (analyte), over the immobilised *in vitro* biotinylated antibodies (ligands). The analyte was injected at a flow rate of 100µl/min, with a contact time of 180s and a dissociation time of 600s. For the calculation of the association ($k_a$) and dissociation ($k_d$) rate constants, a simple Langmuir binding model (red dashed lines) was separately fitted to the association and dissociation parts of the reference subtracted sensorgrams. For the calculation of the equilibrium dissociation constants ($K_D$) reference-subtracted binding data were plotted as a binding curve (steady state curve). The biotinylated antibodies were immobilised on the chip surface at about 600RU. mIgG or hIgG were used as references, accordingly. Concentration range of BSG used in each experiment: MEM-M6/4, 500-3.9nM; MEM-M6/8, 5µM-0.15µM; huMEM-M6/4, 5-0.15µM; huMEM-M6/8, 4-0.125 µM.

***D.*** Tables with the equilibrium and kinetic parameters estimated for the binding of mouse or humanised MEM6-M/4 and MEM6-M/8 to BSG. For each model, the fit to the experimental data is indicated as the Chi$^2$ value. The calculated values for the $K_D$, $k_a$ and $k_d$ are indicated with the standard error.

Whereas huMEM-M6/4 lost a fraction of its affinity for BSG in comparison to the mouse original antibody, the affinity of huMEM-M6/8 was fully retained (Fig. 4.9D). Nevertheless, considering that the $K_D$ between an antibody and its target is typically in the nM range, both (hu)MEM-M6/4 and (hu)MEM-M6/8 are low affinity antibodies.

The low affinity of MEM-M6/8 for BSG is likely the reason for the inability of this to antibody stain human erythrocytes and to prevent erythrocyte invasion in parasite culture. Despite the affinity of MEM-M6/4 for BSG being also low, this antibody was able to bind BSG exposed to human erythrocytes. The latter antibody, however, could only moderately inhibit erythrocyte invasion when tested in erythrocyte invasion assays. As mentioned earlier, it is likely that MEM-M6/4 binds an epitope on BSG which is nearby RH5 binding site, causing a steric effect to the RH5-BSG interaction which in turn reduces invasion efficiency to a certain level.

### 4.3.7 Selection of a mouse anti-BSG monoclonal antibody

As described earlier in this Chapter, two anti-BSG monoclonal antibodies, MEM-M6/4 and MEM-M6/8, were successfully humanised by CDR grafting. Nonetheless, neither parental mouse nor humanised antibodies inhibited the RH5-BSG interaction to the levels required to prevent erythrocyte invasion. Therefore, it was necessary to find an alternative source of anti-BSG antibodies to serve as CDR donors for the development of an anti-BSG humanised antibody, capable of abolishing erythrocyte invasion with high efficacy. In order to maximise the ability to screen for highly efficient antibodies, we decided to create a new panel of anti-BSG monoclonal antibodies, by directly immunising animals and then selecting for high affinity antibodies which are able to potently block erythrocyte invasion.

Following the protocol described in Fig. 4.10A biotinylated BSG-BLH was recombinantly expressed and purified from tissue culture supernatant by affinity chromatography on a nickel loaded Sepharose column (Fig. 4.10B). To confirm that BSG was expressed at the expected size and eluted from the nickel column, the elution peak fraction was analysed by denaturing SDS-PAGE (Fig. 4.10B). A single band at about 56 kDa indicated the presence of BSG in the elution peak fraction. BSG was then used to immunise a five week old BALB/c male mouse, following the prime-boost regime shown in Fig. 4.10A. The immunisation scheme comprised of three injections, of a BSG-TiterMax Gold (adjuvant) emulsion, with a four week
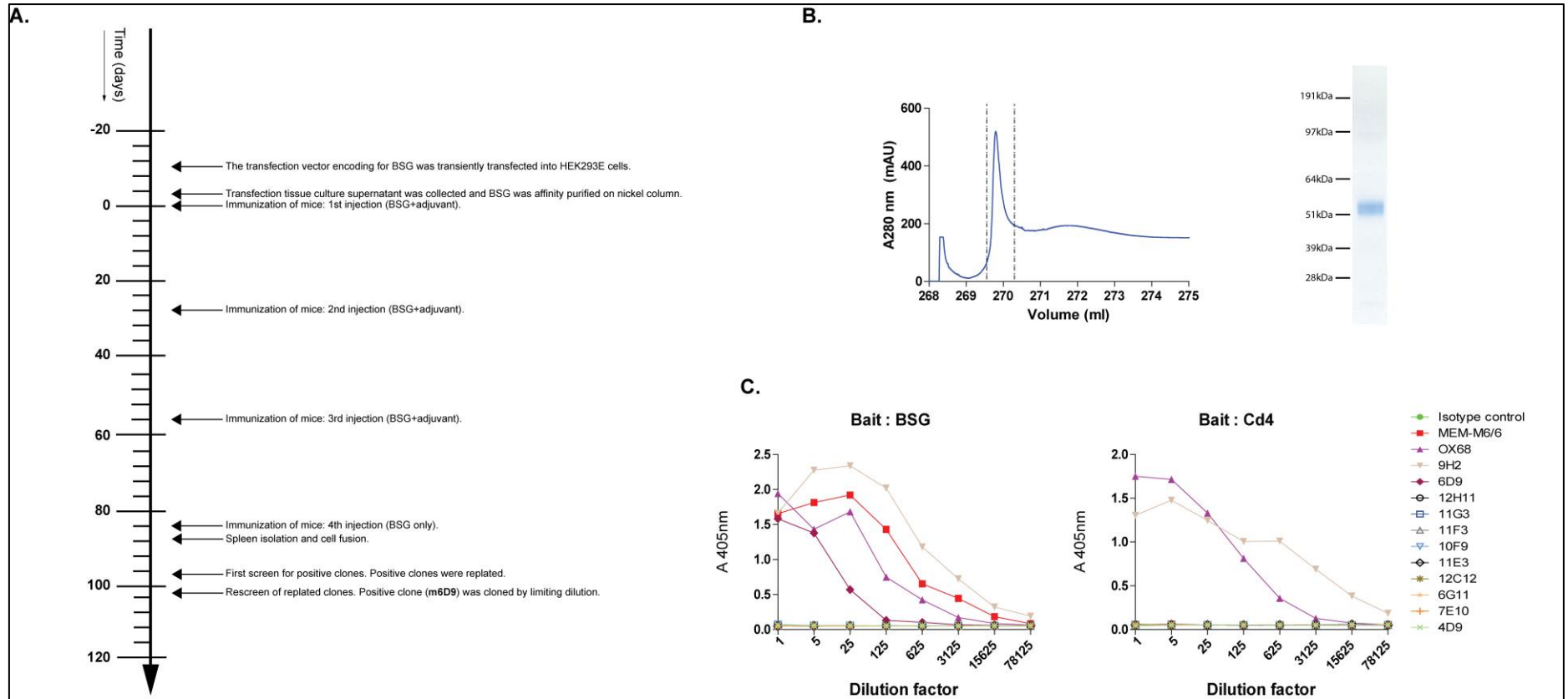
**Figure 4.10 Overview of the procedure followed for creation and establishment of the hybridoma line m6D9 which secretes an anti-BSG monoclonal antibody**.

**A.** Purified BSG (see *B)*, expressed in HEK293E cells, was used to immunise mice. Hybridomas were generated by cell fusion of splenocytes with SP2/0 myeloma cells, and supernatants were screened for positives by using ELISA (data not shown). Positive clones were re-plated and rescreened. M6D9 was the only positive in the second screen and it was cloned by limiting dilution.

**B.** The purification traces of BSG (left) as monitored by obtaining the absorbance at 280nm. Peak fractions containing the protein (between the dashed lines) were pooled, analysed by denaturing SDS-PAGE and visualised using Coomassie brilliant blue (right). The expected band size was 56.3 kDa.

**C.** Hybridoma tissue culture supernatants were tested for the presence of anti-BSG antibodies by ELISA. Biotinylated BSG or Cd4 from tissue culture supernatant were immobilised on a streptavidin-coated plate at concentrations sufficient for complete saturation of the available binding surface, followed by incubation with a five-fold dilution series of each hybridoma supernatant. An alkaline phosphatase-conjugated anti-mIgG antibody was used as secondary antibody. 6D9 hybridoma supernatant was immunoreactive against BSG, whereas 9H2 hybridoma supernatant contained a mAb which bound Cd4 tag. The anti-BSG MEM-M6/6 or the anti-Cd4 OX68 monoclonal antibodies and a mIgG isotype were used as positive and negative controls, respectively (all at starting concentration 1µg/ml).

interval between injections. Four weeks after the last injection, the mouse was boosted with an additional injection of BSG without adjuvant and left for another three days before the spleen was isolated and dissociated to single cells, which were then fused to SP2/0 myeloma cells.

Ten days after fusion, hybridoma tissue culture supernatants were screened for the presence of anti-BSG antibodies by ELISA. The cell culture supernatant of 11 hybridoma clones (9H2, 6D9, 12H11, 11G3, 11F3, 10F9, 11E3, 12C12, 6G11, 7E10, 4D9) was reactive against BSG and negative against Cd4 tag (data not shown; the ELISA screen experiment was entirely done by Dr Nicole Muller-Sienerth and Dr Nicole Staudt). All eleven clones were re-plated in a 48 well plate and rescreened five days later. Out of eleven initially positive clones, nine clones were negative (12H11, 11G3, 11F3, 10F9, 11E3, 12C12, 6G11, 7E10, 4D9) in the rescreen, one secreted antibodies against the Cd4 tag (9H2), and one (6D9) remained positive (Fig. 4.10 C; Dr Nicole Muller-Sienerth and Dr Nicole Staudt are credited for contributing in animal immunisation, cell fusion and first ELISA screen for positive clones). These results show that a hybridoma line secreting an anti-BSG monoclonal antibody was successfully established.

### 4.3.8 Characterisation of m6D9 anti-BSG monoclonal antibody

Mouse 6D9 (m6D9) hybridoma was cloned by limiting dilution and after further expansion, m6D9 mAb was purified from cell culture supernatant by affinity chromatography on a protein G column (Fig. 4.11A). Purified m6D9 retained its ability to bind to BSG by ELISA (Fig. 4.11B). The isotype of m6D9 was determined by using an IsoQuiCκ strip (as described in materials and methods) and was found to be an IgG2A (Fig. 4.11C). To test whether m6D9 was able to block the RH5-BSG interaction *in vitro* in AVEXIS, biotinylated RH5 bait was immobilised on a streptavidin-coated plate and probed with β-lactamase tagged BSG pentamer prey, which was pre-incubated with a dilution series of purified m6D9. M6D9 was able to block the interaction between RH5 and BSG with efficacy levels similar to MEM-M6/6 which was used as positive control (Fig. 4.11D).

The ability of m6D9 to inhibit erythrocyte invasion was tested by *P. falciparum* growth inhibition assay. A parasite culture was synchronised by sorbitol treatment and 36-40 hours post invasion a dilution series of m6D9 was added into the culture
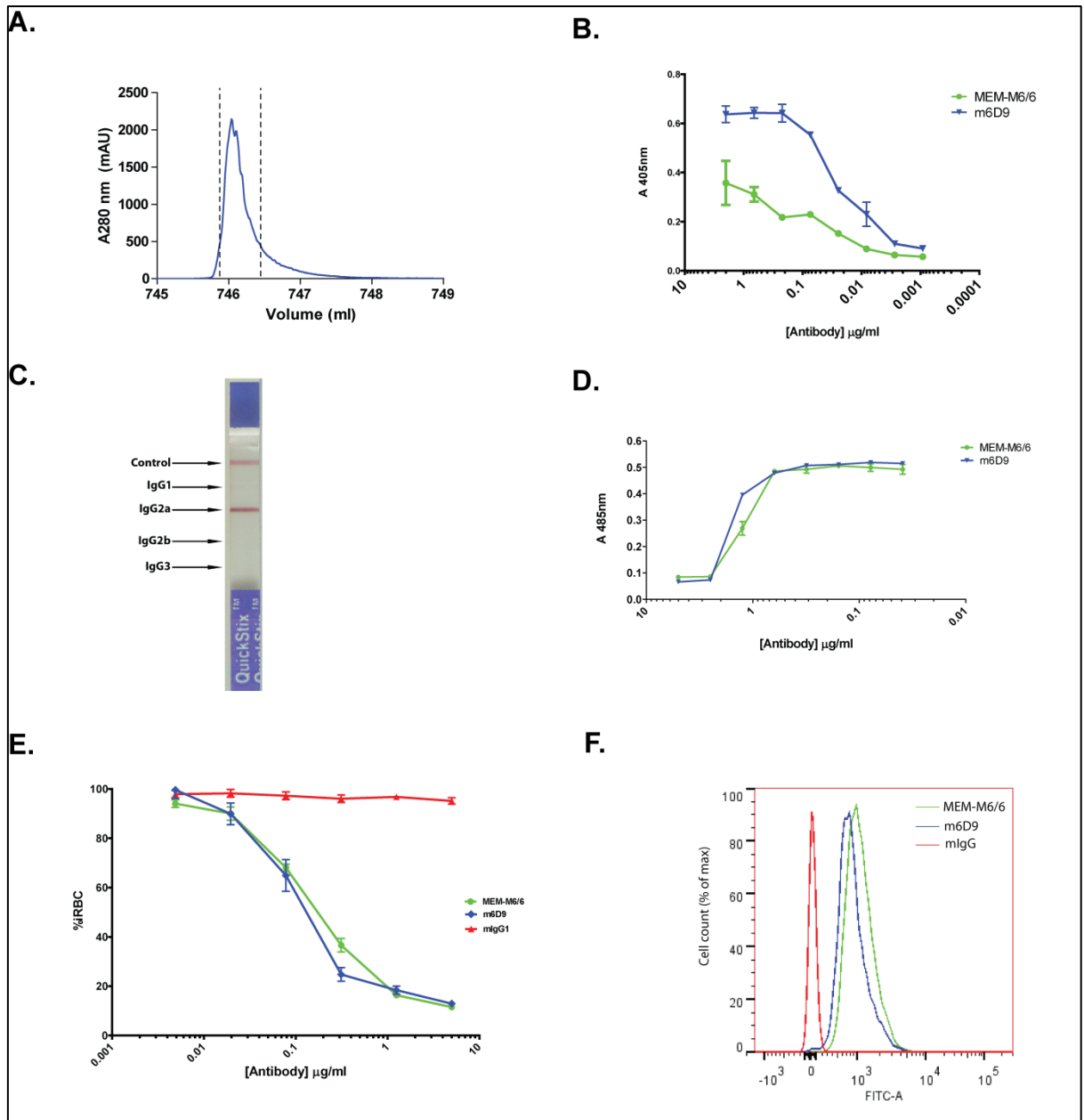
**Figure 4.11 Characterisation of m6D9 monoclonal antibody.**

**A.** M6D9 was affinity purified from hybridoma tissue culture supernatant, on protein G column. The eluate was monitored at 280 nm in real-time and the peak fractions containing antibody (between dashed lines) were pooled.

**B.** Protein G purified m6D9 bound to BSG, in an ELISA assay. BSG-BLH from tissue culture supernatant was immobilised on a streptavidin-coated plate at concentrations sufficient for complete saturation of the available binding surface. A dilution series of purified m6D9 was used as primary antibody and an anti-mouse IgG conjugated with alkaline phosphatase as secondary.

**C.** M6D9 is IgG2A isotype as determined by using an IsoQuiκ strip.

**D.** M6D9 blocked the interaction between RH5 and BSG interaction in an AVEXIS assay**.** RH5-BLH from tissue culture supernatant was immobilised on a streptavidin-coated plate and probed against pentameric β-lactamase tagged BSG which was pre-incubated with a dilution series m6D9.

**E.** Purified m6D9 and was very potent in interfering with erythrocyte invasion when included into the medium of *P.falciparum* infected erythrocytes. A synchronised parasite culture (schizonts) was incubated overnight with a dilution series of m6D9 followed by fixing, staining and analysis by flow cytometry. The graph shows the percentage of infected red blood cells (iRBC) as a function of antibody concentration.

**F**. Purified m6D9 stained human erythrocytes. Red blood cells were incubated with m6D9, followed by incubation with a FITC-conjugated anti mouse-IgG secondary and analysis by flow cytometry. The histogram shows the normalised cell count as a function fluorescence intensity at the FITC emission wavelength.

Data in *B, D* and *E* are shown as mean ± standard error; *n*=3. Where applicable the anti-BSG antibody MEM-M6/6 was used as positive control, and a mIgG isotype as negative.

medium and incubated overnight. Cultured erythrocytes were then fixed, stained and analysed by flow cytometry. M6D9 prevented erythrocyte invasion at the levels similar to the positive control antibody MEM-M6/6 (Fig. 4.11 E). To ensure that the blocking mechanism involved the masking of BSG exposed on the surface of red blood cells by m6D9, the binding of m6D9 to erythrocytes was tested by flow cytometry. M6D9 was capable of binding to erythrocytes at levels comparable to MEM-M6/6 positive control (Fig. 4.11F).

These data demonstrate that m6D9 is a high efficacy antibody which blocks the interaction between RH5 and BSG *in vitro,* and prevents erythrocyte invasion in parasite culture. Therefore, it was considered a suitable antibody to serve as CDR donor for the development of an anti-BSG humanised antibody

### 4.3.9 Development of hu6D9, a humanised anti-BSG monoclonal antibody

The procedure followed for the development of a humanised version of m6D9 (hu6D9), was the same as the one described in section 4.3.4. Sequence analysis of the m6D9 V region sequences (Fig. 4.12A) identified IGHV1-3*01 and IGKV3-15*01 as the human variable segments displaying the highest sequence similarity in FRs to m6D9 variable heavy and light chains sequences, respectively (Fig. 4.12B).

Interestingly, m6D9 variable heavy chain had a cysteine residue within CDR2 (position 58, IMGT numbering) (Fig 4.12A), which was in addition to the two canonical cysteine residues already in place in FR1 and FR3 (positions 23 and 104, IMGT numbering), found in the vast majority of immunoglobulin superfamily domain sequences. While the additional cysteine appears to be a result of affinity maturation of m6D9, it may cause problems in the formation of the correct disulfide bonds in the humanised antibody. Nevertheless, the additional cysteine was retained in the humanised sequence, hoping that it will not cause any conformational issues. Thus, for the development of a humanised 6D9 variable heavy chain (huVH), the CDRs from m6D9 variable heavy chain were engrafted into human IGHV1-3*01 FRs (Fig. 4.12B).

A predicted N-linked glycosylation site within the FR2 of m6D9 variable light chain further complicated the analysis (Fig. 4.12A). This site was to be removed during humanisation by CDR grafting, since all the original FR sequences are replaced by those of the closest human V allele. The size of the putatively attached

**A.**

| Variable region | FR1 | CDR1 | FR2 | CDR2 | FR3 | CDR3 | FR4 |
|---|---|---|---|---|---|---|---|
| VH | EVQLQQSGPELVKTGASVKISCKA | GYSFSDDY | MHWVKQSHGKSLEWIGY | ISCYNGVP | SYNQKFKGKATFTVDTSSSTAYMQFSSLTSEDSAVYYC | ARGGNHGFYYHAMDY | WGQGTSVTVSS |
| VL | DIVLTQSPAILSVSPGERVSFSCRAS | QSIGTG | IHWYQQRTNGSPRLLIK | FAS | ESISGIPSRFSGSGSGTDFTLSINSVESEDIADYFC | QQSTSWPYT | FGGGTKLEIK |

**B.**

| Variable region | Closest human V region | FR1 | CDR1 | FR2 | CDR2 | FR3 | CDR3 | FR4 |
|---|---|---|---|---|---|---|---|---|
| huVH | IGHV1-3*01 | QVQLVQSGAEVKKPGASVKVSCKAS | GYSFSDDY | MHWVRQAPGQRLEWMGW | ISCYNGVP | KYSQKFQGRVTITRDTSASTAYMELSSLRSEDTAVYYC | ARGGNHGFYYHAMDY | WGQGTTVTVSS |
| huVL | IGKV3-15*01 | EIVMTQSPATLSVSPGERATLSCRAS | QSIGTG | LAWYQQKPGQAPRLLIY | FAS | TRATGIPARFSGSGSGTEFTLTISSLQSEDFAVYYC | QQSTSWPYT | FGQGTKLEIK |
| huVLNTCHFR2 | | EIVMTQSPATLSVSPGERATLSCRAS | QSIGTG | IHWYQQRTNGSPRLLIK | FAS | TRATGIPARFSGSGSGTEFTLTISSLQSEDFAVYYC | QQSTSWPYT | FGQGTKLEIK |

**C.**

| Variable region | Closest human V region | Signal peptide sequence |
|---|---|---|
| huVH | IGHV3-1*01 | MDWTWRILFLVAAATGAHS |
| huVL or huVLNTCHFR2 | IGHV3-15*01 | MEAPAQLLFLLLLWLPDTTG |

**D.**
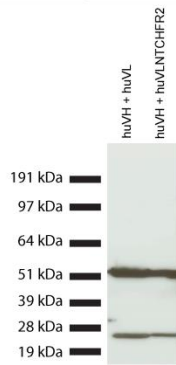


**E.**
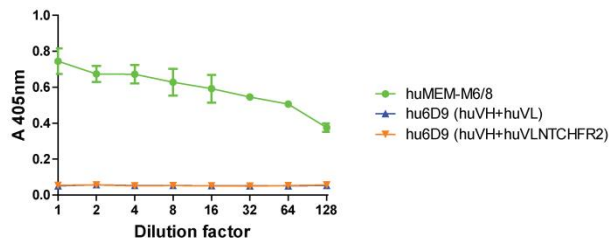


**F.**
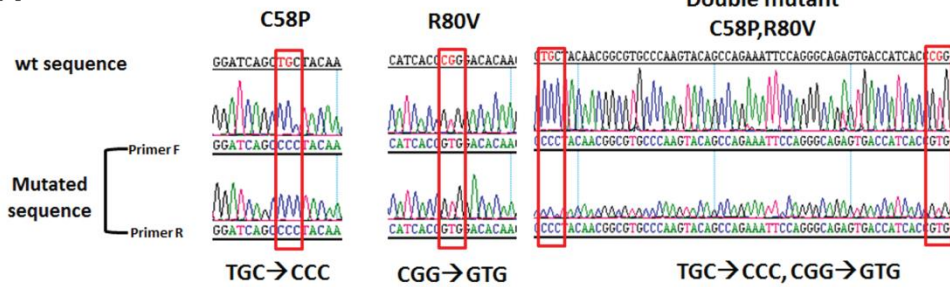


**G.**
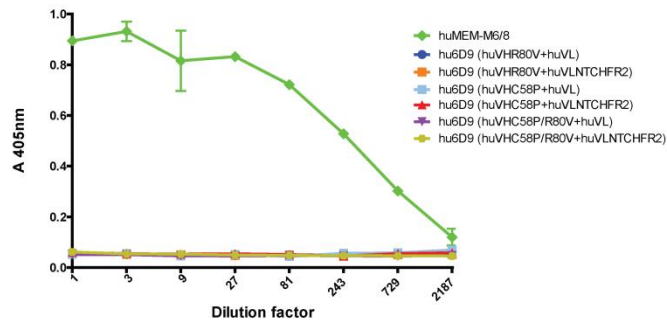
**Figure 4.12 Sequence analysis and humanisation of m6D9 by CDR grafting.**

**A.** Sequence analysis and verification of m6D9 variable regions. The table shows the amino acid sequence of m6D9 rearranged variable heavy (VH) and light (VL) chains as derived from sequence analysis of the amplified variable regions. Of note is the N-linked glycosylation site (green) in FR2 of light chain, and the additional cysteine (red) in heavy chain CDR2. The valine at position 80 (IMGT numbering) of the variable heavy chain is shown in blue.

**B.** The table shows the amino acid sequences of hu6D9 variable heavy (huVH) and light chain, after CDR grafting. Because an N-linked glycosylation site exists within the second FR of m6D9 (see *A.*), two different humanised variable light chains were synthesised: one retaining m6D9 FR2 intact (huVLNTCHFR2), and one exchanging it with the equivalent region of the closest human allele (huVL). The arginine at position 80 (IMGT numbering) of the variable heavy chain is shown in blue.

**C.** The amino acid sequences of the signal peptides that were incorporated upstream the engineered variable regions.

**D.** Western blot showing recombinant expression of hu6D9. Supernatants containing antibodies were harvested, resolved under reducing conditions by SDS-PAGE, blotted, and probed using an HRP conjugated anti-hIgG. Two bands at 55 and 28 kDa were obtained corresponding to the antibody heavy and light chain, respectively.

**E.** Hu6D9 lost an important fraction of its affinity for BSG, as assessed by ELISA.

**F.** Sequencing chromatographs which confirm the mutations introduced in hu6D9 variable heavy chain.

**G.** None of the hu6D9 mutants restored affinity for BSG as demonstrated by ELISA.

Data in *E* and *G* are shown as mean ± standard error; *n*=3.

carbohydrate and how this interplays with the protein moiety is unpredictable, and random removal of the N-linked glycosylation site may affect V region tertiary structure and consequently antibody affinity. Hence, two different humanised variable chains were designed. In the first, m6D9 variable light chain was fully humanised (huVL) by engrafting the mouse CDRs into human IGKV3-15*01 FRs (Fig. 412B). In the second humanised sequence (huNTCHFR2), only FR1, FR3 and FR4 were exchanged, keeping the original mouse FR2 sequence intact. As a result, the N-linked glycosylation site was retained.

Hu6D9 engineered DNA sequences were incorporated downstream of the signal peptide sequence of the respective CDR acceptor chain sequence (Fig. 4.12C), codon optimised for expression in human cells and synthesised by gene synthesis.

## 4.3.10 Characterisation of hu6D9 humanised anti-BSG antibody

For recombinant expression of hu6D9, synthesised variable heavy and light chain sequences were sub-cloned into the antibody heavy and light chain expression plasmids developed in Chapter 3, followed by transfection in HEK293F cells. Six days later, tissue culture supernatant was analysed by Western blot for the presence of antibody. Two bands at 55 and 28 kDa corresponding to antibody heavy and light chain respectively, confirmed recombinant antibody expression of both hu6D9 versions (huVH+huVL and huVH+huVLNTCHFR2) (Fig. 4.12D). The ability of hu6D9 to bind BSG was tested by ELISA. Neither of the two hu6D9 variants was reactive against BSG (Fig. 4.12E), suggesting that hu6D9 has lost a significant fraction of its affinity for BSG during humanisation.

CDR grafted antibodies often exhibit greatly reduced or completely abolished binding affinity as a consequence of incompatibility of non-human CDRs with human FRs (Lo, 2004; Almagro and Fransson, 2008). The affinity can be partially or fully restored, only after re-introducing some of the parental murine FR residues. Nevertheless, the identification of such residues is not straight forward and requires skills in structural biology and *in silico* three dimensional modelling which is beyond the expertise of my laboratory. Hence, as an alternative I sought to mutate the apparent amino acid residue which may have caused incompatibilities between non-human CDRs and human FRs, the cysteine at position 58 (C58; IMGT numbering).

Sequence analysis of m6D9 VH, revealed that it belongs to the mouse IGHV1 subgroup of V regions and it is most similar to IGHV1-31*01. Closer examination of mouse IGHV1 subgroup, demonstrated that 148 out of 155 (95.48%) mouse V alleles classified as IGHV1 (including IGHV1-31*01) in IMGT database, had proline at position 58 (IMGT numbering) of the CDR2, instead of the cysteine in m6D9 VH. Therefore, it was reasonable to assume that mutating cysteine at position 58 (IMGT numbering) to proline might be beneficial for the antibody affinity.

Another amino acid which was potentially involved in the loss of hu6D9 affinity for BSG, was a valine residue in FR3 (position 80 by IMGT numbering, position 71 by Kabat numbering) of m6D9 VH (Fig 4.12A). The positioning and conformation of heavy chain CDR2, has been proposed to be largely dependent on the nature of the amino acid residue that occupies the position 80 of heavy chain FR3, and changes in this amino acid during humanisation may result in displacement of CDR2 (Tramontano *et al.*, 1990). In huVH, the valine at position 80 had been replaced by an arginine (R80). Considering that CDR2 also contains an unusual cysteine, the V80R substitution may have altered CDR2 conformation in a way that disrupts disulfide bond formation, and therefore affecting the correct folding of the variable heavy chain.

To test whether C58 and/or R80 affected antibody binding, I mutated these amino acids to proline and valine respectively. By using site directed mutagenesis, single (C58P or R80V) and double mutants (C58P/R80V) of huVH were generated (Fig. 4.12F). A number of hu6D9 variants were expressed by co-transfecting different combinations of heavy and light chain encoding vectors into HEK293F cells. Hu6D9 variants, contained in tissue culture supernatant, were then tested for binding to BSG by ELISA. None of the hu6D9 mutants bound to BSG (Fig. 4.12G), suggesting that either more radical changes are likely required to restore hu6D9 affinity for BSG, or the loss of affinity is not reversible.

## 4.3.11 Development and characterisation of ch6D9, a chimeric anti-BSG monoclonal antibody

Humanisation of m6D9 resulted in a problematic hu6D9, which had lost a significant fraction of its affinity for BSG. Attempts to restore affinity by mutating certain amino acid residues in hu6D9 variable heavy chain were unsuccessful. Thus,

the antibody chimerisation approach was adopted, as an alternative to humanisation. To this end, m6D9 variable heavy and light chain sequences (Fig. 4.12A) were codon optimised, incorporated downstream of the respective heavy and light chain signal peptide sequences shown in Fig 4.12C, and synthesised by gene synthesis. For recombinant expression of chimeric 6D9 (ch6D9), synthesised DNA sequences were sub-cloned into the antibody heavy and light chain expression plasmids developed in Chapter 3, followed by transfection in HEK293F cells. Six days post transfection, tissue culture supernatant was collected and ch6D9 was purified by affinity chromatography on protein G loaded Sepharose column (Fig 4.13A). Protein G purified ch6D9 was able to bind BSG *in vitro,* as shown by ELISA (Fig 4.13B).

The ability of ch6D9 to block the interaction between RH5 and BSG *in vitro*, was assayed by AVEXIS. Ch6D9 exhibited potent blocking capacity, at levels similar to the MEM-M6/6 positive control (Fig. 4.13C). To validate this result, the efficacy of ch6D9 to inhibit *P. falciparum* erythrocyte invasion was assessed in a parasite growth inhibition assay. Ch6D9, neutralized erythrocyte invasion in a dose dependent manner, in all *P. falciparum* strains tested (3D7, Gb4, HB3 Dd2). The efficacy of ch6D9 to inhibit erythrocyte invasion was analogous to MEM-M6/6 positive control (Fig. 4.13D). These results suggest that ch6D9 is a high efficacy antibody and can be considered for therapeutic purposes.

### 4.3.11.1 Ch6D9 demonstrates reduced binding to FcγRIIA and C1q

The plasmid system for recombinant expression of antibodies described in Chapter 3, was primarily designed for the development and expression of engineered anti-BSG antibodies with therapeutic potential. Such antibodies aim to prevent erythrocyte invasion by inhibiting the interaction between RH5 and BSG. However, the trigger of ADCC and CDC antibody effector functions (section 1.4.2) would be undesirable and detrimental, since the human host would recognise itself as foreign. To eliminate the side effects arising from the stimulation of antibody effector functions, several previously characterised mutations (E233P / L234V / L235A / G236Δ / A327G / A330S/P331S) were introduced to the Fc region of hIgG1 which was incorporated into the heavy chain expression vector (Armour *et al.*, 1999, 2003, 2006). Moreover, to avoid allotype rejection phenomena, the mutations K214T/D356E/L358M (Greenwood and Clark, 1993; Armour *et al.*, 2006) were also introduced to the the Fc region of hIgG1 during gene synthesis (Chapter 3).
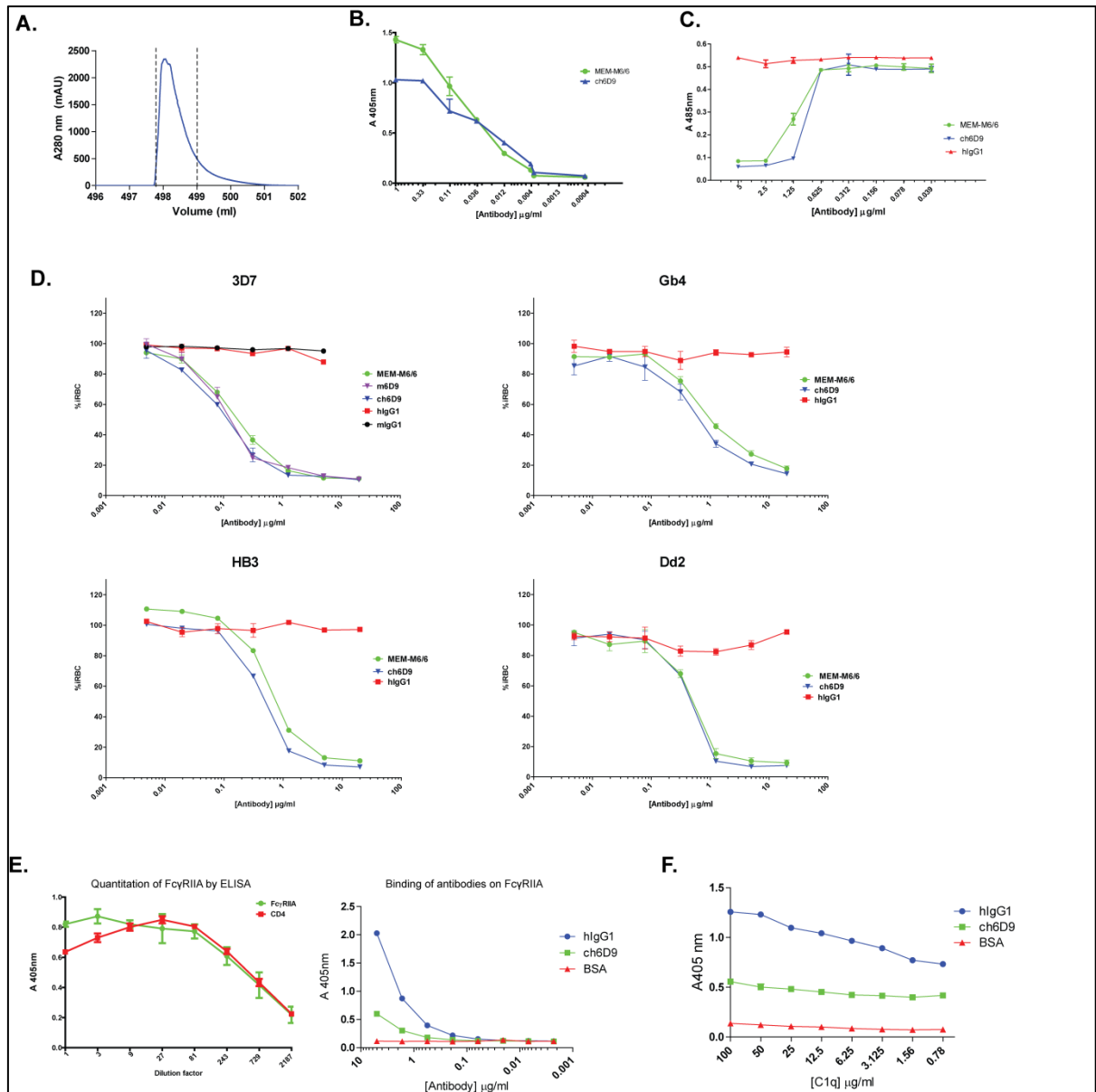
**Figure 4.13 Development and characterisation of ch6D9 chimeric anti-BSG monoclonal antibody.**

**A.** Ch6D9 was expressed recombinantly and affinity purified from tissue culture supernatant on a protein G column. The eluate was monitored at 280 nm in real-time and the peak fractions containing antibody (between dashed lines) were pooled.

**B.** Protein-G purified ch6D9 bound to BSG, in an ELISA assay. BSG-BLH from tissue culture supernatant was immobilised on a streptavidin-coated plate at concentrations sufficient for complete saturation of the available binding surface. A dilution series of purified ch6D9 was used as primary antibody and an anti-human IgG conjugated with alkaline phosphatase as secondary.

**C.** Ch6D9 blocked the interaction between RH5 and BSG interaction, in AVEXIS. RH5-BLH from tissue culture supernatant was immobilised on a streptavidin-coated plate and probed against pentameric β-lactamase tagged BSG which was pre-incubated with a dilution series of protein G purified ch6D9.

**D.** Purified ch6D9 blocked erythrocyte invasion in all *P. falciparum* strains tested. A synchronised parasite culture (schizonts) for each of the 3D7, Gb4, HB3 and Dd2 strains, was incubated overnight with a dilution series of ch6D9 followed by fixing, staining and analysis by flow cytometry. In 3D7 culture, m6D9 was also tested for comparison. The graph shows the percentage of infected red blood cells (iRBC) as a function of antibody concentration.

**E.** Ch6D9 demonstrated reduced binding to FcγRIIA$_{131HIS}$ (right). FcγRIIA α-chain was expressed recombinantly as monomeric biotinylated form and quantitated by ELISA (left). The anti-Cd4 monoclonal antibody OX68 was used as primary antibody and biotinylated Cd4 was used as reference. To test FcγRIIA binding to ch6D9 (right), a dilution 1:9 of tissue culture supernatant containing FcγRIIA was used to immobilise FcγRIIA on a 96 well streptavidin-coated plate. Immobilised FcγRIIA was incubated with a dilution series of ch6D9 or hIgG1 or BSA (negative control). For probing a donkey anti-hIgG F(ab)$_2$ fragment conjugated with alkaline phosphatase was used.

**F.** Ch6D9 demonstrated reduced binding to C1q, in an ELISA-based assay. Equal amounts of ch6D9 or hIgG1 or BSA (negative control) were adsorbed on a 96 well plate, and incubated with a dilution series of human C1q. Then, the plates were incubated with a goat anti-hC1q followed by a rabbit anti-goat conjugated with alkaline phosphatase. Where applicable, the anti-BSG monoclonal antibody MEM-M6/6 was used as positive control. Data in *B, C, D, E* and *F* are shown as mean ± standard error; *n*=3.

To test whether the mutations carried by hIgG1 Fc region were functional, the binding of ch6D9 to FcγRIIA$_{131His}$ was examined. A vector encoding for a biotinylatable form of human FcγRIIA α-chain (P12318) (provided by Dr Yi Sun), was transfected into HEK293E cells. Five days later, the amount of recombinant biotinylated FcγRIIA present in tissue culture supernatant was evaluated by ELISA (Fig. 4.13E). To test whether the binding of ch6D9 to FcγRIIA was diminished, a saturating amount of FcγRIIA was immobilised on a streptavidin coated plate and incubated with a dilution series of ch6D9 or wild type (non-mutated) hIgG1 isotype, followed by probing with an alkaline phosphatase conjugated anti-hIgG F(ab)$_2$ secondary. Ch6D9 demonstrated reduced binding to FcγRIIA in comparison to hIgG1 reference (Fig. 4.13E), providing evidence that the mutations in ch6D9 Fc region are functional in terms of eliminating Fcγ receptor binding. Ideally, the interaction between ch6D9 and other Fcγ receptors would have also been assayed, but attempts to get access to a panel of Fcγ expression constructs optimized for recombinant expression in HEK293 cells (Shields *et al.*, 2001), were unsuccessful.

The activation of the classical complement pathway by ch6D9 was also examined by assaying for its ability to recruit human C1q, in an ELISA based assay. A fixed amount of ch6D9 or unmodified hIgG1 isotype was adsorbed on the plastic bottom of a 96-well plate and incubated with a dilution series of human C1q. The plate was then washed to remove unbound C1q, followed by serial incubation with goat anti-human C1q and rabbit anti-goat IgG conjugated with alkaline phosphatase. The amount of C1q bound to ch6D9 was reduced in comparison to hIgG1 (Fig. 4.13F), suggesting an impaired capability of ch6D9 to activate the classical pathway of complement cascade.

These results demonstrate that the mutations introduced in ch6D9 Fc region are functional, and thus, suggest that ch6D9 is likely to have impaired ability to trigger ADCC and CDC antibody effector functions.

### 4.3.11.2 Epitope mapping of ch6D9 on BSG

To further characterise ch6D9, I attempted to map ch6D9 epitope on BSG by using an array of BSG constructs previously generated in the lab (by Dr Josefin Bartholdson, Dr Cecile Crosnier and Dr Madushi Wanaguru). To narrow down the BSG sequence recognised by ch6D9, soluble, biotinylated, BSG domain 1 (d1) and

2 (d2) were expressed recombinantly and tissue culture supernatants were analysed by ELISA for the presence of recombinant proteins. Both BSG d1 and d2 were reactive against the anti-Cd4 monoclonal OX68, confirming recombinant expression (Fig. 4.14A right panel). The binding of ch6D9 to BSG d1 or d2 contained in tissue culture supernatant was then assayed in another round of ELISA. Ch6D9 bound to BSG d1 but not d2 suggesting that ch6D9 epitope is located somewhere within d1 (Fig. 4.14A left panel).

To refine the epitope of ch6D9 on human BSG (*Hs*BSG), a number of constructs encoding for the Cd4-tagged BSG orthologues in gorilla (*Gorilla gorilla*), chimpanzee (*Pan troglodytes*), and marmoset monkey (*Callithrix jacchus*) were employed. The alignment of the ectodomain from all BSG orthologues is shown in Fig. 4.15. Interestingly, chimpanzee ENSPTRP00000017252 (*Pt*BSG) and gorilla ENSGGOP00000022655 (*Gg*BSG) BSG shared a high degree of similarity with *Hs*BSG (about 94%) whereas the similarity between *Callithrix jacchus* (*Cj*BSG) and *Hs*BSG was lower (about 78%). Leucine at position 175 in *Hs*BSG was missing in chimpanzee BSG (*Pt*BSG) but this was probably due to an error arising from incorrect specification of intron-exon boundaries in ENSEMBL genome browser (www.ensembl.org). The identification and analysis of chimpanzee and gorilla BSG was performed by Dr Madushi Wanaguru based on ENSEMBL 2011. Marmoset monkey BSG was cloned from *Cj*cDNA and sequenced by Dr Leyla Bustamante.

All BSG orthologues were recombinantly expressed in a biotinylated form, by transient transfection of the equivalent expression vector into HEK293E cells. The presence of recombinant protein in tissue culture supernatant was confirmed by ELISA (Fig. 4.14B right panel). The binding of ch6D9 to *Pt*BSG, *Gg*BSG and *Cj*BSG was examined in a second ELISA assay. Ch6D9 bound *Pt*BSG to levels similar to *Hs*BSG (Fig. 4.14B left panel). This was expected because *Hs*BSG and *Pt*BSG are identical in d1 (Fig. 4.15). Ch6D9 was not reactive against *Cj*BSG (Fig. 4.14B left panel). Intriguingly, ch6D9 demonstrated reduced binding to *Gg*BSG in comparison to *Hs*BSG suggesting that certain amino acids that differ between *Hs*BSG and *Gg*BSG are likely to be important for ch6D9 binding to BSG. To further investigate the differential binding to *Gg*BSG, a number of *Hs*BSG mutants (H1-H6) were utilized (provided by Dr Madushi Wanaguru). In these constructs, five residues in *Hs*BSG were singly mutated to those found in *Gg*BSG at

| Site directed mutant | Mutation | Location |
|---|---|---|
| H1 | F27 L | Domain 1 |
| H2 | D32 E | |
| H3 | K75 E | |
| H4 | Q100 K | |
| H5 | Insertion H at 103 | |
| H6 | S113 L | Domain 2 |
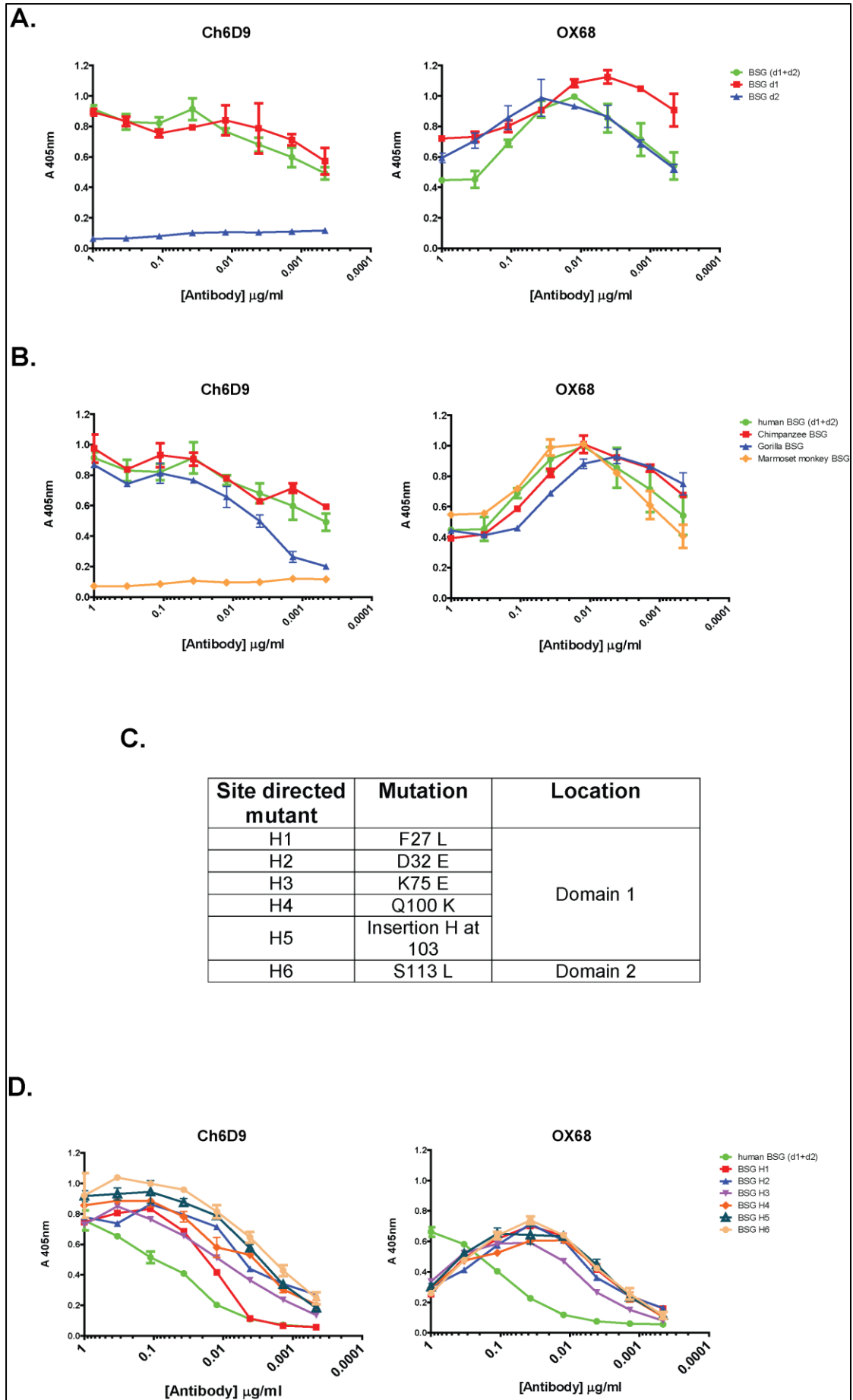
**Figure 4.14 Epitope mapping of ch6D9 on BSG.**

**A.** Ch6D9 bound to HsBSG domain 1, as demonstrated by ELISA.

**B.** Ch6D9 demonstrated binding to Gorilla and Chimpanzee BSG orthologues but not to the marmoset monkey one, as shown by ELISA.

**C.** Site-directed mutants of *Hs*BSG. Five amino acid residues in *Hs*BSG were mutated to those found in *Gg*BSG at the same position. A Histidine residue was also inserted in *Hs*BSG at position 103, as found in *Gg*BSG (constructs made by Dr Madusi Wanaguru).

**D.** Ch6D9 recognises BSG H1 mutant with slightly altered affinity, as assessed by ELISA.

The anti-Cd4 antibody OX68 was used to normalise the amounts of BSG proteins. For all ELISAs, the appropriate BSG species/variant from tissue culture supernatant, was immobilised on a streptavidin-coated plate. A dilution series of purified ch6D9 or OX68 was used as primary antibody and an anti-hIgG or anti-mIgG conjugated with alkaline phosphatase as secondary. Abbreviations: d1, BSG domain 1; d2, BSG domain 2. Data in *A*, *B* and *D* are shown as mean ± standard error; *n*=3.
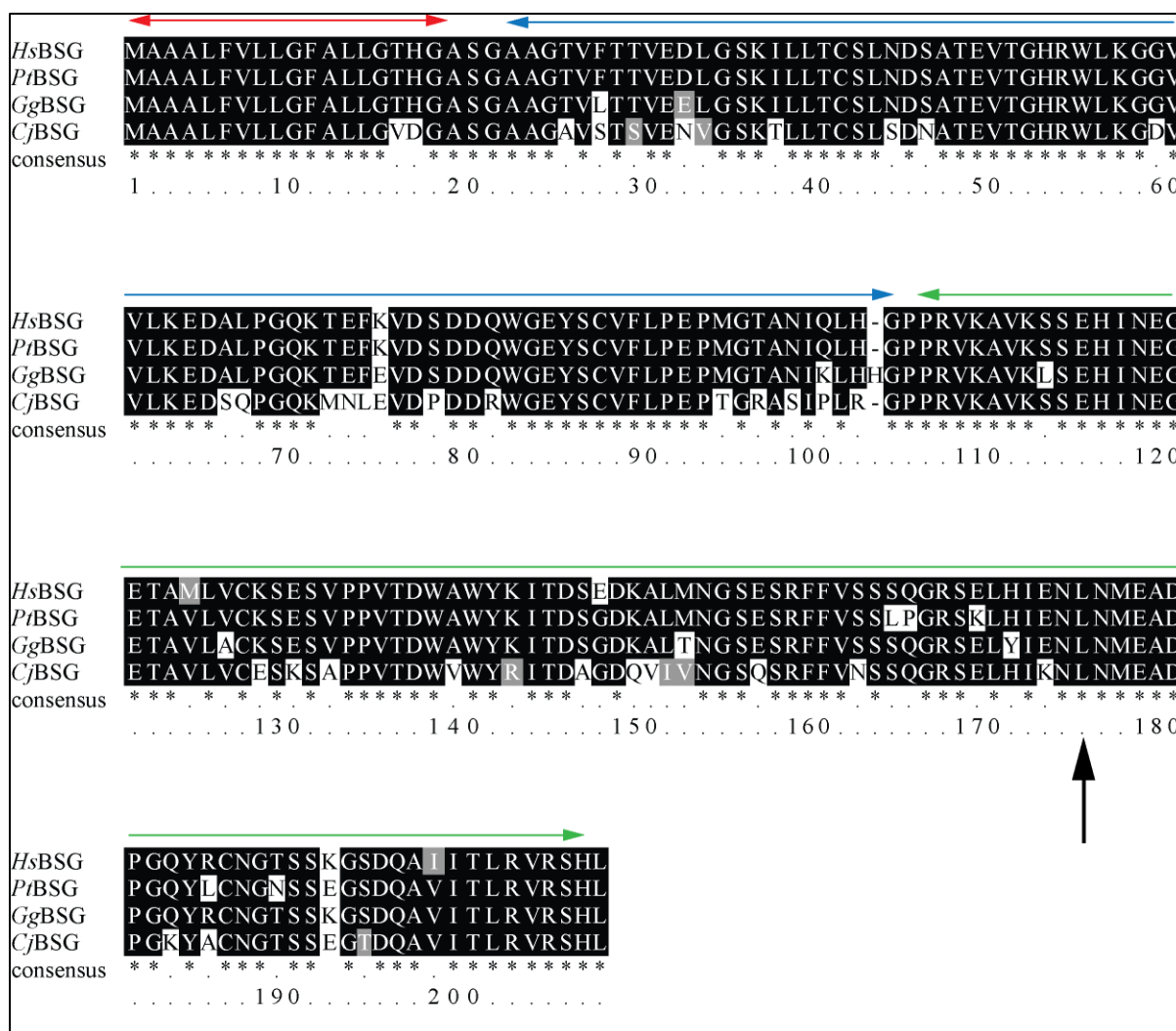
**Figure 4.15 Chimpanzee (*Pan troglodytes*) gorilla (*Gorilla gorilla*) and marmoset (*Callithrix jacchus*) orthologues of human (*Homo sapiens*) BSG.**

Alignment of the full-length ectodomains of BSG orthologues containing two immunoglobulin-like domains, from human (*Hs*BSG, ENSP00000343809, aa 1-206), chimpanzee (*Pt*BSG, ENSPTRP00000017252, aa 1-206) gorilla (*Gg*BSG, ENSGGOP00000022655, aa 1-207), and marmoset monkey (*Cj*BSG, aa 1-206). Conserved residues are shaded in black and semi-conserved residues in grey. The numbering indicated is for *Gg*BSG. The black arrow marks Leu-175, which is missing from the original *Pt*BSG sequence from Ensembl. The sequences were aligned using ClustalW2 software (Larkin *et al.*, 2007). The signal peptide (aa 1-18), IgSF domain 1 (aa 22-104) and IgSF domain 2 (aa 105-206) (Schlegel *et al.*, 2009) are marked with red, blue and green arrows, respectively. The protein sequences of the predicted BSG orthologues from *P. troglodytes* and *G. gorilla*, were retrieved and analysed from the Ensembl genome browser (Flicek *et al.*, 2011) by Dr Madushi Wanaguru. *Cj*BSG nucleotide sequence was amplified from *Cj*cDNA and sequenced by Dr Leyla Bustamante.

the equivalent positions (Fig. 4.14C). Four of these residues are located in domain 1 and the fifth in domain 2. A Histidine residue was also inserted into the *Hs*BSG sequence at position 103, as found in *Gg*BSG. All six biotinylated *Hs*BSG variants were recombinantly expressed, and the amount of biotinylated protein in each of the preparations was normalised against each other by ELISA (Fig. 4.14D right panel). An ELISA assay was also employed to assess the binding of ch6D9 to the six *Hs*BSG mutants. The binding of ch6D9 to mutants H2-H6 was almost indistinguishable (Fig. 4.14D left panel) between each other. Nevertheless, ch6D9 showed reduced binding to H1 (Fig. 4.14D left panel), suggesting that the phenylalanine at position 27 is likely implicated in the binding of ch6D9 to *Hs*BSG.

### 4.3.11.3 Biophysical characterisation of mouse and chimeric 6D9

Mouse and chimeric 6D9 were assed for their affinity for BSG by SPR. For this purpose hexa-histidine tagged BSG was purified from tissue culture supernatant by affinity chromatography on a nickel column followed by gel filtration (Fig 4.16A). The protein eluted from the gel filtration column as a monodisperse peak (Fig. 4.16 A). The expected elution volume for BSG monomer was 34.6ml, corresponding to an estimated size of 56.3kDa. Peak fractions containing monomeric protein were pooled and analysed by denaturing SDS-PAGE to confirm presence of BSG at the expected size (Fig 4.16B).

For kinetic analysis, protein G purified mouse (Fig. 4.11A) and chimeric 6D9 (Fig. 4.13A) were *in vitro* biotinylated and captured on the surface of a sensor chip. A dilution series of gel filtrated BSG was injected over the immobilised antibodies and reference substracted sensorgrams were derived. The $k_a$ and $k_d$ values were estimated by globally fitting a 1:1 binding model to the reference subtracted sensorgrams (Fig. 4.16C). Ch6D9 exhibited almost indistinguishable affinity for BSG, in comparison to m6D9 parental antibody (Fig. 4.16D) suggesting that chimerisation did not affect ch6D9 affinity for BSG. The $K_D$ of both chimeric and mouse 6D9 is in the nM range, which is typical for antibody-antigen interactions.

### 4.3.12 Development and characterisation of a two chimeric anti-RH5 monoclonal antibodies

Dr Simon Draper's group (Jenner Institute, University of Oxford) developed a panel of anti-RH5 monoclonal antibodies, two of which, (2AC7 and 9AD4),

**A.**



Protein purification

Gel filtration

**B.**



191kDa

97kDa

64kDa

51kDa

39kDa

28kDa

**C.**



m6D9

ch6D9

**D.**

| Antibody | $k_a$ ($M^{-1}s^{-1}$) | $k_d$ ($s^{-1}$) | $K_D$ (M) | $Chi^2$ ($RU^2$) |
|---|---|---|---|---|
| m6D9 | $(7.02 \pm 0.01) \times 10^4$ | $(2.600 \pm 0.003) \times 10^{-4}$ | $3.767 \times 10^{-9}$ | 0.0672 |
| ch6D9 | $(6.27 \pm 0.02) \times 10^4$ | $(2.900 \pm 0.006) \times 10^{-4}$ | $4.742 \times 10^{-9}$ | 0.0672 |
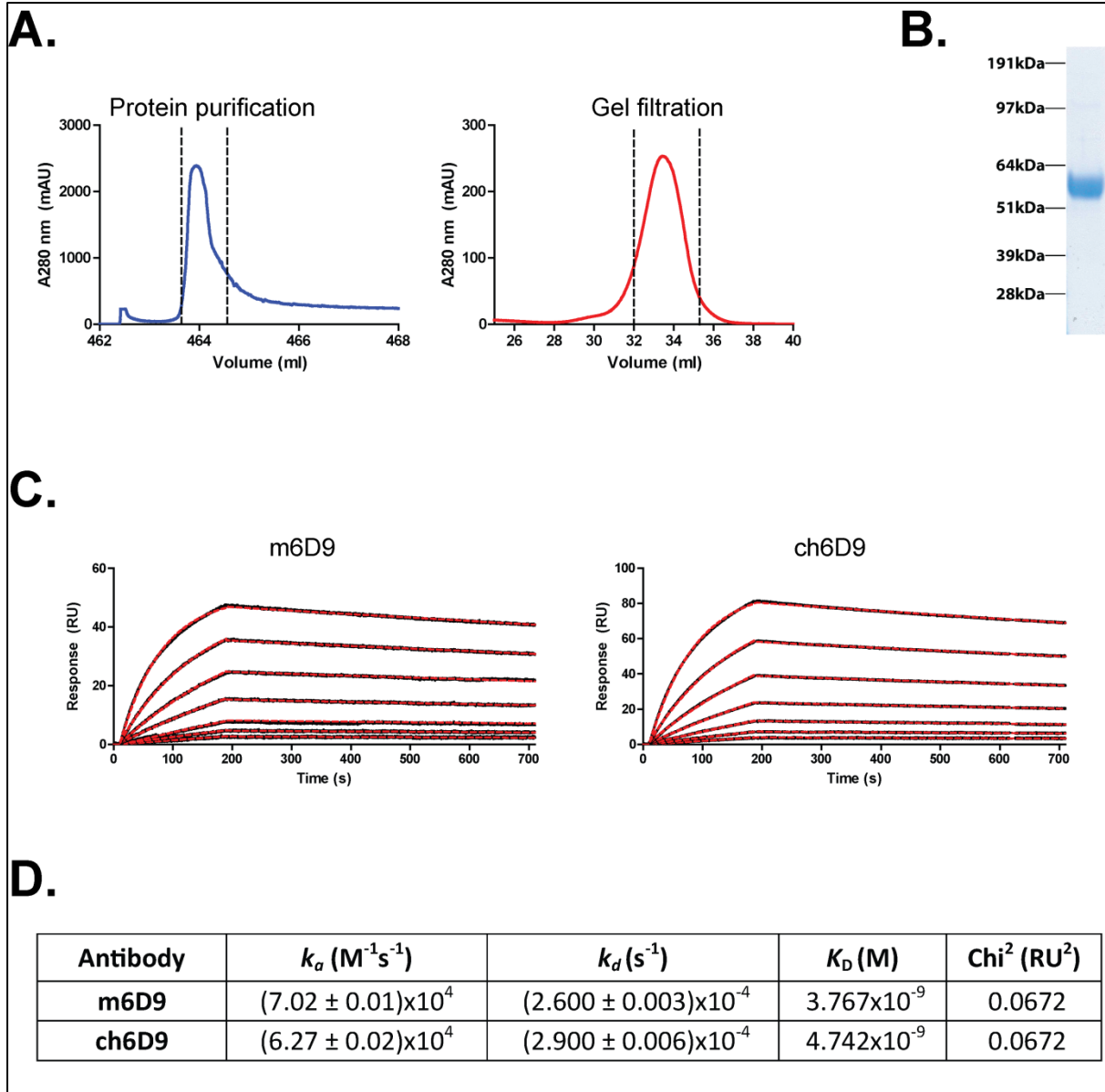
**Figure 4.16 Biophysical analysis of mouse and chimeric 6D9 using SPR.**

*A.* BSG-BLH was affinity purified from tissue culture supernatant, on a nickel column (left), followed by gel filtration (right) to separate monomeric BSG from other forms. The eluate in each of the experiments was monitored at 280 nm in real-time and the peak fractions containing protein (between dashed lines) were pooled. The expected gel filtration elution volume was 34.6ml.

*B.* Denaturing SDS-PAGE analysis of gel filtrated BSG. The protein was visualised using Coomassie brilliant blue. The expected band size was 56.3kDa.

*C.* Reference-subtracted sensorgrams (black lines) from the injection of a 2-fold dilution series of BSG (200 - 3.12nM), over the immobilised *in vitro* biotinylated mouse or chimeric 6D9 (ligands). The analyte was injected at a flow rate of 100 μl/min, with a contact time of 180s and a dissociation time of 530s. For the calculation of the association ($k_a$) and dissociation ($k_d$) rate constants, a simple Langmuir 1:1 binding model (red dashed lines) was globally fitted to the data. The biotinylated antibodies were immobilised on the chip surface at about 700RU. A mIgG2a or a hIgG1 were used as references.

*D.* Tables with the kinetic parameters estimated for the binding of mouse or chimeric 6D9 to BSG. For each model, the fit to the experimental data is indicated as the $Chi^2$ value. The calculated values for the $k_a$ and $k_d$ are indicated with the standard error. $K_D$ was estimated from the equitation $\frac{k\mathrm{d}}{k\mathrm{a}}$.

demonstrated high efficacy in blocking erythrocyte invasion (Douglas *et al.*, 2013). In order to assess their putative therapeutic potential, I attempted to chimerise them and compare their efficacy with ch6D9. For this purpose, 2AC7 and 9AD4 hybridoma lines were grown in culture, and antibody variable heavy and light chains were amplified and sequenced as described in section 4.3.4 (Fig. 4.17A). Based on the sequencing results, primers were designed for the amplification of 2AC7 and 9AD4 variable regions from TOPO vector (Fig. 4.17B). In parallel, ch6D9 variable heavy or light chain sequences were deleted from the equivalent expression vector by inverted PCR, leaving behind a linear vector carrying the associated signal peptide and constant region, but lacking ch6D9 variable regions (Fig 4.17B). Chimeric 2AC7 and 9AD4 encoding vectors (ch2AC7 and ch9AD4) were generated by blunt-end ligation of 2AC7 and 9AD4 amplicons in between the constant region and signal peptide of the linear vectors (Fig 4.17B).

For recombinant antibody expression, ch2AC7 and ch9AD4 heavy and light chain encoding vectors were co-transfected in HEK293F cells. Tissue culture supernatants were analysed by ELISA for the presence of anti-RH5 antibodies. Both tissue culture supernatants were immunoreactive against RH5, confirming recombinant expression of ch2AC7 and ch9AD4 (Fig 4.17C). To test whether ch2AC7 and ch9AD4 retained their efficacy in blocking erythrocyte invasion, chimeric and mouse 2AC7 and 9AD4 were affinity purified on protein G column (Fig 4.17D), and assayed in *P. falciparum* growth inhibition assay. Ch2AC7 and ch9AD4 prevented erythrocyte invasion at levels comparable to the original mouse antibodies, establishing that chimerisation did not significantly alter their efficacy in inhibiting erythrocyte invasion.

To test whether ch2AC7 and ch9AD4 have retained their affinity for RH5, their binding kinetic parameters were estimated by using SPR. Histidine tagged RH5 was recombinantly expressed and purified by affinity chromatography on nickel column followed by gel filtration (Fig 4.18A). The expected elution volume for full length RH5 monomer was 33.8ml, corresponding to an estimated size of 88kDa (Fig 4.18A). Denaturing SDS-PAGE analysis of the gel filtration peak fraction confirmed the presence of RH5 at the expected size (Fig 4.18B).

For the SPR experiment, purified mouse and chimeric 2AC7 and 9AD4 were *in vitro* biotinylated and immobilised on a sensor chip before a dilution series of RH5

**A.**

| Antibody | Variable region | FR1 | CDR1 | FR2 | CDR2 | FR3 | CDR3 | FR4 |
|---|---|---|---|---|---|---|---|---|
| 2AC7 | Heavy | EVKLVESGGGLVQPGGSRKLSCAAS | GFTLSDYG | MAWVRQAPGKGPEWVAF | ISNLAY | SIYYADTVTGRFTISRENDKNTLYLEMNNLRSEDTSMYYC | ARAIFDYDGYWYFDV | WGAGATVTVSS |
| | Light | DIVLTQSPTSLAVSLGQRATISCRAS | ESVEYYGTSL | IHWFQQKPGQPPKLLIY | AAS | NVESGVPARFSGSGSGTDFSLNIHPVEEDDIAMYFC | QQSKNIPWT | FGGGTKLEIK |
| 9AD4 | Heavy | EVKLVESGGGVVQPGGSRKLSCAAS | GFTFSDYG | MAWVRQAPGKGPEWVTF | ISNMAY | SIYYADTVTGRFTISRENAKNTLHLEMSSLRSEDTAMYYC | TRAIFDYAGYWYFDV | WGAGTTVTVSS |
| | Light | DIVLTQSPASLAVSLGQRATISCRAS | ESVEYYGTSL | MQWFQQKPGQPPRLLIH | GAS | NVQSGVPARFSGSGSGTDFSLNIHPVEEDDFAMYFC | QQSTKVPWT | FGGGTKLEIK |

**B.**

TOPO vector

**KEY**
Signal peptide
Ch6D9 VH or VL
hIgG1 or hIgCK
2AC7 or 9AD4 VH or VL

Heavy or Light chain encoding vector

**C.**



**D.**

m2AC7   m9AD4   ch2AC7   ch9AD4



**E.**

**Figure 4.17 Development and characterisation of ch2AC7 and ch9AD4, two chimeric anti-RH5 monoclonal antibodies**

**A.** Sequence analysis of mouse 2AC7 and 9AD4 variable regions. The table shows the amino acid sequence of mouse 2AC7 and 9AD4 rearranged variable heavy (VH) and light (VL) chains as derived from sequence analysis of the amplified variable region from the respective hybridoma cell line.

**B.** The approach that was followed for the cloning of 2AC7 and 9AD4 variable regions into the heavy and light chain encoding vectors. Ch6D9 variable heavy (VH) or light (VL) chain sequence was deleted from the equivalent vector by inverted PCR. 2AC7 and 9AD4 variable regions were amplified from TOPO vector and blunt ligated into the relevant linear heavy or light chain encoding vector. Blue arrowheads indicate the position of primers.

**C.** Ch2AC7 (left) and ch9AD4 (right) anti-RH5 antibodies bound to RH5, in an ELISA assay. RH5-BLH from tissue culture supernatant was immobilised on a streptavidin-coated plate at concentrations sufficient for complete saturation of the available binding surface. A 3-fold dilution series of tissue culture supernatant containing ch2AC7 or ch9AD4 was used as primary antibody and an anti-human IgG conjugated with alkaline phosphatase as secondary. M2AC7 and m9AD4 (at starting concentration 2μg/ml) were used as positive controls.

**D.** Mouse and chimeric 2AC7 and 9AD4 were affinity purified from tissue culture supernatant on protein G column. The eluate in each experiment was monitored at 280 nm in real-time and the peak fractions containing antibody (between dashed lines) were pooled.

**E.** Protein G purified ch2AC7 and ch9AD4 block *P.falciparum* erythrocyte invasion in culture**.** A synchnonised parasite culture (schizonts) was incubated overnight with a dilution series of ch2AC7 or ch9AD4 followed by fixing, staining and analysis by flow cytometry. M2AC7 and m9AD4 were used as positive controls and an isotype matched antibody, as negative control. The graph shows the percentage of infected red blood cells (iRBC) as a function of antibody concentration.

Data in *C* and *E* are shown as mean ± standard error; *n*=3.

A.

Protein purification

Gel filtration

B.

C.

m2AC7

m9AD4

ch2AC7

ch9AD4

D.

| Antibody | $k_a$ (M$^{-1}$s$^{-1}$) | $k_d$ (s$^{-1}$) | $K_D$ (M) | Chi$^2$ (RU$^2$) |
|---|---|---|---|---|
| m2AC7 | $(5.31 \pm 0.01) \times 10^6$ | $(2.059 \pm 0.003) \times 10^{-4}$ | $3.863 \times 10^{-11}$ | 0.273 |
| ch2AC7 | $(3.39 \pm 0.07) \times 10^6$ | $(1.924 \pm 0.006) \times 10^{-4}$ | $5.667 \times 10^{-11}$ | 1.47 |
| m9AD4 | $(4.00 \pm 0.02) \times 10^6$ | $(5.070 \pm 0.001) \times 10^{-4}$ | $1.267 \times 10^{-10}$ | 2.32 |
| ch9AD4 | $(3.95 \pm 0.01) \times 10^6$ | $(5.359 \pm 0.006) \times 10^{-4}$ | $1.356 \times 10^{-10}$ | 0.208 |
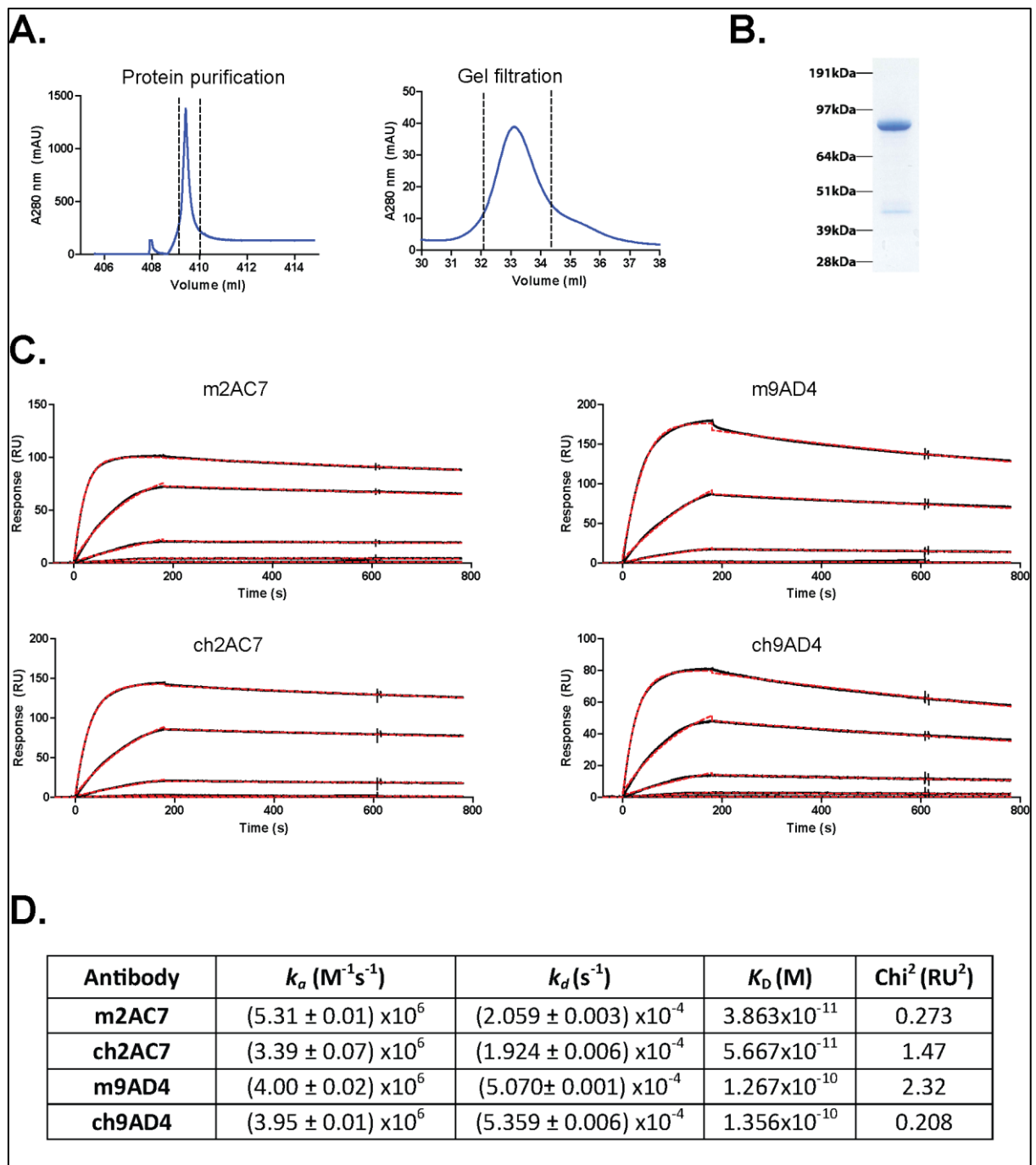
**Figure 4.18 Biophysical characterisation of mouse and chimeric 2AC7 and 9AD4 using SPR.**

**A.** Histidine tagged RH5 was affinity purified from tissue culture supernatant, on a nickel column (left), followed by gel filtration (right). The eluate was monitored at 280 nm in real-time and the peak fractions containing protein (between dashed lines) were pooled. The expected gel filtration elution volume was ~33.8ml.

**B.** Denaturing SDS-PAGE analysis of gel filtrated RH5. The protein was visualised using Coomassie brilliant blue. The expected band size was 88 kDa (including tags).

**C.** Reference subtracted sensorgrams (black lines) from the injection of a 5-fold dilution series of RH5 (10 - $3.2 \times 10^{-3}$nM), over immobilised *in vitro* biotinylated mouse or chimeric 2AC7 or 9AD4 (ligands). The analyte was injected at a flow rate of 100µl/min, with a contact time of 180s and a dissociation time of 600s. For the calculation of the association ($k_a$) and dissociation ($k_d$) rate constants, a simple Langmuir 1:1 binding model (red dashed lines) was globally fitted to the data. The biotinylated antibodies were immobilised on the chip surface at about 550RU. A mIgG2a or a hIgG1 were used as references.

**D.** Tables with the kinetic parameters estimated for the binding of mouse or chimeric 2AC7 and 9AD4 to RH5. For each model, the fit to the experimental data is indicated as the $Chi^2$ value. The calculated values for $k_a$ and $k_d$ are indicated with standard error. $K_D$ was estimated from the equitation $\frac{kd}{ka}$.

was injected across the sensor surface. The $k_a$ and $k_d$ values were measured by globally fitting a simple Langmuir binding model to the reference subtracted sensorgrams (Fig 4.18C). Ch2AC7 and ch9AD9 affinity for RH5 was almost identical to their mouse antibody counterparts (Fig 4.18D) suggesting that chimerisation did not alter their affinity for RH5.

## 4.3.13 Development and characterisation of bi-specific 2AC7-6D9 DVD-Ig

Both humanised anti-BSG (ch6D9) and anti-RH5 (ch2AC7 and ch9AD4) antibodies interfered with erythrocyte invasion in growth inhibition assays. To test whether combining both specificities into a single molecule would have an additive effect in preventing erythrocyte invasion, I sought to combine ch2AC7 and ch6D9 into a single tetravalent immunoglobulin-like molecule which is termed dual-variable-domain immunoglobulin (DVD-Ig; Wu *et al.*, 2007) (Fig. 4.19A).

To develop a 2AC7-6D9 DVD-Ig, 2AC7 variable heavy and light chain sequence was amplified from 2AC7 heavy and light chain encoding vector respectively. Wu and colleagues recommended the development and testing of at least two DVD-Ig versions (short and long), differing in the size of interspace sequence between the two variable domains of different specificity (Wu *et al.*, 2007) (Fig. 4.19A). The size of the linker sequence appears to be important for the flexibility of the variable region, and the appropriate size should be identified by empirical testing. Therefore, two different reverse primers were designed for the amplification of 2AC7 variable heavy or light chain sequence fused to two different sized fragments from hIgG1 or hIgCκ respectively (Fig. 4.19B). In parallel, ch6D9 heavy and light encoding vectors were linearized by inverted PCR. Amplified 2AC7 variable chain sequence fragments (together with the attached sequence encoding for the linker peptide) were ligated in frame to the ch6D9 variable region sequences as shown in Fig. 4.19B.

For recombinant expression, 2AC7-6D9 DVD-Ig heavy and light encoding vectors were co-transfected in HEK293F cells and tissue culture supernatant was collected five days post transfection. Short and long 2AC7-6D9 DVD-Igs were purified from tissue culture supernatant by affinity chromatography on protein G column (Fig. 4.19C). The ability of 2AC7-6D9 DVD-Ig to simultaneously binding to RH5 and BSG was examined by SPR (Fig. 4.19D). *In vitro* biotinylated 2AC7-6D9
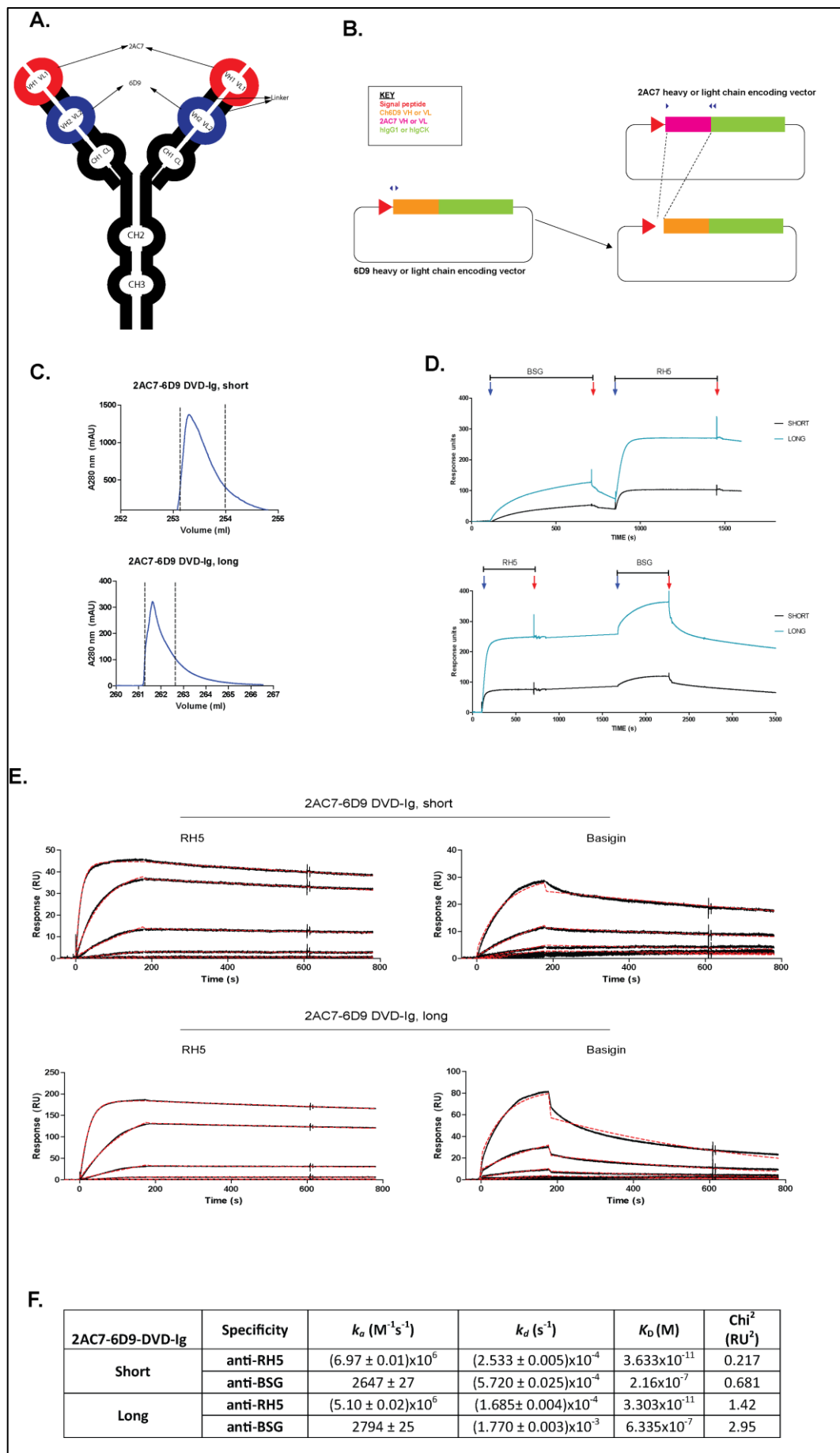
**Figure 4.19 Generation and biophysical characterisation of a dual specificity 2AC7-6D9 DVD-Ig.**

**A.** Schematic diagram of 2AC7-6D9DVD-Ig protein structure, with two tandem variable domains in each heavy and light chain. Abbreviations: VH1 and VH2, Variable heavy chain 1 and 2; VL1 and VL2, Variable light chain 1 and 2; CH1-3, Constant heavy 1-3; CL, Constant Light.

**B.** The cloning strategy that was followed for the development of 2AC7-6D9 DVD-Ig. 2AC7 variable heavy (VH) and light (VL) chain sequences together with a small sequence fragment from hIgG1 or hIgCκ respectively, were amplified and cloned into a linearised ch6D9 encoding vector. For the derivation of short and long versions of 2AC7-6D9 DVD-Ig two different reverse primers were used to amplify the 2AC7 variable chain sequences. For more details, see text.

**C.** 2AC7-6D9 DVD-Igs, short and long, were affinity purified from tissue culture supernatant on protein G column. The eluate in each experiment was monitored at 280 nm in real-time and the peak fractions containing antibody (between dashed lines) were pooled

**D.** Reference-subtracted sensorgrams from the sequential 600s injection of BSG (5µM) and RH5 (10nM) (without regenerating the surface between injections) over immobilised *in vitro* biotinylated 2AC7-6D9 DVD-Ig short or long version. The sensorgrams suggest that 2AC7-6D9 DVD-Ig can simultaneously bind to RH5 and BSG and this is independent of the order of analyte injection. Blue and red arrows demonstrate the start and end of analyte injection. Bars above the sensograms represent the duration of analyte injection.

**E.** Reference subtracted sensorgrams (black lines) from the injection of a 5-fold dilution series of RH5 (10 – 6.4x10$^{-4}$nM) and BSG (5 – 0.32 µM), over the immobilised *in vitro* biotinylated 2AC7-6D9 DVD-Ig short or long. Each time, the analyte was injected at a flow rate of 100µl/min, with a contact time of 180s and a dissociation time of 600s. For the calculation of the association ($k_a$) and dissociation ($k_d$) rate constants, a simple Langmuir 1:1 binding model (red dashed lines) was globally fitted to the data. The biotinylated antibodies were immobilised on the chip surface at about 600RU. A hIgG were used as reference.

**F.** Tables with the kinetic parameters estimated for the binding of 2AC7-6D9 DVD-Ig (short and long) to BSG and RH5. For each model, the goodness of fit to the experimental data is indicated as the Chi$^2$ value. The calculated values for $k_a$ and $k_d$ are indicated with standard error. $K_D$ was estimated from the equitation $\frac{kd}{ka}$.

DVD-Igs were immobilised on the surface of a sensor chip followed by a sequential injection of BSG and RH5 over the sensor surface. 2AC7-6D9 DVD-Ig was able to bind to both BSG and RH5 at the same time, and the order of binding is not important (Fig. 4.19D). For kinetic analysis, a dilution series of BSG or RH5 was injected across 2AC7-6D9 DVD-Ig captured on the sensor surface. For the derivation of $k_a$ and $k_d$, a 1:1 binding model was globally fitted to the datasets (Fig. 4.19E). The affinity of both short and long versions of 2AC7-6D9 DVD-Ig for RH5 was almost indistinguishable from ch2AC7 ($K_D$=~3.5x10$^{-11}$M). Nevertheless, a fraction of the affinity for BSG was lost in both 2AC7-6D9 DVD-Ig short and long ($K_D$=~4x10$^{-7}$M), when compared to ch6D9 (Fig. 4.19F).

The efficacy of 2AC7-6D9 DVD-Ig in preventing erythrocyte invasion was also investigated. A synchronised *P. falciparum* culture at the late trophozoite to early schizont stage was incubated overnight in the presence of a dilution series of purified 2AC7-6D9 DVD-Ig short or long, before analysis of growth inhibition by flow cytometry. The IC$_{50}$ of short 2AC7-6D9 DVD-Ig was significantly lower than ch2AC7 alone, but for the long version the differences were marginal. However, both 2AC7-6D9 DVD-Ig short and long had considerably higher IC$_{50}$ than ch6D9 alone.

These results suggest that ch6D9 is more potent in blocking erythrocyte invasion than 2AC7 or 2AC7-6D9 DVD-Ig, since much lower antibody doses are required for this inhibitory effect (Fig. 4.20).

## 4.4 Discussion

### 4.4.1 MEM-6/4 and MEM-M6/8 inhibit the RH5-BSG interaction *in vitro* but not in parasite culture

The central aim this Chapter was the development and characterisation of an anti-BSG humanised or chimeric antibody, as a potential anti-malarial therapeutic. Two anti-BSG mouse monoclonal antibodies, MEM-M6/4 and MEM-M6/8 (Koch *et al.*, 1999), were initially chosen for humanisation. MEM-M6/8 was found to be unable to inhibit erythrocyte invasion in parasite culture and incapable of binding to human erythrocytes (Fig. 4.2). The same antibody however, appeared to block the RH5-BSG interaction *in vitro*, but this was observed only at very high antibody concentrations (Fig. 4.2). I propose two possible explanations for these observations, which are not necessarily mutually exclusive.
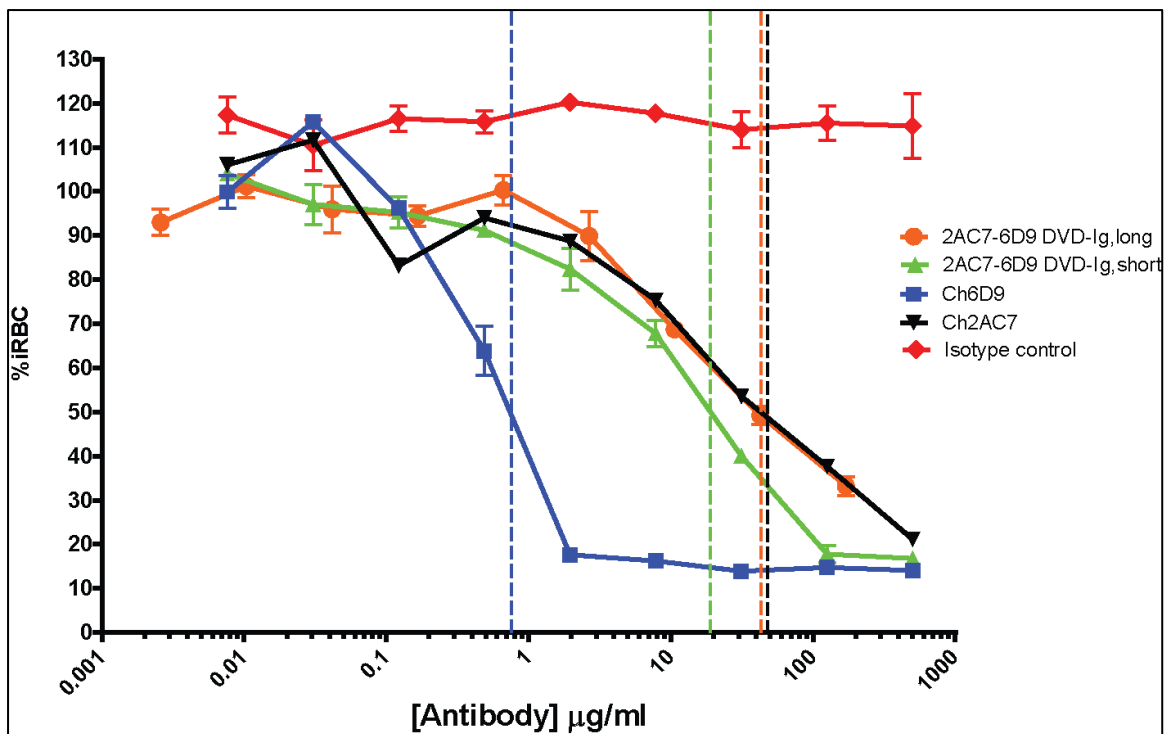
**Figure 4.20 ch6D9 is much more potent than ch2AC7 or 2AC7-6D9 DVD-Ig, in blocking erythrocyte invasion.** A synchronised parasite culture (schizonts) was incubated overnight with a dilution series of each antibody followed by fixing, staining and analysis by flow cytometry. The graph shows the percentage of infected red blood cells (iRBC) as a function of antibody concentration. An isotype matched antibody was used as negative control. Dashed vertical lines indicate the $IC_{50}$ value for each antibody.

The first explanation is based on the fact that when an antibody is tested for its ability to block an interaction in AVEXIS, two equilibria exist and both need to be taken into account, as shown below.

$$Antibody \quad + \quad Prey \quad \underset{\longleftarrow}{\overset{KD1}{\longrightarrow}} \quad \left(Antibody - Prey\,complex\right)$$

$$+$$

$$Bait$$

$$\uparrow\downarrow \; KD2$$

$$\left(Prey\text{-}Bait\,complex\right)$$
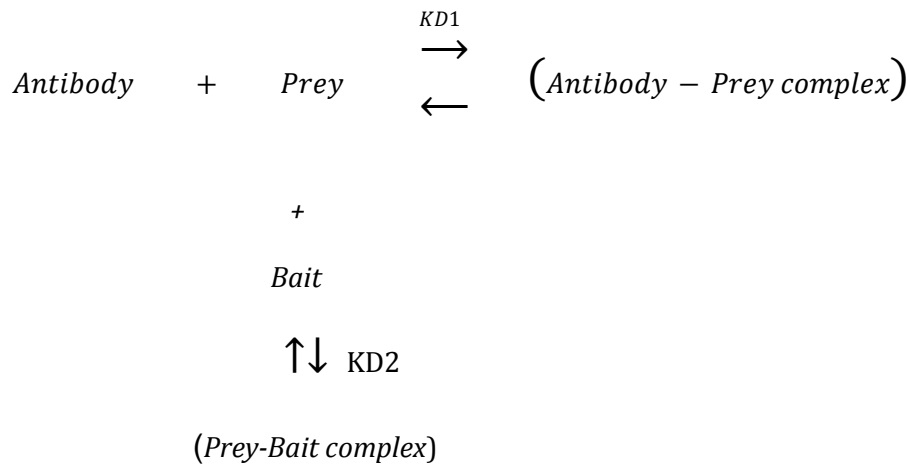
There is one equilibrium between the antibody and prey, and one between the prey and bait. If $K_{D1} \ll K_{D2}$ the antibody is strongly bound to the prey, and the bait cannot compete for binding. When $K_{D1} \geq K_{D2,}$ the bait becomes a significant competitor to the antibody for binding to the prey and therefore, the interaction between bait and prey is not prevented. In this context, the $K_D$ I calculated for the interaction between MEM-M6/8 and BSG ($\sim$1.027 x10$^{-6}$M), is in the range of the $K_D$ previously reported for the RH5-BSG interaction ($\sim$1.2 x10$^{-6}$ M) (Crosnier *et al.*, 2011). Nevertheless, because AVEXIS utilizes pentameric BSG, the overall avidity of the RH5-BSG interaction increases significantly. Therefore, only extraordinary high concentrations of MEM-M6/8 are capable of outcompeting the binding to RH5 and thus inhibiting the interaction. This alone however, does not explain why high concentrations of MEM-M6/8 do not have inhibitory effect in erythrocyte invasion. It is important to mention that there are significant differences in blocking the RH5-BSG interaction *in vitro* by AVEXIS and *ex vivo* in parasite culture. The former system utilizes soluble recombinant proteins of which one of them is a pentamer, whereas the latter is a cell based system where at least one interacting partner (BSG) is membrane embedded. Therefore, parameters which are of little or no importance in first system e.g antibody accessibility, become limiting factors in the second and vice versa.

The second possible explanation – which does not contradict the first one - is based on the fact that antibodies in general are capable of both monovalent and bivalent binding. In the case of clustered antigen, bivalent antibody binding becomes a two state reaction where the engagement of the first antibody binding site brings the second paratope in close vicinity to the target molecule and thereby facilitates its binding. Therefore, the engagement of the first binding site is the limiting factor in this two state reaction.

The soluble pentameric nature of BSG prey used in AVEXIS assay, allows bivalent antibody binding. At (relatively) low concentrations of MEM-M6/8 antibody, monovalent binding occurs, but because the antibody has low affinity for the antigen, it quickly dissociates and cannot be replenished rapidly enough to prevent the binding to bait. Therefore, a significant amount of free BSG still exists, and is capable of binding to RH5 immobilised on the plate. By increasing the concentration of antibody, more monovalent binding exists at a given time point and therefore, bivalent binding is more likely to occur. Bivalently bound MEM-M6/8 results in the formation of stable MEM-M6/8-BSG complexes with extended half-life and thereby the interaction between BSG with RH5 is inhibited.

Bivalent antibody binding requires that two antigen molecules are in close vicinity with each other. Because of the relatively low abundance ($\sim 10^5$ molecules/cell) of BSG on erythrocyte cell surface (Crosnier *et al.*, 2011; Bartholdson *et al.*, 2013), bivalent binding of MEM-M6/8 to BSG likely did not occur when MEM-M6/8 was used to stain human erythrocytes or to inhibit erythrocyte invasion in *P. falciparum* growth inhibition assay. As a result, monovalently bound MEM-M6/8 quickly dissociated leaving behind "unmasked" BSG which was utilized by the parasite to invade erythrocytes. This hypothesis is supported by previous observations that MEM-M6/8 was unable to stain resting T cells on which BSG is expressed but is of low abundance (Koch *et al.*, 1999). When the same experiment was repeated with PHA activated T cells which have threefold more BSG molecules on their cell surface than resting T cells, MEM-M6/8 binding could be readily detected.

In the same experiments, MEM-M6/4 was shown to be able to bind to both resting and stimulated T cells which is in agreement with my observations that this antibody stains human erythrocytes. The latter result indicates that, in contrast to

MEM-M6/8, monovalent MEM-M6/4 binding is strong enough to survive the washes during staining (Fig. 4.2). Indeed, SPR experiments established that MEM-M6/4 exhibits more than two orders of magnitude higher affinity for BSG than MEM-M6/8 (Fig. 4.9; see below). This however, was not enough for MEM-M6/4 to completely block the RH5-BSG interaction by AVEXIS or to abolish erythrocyte invasion. MEM-M6/4 had a moderate inhibitory effect in parasite growth inhibition assay, which appears to be saturable at about 20% inhibition. Therefore, it is more likely that MEM-M6/4 binds an epitope on BSG which is nearby RH5 binding site, causing a steric effect to the RH5-BSG interaction which in turn reduces invasion efficiency to a certain level (20% inhibition).

### 4.4.2 The affinity of MEM-6/4 and MEM-M6/8 for BSG is lower than previously reported

Biophysical analysis of MEM-M6/4 and MEM-M6/8 (Fig. 4.9), suggested that the affinities of these antibodies for BSG were three to four orders of magnitude lower than previously reported (Koch *et al.*, 1999). Koch and colleagues used SPR to biophysically analyse MEM-M6/4 and MEM-M6/8. In their experiments they used Fc-fused recombinant BSG as ligand over which they injected the antibodies. To calculate the affinity of MEM-M6/4 and MEM-M6/8 for BSG, it was assumed that there is 1:1 binding, and a predefined Langmuir 1:1 interaction model was fitted to the SPR sensorgrams (Koch *et al.*, 1999). However, there was an important flaw in their experimental design which affected the final results: despite claiming 1:1 stoichiometry between analyte and ligand, it was not taken into account that both analyte and ligand had two binding sites for each other, which significantly increases the overall avidity of the interaction. As a result, the affinity of MEM-M6/4 and MEM-M6/8 for BSG was overestimated.

### 4.4.3 MEM-6/4 and MEM-M6/8 were successfully humanised

By using the plasmid expression system described in Chapter 3, MEM-M6/4 and MEM-M6/8 were successfully humanised by CDR grafting. HuMEM-M6/4 and huMEM-M6/8 were able to bind BSG *in vitro* by ELISA (Fig. 4.6). HuMEM6/8, similar to the original mouse antibody, had a moderate effect in blocking the RH5-BSG interaction *in vitro*, but could not prevent erythrocyte invasion *ex vivo*. HuMEM-M6/4, unlike its mouse parental antibody, was incapable of staining human erythrocytes

and could not interfere with RH5-BSG interaction *in vitro*, or with erythrocyte invasion in parasite culture, probably due to the decrease in the affinity of huMEM-M6/4 for BSG, in comparison to the mouse parental antibody (Fig. 4.9; see below).

Biophysical analysis of huMEM-M6/4 and huMEM-M6/8 by SPR, suggested that humanisation of these antibodies was accompanied by a decrease in their affinity for BSG. Despite the affinity of huMEM-M6/8 was almost unaltered compared to MEM-M6/8, the affinity of huMEM-M6/4 was reduced by two orders of magnitude in comparison to MEM-M6/4. The decrease in antibody affinities was likely due to incompatibilities between human FRs and murine CDRs. (Lo, 2004; Almagro and Fransson, 2008) Possible ways of restoring the affinity of humanised antibodies for BSG are discussed in Chapter 6.

### 4.4.4 Development and humanisation of m6D9, a high efficacy anti-BSG antibody

In the current Chapter, I demonstrated that (hu)MEM-M6/4 and (hu)MEM-M6/8 inhibited the RH5-BSG interaction with levels of efficacy below those required for the blockade of erythrocyte invasion in parasite culture. To obtain a more effective anti-BSG monoclonal, a new panel of hybridoma lines secreting anti-BSG antibodies was generated, by directly immunising animals. Initially 11 hybridoma clones were found to secrete antibodies against BSG. However, several hybridomas were later found to have lost their ability to secrete anti-BSG antibodies, probably due to the general genetic instability that accompanies hybridoma clones after fusion (Kromenaker and Srienc, 1994).

The monoclonal antibody m6D9, which was secreted by one of the generated hybridoma clones, demonstrated high efficacy in blocking erythrocyte invasion in parasite culture (Fig. 4.11) and thus, it was selected for humanisation. Humanisation by CDR grafting resulted in the loss of a significant fraction of hu6D9 affinity for BSG (Fig. 4.12). The replacement of two amino acids in huVH which were potentially implicated in the loss of hu6D9 affinity for BSG, did not have the desired result. The loss of hu6D9 affinity is most likely to arise from the incorrect conformation of murine CDRs in the human framework context. Experimental procedures which can potentially restore hu6D9 affinity for BSG are described in Chapter 6.

### 4.4.5 Ch6D9 is a high affinity anti-BSG chimeric antibody which binds to BSG domain 1

As an alternative to fully humanised hu6D9 a chimeric version of m6D9, ch6D9 was developed. For the creation of ch6D9, intact murine variable heavy and light chains were used and thus, the affinity for BSG was fully retained (Fig. 4.16). Ch6D9 demonstrated high efficacy in inhibiting the RH5-BSG interaction *in vitro*, and in blocking erythrocyte invasion in all four *P. falciparum* strains tested (Fig. 4.13) Therefore, it can be considered for therapeutic purposes.

Epitope mapping experiments demonstrated that ch6D9 binds to BSG domain 1 (Fig. 4.14). To further refine ch6D9 epitope, recombinant *Gg*BSG, *Pt*BSG, and *Cj*BSG were employed. Ch6D9 bound to *Pt*BSG at levels similar to *Hs*BSG. The latter observation was expected because *Pt*BSG and *Hs*BSG are identical in domain 1 (Fig. 4.15) and therefore, *Pt*BSG served as a good internal control. In contrast, no ch6D9 binding to *Cj*BSG was observed. Intriguingly, ch6D9 demonstrated reduced binding to *Gg*BSG in comparison to *Hs*BSG suggesting that certain amino acids that differ between *Hs*BSG and *Gg*BSG are likely important for ch6D9 binding to BSG.

To further refine ch6D9 epitope, a number of *Hs*BSG mutants were used (H1-H6), in which amino acid residues in *Hs*BSG were singly mutated to those found in *Gg*BSG at the same positions (Fig. 4.14). The binding of ch6D9 to H1 BSG mutant considerably decreased in comparison to wild type *Hs*BSG, suggesting that phenylalanine at position 27 is likely part of ch6D9 epitope. These results fit perfectly with previous experiments in our laboratory showing that H1 mutant has 7-fold lower affinity for RH5 than wild type *Hs*BSG (Dr Madushi Wanaguru, unpublished data). The latter observation suggests that phenylalanine at position 27 – which is solvent exposed (Yu *et al.*, 2008) - is probably implicated in RH5-BSG interaction, and in the presence of ch6D9, is likely inaccessible to RH5. However, the possibility that the mutation introduced at position 27 in H1 mutant, simply caused local unfolding which affected both ch6D9 and RH5 binding, cannot be ruled out.

### 4.4.6 Ch6D9 demonstrates reduced binding to C1q and FcγRIIA

Ch6D9 was very efficient in blocking *P. falciparum* erythrocyte invasion in parasite culture, and it was therefore reasonable to envisage ch6D9 as a putative therapeutic. Nevertheless, the therapeutic value of ch6D9 does not solely rely on its

ability to prevent erythrocyte invasion, but it equally depends on its (in)ability to stimulate ADCC and CDC effector functions which are initiated upon binding of antibody to Fc receptors or recruitment of complement components, respectively. To eliminate antibody effector functions, several mutations were introduced into the Fc region of ch6D9 (Chapter 3)

These mutations were demonstrated to inhibit FcγRIIA and C1q binding to ch6D9. Ideally, the binding of other Fcγ receptors to ch6D9 would have been tested, but attempts to get access to a panel of constructs expressing a range of Fcγ receptors (Shields *et al.,* 2001) were unsuccessful. Nevertheless, the results obtained with FcγRIIA and C1q, suggest that ch6D9 is likely to have reduced ability to trigger ADCC and CDC effector functions.

### 4.4.7 The potency of ch6D9 in inhibiting erythrocyte invasion is higher than ch2AC7, ch9AD4, or 2AC7-6D9 DVD-Ig

Two chimeric anti-RH5 antibodies, namely ch2AC7 and ch9AD4 were developed. Both antibodies retained their high affinity for RH5 after chimerisation, and were able to inhibit erythrocyte invasion with efficacy similar to the murine parental antibodies (Fig. 4.17). Previous experiments demonstrated that a combination of anti-BSG mAb (TRA-185) and polyclonal rabbit anti-RH5 IgG had an additive effect in blocking erythrocyte invasion in *P. falciparum* parasite culture (Dr Andrew Williams, personal communication). To test whether combining both anti-RH5 and anti-BSG specificities into a single molecule would still have an additive effect in preventing erythrocyte invasion, two versions (short and long) of a bi-specific anti-BSG/RH5 antibody, 2AC7-6D9 DVD-Ig, were developed (Fig. 4.19).

Biophysical analysis of 2AC7-6D9 DVD-Ig demonstrated that both versions were capable of simultaneous binding to RH5 and BSG and the order of binding was not important (Fig. 4.19). Nevertheless, while 2AC7-6D9 DVD-Ig affinity for RH5 was retained in comparison to ch2AC7, the affinity for BSG decreased two orders of the magnitude as compared to ch6D9. It appears that the incorporation of 2AC7 variable heavy and light chain, N-terminally to the respective 6D9 chains, constrained the accessibility of 6D9 variable regions to BSG (DiGiammarino *et al.,* 2012). This is further supported by the biophysical data showing that while the BSG dissociation rate constant ($k_d$) was only mildly affected (~6-fold and ~2-fold higher in 2AC7-6D9

DVD-Ig short and long respectively, in comparison to ch6D9), the association rate constant ($k_a$) decreased by a factor of 22 (Fig. 4.19)

Side by side comparison between ch6D9 and ch2AC7 demonstrated that ch6D9 has a considerably higher potency (~50-fold lower $IC_{50}$ than ch2AC7) in inhibiting erythrocyte invasion in parasite culture (Fig. 4.20). Considering that ch2AC7 has two orders of magnitude higher affinity for RH5 than ch6D9 has for BSG, the latter observation cannot be attributed to differences in antibody-antigen affinity between ch2AC7 and ch6D9. The higher potency of ch6D9 is more likely to be due to the binding equilibrium that is reached between ch6D9 and erythrocyte exposed BSG during the invasion assay incubation period. Because of the very transient exposure of RH5 to ch2AC7 during an erythrocyte invasion assay, such equilibrium between ch2AC7 and RH5 can only be achieved by very high concentrations of ch2AC7 (Williams *et al.*, 2012). Similarly, ch6D9 was more potent than 2AC7-6D9 DVD-Ig in preventing erythrocyte invasion. However, as mentioned above, 2AC7-6D9 DVD-Ig has lost a fraction of its affinity for BSG in comparison to ch6D9 and therefore, these data should be interpreted with caution (see Chapter 6).

## 4.5 Conclusions

In this chapter I described the development of a chimeric anti-BSG antibody, ch6D9, as a potential anti-malarial therapeutic. Ch6D9 retained its high affinity for BSG after chimerisation, and demonstrated high potency in blocking erythrocyte invasion in all parasite lines tested. Furthermore, ch6D9 displayed reduced binding to FcγRIIA and C1q *in vitro*, suggesting that this antibody may have reduced ability to trigger antibody effector functions.

Two chimeric anti-RH5 monoclonal antibodies (ch2AC7 or ch9AD4) and a bi-specific antibody (2AC7-6D9 DVD-Ig) targeting both RH5 and BSG, were also developed. Side by side comparison between ch6D9, ch2AC7 and 2AC7-6D9 DVD-Ig demonstrated that ch6D9 had a considerably lower $IC_{50}$ in blocking erythrocyte invasion in parasite culture, suggesting that the anti-BSG ch6D9 has higher potency in inhibiting erythrocyte invasion, than the other two antibodies tested.

# CHAPTER 5

**Systematic screening for extracellular receptor-ligand interactions involved in erythrocyte recognition and invasion by *P. falciparum***

## 5.1 Summary and Aims

Invasion of erythrocytes by *Plasmodium falciparum* merozoites, is an essential step in parasite's lifecycle and has therefore long been thought of as a desirable target for the development of therapeutics, particularly a vaccine. However, the development of a highly efficacious blood stage malaria vaccine has been made difficult by the highly polymorphic nature of merozoite ligands as well as by functional redundancy of the receptor-ligand pairs involved in the invasion process. A more detailed molecular understanding of invasion could lead to identification of cell surface receptor-ligand interactions, which are essential for erythrocyte invasion and therefore, promising intervention targets can be revealed. However, such studies have been hampered by the difficulties in recombinant expression of *Plasmodium* spp. proteins and by the technical challenges in systematically identifying interacting partners for cell surface proteins (Birkholtz *et al.*, 2008; Bartholdson *et al.*, 2013).

In previous work from our laboratory, 53 *P. falciparum* merozoite cell surface and secreted proteins were expressed in a biochemically active recombinant form, by using the HEK293E protein expression system (Crosnier et al, unpublished). By using AVEXIS (Bushell *et al.*, 2008), a system designed to detect low affinity protein-protein interactions that is discussed in more depth below, the *P. falciparum* recombinant merozoite protein array was systematically screened against a protein library consisting of erythrocyte cell surface receptors which was also expressed recombinantly in our laboratory (Crosnier and Bartholdson, unpublished data). The screen identified BSG and Semaphorin7A as the erythrocyte receptors for merozoite RH5 and MTRAP respectively (Crosnier *et al.*, 2011; Bartholdson *et al.*, 2012). Importantly, the interaction between RH5 and BSG is the only one known so far that is essential and universally required for erythrocyte invasion (Crosnier *et al.*, 2011).

In this Chapter I, aimed to expand the previous work from our laboratory, and identify novel receptor-ligand pairs involved in erythrocyte invasion. For this purpose, I expanded the already existing *P. falciparum* merozoite recombinant protein library by 26 proteins, using transcription microarray data and information available in the published literature. Of 26 new *P. falciparum* merozoite proteins targeted, 21 were recombinantly expressed at usable amounts. Biochemical analysis provided evidence that the recombinant merozoite ligands were biochemically active and correctly folded. AVEXIS was then used to systematically screen these new

members of the *P. falciparum* recombinant protein library, against an equivalent library consisting of erythrocyte receptors (Bushell *et al.*, 2008). This screen identified one putative interaction (PF13_0125 – P4HB). Further characterisation of the identified interaction provided inconclusive results, and more experiments are required to confirm its validity. The recombinant *P. falciparum* merozoite proteins reported in this project should prove a useful tool for the deeper understanding of erythrocyte invasion, and *P. falciparum* biology in general.

## 5.2 Introduction

### 5.2.1 Systems for recombinant expression of *Plasmodium* spp. proteins

Expressing *Plasmodium* proteins in heterologous systems has been a technically challenging problem (Birkholtz *et al.*, 2008; Fernández-Robledo and Vasta, 2010). Although the causal reasons why *Plasmodium* proteins are difficult to express in recombinant expression systems are not known, several protein characteristics such as high molecular mass (> 56 kDa) and the presence of export motifs and atypical signal peptide sequences were found to make soluble expression of recombinant *Plasmodium* proteins, in commonly used heterologous expression systems, challenging (Birkholtz *et al.*, 2008). Moreover, the problematic recombinant expression of *Plasmodium* proteins has been attributed to the unusually high (~80%) A+T content of parasite genes which can result in the prevalence of repetitive amino acid stretches (Tsuboi *et al.*, 2008), and the use of codons that are not frequently used by organisms selected for heterologous expression affecting translation efficiency.

Despite, or because of, these challenges, recombinant expression of *Plasmodium* proteins has been tested in a number of expression systems. The *E. coli* bacterial expression system is the most popular (Fernández-Robledo and Vasta, 2010). While *E. coli* expression is inexpensive system and can produce high yields of recombinant proteins, an important drawback is that recombinant proteins lack post-translational modifications and therefore, do not represent eukaryotic proteins as they found *in* vivo (Birkholtz *et al.*, 2008; Fernández-Robledo and Vasta, 2010). Moreover, recombinant proteins are expressed in an insoluble form and, often, sequestered in cytoplasmic inclusion bodies (Birkholtz *et al.*, 2008). Such recombinant protein aggregates require solubilisation followed by refolding

(Rodriguez *et al.*, 2008; Baum *et al.*, 2009; Chen *et al.*, 2011), and the overall success rate for obtaining soluble, immunogenic recombinant products remains low and variable depending on the individual protein being expressed (Fernández-Robledo and Vasta, 2010).

In other implementations of *E. coli* expression systems, the recombinant protein is expressed in a soluble form and is secreted into the periplasmic space. The oxidative environment of the periplasmic space facilitates the formation of disulfide bonds and therefore, increases the chances of obtaining a correctly folded, recombinant protein (De Marco, 2009). Nevertheless, recombinant expression of eukaryotic proteins (including *Plasmodium* proteins) in this way, often requires the co-expression of the protein of interest with other proteins which facilitate secretion to the periplasmic space, or mediate correct protein folding by controlling the disulfide bond formation (Outchkourov *et al.*, 2008; de Marco, 2009). A good example of a recombinant *Plasmodium* protein purified from the periplasmic space is *Pf*s48/45 which is a major candidate for the development of a malaria transmission blocking vaccine (section1.13.1 ;Outchkourov and Roeffen, 2008)

Yeast-based systems have also been used for recombinant expression of *Plasmodium* proteins (Ballou *et al.*, 2004). *Saccharomyces cerevisiae* and *Pichia pastoris* are the most commonly used yeast species for heterologous protein expression of *Plasmodium* proteins (Birkholtz *et al.*, 2008). The advantage of yeast over bacterial expression systems is that the recombinant proteins are expressed in their native conformation and can be secreted in a soluble form in the culture medium, simplifying their subsequent purification (Birkholtz *et al.*, 2008). Similar advantages are shared by baculovirus-insect cell and HEK293 expression systems, both eukaryotic expression systems that have been used for the heterologous expression of *Plasmodium* proteins (Li *et al.*, 2002; Ballou *et al.*, 2004; Fernández-Robledo and Vasta, 2010; Crosnier *et al.*, 2011; Douglas *et al.*, 2011; Williams *et al.*, 2012; Bustamante *et al.*, 2013). One common problem that arises with expression of *Plasmodium* proteins in eukaryotic expression systems is aberrant N-linked and O-linked glycosylation. *Plasmodium* parasites lack the enzymatic machinery necessary for glycosylation, but their proteins do contain canonical N-linked glycosylation sites which can become occupied during expression in heterologous eukaryotic cells (Dieckmann-Schuppert *et al.*, 1992). This problem can easily be circumvented by

mutating the N-linked glycosylation sites found in the transgene coding sequence, or by inclusion of N-glycosylation inhibitors in the culture medium (Birkholtz *et al.*, 2008; Fernández-Robledo and Vasta, 2010)

The protozoa *Dictyostelium discoideum* and *Tetrahymena thermophile* are another example of protein expression systems, employed for recombinant expression of *Plasmodium* proteins. They originally became an attractive system for heterologous expression of *Plasmodium* proteins because of the unusual A+T bias of their gene coding sequence, a characteristic they share with *P. falciparum* genome (Birkholtz *et al.*, 2008; Fernández-Robledo and Vasta, 2010). However, while multiple expression systems have been trialled, it is fair to say that until systematic application of HEK293E expression, no single approach has been consistently successful.

## 5.2.2 Studying extracellular protein-protein interactions between merozoite and erythrocytes- the AVEXIS assay.

Cell surface protein-protein interactions between *Plasmodium* merozoite and erythrocytes have been traditionally studied by using naturally occurring erythrocyte variants which either lack, or express a mutant form of a specific cell surface receptor (Bei and Duraisingh, 2012; Bartholdson *et al.*, 2013). Such erythrocytes variants have been used to derive evidence about the binding specificity of different parasite ligands or to determine the impact of specific mutations on parasite invasion efficiency (Bei and Duraisingh, 2012; Bartholdson *et al.*, 2013). For example, the binding specificity of EBA140 for GYPC was established by using erythrocytes lacking expression of GYPC, or lacking specific exons in the *GYPC* gene (Lobo *et al.*, 2003; Maier *et al.*, 2003; Bartholdson *et al.*, 2013). Likewise, GYPB-deficient red blood cells were utilised to show that GYPB is the receptor for EBL1 (Mayer *et al.*, 2009; Bartholdson *et al.*, 2013). The availability, however, of erythrocytes expressing particular receptor variants can be limited. This fact, combined with the relatively short shelf life of cellular biopsies and the possibility that the absence of some receptors might be incompatible with normal erythrocyte function, make this approach generally impractical for systematically identifying new ligand-receptor pairs (Bartholdson *et al.*, 2013).

Information about the binding characteristics of parasite ligands to erythrocytes can also be obtained by testing the sensitivity of the binding of parasite proteins to enzyme-treated erythrocytes (Bartholdson *et al.*, 2013). For example, initial studies with EBA-175 demonstrated that EBA-175 binds to a neuraminidase and trypsin sensitive receptor (Camus and Hadley, 1985), which was later identified to be GYPA (Sim *et al.*, 1994; Bartholdson *et al.*, 2013). Nevertheless, using binding sensitivity to erythrocytes treated with broad substrate specificity enzymes (e.g. trypsin and chymotrypsin), is only rarely helpful because a large number of receptors are sensitive to this treatment.

Cell-surface interactions between erythrocytes and merozoites can also be examined by using recombinant proteins. Besides the difficulties in recombinant expression of *Plasmodium* proteins (section 5.2.1), another major challenge of this approach has been the limited availability of high-throughput assays for the systematic identification of cell-surface protein-protein interaction which are normally highly transient with half-lives of just a few seconds (Wright, 2009; Bartholdson *et al.*, 2013). High throughput assays for the identification of protein-protein interactions, like the yeast-two-hybrid (Young, 1998) and TAP-tagging methods followed by mass spectrometry (Rigaut *et al.*, 1999; Puig *et al.*, 2001), are generally regarded as unsuitable to detect transient interactions between extracellular proteins (Bushell *et al.*, 2008; Wright, 2009): structurally-important post-translational modifications such as disulfide bonds and glycans are not generally added to proteins within the yeast nucleus and the stringent washing steps of biochemical purifications do not allow the detection of transient interactions (Wright, 2009).

To address the problems associated with identifying novel low affinity extracellular protein interactions (including those involved in erythrocyte invasion), an assay termed AVEXIS (for AVidity-based EXtracellular Interaction Screen) was developed (Bushell *et al.*, 2008) (Fig. 5.1). AVEXIS was designed specifically to detect highly transient extracellular protein-protein interactions. The entire ectodomains of cell surface or secreted proteins are recombinantly expressed as soluble fragments in HEK293 cells. Each protein is expressed as both monomeric biotinylated bait and β-lactamase tagged pentameric prey. The pentamerization is required to increase the overall interaction avidity, allowing the assay to detect very transient interactions (with halflives<0.1s) that are a common feature of this class of
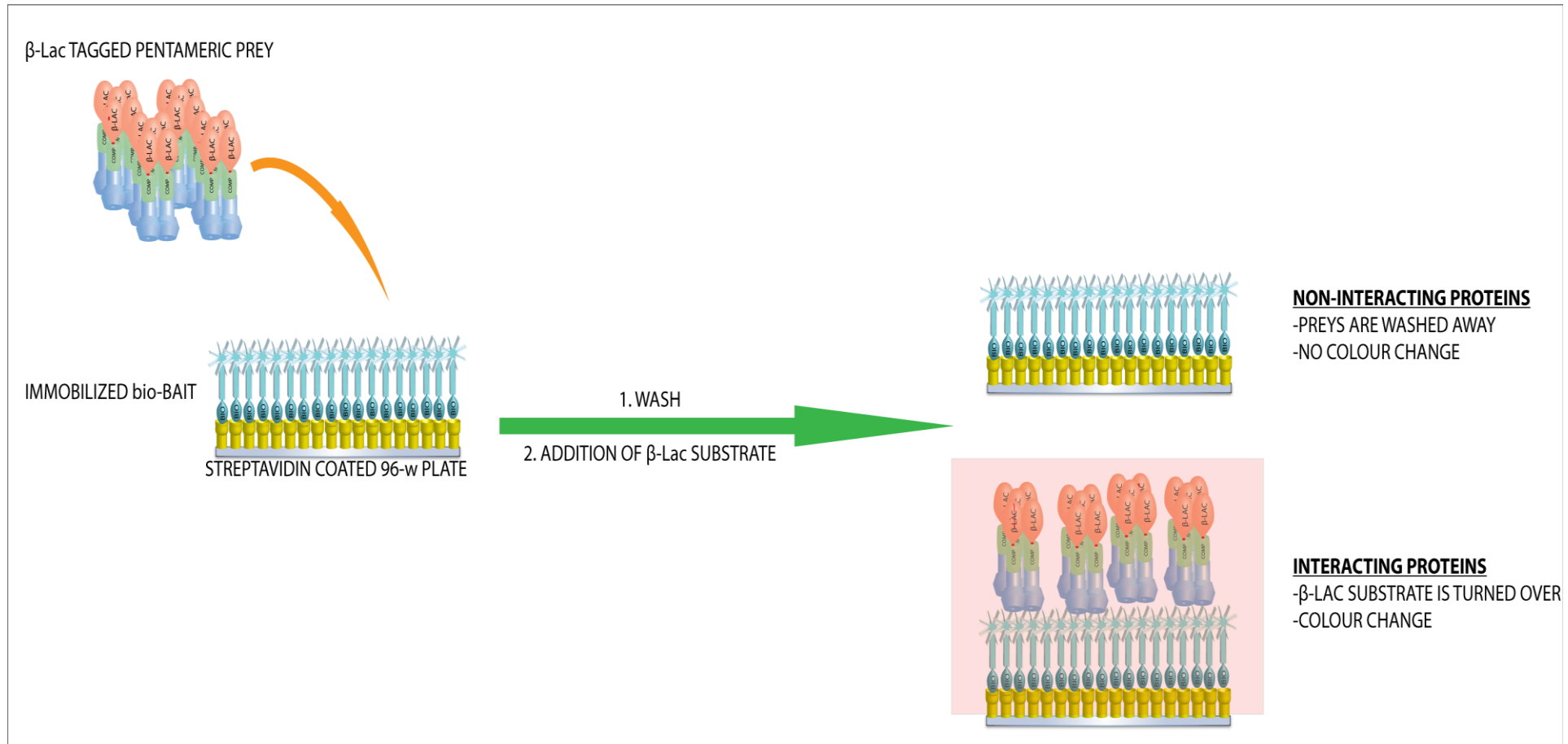
**Figure 5.1 The AVEXIS assay.** Recombinant monobiotinylated bait ectodomains are captured in an oriented manner on a streptavidin-coated micro well plate and systematically screened against β-lactamase tagged pentameric prey ectodomains. Interactions between baits and preys are detected by colourimetric enzymatic turnover of nitrocefin (β-lactamase substrate).

protein interactions. Baits are arrayed by orientated capture on streptavidin-coated plates, and probed for direct interactions with the enzyme-tagged prey proteins (Bushell *et al.*, 2008). By using this assay, BSG and Semaphorin7A were identified as the erythrocyte receptors for merozoite RH5 and MTRAP, respectively (Crosnier *et al.*, 2011; Bartholdson *et al.*, 2012). Notably, the RH5-BSG interaction is the only one known so far that is essential and universally required for erythrocyte invasion (Crosnier *et al.*, 2011). Given the complexity of erythrocyte invasion, it is clear that many additional interactions remain to be identified.

## 5.3 Results

To identify novel cell surface protein-protein interactions implicated in erythrocyte invasion, I sought to expand the *P. falciparum* merozoite recombinant protein library (section 5.1) which is available in our laboratory, and employ AVEXIS to *in vitro* screen the new library members against an erythrocyte cell surface receptor repertoire. To use the AVEXIs assay for the screen, it was necessary to recombinantly express both the merozoite and human erythrocyte protein libraries. The expression constructs encoding the erythrocyte cell surface receptors were available in our laboratory from previous experiments (Crosnier *et al.*, 2011).

### 5.3.1 Compilation of a list of candidate *P. falciparum* merozoite cell surface or secreted proteins

To expand the existing *P. falciparum* merozoite recombinant protein library, I compiled a list of merozoite cell surface or secreted proteins with possible roles in erythrocyte invasion. To identify candidate merozoite cell surface or secreted proteins, I took advantage of publicly available transcription microarray data of *P.falciparum* intra-erythrocytic stages (Bozdech *et al.*, 2003). Bioinformatic analysis of these data, demonstrated that several known merozoite ligands (e.g RH5, AMA1, EBA140, EBA175; Cowman *et al.*, 2012; Bartholdson *et al.*, 2013) follow a similar transcriptional expression pattern which passes through a minimum 20±6 hours post invasion and peak at about 42±6 hours after invasion. Therefore, the latter time-windows were set as criteria for short listing 405 candidate merozoite cell surface proteins (Bozdech *et al.*, 2003). Of 405 shortlisted proteins, 217 carried a signal peptide and/or a single transmembrane domain, as predicted by using the SignalP (http://www.cbs.dtu.dk/services/SignalP/) and TMHMM prediction servers

(http://www.cbs.dtu.dk/services/TMHMM/) respectively, suggesting they are likely cell surface or secreted proteins and therefore considered as candidate proteins. Multipass membrane proteins were excluded because such proteins are unlikely to be expressed in a soluble, secreted form by using the HEK293 expression system.

The 217 candidate proteins included 40 out of the 53 members of the already existing *P. falciparum* merozoite recombinant protein library (Crosnier *et al.*, 2013). This is translated to 75% coverage, indicative of the validity of my methodology. The 40 merozoite proteins which were already available in our laboratory were excluded for further analysis, reducing the number of candidate proteins to 177.

Because I was focused on identifying merozoite cell surface and secreted proteins, all candidate proteins were subject to gene ontology analysis by using the relevant tool in PlasmoDB (www.plasmoDB.org), and to protein domain mapping analysis by using Pfam (www.pfam.sanger.ac.uk). Out of 177 proteins, 121 were removed, because their predicted gene ontology (e.g. involvement in lipid metabolism or nuclear localization) or predicted protein domains (e.g. RNA or DNA binding motif) suggested that they are unlikely to participate in cell surface protein interactions. Another 42 proteins were excluded due to their large size (>1400 amino acids) which are not only prohibitively expensive to codon optimise by gene synthesis, but often expressed at levels below that required for performing additional experiments. After this analysis, 14 candidate merozoite cell surface proteins remained on our shortlist. Seven putative merozoite cell surface proteins were also added onto the candidate list, based on previously published reports in the literature (Haase *et al.*, 2008; Hu *et al.*, 2010) (Fig. 5.2).

The availability of the complete set of proteins belonging to a specific *Plasmodium* paralogous protein family, would allow direct comparison between individual members of the family in the case that one protein-member was found to interact with an erythrocyte cell surface receptor. Several members of the MSP3 (Burgess *et al.*, 2005; Singh *et al.*, 2009) and MSP-7 like (Kadekoppala *et al.*, 2008, 2010; Kadekoppala and Holder, 2010) *P. falciparum* protein families were already available in the laboratory from the previously developed *P. falciparum* merozoite recombinant protein library (Crosnier *et al.*, 2013). However, not all the members of these two families were included in this initial library. The members of

| No | Name | Accession Code | Type | Region to be expressed |
|----|------|----------------|------|------------------------|
| 1 | rhoptry-associated membrane antigen (RAMA) | MAL7P1.208 | GPI | Y17–S840 |
| 2 | prohibitin, putative | PF08_0006 | secreted | L20–F272 |
| 3 | conserved Plasmodium protein, unknown function | PF10_0166 | secreted | Y25–E310 |
| 4 | GLURP | PF10_0344 | secreted | K24–I1233 |
| 5 | MSP3.5 | PF10_0350 | secreted | A20–F710 |
| 6 | MSP3.6 | PF10_0351 | secreted | N22–P566 |
| 7 | MSRP5 | PF13_0191 | secreted | N22–I459 |
| 8 | MSRP4 | MAL13P1.173 | secreted | D22–Q309 |
| 9 | MSP8 | PFE0120c | GPI | E26–S576 |
| 10 | conserved Plasmodium protein, unknown function | PF13_0125 | secreted | N20–S292 |
| 11 | conserved Plasmodium protein, unknown function | PF14_0044 | secreted | Q21–K290 |
| 12 | merozoite-associated tryptophan-rich antigen, putative | PFA0135w | secreted | I25–K276 |
| 13 | LCCL domain-containing protein | PFA0445w | secreted | K22–I1029 |
| 14 | SERA1 | PFB0360c | secreted | M1–V997 |
| 15 | SERA2 | PFB0355c | secreted | E23–V1105 |
| 16 | SERA3 | PFB0350c | secreted | T23–I930 |
| 17 | SERA4 | PFB0345c | secreted | S26–V962 |
| 18 | SERA5 | PFB0340c | secreted | T23–V997 |
| 19 | SERA6 | PFB0335c | secreted | N25–V1031 |
| 20 | SERA7 | PFB0330c | secreted | Q23–V946 |
| 21 | SERA9 | PFI0135c | secreted | E23–V932 |
| 22 | conserved Plasmodium protein, unknown function | PFA0210c | secreted | Y24–D466 |
| 23 | conserved Plasmodium protein, unknown function | PFB0475c | secreted | L23–D446 |
| 24 | conserved Plasmodium protein, unknown function | PFD1130w | secreted | D29–E362 |
| 25 | EBA-165 (corrected ORF) | PFD1155w | I | K22–S1340 |
| 26 | RIPR | PFC1045c | secreted | I20-N1086 |

**Figure 5.2 The merozoite cell surface proteins that were chosen for recombinant expression.** Protein sequences from 3D7 reference *P.falciparum* strain were truncated to remove endogenous signal peptides and sequences corresponding to cytoplasmic and transmembrane domains. The region of each truncated protein that was targeted for recombinant expression is showed on the right column. Abbreviations: GPI, GPI-anchored; I, type I; sec., secreted. Proteins shortlisted from bioinformatic analysis of transcription microarray data are highlighted with grey colour. Proteins chosen from Hu *et al.*, 2010 or Haase *et al.*, 2008, are indicated in green and cyan respectively. The proteins chosen to enable having a complete set of proteins belonging to the MSP3, MSP7 like and SERA families of proteins are highlighted in yellow. EBA-165 was enlisted because it could potentially be useful for experiments that may help to the understanding of host tropism evolution of *P. falciparum.*

these protein families that were missing (MSP3.5, MSP3.6, MSRP4) were also added to our candidate protein list (Fig. 5.2). Similarly, SERA9 was selected because it would complete the set of proteins belonging to the SERA family of proteins (Fig. 5.2); the rest of the SERA family members were short listed from the bioinfomatic analysis of transcription microarray data or from the previously published studies (see above).

*Pf*EBA-165, which is encoded by a likely pseudogene in *Plasmodium falciparum* was also included in my list. Six *P. falciparum* strains investigated in earlier studies, all contained at least one frameshift mutation in the *Pf*eba165 gene that leads to premature termination of protein translation (Triglia *et al.*, 2001; Rayner *et al.*, 2004). The reference *P. falciparum* strain 3D7 contains two such frameshifts, and no *Pf*EBA-165 protein was detected in blood stage parasites (Triglia *et al.*, 2001). It is not currently known whether any naturally occurring *P. falciparum* parasites encode a full-length *Pf*EBA165. Nevertheless, *eba-165* appears to be functional in *Plasmodium reichenowi* in which the frameshifts are missing (Rayner *et al.*, 2004). *P. reichenowi* infects chimpanzee, and is the closest *Plasmodium* species to *Plasmodium falciparum.* Considering the close evolutionary relationship between the two parasite species and also between their primate hosts, EBA-165 could potentially be useful for experiments that may help to understand the evolution of host tropism in *P. falciparum* (see Chapter 6). Therefore, we felt that it was reasonable to add EBA-165 on our protein candidate list, even though it is not currently known whether any *P. falciparum* parasites express it. The two frameshifts in *Pf*eba-165 gene (from 3D7 genome) were corrected before gene synthesis. To correct the 5' frameshift, an adenine was inserted at position 219 of the *Pf*eba-165 coding sequence (CDS). To restore the reading frame towards the 3' end, the adenine at position 1252 of *Pf*eba-165 CDS was deleted (Rayner *et al.*, 2004). The final list consisted of 26 merozoite cell surface proteins (Fig. 5.2).

### 5.3.2 Recombinant expression of an expanded *P.falciparum* merozoite protein library

The 26 shortlisted merozoite candidate proteins were expressed recombinantly as described in section 2.1. Briefly, the sequences encoding for full-length secreted proteins or for ectodomains of cell surface proteins were codon optimised for expression in the human cell line HEK293E, and the potential N-linked glycosylation

sites were systematically removed by substituting alanine for serine/threonine at these sites. Codon optimised expression constructs were synthesised by gene synthesis and provided already sub-cloned into a pTT3-based vector which enables recombinant expression of C-terminally Cd4-hexa-histidine tagged proteins (Fig. 2.1). For recombinant protein expression, the plasmid vectors carrying the synthesised merozoite protein coding sequences, were transfected into HEK293E cells and tissue culture supernatant was harvested six days post transfection. Merozoite proteins were purified from tissue culture supernatant by affinity chromatography on a 96-well nickel column plate.

Purified proteins were quantified relative to Cd4 by ELISA (Fig. 5.3). Most of the proteins were expressed at the levels required for the AVEXIS assay (sufficient amount of protein for complete saturation of the available binding surface Bushell *et al.*, 2008). However, five proteins (GLURP, PF14_0044, PFA0445w, SERA1, SERA6) were almost undetectable by ELISA after five different transfection batches and therefore, excluded from further analysis (indicated in red in Fig. 5.3). The expression level for another three proteins which are indicated in cyan in Fig. 5.3 (SERA7, PFA0210c, RIPR) was below the threshold required for the AVEXIS screen assay, but because some protein was detected, it was considered worth testing them in the experiments described below. These data demonstrate that of 26 recombinant merozoite proteins, 21 (>80%) were successfully expressed at usable amounts.

To confirm expression at the correct size, biotinylated merozoite baits were analysed by western blot (Fig. 5.4). No band was detected for PF14_0044, PFA0445w and SERA1 (data not shown). This observation is consistent with the results obtained by ELISA, and suggests that these proteins failed to express. For SERA 7 and PF08_0006 only a band much lower than the expected size (probably representing the protein tags; section 5.4.1) was detected. In all the remaining proteins, a band representing the full length ectodomain was obtained, but a number of smaller bands were also evident probably due to protein degradation or likely because of proteolytic processing (Fig. 5.4) (section 5.4.1). These observations establish the successful expression of the majority of recombinant merozoite proteins. Overall, 19 of 26 proteins (>73%) were expressed at usable amounts, and a band corresponding to full length recombinant protein was detected by immunoblot.
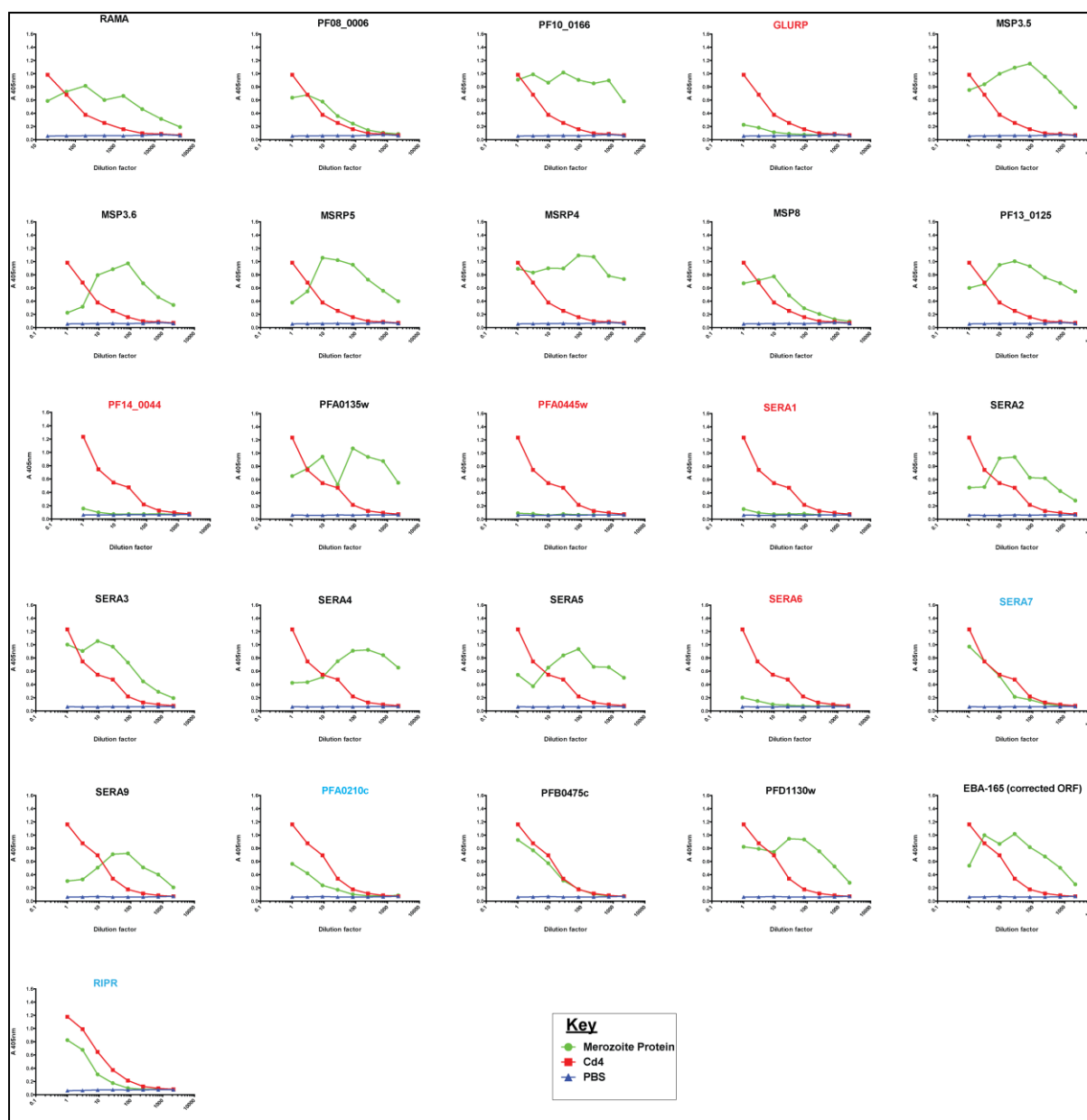
**Figure 5.3 Quantitation of merozoite cell surface protein library by ELISA.** Purified, recombinant merozoite proteins were serially diluted and immobilised on a streptavidin-coated microtiter plate. The anti-Cd4 mouse monoclonal OX68, was used as the primary antibody and an alkaline phosphatase-conjugated anti-mouse IgG antibody as the secondary antibody. Biotinylated Cd4 was used as reference. The proteins where the expression was almost undetectable by ELISA after five different transfection batches are indicated in red. The proteins which did not reach the threshold activity required for the AVEXIS assay are indicated in cyan.
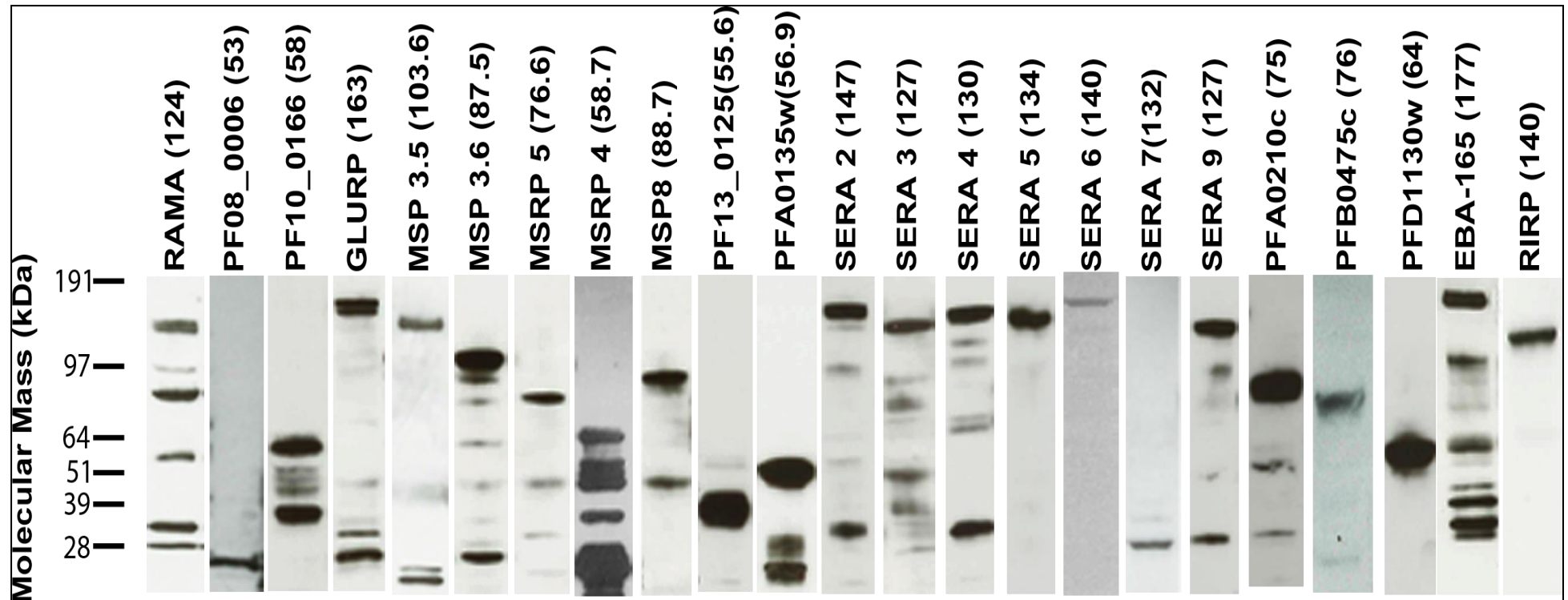
**Figure 5.4 The majority of recombinant merozoite extracellular proteins were expressed at the expected size.** Normalised amounts of purified biotinylated merozoite proteins were resolved under reducing conditions by SDS-PAGE, blotted, and probed using streptavidin-HRP. The expected molecular weight for the each recombinant protein is indicated in brackets above each lane; this includes the Cd4-BioLinker-6xHis tags (28kDa).

### 5.3.3 Biochemical characterisation of the recombinant merozoite protein library

Specific interactions can only detected between proteins that are correctly folded (Bartholdson *et al.*, 2013). Thus, it was considered essential to biochemically characterise the members of the merozoite bait library and confirm that the proteins are active and correctly folded, prior to performing the AVEXIS screen. For this purpose a series of three experiments were designed (described below) to derive evidence for the correct conformation of the recombinant merozoite proteins.

#### 5.3.3.1 Members of the merozoite protein library contain heat-labile epitopes

In nature, proteins are recognised by antibodies in their native conformation. The latter implies that antibodies recognise and bind to conformational epitopes on target proteins. Therefore, denaturation of these epitopes by heat treatment normally reduces immunoreactivity. This logic was used to derive evidence whether recombinant merozoite proteins were correctly folded. Recombinant proteins at the correct conformation were expected to be recognised by naturally occurring antibodies, and immunoreactivity was anticipated to decrease after heat treatment of the same proteins.

For this purpose, recombinant merozoite cell surface proteins were assayed by ELISA, for their immunoreactivity against pooled hyperimmune sera obtained from previously malaria exposed Malawian adults (provided by Dr Faith Osier; Taylor *et al.*, 1992). Each biotinylated merozoite protein was immobilised on a 96-well streptavidin-coated plate (to levels sufficient for complete saturation of the available binding surface) and incubated with protein G purified total IgG from hyperimmune or non-immune sera. In this experiment AMA-1 was used as positive control. AMA-1 is a merozoite cell surface protein which has been previously shown to elicit high antibody titers (Thera *et al.*, 2010; Ellis *et al.*, 2012). The expression construct for AMA-1 was available in our laboratory for previous experiments and it was used for recombinant expression of AMA-1 (Crosnier *et al.*, 2013). The OX68 anti-Cd4 monoclonal antibody was used to confirm bait immobilisation.

Most of the merozoite recombinant proteins gave a signal well above the baseline against the hyperimmune sera and they were negative against the non-immune control sera (Fig. 5.5). For the vast majority of proteins the immunoreactivity

against the immune sera, decreased or completely disappeared when the proteins were heat-inactivated. These data show that antibodies contained in hyperimmune sera bind to heat-labile epitopes on recombinant merozoite proteins. When these proteins are linearized by heat-treatment, they are no longer as immunoreactive suggesting that merozoite recombinant proteins adopt their native conformation.

### 5.3.3.2 *In vitro* interaction of RIPR with RH5

RIPR is a merozoite cell surface protein which has been recently proposed to be an RH5 interaction partner (Chen *et al.*, 2011). Therefore, the recapitulation of this interaction by AVEXIS, using recombinant proteins, would provide evidence that RIPR has the correct conformation. Thus, monomeric biotinylated RIPR bait was recombinantly expressed, purified by affinity chromatography on nickel loaded Sepharose column and quantitated by ELISA (Fig. 5.6 A). Pentameric, β-lactamase tagged RH5 prey was also expressed and quantified by using β-lactamase activity as a proxy (Fig. 5.6A). For the AVEXIS assay, RIPR was immobilised on a streptavidin-coated plate and probed with pentameric RH5. Even though RIPR expression level was below the threshold required for the AVEXIS (sufficient amount of protein for complete saturation of the available binding surface) the interaction between RIPR and RH5 was still detected (Fig. 5.6B). This result suggests that RIPR is active and correctly folded.

### 5.3.3.3 EBA165 demonstrates differential glycan binding in comparison to other Erythrocyte Binding Ligands (EBLs)

The AVEXIS assay was primarily designed for the detection of low affinity protein-protein interactions, but can also be used to detect a range of extracellular interactions (Bushell *et al.*, 2008; Bartholdson *et al.*, 2013). By using AVEXIS, EBA-175 and EBA-140 preys were previously shown to bind a number of biotinylated glycan baits (Dr Madushi Wanaguru, unpublished data). These glycans are members of a larger glycan panel available in our laboratory which is enriched for glycans present on human erythrocytes (www.glycotech.org). It was interesting to test whether EBA-165, which belongs to the same protein family as EBA-175 and EBA-140 (Triglia *et al.*, 2001; Rayner *et al.*, 2004), was also capable of binding to certain
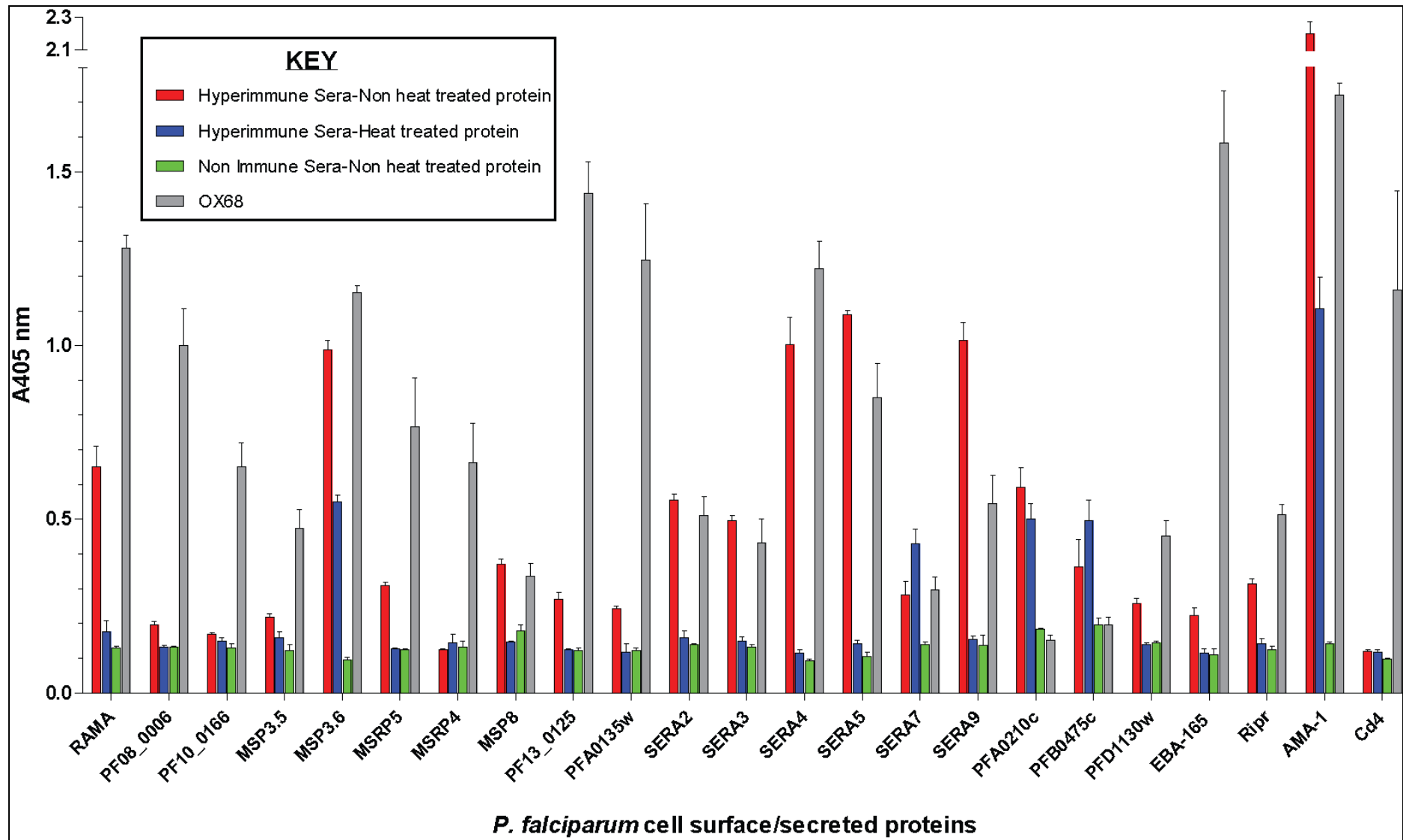
**Figure 5.5 Members of the merozoite cell surface protein library are reactive against hyperimmune sera obtained from previously malaria exposed Malawian adults.**

Biotinylated, purified merozoite cell surface proteins (native or heat treated at $80^{o}C$ for 10mins) were immobilised on a streptavidin-coated plate and incubated for 2 hours in the presence of immune or non-immune sera or OX68 (anti-Cd4) followed by 1 hour incubation with an anti-hIgG or anti-mIgG alkaline phosphatase conjugated secondary antibody. Biotinylated AMA-1 and Cd4 were used as positive and negative control, respectively. Data points are shown as mean ± s.e.m; *n*=3.
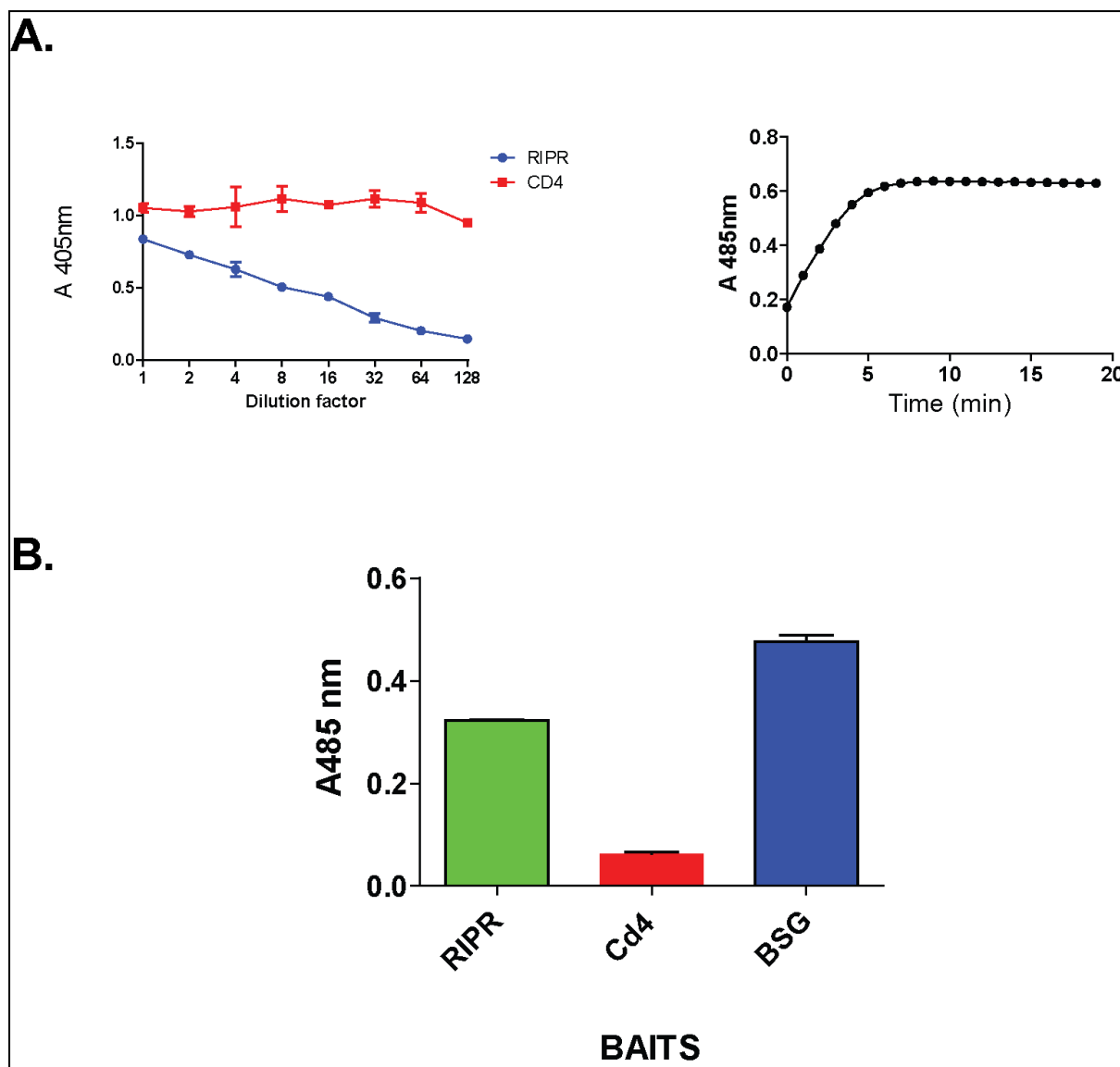
**Figure 5.6    RIPR binds RH5 in AVEXIS.**

*A.* Purified biotinylated RIPR bait (left) and RH5 pentameric prey (right), were quantitated by ELISA and time course monitoring of nitrocefin turnover, respectively. While RH5 activity reached the level required for AVEXIS (section 2.5), the expression level of RIPR was below the threshold required for AVEXIS. Biotinylated Cd4 was used as reference in ELISA.

*B.* RIPR was clearly bound by RH5 in an AVEXIS assay. Biotinylated RIPR was immobilised on a streptavidin-coated plate and probed with RH5-prey, in an AVEXIS assay. Biotinylated Cd4 and BSG were used as negative and positive control, respectively. Data is shown as mean ± s.e.m; *n*=3.

glycans. Such a case would provide evidence that recombinant EBA-165 has adopted the correct conformation.

First, EBA-140, EBA-175 and EBA-165 preys were recombinantly expressed and their activity in tissue culture supernatant was assessed by monitoring nitrocefin turnover over time (Fig 5.7A). For the AVEXIS screen, each glycan was immobilised on a streptavidin-coated plate to levels sufficient for complete saturation of the available binding surface, following by incubation with each of the EBL preys. The EBA-165 prey clearly bound multiple glycans, suggesting that folded domains do exist on the recombinant protein (Fig 5.7B). Interestingly, EBA-165 was able to bind only to glycans containing N-glycolylneuraminic acid (Neu5Gc), whereas EBA-140 and EBA-175 were capable of binding to both N-aceytlneuraminic acid (Neu5Ac) and Neu5Gc containing glycans. Because humans lack the enzyme that converts Ne5Ac to Neu5Gc, Neu5Gc are the dominant sialic-acids in apes but not in humans. (Chou *et al.*, 1998; Varki, 2001). Given that EBA-165 appears to be a pseudogene in the human malaria parasite *P.falciparum,* but is functional *P. reichenowi* (chimpanzee restricted parasite), this observation may have implications for the evolution of *P. falciparum* host specificity, which are discussed Chapter 6.

## 5.3.4 Recombinant expression of a human erythrocyte cell surface protein library

Crosnier and colleagues compiled a list of cell surface and secreted proteins expressed by human erythrocytes (Crosnier *et al.*, 2011), based on published proteomics data (Pasini *et al.*, 2006). Proteins for which the entire ectodomain was expected to be expressed as a soluble recombinant protein were selected and recombinantly expressed in HEK293E cells (Crosnier *et al.*, 2011). The expression constructs encoding for the prey forms of 31 of those erythrocyte cell surface proteins, were employed for the purposes of my experiments (Fig. 5.8).

For recombinant protein expression the above constructs were transfected in HEK293E cells and tissue culture supernatants were analysed for the presence of recombinant β-lactamase-tagged protein preys, by monitoring nitrocefin turnover six days post transfection (Fig. 5.9). To achieve the prey activity which was required for the AVEXIS assay (sufficient protein in 20µl prey tissue culture supernatants to turnover 60 µl of 250 µg/mL nitrocefin within 10mins) (Bushell *et al.*, 2008), repeated
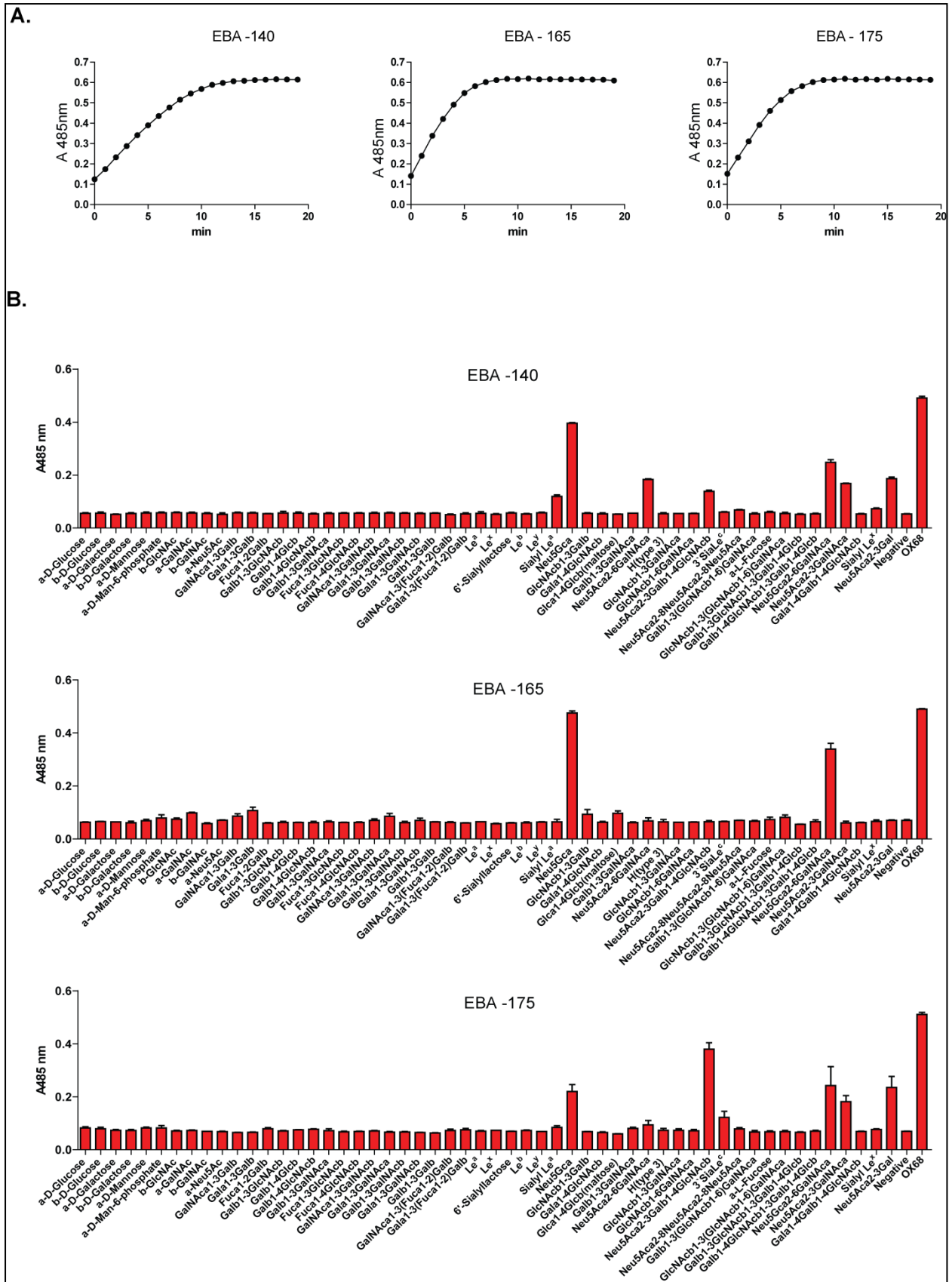
**Figure 5.7 EBA-165 demonstrates differential binding to a glycan panel, in comparison to other members of the EBL family of proteins.**

*A.* EBA-165, EBA-140, EBA-175 were expressed as β lactamase-tagged pentameric preys and quantitated by monitoring their enzymatic activity.

*B.* EBA-165, EBA-140, EBA-175 were screened against a glycan panel, by using AVEXIS. Normalised amounts of biotinylated glycans were immobilised on a streptavidin-coated plate and probed with pentameric preys. The biotinylated monoclonal anti-Cd4 antibody OX68 was used to confirm prey activity. The biotinylated bait used as the negative control contained the linker region carried by all the synthetic glycans. Data are shown as mean ± standard error; *n*=3

| No | Protein Name | Trunc. | Type | Accession code | Blood group |
|----|--------------|--------|------|----------------|-------------|
| 1 | GLYCOPHORIN A | P90 | I | P02724 | MNS |
| 2 | GLYCOPHORIN B | P60 | I | P06028 | MNS |
| 3 | GLYCOPHORIN E | N51 | I | P15421 | |
| 4 | GLYCOPHORIN C | D58 | III | P04921 | Gerbich |
| 5 | MIC2/CD99 | P124 | I | P14209 | Xg |
| 6 | CD44_ISOFORM 1 | P648 | I | P16070 | Indian |
| 7 | COMPLEMENT RECEPTOR 1_ISOFORM S | L2423 | I | NP_000642 | Knops |
| 8 | BASIGIN_ISOFORM 1 | L322 | I | P35613_1 | Ok |
| 9 | BASIGIN_ISOFORM 2 | L206 | I | P35613_2 | Ok |
| 10 | BCAM | G548 | I | P50895 | Lutheran |
| 11 | AMIGO2 | T398 | I | Q86SJ2 | |
| 12 | NICASTRIN | L670 | I | Q92542 | |
| 13 | ERMAP | S154 | I | Q96PL5 | Scianna/Radin |
| 14 | C1ORF9 | R1010 | I | Q9UBS9 | |
| 15 | JAM1 | V238 | I | Q9Y624 | |
| 16 | NEUROPLASTIN | P223 | I | Q9Y639 | |
| 17 | PROGESTERON RECEPTOR COMPONENT 2 | A46 | I | O15173 | |
| 18 | LFA3/CD58 | L218 | I | P19256 | |
| 19 | ENDOD1 | P338 | I | O94919 | |
| 20 | SEMAPHORIN7A | A644 | GPI | O75326 | John Milton Hagen |
| 21 | COMPLEMENT DECAY ACCELERATING FACTOR | S353 | I/GPI | P08174 | Cromer |
| 22 | MACIF/CD59 | N102 | GPI | P13987 | |
| 23 | ACETYLCHOLINESTERASE_ISOFORM H | T581 | GPI | P22303-2 | Yt |
| 24 | MULTIDRUG RESISTANCE PROTEIN 1/MRP1 | T36 | 17TM | P33527-2 | |
| 25 | DUFFY_ISOFORM 1 | P63 | 7TM | Q16570-2 | |
| 26 | PROLACTIN | n.a. | sec. | P01236 | |
| 27 | LACTOTRANSFERRIN | n.a. | sec. | P02788 | |
| 28 | C8ORF55 | n.a. | sec. | Q8WUY1 | |
| 29 | METHYLTRANSFERASE-LIKE PROTEIN 7A | n.a. | sec. | Q9H8H3 | |
| 30 | GALECTIN-3/LGALS3 | n.a. | sec. | P17931 | |
| 31 | PROTEIN DISULFIDE-ISOMERASE/P4HB | n.a. | sec. | P07237 | |

**Figure 5.8 The erythrocyte cell surface receptor library.** Abbreviations: Trunc.,the ectodomain truncation residue; I, type I; III, type III; GPI, GPI-anchored; #TM, multipass transmembrane protein with number of predicted transmembrane domains; n.a, not applicable; sec., secreted. Figure adapted from Crosnier *et al.*, 2011.
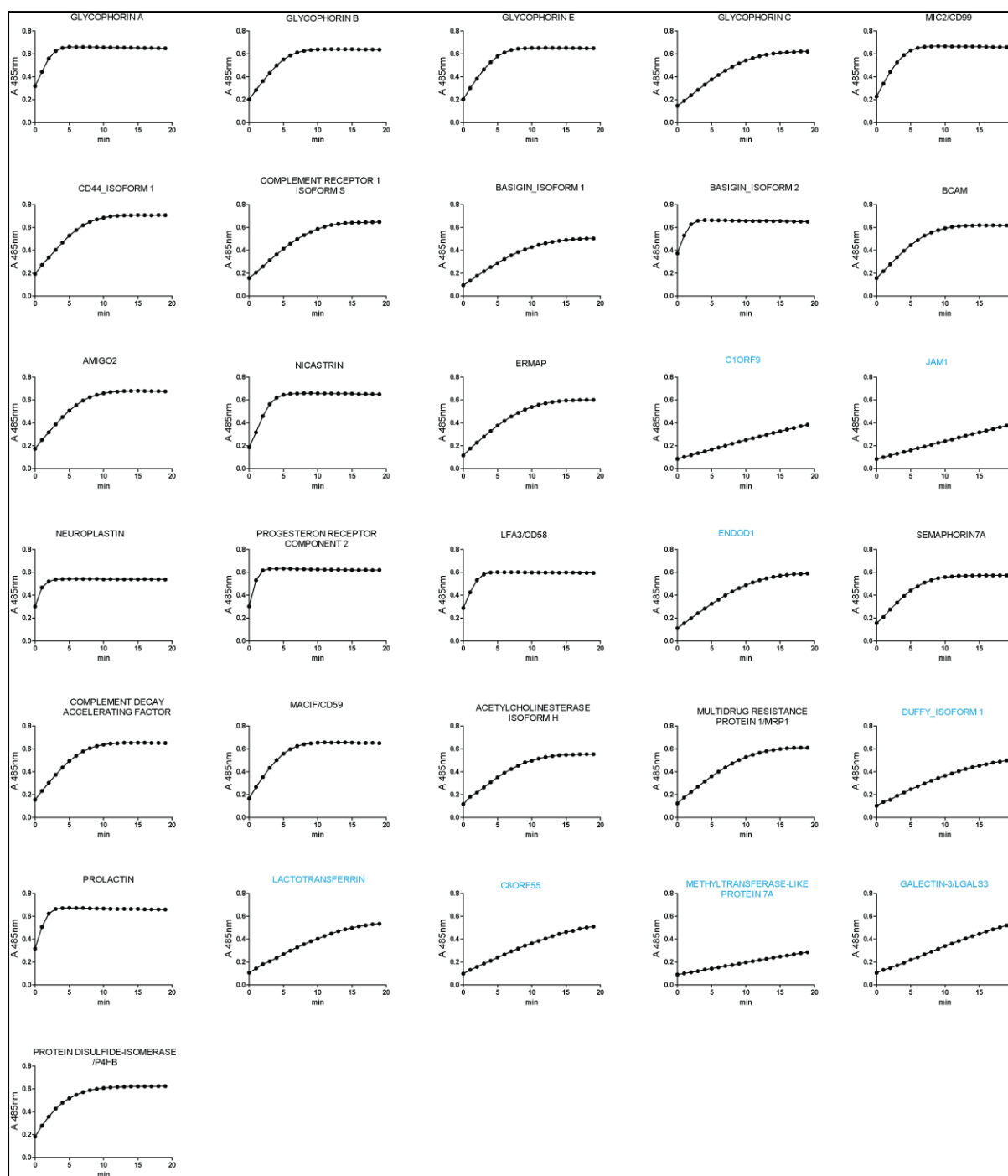
**Figure 5.9 Expression and activity assessment of erythrocyte receptor preys.** The activity of erythrocyte β-lactamase tagged pentameric preys was assessed by quantifying the turnover of the colourimetric β-lactamase substrate as a function of time. The proteins which did not reach the threshold activity required for the AVEXIS assay are indicated in cyan. The tissue culture supernatants containing the latter proteins were concentrated five times before assessment of β-lactamase activity.

rounds of transfection-analysis were performed. Proteins which did not reach the required expression level after five transfection batches, were concentrated five times, before used for probing on AVEXIS (indicated in cyan in Fig. 5.9)

## 5.3.5 The AVEXIS screen identified a putative interaction

After biochemically characterising the recombinant merozoite cell surface protein library, and recombinantly expressing a panel of erythrocyte cell surface receptors, I proceeded to the AVEXIS screen. For the screen the merozoite bait array was immobilised on a streptavidin-coated 96 well plate followed by incubation with each of the erythrocyte pentameric preys. The interaction between RH5 and BSG was used as a positive control (Crosnier *et al.*, 2011). Because the activity of several baits and preys was below the threshold required for the AVEXIS assay, to cover a range of bait and prey activities, a dilution series of RH5 bait was probed against BSG prey and vice versa (Fig. 5.10A). Cd4 was used as negative control, and biotinylated OX68 was used to capture the preys on the plate and thereby to confirm prey activity. No robust interaction with z-scores > 2 was detected (Fig 5.10B). Therefore, the three interactions (PF13_0125 – Prolactin, PF13_0125 – P4HB, PFA0135w – P4HB) which had z-scores > 1.5 (Fig 5.11) were investigated further.

Interactions detected by AVEXIS are only considered positive if they are independent of the bait–prey orientation (Bushell *et al.*, 2008). Therefore, I attempted to reciprocate the orientation of the proteins implicated in the three putative interactions identified in my screen. For this purpose, pentamerized β-lactamase tagged PF13_0125 and PFA0135w were recombinantly expressed and quantitated by monitoring β-lactamase activity over time (Fig. 5.12A). Monomeric biotinylated P4HB and Prolactin were also recombinantly expressed and quantitated by ELISA (Fig. 5.13C). All recombinant proteins were used for another AVEXIS assay. While the interactions PF13_0125 - P4HB, and PFA0135w – P4HB were detected again, the interaction between PF13_0125 and Prolactin was not (Fig. 5.12B). These reciprocation data suggest that while the interactions PF13_0125 – P4HB, and PFA0135w – P4HB were likely to be valid, the interaction between PF13_0125 and Prolactin was probably a false positive hit of the AVEXIS screen.
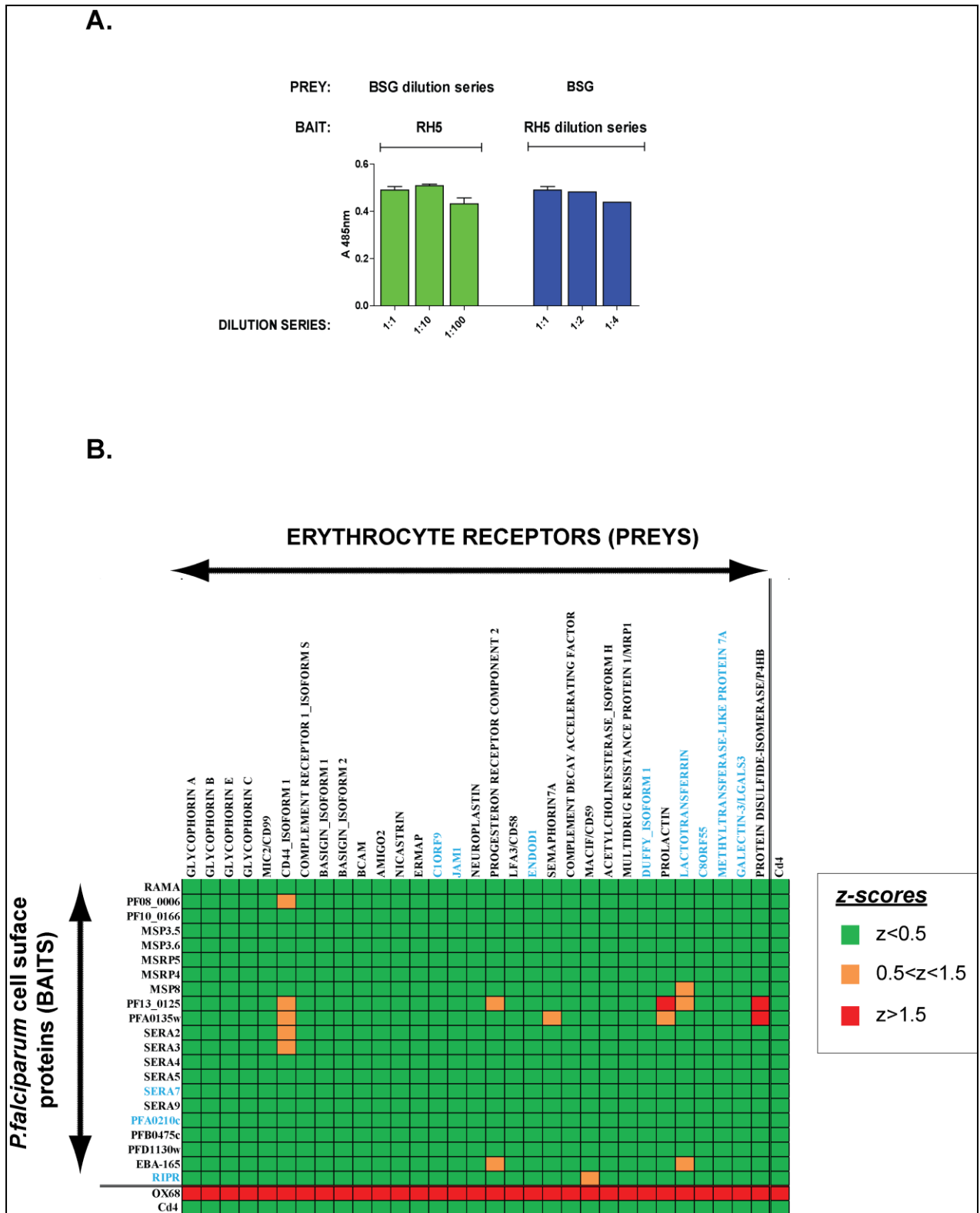
**Figure 5.10 The systematic screen between the merozoite and erythrocyte protein libraries resulted in three interactions with z-score>1.5.**

**A.** A bar chart demonstrating the interaction between Basigin-prey and RH5-bait (both from tissue culture supernatant) which was used as positive control in the screen. To cover a range of bait and prey activities a dilution series of RH5 was probed against Basigin and vice versa. Data are shown as mean ± s.e.m; *n*=3.

**B.** A z-score heat-map summarizing the results of the screen. Three interactions (PF13_0125 – Prolactin, PF13_0125 – P4HB, PFA0135w – P4HB) had z-score>1.5. Biotinylated merozoite protein baits were immobilised on a streptavidin-coated plate and probed with erythrocyte pentameric preys. Where applicable preys or baits activities were normalised against each other. The biotinylated monoclonal anti-Cd4 antibody OX68 was used to confirm prey activity. The proteins which did not reach the expression levels required for the AVEXIS assay are indicated in cyan.
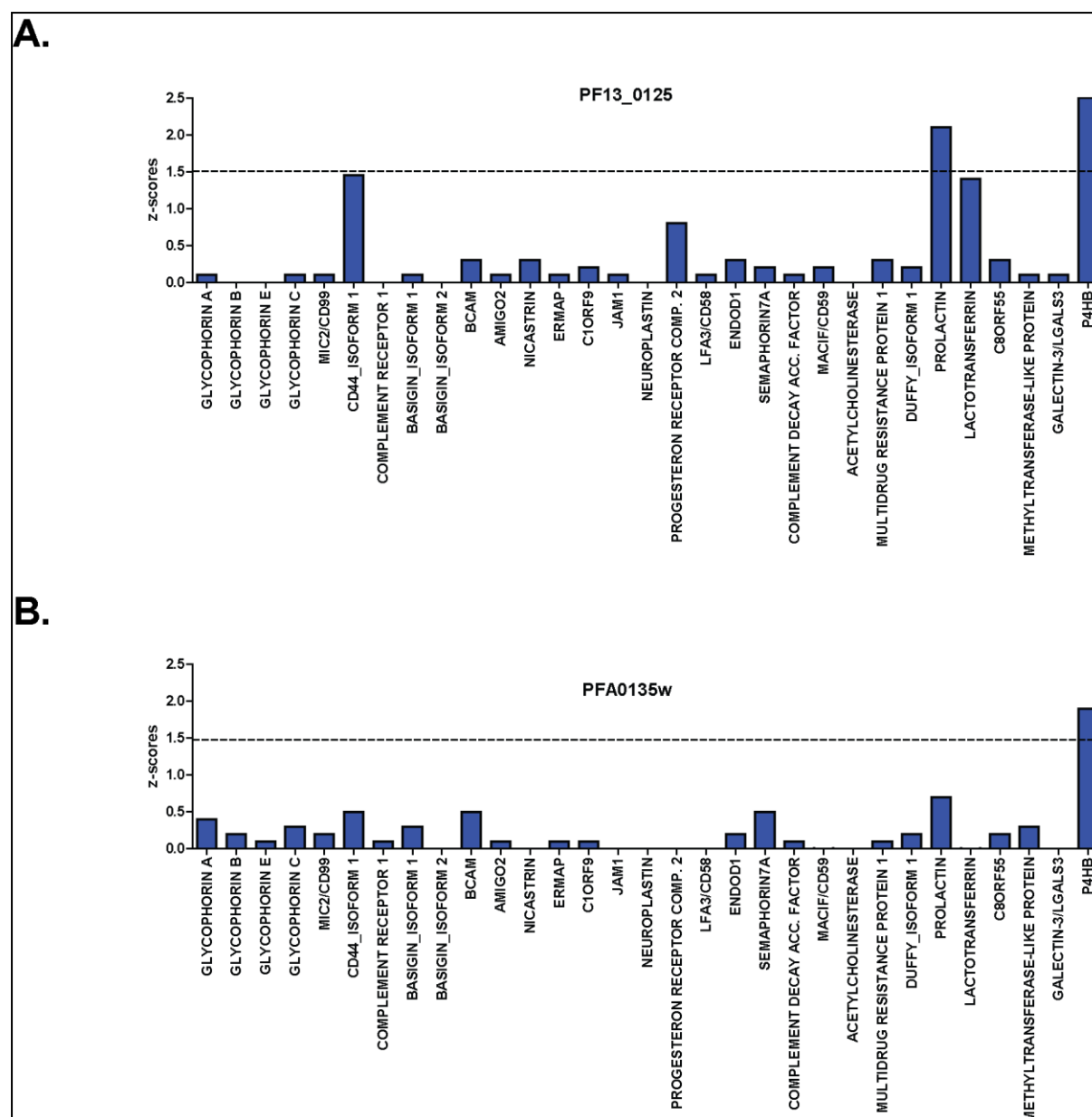
**Figure 5.11 The interactions between PF13_0125, PFA0135w and P4HB, and between PF13_0125 and Prolactin had z scores>1.5.** The bar charts show the normalised binding (z scores) of PF13_0125 (*A.*) and PFA0135w (*B.*) to the panel of erythrocyte receptors. Dashed line indicates z-score=1.5 which was set as threshold.
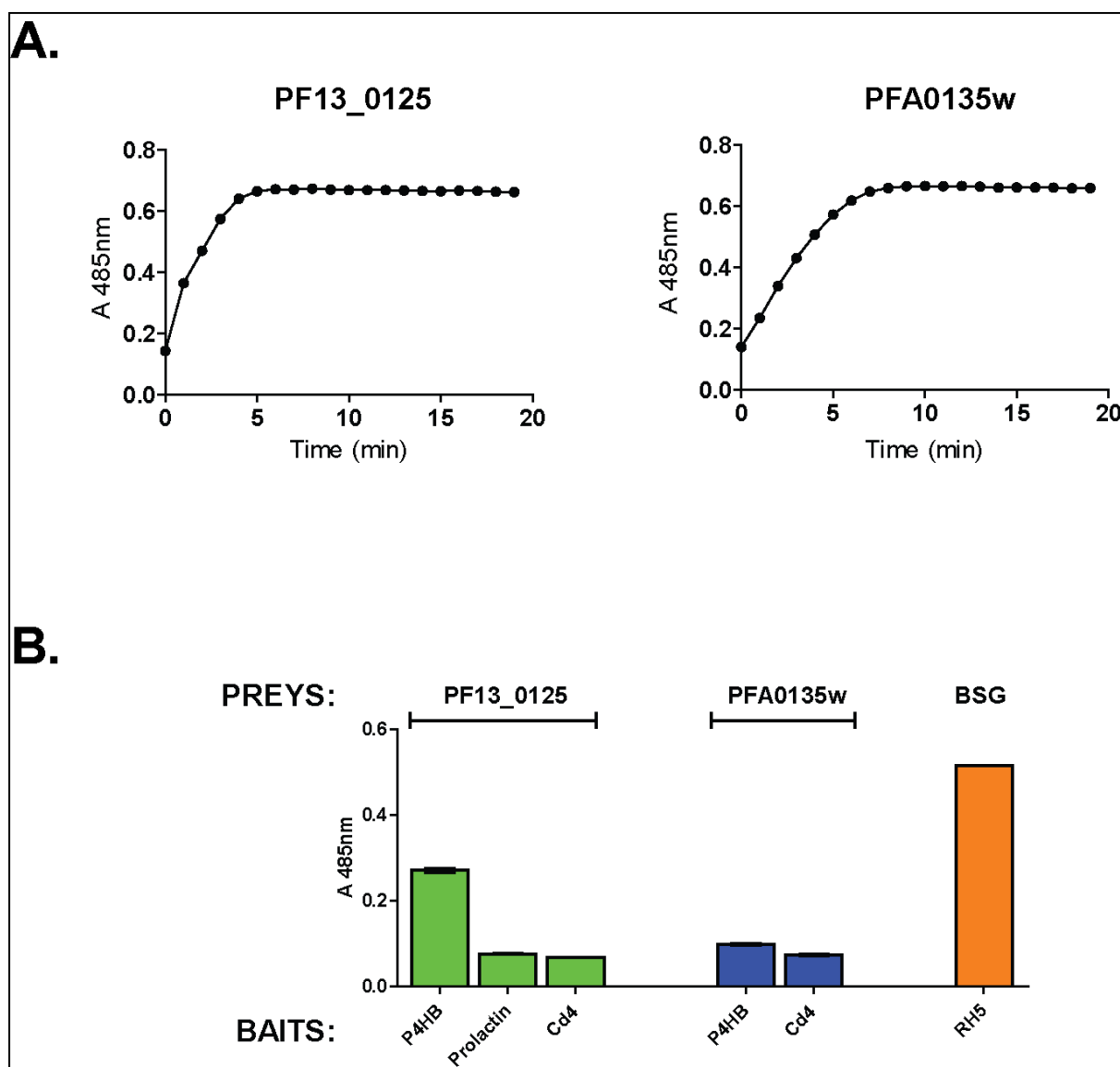
**Figure 5.12 The interactions between PF13_0125, PFA0135w and P4HB are independent of bait-prey orientation.**

*A.* PF13_0125 and PFA0135w were expressed in the pentameric β-lactamse prey form and their activity was normalised by monitoring nitrocefin turnover

*B.* Normalised amounts of biotinylated P4HB and Prolactin baits from tissue culture supernatant, were immobilised on a streptavidin-coated plate and probed with affinity purified PF13_0125 or PFA0135w preys. The interactions PF13_0125 - P4HB, and PFA0135w – P4HB were detectable, whereas the interaction between PF13_0125 and Prolactin was not. The interaction between RH5 and BSG was used as positive control. Data are shown as mean ± s.e.m; *n*=3. Cd4-bio was used as negative control.
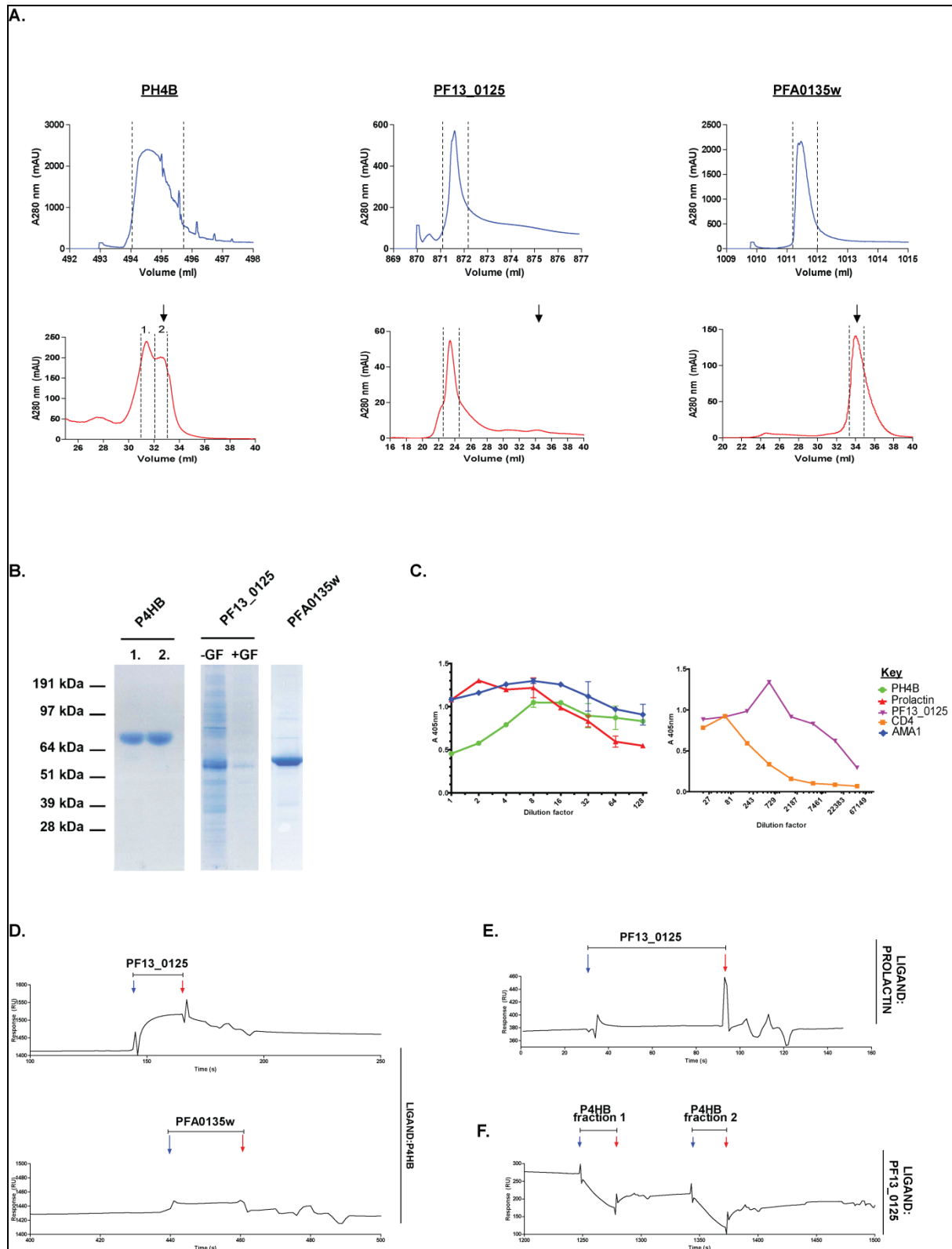
**Figure 5.13 Biophysical analysis of the putative interactions between PF13_0125, PFA0135w and P4HB, and between PF13_0125 and Prolactin, by Surface Plasmon Resonance**.

***A.*** Histidine tagged P4HB, PF13_0125 and PFA0135w were affinity purified from tissue culture supernatant on a nickel column (top), followed by gel filtration (bottom). The eluate in each experiment, was monitored at 280 nm in real-time and the peak fractions containing protein (between dashed lines) were pooled. Two gel filtration peak fractions (1 and 2) were collected for P4HB. The expected gel filtration elution volumes, which are indicated by arrows, were 32.8ml, 34.6ml, and 34.5ml for P4HB, PF13_0125 and PFA0135w respectively.

***B.*** The gel filtrated proteins were analysed by denaturing SDS-PAGE and visualised using Coomassie brilliant blue. Because of the non-expected elution volume of PF13_0125, a purified non gel-filtrated fraction of this protein was analysed as well. The expected band sizes are 83kDa, 55.3kDa and 56.6kDa for P4HB, PF13_0125 and PFA0135w respectively. Abbreviations: -GF, without gel filtration; +GF, gel filtrated.

***C.*** P4HB, Prolactin and PF13_0125 were expressed as monomeric biotinylated forms and quantified by ELISA***.*** A dilution series of each protein was immobilised on a streptavidin-coated plate and probed with the anti-Cd4 mouse monoclonal OX68. An alkaline phosphatase-conjugated anti-mouse IgG antibody as the secondary antibody. In this experiment P4HB and Prolactin were used unpurified from tissue culture supernatant whereas PF13_0125 was affinity purified on nickel column. Biotinylated AMA1 and Cd4 were used as references. Data is shown as mean ± s.e.m; *n*=3.

***D.*** Reference subtracted sensorgrams from the pulse injection of gel filtrated PF13_0125 (top) or PFA0135w (bottom), each at 3 µM, over biotinylated P4HB immobilised on a streptavidin-coated sensor chip. PF13_0125 and PFA0135w were injected at a flow rate of 20 µl/min. The biotinylated ligands were immobilised at: Cd4 (reference)-800 RU, P4HB-2600 RU.

***E.*** Reference subtracted sensorgram from the injection of gel filtrated PF13_0125, at 3 µM, over biotinylated Prolactin immobilised on a streptavidin-coated sensor chip. PF13_0125 was injected at a flow rate of 20 µl/min. The biotinylated ligands were immobilised at: Cd4 (reference)-800 RU, Prolactin-1600RU

***F.*** Reference subtracted sensorgram from the injection of gel filtrated P4HB, at 3 µM, over biotinylated PF13_0125. P4HB was injected at a flow rate of 20 µl/min. The biotinylated baits were immobilised at: Cd4 (reference)-500RU, PF13_0125-1100RU.

Blue and red arrows indicate the start and end of analyte injection and bars above the sensograms represent the duration of injection

## 5.3.6 SPR analysis of the putative novel interactions identified by using AVEXIS

Specific interactions are saturable, and this is normally determined by biophysical analysis. To test whether the putative interactions identified by AVEXIS, were saturable they were further examined by SPR. For this purpose, PFA0135w and PF13_0125 analytes were purified from tissue culture supernatant by affinity chromatography on a nickel column followed by gel filtration (Fig 5.13A). PFA0135w was eluted from the gel filtration column as a monodispersed peak at the expected elution volume (34.5ml) corresponding to an estimated size of 56.6kDa which was confirmed by SDS-PAGE (Fig 5.13B). Despite the expected elution volume for PF13_0125 being 32.8ml, a single elution peak at about 24ml (corresponding to an approximate size of 195kDa) was consistently obtained, suggesting that PF13_0125 could have been aggregated or associated with other proteins (Fig 5.13A). Analysis of PF13_0125 prior to and after gel filtration demonstrated that a band at the expected size (55.3kDa) was present, confirming the presence of protein in the elutant. However, a number of other bands with higher and lower molecular weights were also evident, suggesting protein aggregation or association with other proteins.

To test whether saturable binding can be observed between the putative interacting partners PF13_0125 – P4HB, PFA0135w – P4HB and PF13_0125 – Prolactin, biotinylated P4HB and Prolactin contained in tissue culture supernatant (Fig. 5.13C) were immobilised on the surface of a sensor chip. Gel filtrated PF13_0125 and PFA0135w were injected over the immobilised proteins and reference subtracted sensorgrams were obtained (Fig. 5.13D, E). No binding of PFA0135w to P4HB and of PF13_0125 to Prolactin was observed, suggesting that these interactions were most likely false positive hits of the AVEXIS screen. In contrast, PF13_0125 consistently bound to P4HB and the binding was saturable (Fig. 5.13D). Nevertheless, PF13_0125 did not dissociate, even after injecting 5M NaCl to facilitate dissociation (data not shown). Complexes from specific interaction between two proteins are expected to dissociate after some time and therefore, the latter observation raised questions for the specificity of this interaction.

To further investigate this result, I tested whether the observation could be replicated when P4HB is used as analyte and PF13_0125 as ligand. P4HB analyte was recombinantly expressed and purified from tissue culture on a nickel column

followed by gel filtration (Fig 5.13A). Two peaks were obtained from gel filtration, and both appeared to contain P4HB as confirmed after analysis by SDS-PAGE (Fig 5.13B). To repeat the SPR experiment in the reverse orientation, biotinylated PF13_0125 (Fig 3.13C) was captured on the surface of a sensor chip, followed by injection of P4HB analyte. Reference subtracted sensorgrams indicated that P4HB contained in both elution peak fractions (Fig 5.13A) demonstrated higher level of binding to Cd4, which was used as reference, than to PF13_0125 (Fig. 513F). These results are not conclusive whether PF13_0125 interacts with P4HB and more experiments are required to validate this interaction (Chapter 6).

## 5.4 Discussion

### 5.4.1 Recombinant expression of recombinant merozoite proteins

Based on microarray data and observations reported in the literature a total of 26 merozoite cell surface proteins were chosen for recombinant expression. Of 26 recombinant merozoite proteins, 21 (>80%) were successfully expressed at levels detectable by ELISA. Five proteins (GLURP, SERA6, SERA1, PF14_0044, PFA0445w) were not readily detectable by ELISA (Fig. 5.3). However, a band corresponding to full length ectodomain of GLURP and SERA6 was detected by western, indicating that these proteins were expressed at low levels. The low expression level for SERA6 is in agreement with previous attempts for recombinant expression of a full length form of this protein (Ruecker *et al.*, 2012). Full length recombinant GLURP was previously expressed in *E.coli* but the authors did not report the expression levels (Theisen *et al.*, 1995).

As mentioned in the introduction of this Chapter, recombinant expression of *Plasmodium* proteins is generally problematic (Birkholtz *et al.*, 2008). A possible explanation for the low or no recombinant expression observed for five merozoite proteins might simply be their incompatibility with the HEK293 protein expression system or with heterologous expression in general. An experiment which could potentially improve recombinant expression is discussed in Chapter 6.

For twenty one out of 23 merozoite recombinant proteins that were detectable by western (>88%), a band corresponding the full length ectodomain was observed (Fig. 5.4). Some processing was also evident for several proteins. The lower than the expected size bands likely origin from proteolytic activity of foetal bovine serum

proteases, contained in complete tissue culture medium (Shimomura *et al.*, 1992) or from other proteases released from dead cells in culture. A common band at about 28kDa was detected in most of the processed proteins. This band was observed in previous experiments in our laboratory and represents the protein tags (biotinylatable peptide-Cd4-6xHis). The latter protein fragment appears to be the result of a cleavage event within a presumed proteolytically prone area, nearby the C-terminus of the protein ectodomain sequence. It is possible that full length ectodomain was still recombinantly expressed, but because all tags are located C-terminally, purification on nickel column and detection with streptavidin based probes cannot be achieved.

Naturally occurring proteolytic processing for RAMA (Topolska *et al.*, 2004), GLURP (Borre *et al.*, 1991) and MSP8 (Black *et al.*, 2001; Drew *et al.*, 2005) has been reported in earlier studies. Nonetheless, it is difficult to compare the processing pattern I observed with those reported previously, due to differences in the detection probes that were used in each case. Of note is that only the unprocessed, full length SERA5 and SERA6 and a slightly processed form of SERA4 were obtained, consistent with previous findings that processing of those proteins requires the presence of *Pf*SUB1(Yeoh *et al.*, 2007; Blackman, 2008; Ruecker *et al.*, 2012).

## 5.4.2 Recombinant merozoite proteins are biochemically active

Evidence that recombinant merozoite proteins were active and correctly folded was provided by a series of experiments. Twenty out of 21 (~95%) merozoite cell surface proteins tested, were immunoreactive against hyperimmune sera obtained from previously malaria experienced individuals (Fig. 5.5). In 18 out of the 20 immunoreactive proteins (~86% of the total proteins tested) the immunoreactivity decreased, or was completely lost, when these proteins were heat-treated prior to probing with hyperimmune sera. These results suggest that antibodies contained in hyperimmune sera recognised conformational epitopes on the merozoite proteins, suggesting correct protein folding.

Another experiment that provided evidence for the correct conformation and activity of merozoite proteins was that RIPR was capable of interacting with RH5 by AVEXIS. Because only active and correctly folded proteins are expected to specifically interact, the observation that RIPR interacts with RH5 *in vitro* suggests

that RIPR has the correct conformation. Indications that this interaction happens *in vivo* was first provided by Chen and colleagues (Chen *et al.*, 2011), but there are a few important questions that are yet to be answered. It would be interesting to derive the kinetic and affinity parameters of this interaction and to test how the interaction between RH5 and RIPR (Chen *et al.*, 2011) influences the interaction between RH5 and BSG (Crosnier *et al.*, 2011). Experiments to further characterise the interaction between RH5-RIPR were hampered by the low expression yields of RIPR. Attempts to recombinantly express the two naturally occurring RIPR halves (Chen *et al.*, 2011) did not improve expression levels.

Finally, evidence for the correct folding of the recombinant merozoite proteins were provided by the observation that *Pf*EBA-165 was able to interact with a number of glycans on AVEXIS, suggesting that folded domains do exist on *Pf*EBA-165.

### 5.4.3 PF13_0125, PFA0135w, Prolactin and P4HB participated in the three interactions with the highest z-scores

Three interactions (PF13_0125 – Prolactin, PF13_0125 – P4HB, PFA0135w – P4HB) with z-scores higher than 1.5 were observed in the AVEXIS screen where the recombinant merozoite protein library was systematically screened against an equivalent protein library of erythrocyte receptors. While no information was found in the literature about PF13_0125, apart from that is localised apically in the mature merozoite (Hu *et al.*, 2010), PFA0135w (also known as MaTrA, for merozoite associated tryptophan-rich antigen) has been shown to co-localize with MSP-1 in segmented schizonts and free merozoites (Ntumngia *et al.*, 2004). It contains a tryptophan-rich domain which is also found in the *P. falciparum* paralogues TrpA-3 (PF10_0026), TryThrA (PF08_0003) and LysTrpA (MAL13P1.269) (Ntumngia *et al.*, 2005). MaTrA has orthologues in *P vivax, P. yoelii and P.knowlesi* (Burns *et al.*, 1999, 2000; Uhlemann *et al.*, 2001; Jalah *et al.*, 2005; Ntumngia *et al.*, 2005; Bora *et al.*, 2013). Synthetic peptides spanning the PFA0135w orthologue TryThrA sequence, have been shown to be highly active in binding human erythrocytes and were able to inhibit erythrocyte invasion (Curtidor *et al.*, 2006).

Interestingly, recombinant PFA0135w tryptophan rich domain, expressed in *E. coli,* was specifically recognised by IgG serum antibodies from previously *P. falciparum* exposed individuals living in Lambarene, Gabon, an area of high malaria

transmission (Ntumngia *et al.*, 2004). However, out of 135 serum samples tested, only 30 (23%) contained antibodies against the recombinant protein. These results are in agreement with my observation that full length recombinant PFA0135w exhibits relatively low immunoreactivity against pooled hyperimmune sera obtained from Malawians (Fig. 5.5), suggesting that PFA0135w is not under significant immune pressure.

On the other hand prolactin is an all α-helix protein hormone, secreted by the anterior pituitary gland (Teilum *et al.*, 2005). More than 300 biological functions have been assigned to prolactin, all mediated by prolactin receptor (Bole-Feysot *et al.*, 1998). Apart from the binding to prolactin receptor, an extracellular interaction between prolactin and cyclophilin B has also been described (Rycyzyn *et al.*, 2000).

Finally P4HB (also known as Prolyl 4-hydroxylase subunit beta or p55) is a protein disulfde isomerase and is found both in the endoplasmic reticulum (ER) and at the cell surface. Its function on the cell surface is not well understood (Wilkinson and Gilbert, 2004). Of note, is that P4HB has been linked with the events that mediate HIV entry into human leukocytes. It has been shown to that P4HB is clustered together with CD4 on human CD4$^+$ lymphocytes during HIV entry (Fenouillet *et al.*, 2001). Although P4HB is not necessary for the initial adherence of HIV (Barbouche *et al.*, 2003), it is indispensable from the fusion of the viral envelope with the host cell membrane (Fenouillet *et al.*, 2001; Gallina *et al.*, 2002; Barbouche *et al.*, 2003, 2005; Markovic *et al.*, 2004).

Structurally, P4HB harbours two thioredoxin-like domains and it interacts with a number of proteins where it catalyzes the reduction, formation and rearrangement of disulfide bonds (Wilkinson and Gilbert, 2004). P4HB has been shown to exhibit both chaperone (prevents protein aggregation) and anti-chaperone (facilitates protein aggregation) activity, depending on its concentration (Mezghrani *et al.*, 2000; Wilkinson and Gilbert, 2004). Because there is no apparent consensus sequence that P4HB recognises (Wilkinson and Gilbert, 2004) it can theoretically interact with a range of different proteins which carry disulfide bonds. This might be a reason why two putative interactions in my screen involved P4HB. Other independent protein screens in our laboratory (Dr Yi Sun, unpublished), also found P4HB to interact with numerous proteins. It is likely that a number of those interactions were specific, without though implying their existence in nature.

The interaction between P4HB and PF13_0125 was reversible in AVEXIS (Fig. 5.12). This interaction was saturable by SPR, only when P4HB was used as ligand and PF13_0125 as analyte. PF13_0125 remained bound to P4HB and did not dissociate, even after injecting a regeneration solution to facilitate dissociation (Fig. 5.13). The latter observation, together with the fact that PF13_0125 was consistently eluted from the gel filtration column much earlier than expected (Fig. 5.13), suggests that PF13_0125 analyte could have been aggregated. However, it is not yet clear why PF13_0125 demonstrated saturable binding to P4HB. Moreover, the reason why P4HB, when used as analyte, bound more to the Cd4 reference than PF13_0125 still remains an enigma.

In contrast to the interaction between PF13_0125 and P4HB, the interaction between PF13_0125 and Prolactin could not be repeated in the reciprocate bait-prey orientation (Fig. 5.12). Similarly, the interaction between PFA0135w and P4HB could only barely be detected when PFA0135w was used as prey and P4HB as bait. None of the latter two interactions was reproducible by SPR, suggesting that they may be false positive hits of AVEXIS. AVEXIS has a general low false-positive rate, and a stringent prey activity is thought to be appropriate for the testing of most interaction pairs by AVEXIS (Bushell *et al.*, 2008). However, because the stringency range varies significantly from protein pair to protein pair under investigation, inevitably some false positives and negatives do exist (Fig. 5.14). Therefore it is not unlikely that some of the interactions I observed are simply false positives.

## 5.5 Conlcusions

In this chapter I described the recombinant expression of 23 putative *P. falciparum* merozoite cell surface and secreted proteins. Of 23 *P. falciparum* merozoite recombinant proteins, 19 were expressed at usable amounts, and a band corresponding to full length recombinant protein was detected by immunoblot. Biochemical characterisation of the recombinant proteins provided evidence that the the majority of merozoite ligands were biochemically active and correctly folded.

The *P. falciparum* recombinant protein library was then systematically screened against an equivalent library consisting of erythrocyte receptors, by using AVEXIS
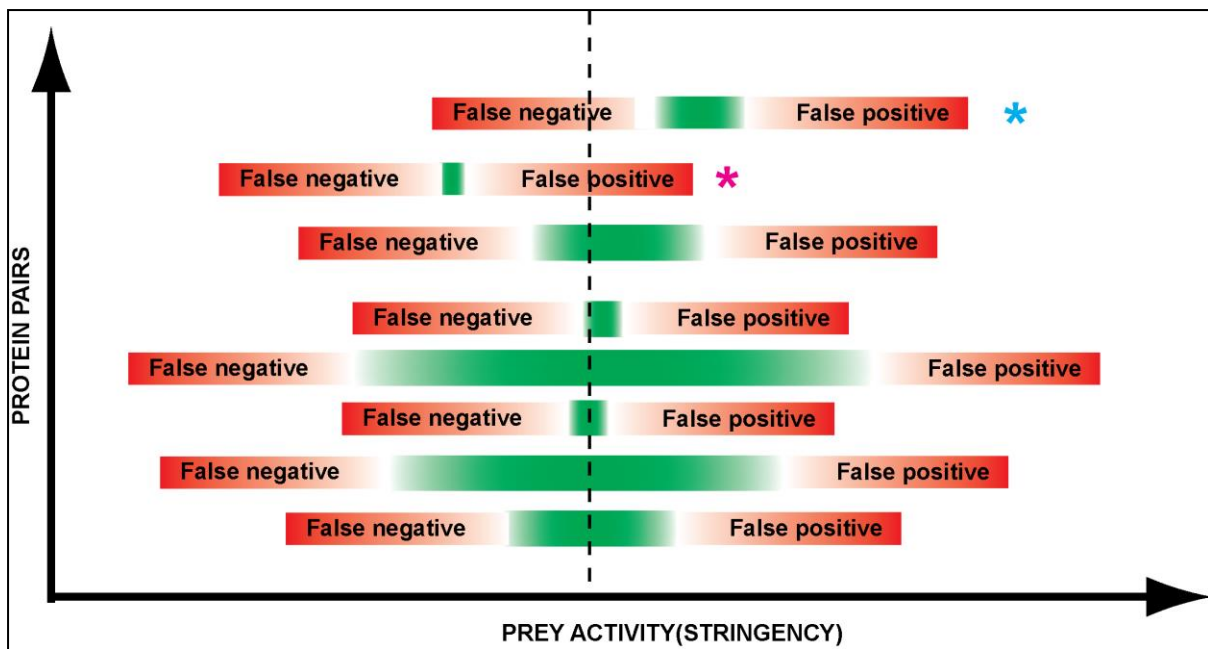
**Figure 5.14 The false positive and negative rate in AVEXIS is dependent on prey activity.** A diagram showing the prey activity in relation to the stringency of each protein pair tested for interaction in AVEXIS. Prey activity (dashed line) is chosen to fall within the stringency range (green) of most protein pairs. Nevertheless, because the stringency range varies significantly from protein pair to protein pair, inevitably some false positives (magenta asterisk) and negatives (cyan asterisk) arise.

(Bushell *et al.*, 2008). The screen identified one putative interaction (PF13_0125 – P4HB). Further characterisation of the identified interaction provided inconclusive results, and more experiments are required to confirm its validity. However, the expanded library of recombinant *P. falciparum* merozoite proteins reported in this project, should prove to be a useful tool for the deeper understanding of erythrocyte invasion, and *P. falciparum* merozoite biology.

# CHAPTER 6

**Discussion**

### 6.1 Summary and Aims

Chapters 3 and 4 described the first steps in developing humanised monoclonal antibodies targeting the RH5-Basigin interaction, as potential novel anti-malarial therapeutics. In this Chapter, I describe a number of future experiments that could be done to improve these pilot therapeutics, including increasing the affinity of huMEM-M6/4, huMEM-M6/8 and huD9 antibodies for BSG, further characterisation of ch6D9 *in vitro* and *in vivo* and future work on the bi-specific monoclonal 2AC7-6D9 DVD-Ig.

In the second half of this Chapter I build on the AVEXIS screen described in Chapter 5 by discussing future experiments aiming to improve the recombinant expression of *Plasmodium* proteins. Finally, I discuss the future directions for the recombinant merozoite protein library, focusing specifically on the putative interaction between PF13_0125 and P4HB, and also on EBA-165.

### 6.2 The affinity of huMEM-M6/4 and huMEM-M6/8 for BSG can potentially be restored

To easily engineer and recombinantly express antibodies, I employed a plasmid vector system that allows the recombinant expression of rearranged antibody heavy and light chains in HEK293 cells. The plasmid system is based on the pTT3 expression vector and similar plasmid systems have been successfully used in the past for the recombinant expression of humanised or chimeric antibodies (Clarke *et al.*, 2010; Yu *et al.*, 2010).

By using this plasmid expression system, two anti-BSG monoclonals, MEM-M6/4 and MEM-M6/8, were successfully humanised by CDR grafting. Both huMEM-M6/4 and huMEM-M6/8 retained their specificity for BSG, but a biophysical analysis of the humanised antibodies demonstrated that the affinity for BSG decreased in comparison to the original mouse antibodies. While the decrease in affinity for huMEM-M6/8 was subtle, the affinity of huMEM-M6/4 decreased by at least two orders of the magnitude in comparison to MEM-M6/4. It is not an unusual phenomenon that the affinity of a humanised antibody is reduced in comparison to the parental mouse one (Lo, 2004; Almagro and Fransson, 2008). However, antibody affinity plays an important role in biological efficacy, and hence, antibodies with low affinity are unlikely to be used for therapeutic purposes (Ho and Pastan,

2009). An increased affinity may allow for a low dosage of a therapeutic antibody and toxic side effects may therefore be reduced (Ho and Pastan, 2009).

The decrease in affinity in humanised antibodies likely arises from interference between human FRs and murine CDRs. Such interference may involve CDR loop displacement or loss of CDR flexibility. Antibody affinity can potentially be restored by mutating certain amino acids in the FRs of the humanised antibody to match those found at the same positions in the murine antibody, but the identification of the residues to be mutated often requires three dimensional modelling (Lo, 2004; Almagro and Fransson, 2008). Because of the lack of such expertise in our laboratory, future directions may include the collaboration with other laboratories which specialise in structural biology and *in silico* modelling. If such an effort was to be undertaken, huMEM-M6/4, which appears to inhibit the RH5-BSG interaction through steric hindrance, is clearly not a high priority target. Collaborations with the aim of increasing the affinity of huMEM-M6/8 for BSG could however be fruitful.

Instead of mutating targeted candidate amino acids, which often requires detailed structural knowledge of the antibody-antigen interaction, high-throughput experimental approaches could be used to increase affinity of huMEM-M6/8 for BSG. Error prone PCR which introduces random mutations within the variable region is a common procedure for antibody affinity maturation, and is normally followed by large scale, display based screens, to isolate highly avid mutants (Hoogenboom, 2005; Sergeeva *et al.*, 2006; Geyer *et al.*, 2012).To reduce the number of mutants to be screened Chowdhury and colleagues developed another approach in which mutations are introduced only at germline hotspots which are naturally mutated during somatic hypermutation in antibody secreting B-cells (Chowdhury and Pastan, 1999). Nevertheless, all these approaches require display technologies which are not available in our laboratory, and therefore these experiments should also be performed in the terms of collaborations with other laboratories which are set up for this work.

## 6.3 The identification of structurally important amino acid residues within V region, may facilitate the restoration of hu6D9 affinity for BSG

The humanisation process for the novel anti-BSG monoclonal antibody developed in this thesis, m6D9, was less successful than the humanisation of MEM-

M6/4 and MEM-M6/8, although a chimeric 6D9 antibody was successfully developed. Several alternate approaches could be trialled to improve the humanisation of 6D9. In the present PhD thesis, the IMGT numbering system was used to identify CDR and FR sequences. The choice of this numbering system was simply because it is the most recent one and various useful bioinformatic tools are publicly available through the official IMGT website (www.imgt.org). However, other numbering systems do exist and could be applied. In particular, it would be interesting to repeat the humanisation process for the development of hu6D9 by engrafting the CDRs as defined by Kabat (Kabat *et al.*, 1991) which is likely the most widely used numbering system (Fig. 6.1).

Additionally, the amino acid residues at certain positions in the V region have been proposed to participate in the formation of a platform, known as the Vernier zone (Foote and Winter, 1992; Lo, 2004), which is necessary to support correct CDR conformation. Re-introduction of the murine residues at these positions could reinstate hu6D9 binding to BSG. Hence, the following mutations could be considered for introduction in hu6D9: M4L, Y49K in variable light chain and M48I, V67A, I69F in variable heavy chain (Kabat numbering). Other residues that have been proposed to be responsible for retaining the structure of CDRs should also be examined (Lo, 2004). Alternatively, *in silico* molecular modelling of hu6D9 will accurately indicate which amino acids interfere with binding to BSG.

## 6.4 Future directions for 2AC7-6D9 DVD-Ig

Side by side comparison between anti-BSG ch6D9 and the anti-RH5 monoclonal antibody ch2AC7, demonstrated that ch6D9 had a considerably lower $IC_{50}$ in blocking erythrocyte invasion in parasite culture. The higher inhibitory capacity of ch6D9 in comparison to ch2AC7, is likely related to the exposure time of the BSG and RH5 to ch6D9 and ch2AC7, respectively, during an invasion assay. Whereas erythrocyte BSG is constantly exposed to ch6D9, there is only a short timing window (30-40s) following schizont rupture where RH5 is available for binding by ch2AC7.

```
    hu6D9VH    QVQLVQSGAEVKKPGASVKVSCKASGYSFSDDYMHWVRQAPGQRLEWM
    m6D9VH     EVQLQQSGPELVKTGASVKISCKASGYSFSDDYMHWVKQSHGKSLEWI
    Kabat                                          ←——→
    IMGT                                        ←——→


    hu6D9VH    GWISCYNGVPKYSQKFQGRVTITRDTSASTAYMELSSLRSEDTAVYYC
    m6D9VH     GYISCYNGVPSYNQKFKGKATFTVDTSSSTAYMQFSSLTSEDSAVYYC
    Kabat          ←——————————————→
    IMGT           ←———→


    hu6D9VH    ARGGNHGFYYHAMDYWGQGTTVTVSS
    m6D9VH     ARGGNHGFYYHAMDYWGQGTSVTVSS
    Kabat          ←—————————→
    IMGT       ←———————————→
```

```
    hu6D9VL    EIVMTQSPATLSVSPGERATLSCRASQSIGTGLAWYQQKPGQ
    m6D9VL     DIVLTQSPAILSVSPGERVSFSCRASQSIGTGIHWYQQRTNG
    Kabat                               ←—————————→
    IMGT                                  ←———→


    hu6D9VL    APRLLIYFASTRATGIPARFSGSGSGTEFTLTISSLQSEDFAV
    m6D9VL     SPRLLIKFASESISGIPSRFSGSGSGTDFTLSINSVESEDIAD
    Kabat          ←————→
    IMGT           ←→


    hu6D9VL    YYCQQSTSWPYTFGQGTKLEIK
    m6D9VL     YFCQQSTSWPYTFGGGTKLEIK
    Kabat          ←———————→
    IMGT           ←———————→
```

**Figure 6.1 Kabat and IMGT numbering systems have different definitions for CDRs and FRs.** Alignment between hu6D9 and m6D9 variable heavy (top) and light (bottom) chains. Green, cyan and magenta arrows indicate the position of CDR1, CDR2 and CDR3 respectively as defined by Kabat and IMGT numbering systems.

Similarly, ch6D9 was more potent than the bi-specific antibody 2AC7-6D9 DVD-Ig in preventing erythrocyte invasion. However, these data should be interpreted with caution. Because there is a decrease in affinity for BSG in 2AC7-6D9 DVD-Ig, no conclusions can be drawn for the therapeutic potential of an anti-BSG/RH5 bi-specific agent. It will be interesting to test the effect of such an agent when the anti-BSG affinity is retained. Swapping the fusion orientation of the two variable domains in 2AC7-6D9 DVD-Ig is one approach that could restore anti-BSG affinity to that of its parent monoclonal, 6D9 (DiGiammarino *et al.*, 2012). It will also be important to test the efficiency of the anti-RH5/BSG bi-specific agent in blocking erythrocyte invasion in parallel with a combination of individual ch6D9 and ch2AC7 used in various ratios. These experiments are necessary to establish whether anti-RH5 and anti-BSG monoclonals have synergistic or additive effects in preventing erythrocyte invasion, which would greatly inform future development of the anti-BSG/RH5 bispecific agent.

## 6.5 Ch6D9 – Future directions

### 6.5.1 Epitope mapping refinement

To narrow down the BSG sequence recognised by ch6D9, future experiments may include the testing of ch6D9 binding to an array of overlapping synthetic peptides covering BSG domain 1. Although such screening experiments would be informative, the precise amino acids that are in contact between ch6D9 and BSG can only be elucidated by solving the crystal structure of the ch6D9-BSG complex. Some indications as to whether ch6D9 recognises a conformational epitope can be taken by testing the binding of ch6D9 to heat treated BSG.

### 6.5.2 Further investigation of the (in)ability of ch6D9 to stimulate antibody effector functions

Ch6D9 was demonstrated to have a reduced ability to bind FcγRIIA and C1q in *vitro*. Whilst important information about antibody effector functions can be obtained by *in vitro* experiments, it is very difficult to predict how an antibody will behave *in vivo*. Therefore, the capability of ch6D9 to elicit ADCC and CDC should be tested under conditions that are more representative of the *in vivo* environment.

The capacity of an antibody to induce ADCC and CDC, is usually assessed by using the chromium release assay (Brunner *et al.*, 1968). This assay is based on the

measurement of $^{51}$Cr released from metabolically labelled target cells, following the incubation with the antibody under investigation in the presence of FcγR-bearing effector cells or serum (as a source of complement) in a given period of time (Brunner *et al.*, 1968; Otz, 2010). Europium (Eu$^{3+}$) and the naturally occurring cell marker lactate dehydrogenase (LDH) have also been used in the same way as safer alternatives to the radioactive $^{51}$Cr (Korzeniewski and Callewaert, 1983; Blomberg *et al.*, 1986; von Zons *et al.*, 1997). In recent years, more sophisticated approaches have been developed, providing much higher accuracy. In the vast majority of them, the binding of the antibody of interest to an FcγR expressing cell line, as well as the ability of an antibody to trigger ADCC and CDC mediated cell lysis, is assessed by flow cytometric methods (Armour *et al.*, 1999, 2003; Lee-MacAry *et al.*, 2001; Kim *et al.*, 2007; Helguera *et al.*, 2011; Hernandez *et al.*, 2012).

The ability of ch6D9 to induce ADCC can also be examined *in vivo* in mouse models developed for such purposes (Bruhns, 2012). These mouse models have been genetically engineered to express a single or a combination of human FcγRs (Chapman *et al.*, 2007; Bruhns, 2012; Lux and Nimmerjahn, 2013). However, aberrant expression of some hFcγRs in cell types which are not normally expressed, has been reported (Bruhns, 2012). The latter observations suggest that data obtained from studies in animal models require careful interpretation to remain meaningful.

Besides the amino acids that have already been mutated in the Fc region of ch6D9 for the elimination of antibody effector functions, the presence of oligosaccharides attached to the asparagine at position 297 of hIgG1 Fc region has also been shown to be important for the stimulation of ADCC and CDC (Idusogie *et al.*, 2000; Jefferis, 2009). Therefore, future experiments may include the development and testing of an aglycosylated form of ch6D9. By using site directed mutagenesis, and exploiting the versatility of the plasmid system described in Chapter 3, the asparagine at position 297 of the hIgG1 Fc region can be mutated to another amino acid (normally alanine) and thereby destroying the N-linked glycosylation site.

### 6.5.3 Testing the safety, efficacy and pharmacokinetics of ch6D9 *in vivo*

Ch6D9 safety and pharmacokinetics are currently being assessed *in vivo,* in NOD-*scid IL2Rγ^{null}* mice which have been engrafted with human erythrocytes (Jiménez-Díaz *et al.*, 2009). The next step will be to challenge these mice with *P. falciparum* infected erythrocytes, and test the anti-malarial efficacy of ch6D9 at various doses. These experiments are being performed in collaboration with Prof. Peter Preiser group in NTU, Singapore.

We are still at the very early stages in testing ch6D9 in mouse (and *in vitro*), but If the preclinical studies provide satisfactory results, the next step may be to test ch6D9 in man, in a Phase I clinical trial. Administration of ch6D9 to volunteers will require the production of ch6D9 under European Union good manufacturing practice (GMP) conditions. The production process should be capable of producing product of consistent quality, with minimal impurities and free of pathogens. In a potential Phase I clinical trial, GMP-produced ch6D9 will be administered to a small group (normally 20–100) of healthy volunteers and will be assessed for its safety, tolerability and pharmacokinetics. Also, Phase I clinical trials usually include dose ranging and therefore, the maximum dose of ch6D9 which is safe to be administered can be identified.

Based on the results of Phase I clinical trial, ch6D9 dosing requirements and efficacy can be determined in a Phase II clinical trial. For this purpose, a range of ch6D9 doses could be administered to individuals who have been challenged with *P. falciparum* via mosquito bite. If ch6D9 passes successfully through a Phase II clinical trial, then the next step will probably be to test the efficacy of ch6D9 in a large scale, randomized Phase III clinical trial.

### 6.5.4 Possible complications of using ch6D9 *in vivo* in man

Monoclonal antibodies against erythrocyte cell surface proteins but also against cell surface proteins expressed on other cells have previously been shown to be effective and safe for administration (Armour *et al.*, 2006; Ghevaert *et al.*, 2008, 2013). For example, an anti-D antibody (Fog-1) which carries the same mutations in the Fc region as ch6D9, has been demonstrated to be able to coat circulation erythrocytes without however promoting clearance and haemolysis (Armour *et al.*, 2006)

Specifically for Basigin, an anti-Basigin monoclonal antibody has been used before in the clinic, for the treatment of steroid-refractory acute graft-versus-host disease (Heslop *et al.*, 1995; Deeg *et al.*, 2001; Macmillan *et al.*, 2007). Moreover, in 2005, the Chinese Food and Drug Administration licenced the use of an anti-BSG iodine-131-labeled $F(ab)_2$ fragment under the brand name Licartin (also known as metuximab), for the treatment of patients suffering from hepatocellular carcinoma (HCC) (Yu *et al.*, 2008; He *et al.*, 2013). The previous safe use of anti-Basigin monoclonal antibodies in the clinic (section 1.10.6.2.2 and 1.10.6.2.3) is encouraging that antibodies against Basigin would be safe and very effective in treating malaria infected individuals. If successful, this would be the first time that a host-directed anti-malarial has ever been developed.

It is important however, to make some critical considerations about the possible problems that may arise from the administration of ch6D9 to man as a putative anti-malarial. First, because ch6D9 targets Basigin exposed on the cell surface of erythrocytes, it should be administered intravenously and this could prove clinically impractical on a large scale. Moreover, the requirement of manufacturing and scaling up the product, as well as the cost and feasibility of delivering an antibody which should be refrigerated, could be major logistic challenges. Furthermore, ch6D9 would potentially treat malaria infected individuals, but it would only confer protection against malaria for a limited amount of time (several days) depending on ch6D9 pharmacokinetics. Therefore, ch6D9 is not a replacement of a highly efficient malaria vaccine, but it could potentially be used in combination with it.

From safety point of view, Basigin is widely expressed in human body, and ch6D9 could potentially bind to Basigin expressed in cell types other than erythrocytes, with unpredicted outcomes. Indeed, some side effects arising from administration of anti-Basigin antibodies to patients have been reported in previous studies (Deeg *et al.*, 2001; Macmillan *et al.*, 2007). Previous experiments in mice, where erythrocyte exposed Basigin was blocked by an anti-BSG $F(ab)_2$ fragment, resulted in the selective trapping of erythrocytes in the spleen (Coste, 2001).Therefore, the pre-clinical studies in humanised mice which are currently under way for ch6D9, should closely monitor for rapid erythrocyte clearance. Finally ch6D9 is a chimeric antibody and therefore, it may cause some human-anti-mouse

antibody (HAMA) responses. This problem can be minimized if ch6D9 is fully humanised.

## 6.6 Improving recombinant protein expression levels by molecular chaperones

While Chapters 3 and 4 focused on a known merozoite-erythrocyte protein-protein interaction, Chapter 5 detailed a screen carried out to identify novel interactions. That screen, and the RH5-BSG interaction itself, were facilitated by recent advances in the recombinant protein expression of *Plasmodium* proteins. Expressing *Plasmodium* proteins in heterologous systems has traditionally been a technically challenging problem and the general success rate of expressing *Plasmodium* spp. proteins in a biochemically active recombinant form has been very low (Birkholtz *et al.*, 2008; Fernández-Robledo and Vasta, 2010). For example, Mehlin and colleagues reported only a 6.3% success rate in recombinant expression of *Plasmodium* proteins in a soluble form and at levels sufficient to be purified (Mehlin *et al.*, 2006). In Chapter 5, I demonstrated that 18 out of 26 (~70%) merozoite proteins were expressed in a biochemically active recombinant form and at usable amounts.

While the overall success rate was high, in keeping with previous experience of the HEK293 system, and in stark contrast to the historical experience with expressing *P. falciparum* proteins in other systems, a few merozoite proteins still failed to express as a recombinant form or expressed at very low levels. Although the genes were codon-optimised for HEK293 cells, *P. falciparum* proteins still have relatively unusual amino acid distributions, with an enrichment for asparagine, glutamic acid and lysine, and frequent homopolymeric runs. Indeed, it has been recently demonstrated that the stability of several *Plasmodium* proteins depends upon their association with heat shock proteins which act as molecular chaperones, presumably specifically evolved to handle the unusual amino acid composition (Muralidharan *et al.*, 2012). It will be interesting to test if there is any improvement in protein expression in the presence of *Pf*Hsp110c which has been proposed to be a protein-stabilizing chaperone (Muralidharan *et al.*, 2012).

## 6.7 Future directions for the recombinant merozoite protein library

A previously developed protein library consisting of merozoite cell surface or secreted proteins was expanded by 21 proteins. The 21 new protein members were

systematically screened for interacting partners against a protein library consisting of erythrocyte cell surface receptors. Apart from the interaction between PF13_0125 and P4HB which was not confirmed, no other interaction was detected. However, the erythrocyte receptors included in the AVEXIS screen do not cover the complete repertoire of receptors exposed on the erythrocyte cell surface. For example, multipass receptors were largely excluded due to their low likelihood for recombinant expression in a soluble form. Therefore, it is likely that several of the 21 recombinantly expressed merozoite cell surface and secreted proteins bind to erythrocyte receptors that were not included in the screen. To test this possibility, future experiments may include the raising of antibodies against the 21 merozoite proteins which can then be used for immunofluorescence and erythrocyte invasion assays. Moreover, the 21 purified merozoite proteins can be tested in erythrocyte invasion assays and also for their ability to bind human erythrocytes.

## 6.8 Further investigation of the putative interaction between P4HB- PF13_0125 is required

Future experiments are required to validate the interaction between P4HB and PF13_0125. Although PF13_0125 has been shown to localise apically in merozoites (Hu *et al.*, 2010), it remains a largely uncharacterised protein. It will be interesting to test whether co-transfection of PF13_0125 with *Pf*Hsp110c prevents aggregation of the former (Muralidharan *et al.*, 2012) (see section 6.5). This will enable the reliable analysis of the putative interaction between P4HB and PF13_0125 by SPR. Other future experiments may include testing the ability of PF13_0125 to bind to human erythrocytes, and the inclusion of purified PF13_0125 and P4HB in erythrocyte invasion assays. Antibodies raised against PF13_0125 together with anti-P4HB can be used for immunofluorescence and invasion assays.

## 6.9 *Pf*EBA-165 – a merozoite cell surface ligand with possible implications in *Plasmodium* host specificity?

Experiments described in Chapter 5 demonstrated that *Pf*EBA-165 was capable of *in vitro* binding to Neu5Gc but not to Neu5Ac containing glycans. Neu5Ac and its hydroxylated derivative Neu5Gc are the most common sialic acid forms found in mammalian cells; the former is converted to the latter by an enzyme encoded by the CMP-N-acetylneuraminic acid hydroxylase (*CMAH*) gene (Chou *et al.*, 1998).

Early studies showed that Neu5Ac but not Neu5Gc was detectable in human tissues whereas body fluids and tissue samples from all four great apes (chimpanzee, bonobo, gorilla and orangutan) contained high levels of both sialic acid forms, with Neu5Gc being predominant (Muchmore *et al.*, 1998). It was later reported that the reason for the absence of Neu5Gc in human sialoglycoproteins, was the inactivation of *CMAH* gene due to a 92-bp deletion resulting in a frameshift mutation (Chou *et al.*, 1998). The inactivation of the *CMAH* gene must have occurred sometime after the separation of human from the common ancestor with bonobo/chimpanzee (Varki, 2001; Olson and Varki, 2003; Hayakawa *et al.*, 2006) which is estimated to happened five to seven million years ago (Olson and Varki, 2003).

Around the same time (~5 million years ago), *P. falciparum* and *P. reichenowi* diverged from their common ancestor (Escalante *et al.*, 1998). In the early days, because *P. reichenowi* was morphologically indistinguishable from *P. falciparum* which was already known, it was proposed that apes might be a natural reservoir for *P. falciparum* (Martin *et al.*, 2005). Evidence that *P. reichenowi* is a separate species was provided by *in vivo* experiments which demonstrated that *P. reichenowi* is unable to infect humans, and *P. falciparum* infection cannot be easily established in chimpanzees (Varki, 2001; Martin *et al.*, 2005; Rayner *et al.*, 2011).

Sialic acid residues on erythrocytes are important for erythrocyte binding and invasion by a number of *Plasmodium falciparum* strains (Stubbs *et al.*, 2005). Therefore, the strong preference of *P. falciparum* and *P. reichenowi* for humans and chimpanzees, respectively, was suggested to be due to the differences in Neu5Ac and Neu5Gc content between the two hosts (Muchmore *et al.*, 1998; Varki, 2001; Martin *et al.*, 2005; Rayner *et al.*, 2011). Direct evidence for the role of sialic acids in *Plasmodium* host specificity was provided by Martin and colleagues (Martin *et al.*, 2005). In that study it was demonstrated that *Pf*EBA175 prefers Neu5Ac than Neu5Gc, which could explain why *P. falciparum* infection was not easily established in chimpanzees, in previous studies. Conversely *Pr*EBA-175 strongly prefers Neu5Gc, perhaps explaining the previously reported inability of *P. reichenowi* to infect human subjects (Martin *et al.*, 2005). However, recent data in our lab suggests that *Pf*EBA-175 is less discriminatory between Neu5Ac and Neu5GC than previously thought, suggesting that more studies are needed (Wanaguru *et al.*, 2013).

My observation that a corrected *Pf*EBA-165 protein binds to Neu5Gc but not to Neu5Ac containing glycans suggests that EBA-165 might also be implicated in the molecular mechanisms mediating the strong host preference exhibited by *P. falciparum* and *P. reichenowi*. It is possible that the frameshifts in *Pfeba-165* may have been essential for the adaptation of *P. falciparum* to its human host, which carry Neu5Ac but not Neu5Gc containing sialoglycoproteins. Even if they were not required for the host transition event itself, the frameshifts observed in *Pfeba-165* could have played a role towards the isolation of *P. falciparum* from *P. reichenowi*.

To establish whether *Pf*EBA-165 mutations are indeed involved in host specificity, a number of experiments are required. First, in this study only a "corrected" *Pf*EBA-165 was expressed. It is therefore necessary to recombinantly express *Pr*EBA-165 and assess its binding to the glycan panel available in our laboratory, and also to human and chimpanzee erythrocytes. If the hypothesis is correct, recombinant *Pr*EBA-165 is expected to preferentially bind to Neu5Gc containing glycans and to chimpanzee erythrocytes. An alternative experimental angle would be to test the binding of *Pf*EBA-165 to human erythrocytes derived from stem cells which have been genetically engineered to express CMAH. Ideally, downstream experiments would include the generation and phenotypic analysis of a *Preba-165* knockout mutant. Such experimental designs are hampered by the fact that no *in vitro* culture system for *P. reichenowi* has been established, nor is it likely to be, given that chimpanzees are highly protected species. Finally, it will be critical to use the population genomic data being generated at the Sanger Institute to establish whether any clinical *P. falciparum* isolates possess a non-frameshifted *Pf*EBA-165. Several of those experiments are currently underway and are led by Dr William Proto in Julian Rayner's lab.

## 6.10 Concluding remarks

In the current PhD thesis I described the establishment of a versatile expression system which rapidly enables the recombinant expression of engineered antibodies. By using this system a high affinity anti-BSG chimeric antibody, ch6D9, was developed as a potential anti-malarial therapeutic. Ch6D9 demonstrated high efficacy in inhibiting erythrocyte invasion *in* vitro. Furthermore, ch6D9 displayed reduced binding to FcγRIIA and C1q *in vitro*, suggesting that this antibody may have reduced ability to trigger antibody effector functions. To the best of my knowledge

this is the first attempt to challenge malaria by targeting a host derived molecule. Further characterisation of ch6D9 is currently under way.

In a parallel project I expanded an existing *P. falciparum* merozoite recombinant protein library by 26 proteins, which were chosen based on transcription microarray data and information available in the literature. Twenty one out of 26 (>80%) merozoite proteins were expressed in a recombinant form and at usable amounts. These proteins will be a useful tool for the deeper understanding of erythrocyte invasion, and *Plasmodium falciparum* merozoite biology, in general.

# CHAPTER 7

**Bibliography**

## Bibliography

A G N (1931). The Late Baron Shibasaburo Kitasato. Canadian Medical Association Journal *25*, 206.

Abbas, A., Lichtman, A., and Pillai, S. (2011). Cellular and molecular immunology (Elsevier Health Sciences).

Agnandji, S.T., Lell, B., Fernandes, J.F., Abossolo, B.P., Methogo, B.G.N.O., Kabwende, A.L., Adegnika, A.A., Mordmüller, B., Issifou, S., Kremsner, P.G., et al. (2012). A phase 3 trial of RTS,S/AS01 malaria vaccine in African infants. The New England Journal of Medicine *367*, 2284–2295.

Agnandji, S.T., Lell, B., Soulanoudjingar, S.S., Fernandes, J.F., Abossolo, B.P., Conzelmann, C., Methogo, B.G.N.O., Doucka, Y., Flamen, A., Mordmüller, B., et al. (2011). First results of phase 3 trial of RTS,S/AS01 malaria vaccine in African children. The New England Journal of Medicine *365*, 1863–1875.

Aikawa, M., Miller, L.H., Johnson, J., and Rabbege, J. (1978). Erythrocyte entry by malarial parasites. A moving junction between erythrocyte and parasite. The Journal of Cell Biology *77*, 72–82.

Almagro, J.C., and Fransson, J. (2008). Humanization of antibodies. Frontiers in Bioscience : a Journal and Virtual Library *13*, 1619–1633.

Andersson, K., Hämäläinen, M., and Malmqvist, M. (1999). Identification and optimization of regeneration conditions for affinity-based biosensor assays. A multivariate cocktail approach. Analytical Chemistry *71*, 2475–2481.

Angrisano, F., Riglar, D.T., Sturm, A., Volz, J.C., Delves, M.J., Zuccala, E.S., Turnbull, L., Dekiwadia, C., Olshina, M. a, Marapana, D.S., et al. (2012). Spatial localisation of actin filaments across developmental stages of the malaria parasite. PloS One *7*, e32188.

Antinori, S., Galimberti, L., Milazzo, L., and Corbellino, M. (2013). Plasmodium knowlesi: the emerging zoonotic malaria parasite. Acta Tropica *125*, 191–201.

Armour, K.L., Clark, M.R., Hadley, A.G., and Williamson, L.M. (1999). Recombinant human IgG molecules lacking Fcgamma receptor I binding and monocyte triggering activities. European Journal of Immunology *29*, 2613–2624.

Armour, K.L., Parry-Jones, D.R., Beharry, N., Ballinger, J.R., Mushens, R., Williams, R.K., Beatty, C., Stanworth, S., Lloyd-Evans, P., Scott, M., et al. (2006). Intravascular survival of red cells coated with a mutated human anti-D antibody engineered to lack destructive activity. Blood *107*, 2619–2626.

Armour, K.L., Van de Winkel, J.G.J., Williamson, L.M., and Clark, M.R. (2003). Differential binding to human FcγRIIa and FcγRIIb receptors by human IgG wildtype and mutant antibodies. Molecular Immunology *40*, 585–593.

Baillie, J.K., and Digard, P. (2013). Influenza--time to target the host? The New England Journal of Medicine *369*, 191–193.

Ballou, W.R., Arevalo-Herrera, M., Carucci, D., Richie, T.L., Corradin, G., Diggs, C., Druilhe, P., Giersing, B.K., Saul, A., Heppner, D.G., et al. (2004). Update on the clinical development of candidate malaria vaccines. The American Journal of Tropical Medicine and Hygiene *71*, 239–247.

Bannister, L., and Mitchell, G. (2003). The ins, outs and roundabouts of malaria. Trends in Parasitology *19*, 209–213.

Bannister, L.H., and Mitchell, G.H. (2009). The malaria merozoite, forty years on. Parasitology *136*, 1435–1444.

Bannister, L.H., and Sherman, I.W. (2009). Plasmodium. Encyclopedia of Life Sciences (ELS). John Wiley & Sons, Ltd: Chichester. 1–12.

Barbouche, R., Lortat-Jacob, H., Jones, I.M., and Fenouillet, E. (2005). Glycosaminoglycans and protein disulfide isomerase-mediated reduction of HIV Env. Molecular Pharmacology *67*, 1111–1118.

Barbouche, R., Miquelis, R., Jones, I.M., and Fenouillet, E. (2003). Protein-disulfide isomerase-mediated reduction of two disulfide bonds of HIV envelope glycoprotein 120 occurs post-CXCR4 binding and is required for fusion. The Journal of Biological Chemistry *278*, 3131–3136.

Bartholdson, S.J., Bustamante, L.Y., Crosnier, C., Johnson, S., Lea, S., Rayner, J.C., and Wright, G.J. (2012). Semaphorin-7A is an erythrocyte receptor for P. falciparum merozoite-specific TRAP homolog, MTRAP. PLoS Pathogens *8*, e1003031.

Bartholdson, S.J., Crosnier, C., Bustamante, L.Y., Rayner, J.C., and Wright, G.J. (2013). Identifying novel Plasmodium falciparum erythrocyte invasion receptors using systematic extracellular protein interaction screens. Cellular Microbiology *15*, 1304–1312.

Bartlett, J.G. (1996). A Guide to Primary Care of People with HIV/AIDS.

Baselga, J., Cortés, J., Kim, S.-B., Im, S.-A., Hegg, R., Im, Y., Roman, L., Pedrini, J.L., Pienkowski, T., Knott, A., et al. (2012). Pertuzumab plus trastuzumab plus docetaxel for metastatic breast cancer. The New England Journal of Medicine *366*, 109–119.

Baum, J., Chen, L., Healer, J., Lopaticki, S., Boyle, M., Triglia, T., Ehlgen, F., Ralph, S. a, Beeson, J.G., and Cowman, A.F. (2009). Reticulocyte-binding protein homologue 5 - an essential adhesin involved in invasion of human erythrocytes by Plasmodium falciparum. International Journal for Parasitology *39*, 371–380.

Baum, J., Maier, A.G., Good, R.T., Simpson, K.M., and Cowman, A.F. (2005). Invasion by P. falciparum merozoites suggests a hierarchy of molecular interactions. PLoS Pathogens *1*, e37.

Baum, J., Richard, D., Healer, J., Rug, M., Krnajski, Z., Gilberger, T.-W., Green, J.L., Holder, A. a, and Cowman, A.F. (2006). A conserved molecular motor drives cell invasion and gliding motility across malaria life cycle stages and other apicomplexan parasites. The Journal of Biological Chemistry *281*, 5197–5208.

Beck, A., Wurch, T., Bailly, C., and Corvaia, N. (2010). Strategies and challenges for the next generation of therapeutic antibodies. Nature Reviews. Immunology *10*, 345–352.

Bei, A.K., and Duraisingh, M.T. (2012). Functional analysis of erythrocyte determinants of Plasmodium infection. International Journal for Parasitology *42*, 575–582.

Belton, R.J., Chen, L., Mesquita, F.S., and Nowak, R. a (2008). Basigin-2 is a cell surface receptor for soluble basigin ligand. The Journal of Biological Chemistry *283*, 17805–17814.

Besteiro, S., Dubremetz, J.-F., and Lebrun, M. (2011). The moving junction of apicomplexan parasites: a key structure for invasion. Cellular Microbiology *13*, 797–805.

Birch, J.R., and Racher, A.J. (2006). Antibody production. Advanced Drug Delivery Reviews *58*, 671–685.

Birkholtz, L.-M., Blatch, G., Coetzer, T.L., Hoppe, H.C., Human, E., Morris, E.J., Ngcete, Z., Oldfield, L., Roth, R., Shonhai, A., et al. (2008). Heterologous expression of plasmodial proteins for structural studies and functional annotation. Malaria Journal *7*, 197.

Black, C.G., Wu, T., Wang, L., Hibbs, a R., and Coppel, R.L. (2001). Merozoite surface protein 8 of Plasmodium falciparum contains two epidermal growth factor-like domains. Molecular and Biochemical Parasitology *114*, 217–226.

Blackman, M.J. (2008). Malarial proteases and host cell egress: an "emerging" cascade. Cellular Microbiology *10*, 1925–1934.

Blackman, M.J., Scott-Finnigan, T.J., Shai, S., and Holder, A.A. (1994). Antibodies inhibit the protease-mediated processing of a malaria merozoite surface protein. The Journal of Experimental Medicine *180*, 389–393.

Blomberg, K., Granberg, C., Hemmilä, I., and Lövgren, T. (1986). Europium-labelled target cells in an assay of natural killer cell activity. I. A novel non-radioactive method based on time-resolved fluorescence. Journal of Immunological Methods *86*, 225–229.

Blumenthal, G.M., Scher, N.S., Cortazar, P., Chattopadhyay, S., Tang, S., Song, P., Liu, Q., Ringgold, K., Pilaro, A.M., Tilley, A., et al. (2013). First FDA approval of dual anti-HER2 regimen: pertuzumab in combination with trastuzumab and docetaxel for HER2-positive metastatic breast cancer. Clinical Cancer Research : an Official Journal of the American Association for Cancer Research *19*, 4911–4916.

Bole-Feysot, C., Goffin, V., Edery, M., Binart, N., and Kelly, P. a (1998). Prolactin (PRL) and its receptor: actions, signal transduction pathways and phenotypes observed in PRL receptor knockout mice. Endocrine Reviews *19*, 225–268.

Bora, H., Tyagi, R.K., and Sharma, Y.D. (2013). Defining the erythrocyte binding domains of Plasmodium vivax tryptophan rich antigen 33.5. PloS One *8*, e62829.

Borre, M.B., Dziegiel, M., Høgh, B., Petersen, E., Rieneck, K., Riley, E., Meis, J.F., Aikawa, M., Nakamura, K., and Harada, M. (1991). Primary structure and localization of a conserved immunogenic Plasmodium falciparum glutamate rich protein (GLURP) expressed in both the preerythrocytic and erythrocytic stages of the vertebrate life cycle. Molecular and Biochemical Parasitology *49*, 119–131.

Boyle, M.J., Richards, J.S., Gilson, P.R., Chai, W., and Beeson, J.G. (2010). Interactions with heparin-like molecules during erythrocyte invasion by Plasmodium falciparum merozoites. Blood *115*, 4559–4568.

Bozdech, Z., Llinás, M., Pulliam, B.L., Wong, E.D., Zhu, J., and DeRisi, J.L. (2003). The transcriptome of the intraerythrocytic developmental cycle of Plasmodium falciparum. PLoS Biology *1*, E5.

Brown, M.H., and Barclay, a N. (1994). Expression of immunoglobulin and scavenger receptor superfamily domains as chimeric proteins with domains 3 and 4 of CD4 for ligand analysis. Protein Engineering *7*, 515–521.

Bruhns, P. (2012). Properties of mouse and human IgG receptors and their contribution to disease models. Blood *119*, 5640–5649.

Brunner, K.T., Mauel, J., Cerottini, J.C., and Chapuis, B. (1968). Quantitative assay of the lytic action of immune lymphoid cells on 51-Cr-labelled allogeneic target cells in vitro; inhibition by isoantibody and by drugs. Immunology *14*, 181–196.

Bruno, C.J., and Jacobson, J.M. (2010). Ibalizumab: an anti-CD4 monoclonal antibody for the treatment of HIV-1 infection. The Journal of Antimicrobial Chemotherapy *65*, 1839–1841.

Burgess, B.R., Schuck, P., and Garboczi, D.N. (2005). Dissection of merozoite surface protein 3, a representative of a family of Plasmodium falciparum surface proteins, reveals an oligomeric and highly elongated molecule. The Journal of Biological Chemistry *280*, 37236–37245.

Burns, J.M., Adeeku, E.K., Belk, C.C., and Dunn, P.D. (2000). An unusual tryptophan-rich domain characterizes two secreted antigens of Plasmodium yoelii-infected erythrocytes. Molecular and Biochemical Parasitology *110*, 11–21.

Burns, J.M., Adeeku, E.K., and Dunn, P.D. (1999). Protective immunization with a novel membrane protein of Plasmodium yoelii-infected erythrocytes. Infection and Immunity *67*, 675–680.

Bushell, K.M., Söllner, C., Schuster-Boeckler, B., Bateman, A., and Wright, G.J. (2008). Large-scale screening for novel low-affinity extracellular protein interactions. Genome Research *18*, 622–630.

Bustamante, L.Y., Bartholdson, S.J., Crosnier, C., Campos, M.G., Wanaguru, M., Nguon, C., Kwiatkowski, D.P., Wright, G.J., and Rayner, J.C. (2013). A full-length recombinant Plasmodium falciparum PfRH5 protein induces inhibitory antibodies that are effective across common PfRH5 genetic variants. Vaccine *31*, 373–379.

Camus, D., and Hadley, T.J. (1985). A Plasmodium falciparum antigen that binds to host erythrocytes and merozoites. Science (New York, N.Y.) *230*, 553–556.

Canfield, S.M., and Morrison, S.L. (1991). The binding affinity of human IgG for its high affinity Fc receptor is determined by multiple amino acids in the CH2 domain and is modulated by the hinge region. The Journal of Experimental Medicine *173*, 1483–1491.

Carter, P.J. (2006). Potent antibody therapeutics by design. Nature Reviews. Immunology *6*, 343–357.

Carter, R., Mendis, K.N., Miller, L.H., Molineaux, L., and Saul, A. (2000). Malaria transmission-blocking vaccines--how can their development be supported? Nature Medicine *6*, 241–244.

Casares, S., Brumeanu, T.-D., and Richie, T.L. (2010). The RTS,S malaria vaccine. Vaccine *28*, 4880–4894.

Chadd, H.E., and Chamow, S.M. (2001). Therapeutic antibody expression technology. Current Opinion in Biotechnology *12*, 188–194.

Chames, P., and Baty, D. (2009). Bispecific antibodies for cancer therapy: the light at the end of the tunnel? mAbs *1*, 539–547.

Chan, A.C., and Carter, P.J. (2010). Therapeutic antibodies for autoimmunity and inflammation. Nature Reviews. Immunology *10*, 301–316.

Chapman, K., Pullen, N., Graham, M., and Ragan, I. (2007). Preclinical safety testing of monoclonal antibodies: the significance of species relevance. Nature Reviews. Drug Discovery *6*, 120–126.

Chappel, M.S., Isenman, D.E., Everett, M., Xu, Y.Y., Dorrington, K.J., and Klein, M.H. (1991). Identification of the Fc gamma receptor class I binding site in human IgG through the use of recombinant IgG1/IgG2 hybrid and point-mutated antibodies. Proceedings of the National Academy of Sciences of the United States of America *88*, 9036–9040.

Chen, L., Lopaticki, S., Riglar, D.T., Dekiwadia, C., Uboldi, A.D., Tham, W.-H., O'Neill, M.T., Richard, D., Baum, J., Ralph, S. a., et al. (2011). An EGF-like Protein Forms a Complex with PfRh5 and Is Required for Invasion of Human Erythrocytes by Plasmodium falciparum. PLoS Pathogens *7*, e1002199.

Chen, Q., Schlichtherle, M., and Wahlgren, M. (2000). Molecular Aspects of Severe Malaria. Clinical Microbiology Reviews *13*, 439–450.

Chou, H.H., Takematsu, H., Diaz, S., Iber, J., Nickerson, E., Wright, K.L., Muchmore, E. a, Nelson, D.L., Warren, S.T., and Varki, a (1998). A mutation in human CMP-sialic acid hydroxylase occurred after the Homo-Pan divergence. Proceedings of the National Academy of Sciences of the United States of America *95*, 11751–11756.

Chowdhury, P.S., and Pastan, I. (1999). Improving antibody affinity by mimicking somatic hypermutation in vitro. Nature Biotechnology *17*, 568–572.

Clarke, A.W., Poulton, L., Wai, H.Y., Walker, S. a, Victor, S.D., Domagala, T., Mraovic, D., Butt, D., Shewmaker, N., Jennings, P., et al. (2010). A novel class of anti-IL-12p40 antibodies: potent neutralization via inhibition of IL-12-IL-12Rβ2 and IL-23-IL-23R. mAbs *2*, 539–549.

Clyde, D.F., Most, H., McCarthy, V.C., and Vanderberg, J.P. (1973). Immunization of man against sporozite-induced falciparum malaria. The American Journal of the Medical Sciences *266*, 169–177.

Cobleigh, M. a, Vogel, C.L., Tripathy, D., Robert, N.J., Scholl, S., Fehrenbacher, L., Wolter, J.M., Paton, V., Shak, S., Lieberman, G., et al. (1999). Multinational study of the efficacy and safety of humanized anti-HER2 monoclonal antibody in women who have HER2-overexpressing metastatic breast cancer that has progressed after chemotherapy for metastatic disease. Journal of Clinical Oncology : Official Journal of the American Society of Clinical Oncology *17*, 2639–2648.

Coggeshall, L.T., and Kumm, H.W. (1937). DEMONSTRATION OF PASSIVE IMMUNITY IN EXPERIMENTAL MONKEY MALARIA. The Journal of Experimental Medicine *66*, 177–190.

Cohen, S., Butcher, G.A., and Crandall, R.B. (1969). Action of malarial antibody in vitro. Nature *223*, 368–371.

Cohen, S., McGregor, I.A., and Carrington, S. (1961). Gamma-globulin and acquired immunity to human malaria. Nature *192*, 733–737.

Coles, A.J. (2013). Alemtuzumab therapy for multiple sclerosis. Neurotherapeutics : the Journal of the American Society for Experimental NeuroTherapeutics *10*, 29–33.

Conway, D.J., Cavanagh, D.R., Tanabe, K., Roper, C., Mikes, Z.S., Sakihama, N., Bojang, K.A., Oduola, A.M., Kremsner, P.G., Arnot, D.E., et al. (2000). A principal target of human immunity to malaria identified by molecular population genetic and immunological analyses. Nature Medicine *6*, 689–692.

Cooper, M. (2002). Optical biosensors in drug discovery. Nature Reviews. Drug Discovery *1*, 515–528.

Coste, I. (2001). Unavailability of CD147 leads to selective erythrocyte trapping in the spleen. Blood *97*, 3984–3988.

Cowman, A.F., Berry, D., and Baum, J. (2012). The cellular and molecular basis for malaria parasite invasion of the human red blood cell. The Journal of Cell Biology *198*, 961–971.

Cowman, A.F., and Crabb, B.S. (2006). Invasion of red blood cells by malaria parasites. Cell *124*, 755–766.

Crombet, T., Osorio, M., Cruz, T., Roca, C., Del Castillo, R., Mon, R., Iznaga-Escobar, N., Figueredo, R., Koropatnick, J., Renginfo, E., et al. (2004). Use of the humanized anti-epidermal growth factor receptor monoclonal antibody h-R3 in combination with radiotherapy in the treatment of locally advanced head and neck cancer patients. Journal of Clinical Oncology : Official Journal of the American Society of Clinical Oncology *22*, 1646–1654.

Crompton, P.D., Pierce, S.K., and Miller, L.H. (2010). Advances and challenges in malaria vaccine development. The Journal of Clinical Investigation *120*, 4168–4178.

Crosnier, C., Bustamante, L.Y., Bartholdson, S.J., Bei, A.K., Theron, M., Uchikawa, M., Mboup, S., Ndir, O., Kwiatkowski, D.P., Duraisingh, M.T., et al. (2011). Basigin is a receptor essential for erythrocyte invasion by Plasmodium falciparum. Nature *480*, 534–537.

Crosnier, C., Staudt, N., and Wright, G.J. (2010). A rapid and scalable method for selecting recombinant mouse monoclonal antibodies. BMC Biology *8*, 76.

Crosnier, C., Wanaguru, M., McDade, B., Osier, F.H., Marsh, K., Rayner, J.C., and Wright, G.J. (2013). A Library of Functional Recombinant Cell-surface and Secreted P. falciparum Merozoite Proteins. Molecular & Cellular Proteomics : MCP *12*, 3976–3986.

Culleton, R., and Kaneko, O. (2010). Erythrocyte binding ligands in malaria parasites: intracellular trafficking and parasite virulence. Acta Tropica *114*, 131–137.

Curtidor, H., Ocampo, M., Rodríguez, L.E., López, R., García, J.E., Valbuena, J., Vera, R., Puentes, A., Leiton, J., Cortes, L.J., et al. (2006). Plasmodium falciparum TryThrA antigen synthetic peptides block in vitro merozoite invasion to erythrocytes. Biochemical and Biophysical Research Communications *339*, 888–896.

Davis, J.H., Aperlo, C., Li, Y., Kurosawa, E., Lan, Y., Lo, K.-M., and Huston, J.S. (2010). SEEDbodies: fusion proteins based on strand-exchange engineered domain (SEED) CH3 heterodimers in an Fc analogue platform for asymmetric binders or immunofusions and bispecific antibodies. Protein Engineering, Design & Selection : PEDS *23*, 195–202.

Deeg, H.J., Blazar, B.R., Bolwell, B.J., Long, G.D., Schuening, F., Cunningham, J., Rifkin, R.M., Abhyankar, S., Briggs, A.D., Burt, R., et al. (2001). Treatment of steroid-refractory acute graft-versus-host disease with anti-CD147 monoclonal antibody ABX-CBL. Blood *98*, 2052–2058.

Desjarlais, J.R., and Lazar, G. a (2011). Modulation of antibody effector function. Experimental Cell Research *317*, 1278–1285.

Diacon, A.H., Dawson, R., Von Groote-Bidlingmaier, F., Symons, G., Venter, A., Donald, P.R., Van Niekerk, C., Everitt, D., Winter, H., Becker, P., et al. (2012). 14-day bactericidal activity of PA-824, bedaquiline, pyrazinamide, and moxifloxacin combinations: a randomised trial. Lancet *380*, 986–993.

Dieckmann-Schuppert, a, Bender, S., Odenthal-Schnittler, M., Bause, E., and Schwarz, R.T. (1992). Apparent lack of N-glycosylation in the asexual intraerythrocytic stage of Plasmodium falciparum. European Journal of Biochemistry / FEBS *205*, 815–825.

DiGiammarino, E., Ghayur, T., and Liu, J. (2012). Design and generation of DVD-Ig$^{TM}$ molecules for dual-specific targeting. Methods in Molecular Biology (Clifton, N.J.) *899*, 145–156.

Dodoo, D., Aikins, A., Kusi, K.A., Lamptey, H., Remarque, E., Milligan, P., Bosomprah, S., Chilengi, R., Osei, Y.D., Akanmori, B.D., et al. (2008). Cohort study of the association of antibody levels to AMA1, MSP119, MSP3 and GLURP with protection from clinical malaria in Ghanaian children. Malaria Journal *7*, 142.

Dodoo, D., Theisen, M., Kurtzhals, J. a, Akanmori, B.D., Koram, K. a, Jepsen, S., Nkrumah, F.K., Theander, T.G., and Hviid, L. (2000). Naturally acquired antibodies to the glutamate-rich protein are associated with protection against Plasmodium falciparum malaria. The Journal of Infectious Diseases *181*, 1202–1205.

Douglas, A.D., Williams, A.R., Illingworth, J.J., Kamuyu, G., Biswas, S., Goodman, A.L., Wyllie, D.H., Crosnier, C., Miura, K., Wright, G.J., et al. (2011). The blood-stage malaria antigen PfRH5 is susceptible to vaccine-inducible cross-strain neutralizing antibody. Nature Communications *2*, 601.

Douglas, A.D., Williams, A.R., Knuepfer, E., Illingworth, J.J., Furze, J.M., Crosnier, C., Choudhary, P., Bustamante, L.Y., Zakutansky, S.E., Awuah, D.K., et al. (2013). Neutralization of Plasmodium falciparum Merozoites by Antibodies against PfRH5. Journal of Immunology (Baltimore, Md. : 1950).

Draper, S.J., and Heeney, J.L. (2010). Viruses as vaccine vectors for infectious diseases and cancer. Nature Reviews. Microbiology *8*, 62–73.

Drew, D.R., Sanders, P.R., and Crabb, B.S. (2005). Plasmodium falciparum merozoite surface protein 8 is a ring-stage membrane protein that localizes to the parasitophorous vacuole of infected erythrocytes. Infection and Immunity *73*, 3912–3922.

Drew, M.E., Banerjee, R., Uffman, E.W., Gilbertson, S., Rosenthal, P.J., and Goldberg, D.E. (2008). Plasmodium food vacuole plasmepsins are activated by falcipains. The Journal of Biological Chemistry *283*, 12870–12876.

Drummond, P.B., and Peterson, D.S. (2005). An analysis of genetic diversity within the ligand domains of the Plasmodium falciparum ebl-1 gene. Molecular and Biochemical Parasitology *140*, 241–245.

Duffy, P.E., Sahu, T., Akue, A., Milman, N., and Anderson, C. (2012). Pre-erythrocytic malaria vaccines: identifying the targets. Expert Review of Vaccines *11*, 1261–1280.

Duraisingh, M.T., Triglia, T., Ralph, S. a, Rayner, J.C., Barnwell, J.W., McFadden, G.I., and Cowman, A.F. (2003). Phenotypic variation of Plasmodium falciparum merozoite proteins directs receptor targeting for invasion of human erythrocytes. The EMBO Journal *22*, 1047–1057.

Durocher, Y., Perret, S., and Kamen, A. (2002). High-level and high-throughput recombinant protein production by transient transfection of suspension-growing human 293-EBNA1 cells. Nucleic Acids Research *30*, E9.

Dvorak, J.A., Miller, L.H., Whitehouse, W.C., and Shiroishi, T. (1975). Invasion of erythrocytes by malaria merozoites. Science (New York, N.Y.) *187*, 748–750.

Dziegiel, M., Rowe, P., Bennett, S., Allen, S.J., Olerup, O., Gottschau, A., Borre, M., and Riley, E.M. (1993). Immunoglobulin M and G antibody responses to Plasmodium falciparum glutamate-rich protein: correlation with clinical immunity in Gambian children. Infection and Immunity *61*, 103–108.

Edozien, J.C., Gilles, H.M., and Udeozo, I.O.K. (1962). ADULT AND CORD-BLOOD GAMMA-GLOBULIN AND IMMUNITY TO MALARIA IN NIGERIANS. The Lancet *280*, 951–955.

Elliott, S.R., and Beeson, J.G. (2008). Estimating the burden of global mortality in children aged <5 years by pathogen-specific causes. Clinical Infectious Diseases: an Official Publication of the Infectious Diseases Society of America *46*, 1794–1795.

Ellis, R.D., Sagara, I., Doumbo, O., and Wu, Y. (2010). Blood stage vaccines for Plasmodium falciparum: current status and the way forward. Human Vaccines *6*, 627–634.

Ellis, R.D., Wu, Y., Martin, L.B., Shaffer, D., Miura, K., Aebig, J., Orcutt, A., Rausch, K., Zhu, D., Mogensen, A., et al. (2012). Phase 1 study in malaria naïve adults of BSAM2/Alhydrogel®+CPG 7909, a blood stage vaccine against P. falciparum malaria. PloS One *7*, e46094.

Enea, V., Ellis, J., Zavala, F., Arnot, D.E., Asavanich, A., Masuda, A., Quakyi, I., and Nussenzweig, R.S. (1984). DNA cloning of Plasmodium falciparum circumsporozoite gene: amino acid sequence of repetitive epitope. Science (New York, N.Y.) *225*, 628–630.

Van Epps, H.L. (2006). Michael Heidelberger and the demystification of antibodies. Journal of Experimental Medicine *203*, 5–5.

Epstein, J.E., Tewari, K., Lyke, K.E., Sim, B.K.L., Billingsley, P.F., Laurens, M.B., Gunasekera, A., Chakravarty, S., James, E.R., Sedegah, M., et al. (2011). Live attenuated malaria vaccine designed to protect through hepatic CD8$^+$ T cell immunity. Science (New York, N.Y.) *334*, 475–480.

Escalante, a a, Freeland, D.E., Collins, W.E., and Lal, a a (1998). The evolution of primate malaria parasites based on the gene encoding cytochrome b from the linear mitochondrial genome. Proceedings of the National Academy of Sciences of the United States of America *95*, 8124–8129.

Fadool, J.M., and Linser, P.J. (1993). Differential glycosylation of the 5A11/HT7 antigen by neural retina and epithelial tissues in the chicken. Journal of Neurochemistry *60*, 1354–1364.

Farrow, R.E., Green, J., Holder, A. a, and Molloy, J.E. (2011). The mechanism of erythrocyte invasion by the malarial parasite, Plasmodium falciparum. Seminars in Cell & Developmental Biology *22*, 953–960.

Fenouillet, E., Barbouche, R., Courageot, J., and Miquelis, R. (2001). The catalytic activity of protein disulfide isomerase is involved in human immunodeficiency virus envelope-mediated membrane fusion after CD4 cell binding. The Journal of Infectious Diseases *183*, 744–752.

Fernández-Robledo, J. a, and Vasta, G.R. (2010). Production of recombinant proteins from protozoan parasites. Trends in Parasitology *26*, 244–254.

Fessel, W.J., Anderson, B., Follansbee, S.E., Winters, M. a, Lewis, S.T., Weinheimer, S.P., Petropoulos, C.J., and Shafer, R.W. (2011). The efficacy of an anti-CD4 monoclonal antibody for HIV-1 treatment. Antiviral Research *92*, 484–487.

Flicek, P., Amode, M.R., Barrell, D., Beal, K., Brent, S., Chen, Y., Clapham, P., Coates, G., Fairley, S., Fitzgerald, S., et al. (2011). Ensembl 2011. Nucleic Acids Research *39*, D800–6.

Foote, J., and Winter, G. (1992). Antibody framework residues affecting the conformation of the hypervariable loops. Journal of Molecular Biology *224*, 487–499.

Fowkes, F.J.I., Richards, J.S., Simpson, J. a, and Beeson, J.G. (2010). The relationship between anti-merozoite antibodies and incidence of Plasmodium falciparum malaria: A systematic review and meta-analysis. PLoS Medicine *7*, e1000218.

Gabison, E.E., Hoang-Xuan, T., Mauviel, A., and Menashi, S. (2005). EMMPRIN/CD147, an MMP modulator in cancer, development and tissue repair. Biochimie *87*, 361–368.

Gallina, A., Hanley, T.M., Mandel, R., Trahey, M., Broder, C.C., Viglianti, G. a, and Ryser, H.J.-P. (2002). Inhibitors of protein-disulfide isomerase prevent cleavage of disulfide bonds in receptor-bound glycoprotein 120 and prevent HIV-1 entry. The Journal of Biological Chemistry *277*, 50579–50588.

Garcia, C.R.S., De Azevedo, M.F., Wunderlich, G., Budu, A., Young, J. a, and Bannister, L. (2008). Plasmodium in the postgenomic era: new insights into the molecular cell biology of malaria parasites. International Review of Cell and Molecular Biology *266*, 85–156.

Gardner, M.J., Hall, N., Fung, E., White, O., Berriman, M., Hyman, R.W., Carlton, J.M., Pain, A., Nelson, K.E., Bowman, S., et al. (2002). Genome sequence of the human malaria parasite Plasmodium falciparum. Nature *419*, 498–511.

Geels, M.J., Imoukhuede, E.B., Imbault, N., Van Schooten, H., McWade, T., Troye-Blomberg, M., Dobbelaer, R., Craig, A.G., and Leroy, O. (2011). European Vaccine Initiative: lessons from developing malaria vaccines. Expert Review of Vaccines *10*, 1697–1708.

Gerloff, D.L., Creasey, A., Maslau, S., and Carter, R. (2005). Structural models for the protein family characterized by gamete surface protein Pfs230 of Plasmodium falciparum. Proceedings of the National Academy of Sciences of the United States of America *102*, 13598–13603.

Geyer, C.R., McCafferty, J., Dübel, S., Bradbury, A.R.M., and Sidhu, S.S. (2012). Recombinant antibodies and in vitro selection technologies. Methods in Molecular Biology (Clifton, N.J.) *901*, 11–32.

Ghevaert, C., Herbert, N., Hawkins, L., Grehan, N., Cookson, P., Garner, S.F., Crisp-Hihn, A., Lloyd-Evans, P., Evans, A., Balan, K., et al. (2013). Recombinant HPA-1a antibody therapy for treatment of fetomaternal alloimmune thrombocytopenia: proof of principle in human volunteers. Blood *122*, 313–320.

Ghevaert, C., Wilcox, D.A., Fang, J., Armour, K.L., Clark, M.R., Ouwehand, W.H., and Williamson, L.M. (2008). Developing recombinant HPA-1a-specific antibodies with abrogated Fcgamma receptor binding for the treatment of fetomaternal alloimmune thrombocytopenia. The Journal of Clinical Investigation *118*, 2929–2938.

Gilberger, T.-W., Thompson, J.K., Triglia, T., Good, R.T., Duraisingh, M.T., and Cowman, A.F. (2003). A novel erythrocyte binding antigen-175 paralogue from Plasmodium falciparum defines a new trypsin-resistant receptor on human erythrocytes. The Journal of Biological Chemistry *278*, 14480–14486.

Gilson, P.R., and Crabb, B.S. (2009). Morphology and kinetics of the three distinct phases of red blood cell invasion by Plasmodium falciparum merozoites. International Journal for Parasitology *39*, 91–96.

Githui, E.K., Peterson, D.S., Aman, R. a, and Abdi, A.I. (2010). Prevalence of 5' insertion mutants and analysis of single nucleotide polymorphism in the erythrocyte binding-like 1 (ebl-1) gene in Kenyan Plasmodium falciparum field isolates. Infection,

Genetics and Evolution : Journal of Molecular Epidemiology and Evolutionary Genetics in Infectious Diseases *10*, 834–839.

Goel, V.K., Li, X., Chen, H., Liu, S., Chishti, A.H., and Oh, S.S. (2003). Band 3 is a host receptor binding merozoite surface protein 1 during the Plasmodium falciparum invasion of erythrocytes. Proceedings of the National Academy of Sciences of the United States of America *100*, 5164–5169.

Gonzales, N.R., De Pascalis, R., Schlom, J., and Kashmiri, S.V.S. (2005). Minimizing the immunogenicity of antibodies for clinical application. Tumour Biology : the Journal of the International Society for Oncodevelopmental Biology and Medicine *26*, 31–43.

Gordon, D.M., McGovern, T.W., Krzych, U., Cohen, J.C., Schneider, I., LaChance, R., Heppner, D.G., Yuan, G., Hollingdale, M., and Slaoui, M. (1995). Safety, immunogenicity, and efficacy of a recombinantly produced Plasmodium falciparum circumsporozoite protein-hepatitis B surface antigen subunit vaccine. The Journal of Infectious Diseases *171*, 1576–1585.

Gorman, S.D., and Clark, M.R. (1990). Humanisation of monoclonal antibodies for therapy. Seminars in Immunology *2*, 457–466.

Gowda, D.C., and Davidson, E. (2000). Reply. Parasitology Today *16*, 39–40.

Gowda, D.C., and Davidson, E. a (1999). Protein glycosylation in the malaria parasite. Parasitology Today (Personal Ed.) *15*, 147–152.

Graham, F.L., Smiley, J., Russell, W.C., and Nairn, R. (1977). Characteristics of a human cell line transformed by DNA from human adenovirus type 5. The Journal of General Virology *36*, 59–74.

Graves, P., and Gelband, H. (2006). Vaccines for preventing malaria (pre-erythrocytic). The Cochrane Database of Systematic Reviews CD006198.

Greenwood, B.M., and Targett, G. a T. (2011). Malaria vaccines and the new malaria agenda. Clinical Microbiology and Infection : the Official Publication of the European Society of Clinical Microbiology and Infectious Diseases *17*, 1600–1607.

Greenwood, J., and Clark, M. (1993). Effector functions of matched sets of recombinant human IgG subclass antibodies. In Protein Engineering of Antibody Molecules for Prophylactic and Therapeutic Applications in Man, pp. 85–100.

Haase, S., Cabrera, A., Langer, C., Treeck, M., Struck, N., Herrmann, S., Jansen, P.W., Bruchhaus, I., Bachmann, A., Dias, S., et al. (2008). Characterization of a conserved rhoptry-associated leucine zipper-like protein in the malaria parasite Plasmodium falciparum. Infection and Immunity *76*, 879–887.

Harris, P.K., Yeoh, S., Dluzewski, A.R., O'Donnell, R. a, Withers-Martinez, C., Hackett, F., Bannister, L.H., Mitchell, G.H., and Blackman, M.J. (2005). Molecular identification of a malaria merozoite surface sheddase. PLoS Pathogens *1*, 241–251.

Harvey, K.L., Gilson, P.R., and Crabb, B.S. (2012). A model for the progression of receptor-ligand interactions during erythrocyte invasion by Plasmodium falciparum. International Journal for Parasitology *42*, 567–573.

Hayakawa, T., Aki, I., Varki, A., Satta, Y., and Takahata, N. (2006). Fixation of the human-specific CMP-N-acetylneuraminic acid hydroxylase pseudogene and implications of haplotype diversity for human evolution. Genetics *172*, 1139–1146.

Hayton, K., Gaur, D., Liu, A., Takahashi, J., Henschen, B., Singh, S., Lambert, L., Furuya, T., Bouttenot, R., Doll, M., et al. (2008). Erythrocyte binding protein PfRH5 polymorphisms determine species-specific pathways of Plasmodium falciparum invasion. Cell Host & Microbe *4*, 40–51.

He, B., Mao, C., Ru, B., Han, H., Zhou, P., and Huang, J. (2013). Epitope mapping of metuximab on CD147 using phage display and molecular docking. Computational and Mathematical Methods in Medicine *2013*, 983829.

Helguera, G., Rodríguez, J.A., Luria-Pérez, R., Henery, S., Catterton, P., Bregni, C., George, T.C., Martínez-Maza, O., and Penichet, M.L. (2011). Visualization and quantification of cytotoxicity mediated by antibodies using imaging flow cytometry. Journal of Immunological Methods *368*, 54–63.

Hernandez, A., Parmentier, J., Wang, Y., Cheng, J., and Bornstein, G.G. (2012). Antibody Engineering (Totowa, NJ: Humana Press).

Herold, K.C., Gitelman, S.E., Masharani, U., Hagopian, W., Bisikirska, B., Donaldson, D., Rother, K., Diamond, B., Harlan, D.M., and Bluestone, J.A. (2005). A single course of anti-CD3 monoclonal antibody hOKT3gamma1(Ala-Ala) results in improvement in C-peptide responses and clinical parameters for at least 2 years after onset of type 1 diabetes. Diabetes *54*, 1763–1769.

Heslop, H.E., Benaim, E., Brenner, M.K., Krance, R. a, Stricklin, L.M., Rochester, R.J., and Billing, R. (1995). Response of steroid-resistant graft-versus-host disease to lymphoblast antibody CBL1. Lancet *346*, 805–806.

Hezareh, M., Hessell, A.N.N.J., Jensen, R.C., and J, J.A.N.G. (2001). Effector Function Activities of a Panel of Mutants of a Broadly Neutralizing Antibody against Human Immunodeficiency Virus Type 1. Society *75*, 12161–12168.

Hill, A.V.S. (2011). Vaccines against malaria. Philosophical Transactions of the Royal Society of London. Series B, Biological Sciences *366*, 2806–2814.

Hirsch, A.J., Medigeshi, G.R., Meyers, H.L., DeFilippis, V., Früh, K., Briese, T., Lipkin, W.I., and Nelson, J.A. (2005). The Src family kinase c-Yes is required for maturation of West Nile virus particles. Journal of Virology *79*, 11943–11951.

Hirsch, M.S., Brun-Vézinet, F., Clotet, B., Conway, B., Kuritzkes, D.R., D'Aquila, R.T., Demeter, L.M., Hammer, S.M., Johnson, V.A., Loveday, C., et al. (2003). Antiretroviral drug resistance testing in adults infected with human immunodeficiency virus type 1: 2003 recommendations of an International AIDS Society-USA Panel.

Clinical Infectious Diseases : an Official Publication of the Infectious Diseases Society of America *37*, 113–128.

Ho, M., and Pastan, I. (2009). In vitro antibody affinity maturation targeting germline hotspots. Methods in Molecular Biology (Clifton, N.J.) *525*, 293–308, xiv.

Hodder, A.N., Czabotar, P.E., Uboldi, A.D., Clarke, O.B., Lin, C.S., Healer, J., Smith, B.J., and Cowman, A.F. (2012). Insights into Duffy binding-like domains through the crystal structure and function of the merozoite surface protein MSPDBL2 from Plasmodium falciparum. The Journal of Biological Chemistry *287*, 32922–32939.

Hoffman, S.L., Goh, L.M.L., Luke, T.C., Schneider, I., Le, T.P., Doolan, D.L., Sacci, J., De la Vega, P., Dowler, M., Paul, C., et al. (2002). Protection of humans against malaria by immunization with radiation-attenuated Plasmodium falciparum sporozoites. The Journal of Infectious Diseases *185*, 1155–1164.

Hoffman, T.L., Canziani, G., Jia, L., Rucker, J., and Doms, R.W. (2000). A biosensor assay for studying ligand-membrane receptor interactions: binding of antibodies and HIV-1 Env to chemokine receptors. Proceedings of the National Academy of Sciences of the United States of America *97*, 11215–11220.

Hogarth, P.M., and Pietersz, G. a (2012). Fc receptor-targeted therapies for the treatment of inflammation, cancer and beyond. Nature Reviews. Drug Discovery *11*, 311–331.

Holliger, P., and Hudson, P. (2005). Engineered antibody fragments and the rise of single domains. Nature Biotechnology *23*, 1126–1136.

Hoogenboom, H.R. (2005). Selecting and screening recombinant antibody libraries. Nature Biotechnology *23*, 1105–1116.

Howell, S. a, Withers-Martinez, C., Kocken, C.H., Thomas, a W., and Blackman, M.J. (2001). Proteolytic processing and primary structure of Plasmodium falciparum apical membrane antigen-1. The Journal of Biological Chemistry *276*, 31311–31320.

Hu, G., Cabrera, A., Kono, M., Mok, S., Chaal, B.K., Haase, S., Engelberg, K., Cheemadan, S., Spielmann, T., Preiser, P.R., et al. (2010). Transcriptional profiling of growth perturbations of the human malaria parasite Plasmodium falciparum. Nature Biotechnology *28*, 91–98.

Hwang, W.Y.K., and Foote, J. (2005). Immunogenicity of engineered antibodies. Methods (San Diego, Calif.) *36*, 3–10.

Iacono, K.T., Brown, A.L., Greene, M.I., and Saouaf, S.J. (2007). CD147 immunoglobulin superfamily receptor function and role in pathology. Experimental and Molecular Pathology *83*, 283–295.

Idusogie, E.E., Presta, L.G., Gazzano-Santoro, H., Totpal, K., Wong, P.Y., Ultsch, M., Meng, Y.G., and Mulkerrin, M.G. (2000). Mapping of the C1q binding site on

rituxan, a chimeric antibody with a human IgG1 Fc. Journal of Immunology (Baltimore, Md. : 1950) *164*, 4178–4184.

Igakura, T., Kadomatsu, K., Kaname, T., Muramatsu, H., Fan, Q.W., Miyauchi, T., Toyama, Y., Kuno, N., Yuasa, S., Takahashi, M., et al. (1998). A null mutation in basigin, an immunoglobulin superfamily member, indicates its important roles in peri-implantation development and spermatogenesis. Developmental Biology *194*, 152–165.

Iyer, J., Grüner, A.C., Rénia, L., Snounou, G., and Preiser, P.R. (2007). Invasion of host cells by malaria parasites: a tale of two protein families. Molecular Microbiology *65*, 231–249.

Jacobson, J.M., Lalezari, J.P., Thompson, M. a, Fichtenbaum, C.J., Saag, M.S., Zingman, B.S., D'Ambrosio, P., Stambler, N., Rotshteyn, Y., Marozsan, A.J., et al. (2010). Phase 2a study of the CCR5 monoclonal antibody PRO 140 administered intravenously to HIV-infected adults. Antimicrobial Agents and Chemotherapy *54*, 4137–4142.

Jakobovits, A., Amado, R.G., Yang, X., Roskos, L., and Schwab, G. (2007). From XenoMouse technology to panitumumab, the first fully human antibody product from transgenic mice. Nature Biotechnology *25*, 1134–1143.

Jalah, R., Sarin, R., Sud, N., Alam, M.T., Parikh, N., Das, T.K., and Sharma, Y.D. (2005). Identification, expression, localization and serological characterization of a tryptophan-rich antigen from the human malaria parasite Plasmodium vivax. Molecular and Biochemical Parasitology *142*, 158–169.

Jefferis, R. (2009). Glycosylation as a strategy to improve antibody-based therapeutics. Nature Reviews. Drug Discovery *8*, 226–234.

Jiménez-Díaz, M.B., Mulet, T., Viera, S., Gómez, V., Garuti, H., Ibáñez, J., Alvarez-Doval, A., Shultz, L.D., Martínez, A., Gargallo-Viola, D., et al. (2009). Improved murine model of malaria using Plasmodium falciparum competent strains and non-myelodepleted NOD-scid IL2Rgammanull mice engrafted with human erythrocytes. Antimicrobial Agents and Chemotherapy *53*, 4533–4536.

Jones, P.T., Dear, P.H., Foote, J., Neuberger, M.S., and Winter, G. (1986). Replacing the complementarity-determining regions in a human antibody with those from a mouse. Nature *321*, 522–525.

Kabat, E.A., Wu, T.T., Perry, H.M., Gottesman, K.S., and Foeller, C. (1991). Sequences of Proteins of Immunological Interest (United States Public Health Service, National Institutes of Health, Bethesda).

Kadekoppala, M., and Holder, A. a (2010). Merozoite surface proteins of the malaria parasite: the MSP1 complex and the MSP7 family. International Journal for Parasitology *40*, 1155–1161.

Kadekoppala, M., O'Donnell, R. a, Grainger, M., Crabb, B.S., and Holder, A. a (2008). Deletion of the Plasmodium falciparum merozoite surface protein 7 gene impairs parasite invasion of erythrocytes. Eukaryotic Cell *7*, 2123–2132.

Kadekoppala, M., Ogun, S. a, Howell, S., Gunaratne, R.S., and Holder, A. a (2010). Systematic genetic analysis of the Plasmodium falciparum MSP7-like family reveals differences in protein expression, location, and importance in asexual growth of the blood-stage parasite. Eukaryotic Cell *9*, 1064–1074.

Kalunian, K.C., Davis, J.C., Merrill, J.T., Totoritis, M.C., and Wofsy, D. (2002). Treatment of systemic lupus erythematosus by inhibition of T cell costimulation with anti-CD154: a randomized, double-blind, placebo-controlled trial. Arthritis and Rheumatism *46*, 3251–3258.

Kanekura, T., Miyauchi, T., Tashiro, M., and Muramatsu, T. (1991). Basigin, a new member of the immunoglobulin superfamily: genes in different mammalian species, glycosylation changes in the molecule from adult organs and possible variation in the N-terminal sequences. Cell Structure and Function *16*, 23–30.

Karu, A.E., Bell, C.W., and Chin, T.E. (1995). Recombinant Antibody Technology. ILAR Journal *37*, 132–141.

Kashmiri, S.V.S., De Pascalis, R., Gonzales, N.R., and Schlom, J. (2005). SDR grafting--a new approach to antibody humanization. Methods (San Diego, Calif.) *36*, 25–34.

Kats, L.M., Black, C.G., Proellocks, N.I., and Coppel, R.L. (2006). Plasmodium rhoptries: how things went pear-shaped. Trends in Parasitology *22*, 269–276.

Kim, G.G., Donnenberg, V.S., Donnenberg, A.D., Gooding, W., and Whiteside, T.L. (2007). A novel multiparametric flow cytometry-based cytotoxicity assay simultaneously immunophenotypes effector cells: comparisons to a 4 h 51Cr-release assay. Journal of Immunological Methods *325*, 51–66.

Kim, S.J., and Hong, H.J. (2012). Humanization by guided selections. Methods in Molecular Biology (Clifton, N.J.) *907*, 237–257.

Kimura, E.A., Katzin, A.M., and Couto, A.S. (2000). More on protein glycosylation in the malaria parasite. Parasitology Today *16*, 38–40.

Koch, C., Staffler, G., Huttinger, R., Hilgert, I., Prager, E., Cerny, J., Steinlein, P., Majdic, O., Horejsi, V., and Stockinger, H. (1999). T cell activation-associated epitopes of CD147 in regulation of the T cell response, and their definition by antibody affinity and antigen density. International Immunology *11*, 777.

Köhler, G., and Milstein, C. (1975). Continuous cultures of fused cells secreting antibody of predefined specificity. Nature *256*, 495–497.

Korzeniewski, C., and Callewaert, D.M. (1983). An enzyme-release assay for natural cytotoxicity. Journal of Immunological Methods *64*, 313–320.

Koussis, K., Withers-Martinez, C., Yeoh, S., Child, M., Hackett, F., Knuepfer, E., Juliano, L., Woehlbier, U., Bujard, H., and Blackman, M.J. (2009). A multifunctional serine protease primes the malaria parasite for red blood cell invasion. The EMBO Journal *28*, 725–735.

Kromenaker, S.J., and Srienc, F. (1994). Stability of producer hybridoma cell lines after cell sorting: a case study. Biotechnology Progress *10*, 299–307.

Labrijn, A.F., Meesters, J.I., De Goeij, B.E.C.G., Van den Bremer, E.T.J., Neijssen, J., Van Kampen, M.D., Strumane, K., Verploegen, S., Kundu, A., Gramer, M.J., et al. (2013). Efficient generation of stable bispecific IgG1 by controlled Fab-arm exchange. Proceedings of the National Academy of Sciences of the United States of America *110*, 5145–5150.

Larkin, M.A., Blackshields, G., Brown, N.P., Chenna, R., McGettigan, P.A., McWilliam, H., Valentin, F., Wallace, I.M., Wilm, A., Lopez, R., et al. (2007). Clustal W and Clustal X version 2.0. Bioinformatics (Oxford, England) *23*, 2947–2948.

Lee-MacAry, A.E., Ross, E.L., Davies, D., Laylor, R., Honeychurch, J., Glennie, M.J., Snary, D., and Wilkinson, R.W. (2001). Development of a novel flow cytometric cell-mediated cytotoxicity assay using the fluorophores PKH-26 and TO-PRO-3 iodide. Journal of Immunological Methods *252*, 83–92.

Leykauf, K., Treeck, M., Gilson, P.R., Nebl, T., Braulke, T., Cowman, A.F., Gilberger, T.W., and Crabb, B.S. (2010). Protein kinase a dependent phosphorylation of apical membrane antigen 1 plays an important role in erythrocyte invasion by the malaria parasite. PLoS Pathogens *6*, e1000941.

Li, J., Matsuoka, H., Mitamura, T., and Horii, T. (2002). Characterization of proteases involved in the processing of Plasmodium falciparum serine repeat antigen (SERA). Molecular and Biochemical Parasitology *120*, 177–186.

Liao, C.-G., Kong, L.-M., Song, F., Xing, J.-L., Wang, L.-X., Sun, Z.-J., Tang, H., Yao, H., Zhang, Y., Wang, L., et al. (2011a). Characterization of basigin isoforms and the inhibitory function of basigin-3 in human hepatocellular carcinoma proliferation and invasion. Molecular and Cellular Biology *31*, 2591–2604.

Liao, H.-X., Chen, X., Munshaw, S., Zhang, R., Marshall, D.J., Vandergrift, N., Whitesides, J.F., Lu, X., Yu, J.-S., Hwang, K.-K., et al. (2011b). Initial antibodies binding to HIV-1 gp41 in acutely infected subjects are polyreactive and highly mutated. The Journal of Experimental Medicine *208*, 2237–2249.

Liao, H.-X., Lynch, R., Zhou, T., Gao, F., Alam, S.M., Boyd, S.D., Fire, A.Z., Roskin, K.M., Schramm, C. a., Zhang, Z., et al. (2013). Co-evolution of a broadly neutralizing HIV-1 antibody and founder virus. Nature *496*, 469–476.

Lieberman-Blum, S.S., Fung, H.B., and Bandres, J.C. (2008). Maraviroc: a CCR5-receptor antagonist for the treatment of HIV-1 infection. Clinical Therapeutics *30*, 1228–1250.

Lindenmann, J. (1984). Origin of the terms "antibody" and "antigen". Scandinavian Journal of Immunology *19*, 281–285.

Lo, B.K.C. (2004). Antibody humanization by CDR grafting. Methods in Molecular Biology (Clifton, N.J.) *248*, 135–159.

Lobo, C.-A., Rodriguez, M., Reid, M., and Lustigman, S. (2003). Glycophorin C is the receptor for the Plasmodium falciparum erythrocyte binding ligand PfEBP-2 (baebl). Blood *101*, 4628–4631.

Lonberg, N. (2005). Human antibodies from transgenic animals. Nature Biotechnology *23*, 1117–1125.

Lopaticki, S., Maier, A.G., Thompson, J., Wilson, D.W., Tham, W.-H., Triglia, T., Gout, A., Speed, T.P., Beeson, J.G., Healer, J., et al. (2011). Reticulocyte and erythrocyte binding-like proteins function cooperatively in invasion of human erythrocytes by malaria parasites. Infection and Immunity *79*, 1107–1117.

Lux, A., and Nimmerjahn, F. (2013). Of mice and men: the need for humanized mouse models to study human IgG activity in vivo. Journal of Clinical Immunology *33 Suppl 1*, S4–8.

Macmillan, M.L., Couriel, D., Weisdorf, D.J., Schwab, G., Havrilla, N., Fleming, T.R., Huang, S., Roskos, L., Slavin, S., Shadduck, R.K., et al. (2007). A phase 2/3 multicenter randomized clinical trial of ABX-CBL versus ATG as secondary therapy for steroid-resistant acute graft-versus-host disease. Blood *109*, 2657–2662.

Magliocca, J.F., and Knechtle, S.J. (2006). The evolving role of alemtuzumab (Campath-1H) for immunosuppressive therapy in organ transplantation. Transplant International : Official Journal of the European Society for Organ Transplantation *19*, 705–714.

Maier, A.G., Baum, J., Smith, B., Conway, D.J., and Cowman, A.F. (2009). Polymorphisms in erythrocyte binding antigens 140 and 181 affect function and binding but not receptor specificity in Plasmodium falciparum. Infection and Immunity *77*, 1689–1699.

Maier, A.G., Duraisingh, M.T., Reeder, J.C., Patel, S.S., Kazura, J.W., Zimmerman, P. a, and Cowman, A.F. (2003). Plasmodium falciparum erythrocyte invasion through glycophorin C and selection for Gerbich negativity in human populations. Nature Medicine *9*, 87–92.

Male, D., Brostoff, J., Roth, D., and Roitt, I. (2006). Essential immunology.

Manske, M., Miotto, O., Campino, S., Auburn, S., Almagro-Garcia, J., Maslen, G., O'Brien, J., Djimde, A., Doumbo, O., Zongo, I., et al. (2012). Analysis of Plasmodium falciparum diversity in natural infections by deep sequencing. Nature *487*, 375–379.

De Marco, A. (2009). Strategies for successful recombinant expression of disulfide bond-dependent proteins in Escherichia coli. Microbial Cell Factories *8*, 26.

Markovic, I., Stantchev, T.S., Fields, K.H., Tiffany, L.J., Tomiç, M., Weiss, C.D., Broder, C.C., Strebel, K., and Clouse, K. a (2004). Thiol/disulfide exchange is a prerequisite for CXCR4-tropic HIV-1 envelope-mediated T-cell fusion during viral entry. Blood *103*, 1586–1594.

Marsh, K., and Kinyanjui, S. (2006). Immune effector mechanisms in malaria. Parasite Immunology *28*, 51–60.

Martin, M.J., Rayner, J.C., Gagneux, P., Barnwell, J.W., and Varki, A. (2005). Evolution of human-chimpanzee differences in malaria susceptibility: relationship to human genetic loss of N-glycolylneuraminic acid. Proceedings of the National Academy of Sciences of the United States of America *102*, 12819–12824.

Marvin, J.S., and Zhu, Z. (2005). Recombinant approaches to IgG-like bispecific antibodies. *26*, 649–658.

Mason, D.W., and Williams, a F. (1980). The kinetics of antibody binding to membrane antigens in solution and at the cell surface. The Biochemical Journal *187*, 1–20.

Massie, B., Couture, F., Lamoureux, L., Mosser, D.D., Guilbault, C., Jolicoeur, P., Bélanger, F., and Langelier, Y. (1998). Inducible overexpression of a toxic protein by an adenovirus vector with a tetracycline-regulatable expression cassette. Journal of Virology *72*, 2289–2296.

Mayer, D.C.G., Cofie, J., Jiang, L., Hartl, D.L., Tracy, E., Kabat, J., Mendoza, L.H., and Miller, L.H. (2009). Glycophorin B is the erythrocyte receptor of Plasmodium falciparum erythrocyte-binding ligand, EBL-1. Proceedings of the National Academy of Sciences of the United States of America *106*, 5348–5352.

Mayer, D.C.G., Mu, J.-B., Feng, X., Su, X. -z., and Miller, L.H. (2002). Polymorphism in a Plasmodium falciparum Erythrocyte-binding Ligand Changes Its Receptor Specificity. Journal of Experimental Medicine *196*, 1523–1528.

Mayer, D.C.G., Mu, J.-B., Kaneko, O., Duan, J., Su, X., and Miller, L.H. (2004). Polymorphism in the Plasmodium falciparum erythrocyte-binding ligand JESEBL/EBA-181 alters its receptor specificity. Proceedings of the National Academy of Sciences of the United States of America *101*, 2518–2523.

McConkey, S.J., Reece, W.H.H., Moorthy, V.S., Webster, D., Dunachie, S., Butcher, G., Vuola, J.M., Blanchard, T.J., Gothard, P., Watkins, K., et al. (2003). Enhanced T-cell immunogenicity of plasmid DNA vaccines boosted by recombinant modified vaccinia virus Ankara in humans. Nature Medicine *9*, 729–735.

McCoubrie, J.E., Miller, S.K., Sargeant, T., Good, R.T., Hodder, A.N., Speed, T.P., De Koning-Ward, T.F., and Crabb, B.S. (2007). Evidence for a common role for the serine-type Plasmodium falciparum serine repeat antigen proteases: implications for vaccine and drug design. Infection and Immunity *75*, 5565–5574.

McGregor, I.., Carrington, S.., and Cohen, S. (1963). Treatment of east african P. falciparum malaria with west african human γ-globulin. Transactions of the Royal Society of Tropical Medicine and Hygiene *57*, 170–175.

Mehlin, C., Boni, E., Buckner, F.S., Engel, L., Feist, T., Gelb, M.H., Haji, L., Kim, D., Liu, C., Mueller, N., et al. (2006). Heterologous expression of proteins from Plasmodium falciparum: results from 1000 genes. Molecular and Biochemical Parasitology *148*, 144–160.

Meissner, P., Pick, H., Kulangara, a, Chatellard, P., Friedrich, K., and Wurm, F.M. (2001). Transient gene expression: recombinant protein production with suspension-adapted HEK293-EBNA cells. Biotechnology and Bioengineering *75*, 197–203.

Mezghrani, A., Courageot, J., Mani, J.C., Pugniere, M., Bastiani, P., and Miquelis, R. (2000). Protein-disulfide isomerase (PDI) in FRTL5 cells. pH-dependent thyroglobulin/PDI interactions determine a novel PDI function in the post-endoplasmic reticulum of thyrocytes. The Journal of Biological Chemistry *275*, 1920–1929.

Miller, L.H., Ackerman, H.C., Su, X.-Z., and Wellems, T.E. (2013). Malaria biology and disease pathogenesis: insights for new treatments. Nature Medicine *19*, 156–167.

Miller, L.H., Baruch, D.I., Marsh, K., and Doumbo, O.K. (2002a). The pathogenic basis of malaria. Nature *415*, 673–679.

Miller, L.H., Hudson, D., Rener, J., Taylor, D., Hadley, T.J., and Zilberstein, D. (1983). A monoclonal antibody to rhesus erythrocyte band 3 inhibits invasion by malaria (Plasmodium knowlesi) merozoites. The Journal of Clinical Investigation *72*, 1357–1364.

Miller, S.K., Good, R.T., Drew, D.R., Delorenzi, M., Sanders, P.R., Hodder, A.N., Speed, T.P., Cowman, A.F., De Koning-Ward, T.F., and Crabb, B.S. (2002b). A subset of Plasmodium falciparum SERA genes are expressed and appear to play an important role in the erythrocytic cycle. The Journal of Biological Chemistry *277*, 47524–47532.

Milstein, C., and Cuello, A.C. (1983). Hybrid hybridomas and their use in immunohistochemistry. Nature *305*, 537–540.

Moorthy, V.S., Hutubessy, R., Newman, R.D., and Hombach, J. (2012). Decision-making on malaria vaccine introduction: the role of cost-effectiveness analyses. Bulletin of the World Health Organization *90*, 864–866.

Morahan, B.J., Wang, L., and Coppel, R.L. (2008). No TRAP , no invasion. Trends in Parasitology 77–84.

Moran, N. (2013). Mouse platforms jostle for slice of humanized antibody market. Nature Biotechnology *31*, 267–268.

Morgan, A., Jones, N., Nesbitt, A., and Chaplin, L. (1995). The N-terminal end of the CH2 domain of chimeric human IgG1 anti-HLA-DR is necessary for Clq, FcyRI and FcyRIII binding. Immunology *86*, 319–324.

Morita, M., Kuba, K., Ichikawa, A., Nakayama, M., Katahira, J., Iwamoto, R., Watanebe, T., Sakabe, S., Daidoji, T., Nakamura, S., et al. (2013). The lipid mediator protectin D1 inhibits influenza virus replication and improves severe influenza. Cell *153*, 112–125.

Morrison, S.L. (2007). Two heads are better than one. Nature Biotechnology *25*, 1233–1234.

Morrison, S.L., Johnson, M.J., Herzenberg, L.A., and Oi, V.T. (1984). Chimeric human antibody molecules: mouse antigen-binding domains with human constant region domains. Proceedings of the National Academy of Sciences of the United States of America *81*, 6851–6855.

Muchmore, E.A., Diaz, S., and Varki, A. (1998). A structural difference between the cell surfaces of humans and the great apes. American Journal of Physical Anthropology *107*, 187–198.

Muralidharan, V., Oksman, A., Pal, P., Lindquist, S., and Goldberg, D.E. (2012). Plasmodium falciparum heat shock protein 110 stabilizes the asparagine repeat-rich parasite proteome during malarial fevers. Nature Communications *3*, 1310.

Muramatsu, T., and Miyauchi, T. (2003). Basigin (CD147): a multifunctional transmembrane protein involved in reproduction, neural function, inflammation and tumor invasion. Histology and Histopathology *18*, 981–987.

Murray, C.J.L., Rosenfeld, L.C., Lim, S.S., Andrews, K.G., Foreman, K.J., Haring, D., Fullman, N., Naghavi, M., Lozano, R., and Lopez, A.D. (2012). Global malaria mortality between 1980 and 2010: a systematic analysis. Lancet *379*, 413–431.

Naglich, J.G., Metherall, J.E., Russell, D.W., and Eidels, L. (1992). Expression cloning of a diphtheria toxin receptor: identity with a heparin-binding EGF-like growth factor precursor. Cell *69*, 1051–1061.

Nelson, A.L., Dhimolea, E., and Reichert, J.M. (2010). Development trends for human monoclonal antibody therapeutics. Nature Reviews. Drug Discovery *9*, 767–774.

Nikodem, D., and Davidson, E. (2000). Identification of a novel antigenic domain of Plasmodium falciparum merozoite surface protein-1 that specifically binds to human erythrocytes and inhibits parasite invasion, in vitro. Molecular and Biochemical Parasitology *108*, 79–91.

Nimmerjahn, F., and Ravetch, J. V (2006). Fcgamma receptors: old friends and new family members. Immunity *24*, 19–28.

Nimmerjahn, F., and Ravetch, J. V (2008). Fcgamma receptors as regulators of immune responses. Nature Reviews. Immunology *8*, 34–47.

Ntumngia, F.B., Bahamontes-Rosa, N., and Kun, J.F.J. (2005). Genes coding for tryptophan-rich proteins are transcribed throughout the asexual cycle of Plasmodium falciparum. Parasitology Research *96*, 347–353.

Ntumngia, F.B., Bouyou-Akotet, M.K., Uhlemann, A.-C., Mordmüller, B., Kremsner, P.G., and Kun, J.F.J. (2004). Characterisation of a tryptophan-rich Plasmodium falciparum antigen associated with merozoites. Molecular and Biochemical Parasitology *137*, 349–353.

Nussenzweig, R.S., Vanderberg, J., Most, H., and Orton, C. (1967). Protective immunity produced by the injection of x-irradiated sporozoites of plasmodium berghei. Nature *216*, 160–162.

Ogutu, B.R., Apollo, O.J., McKinney, D., Okoth, W., Siangla, J., Dubovsky, F., Tucker, K., Waitumbi, J.N., Diggs, C., Wittes, J., et al. (2009). Blood stage malaria vaccine eliciting high antigen-specific antibody concentrations confers no protection to young children in Western Kenya. PloS One *4*, e4708.

Ogwang, C., Afolabi, M., Kimani, D., Jagne, Y.J., Sheehy, S.H., Bliss, C.M., Duncan, C.J.A., Collins, K.A., Garcia Knight, M.A., Kimani, E., et al. (2013). Safety and immunogenicity of heterologous prime-boost immunisation with Plasmodium falciparum malaria candidate vaccines, ChAd63 ME-TRAP and MVA ME-TRAP, in healthy Gambian and Kenyan adults. PloS One *8*, e57726.

Okech, B., Mujuzi, G., Ogwal, A., Shirai, H., Horii, T., and Egwang, T.G. (2006). High titers of IgG antibodies against Plasmodium falciparum serine repeat antigen 5 (SERA5) are associated with protection against severe malaria in Ugandan children. The American Journal of Tropical Medicine and Hygiene *74*, 191–197.

Olson, M. V, and Varki, A. (2003). Sequencing the chimpanzee genome: insights into human evolution and disease. Nature Reviews. Genetics *4*, 20–28.

Otz, T. (2010). Antibody Engineering (Berlin, Heidelberg: Springer Berlin Heidelberg).

Outchkourov, N.S., Roeffen, W., Kaan, A., Jansen, J., Luty, A., Schuiffel, D., Van Gemert, G.J., Van de Vegte-Bolmer, M., Sauerwein, R.W., and Stunnenberg, H.G. (2008). Correctly folded Pfs48/45 protein of Plasmodium falciparum elicits malaria transmission-blocking immunity in mice. Proceedings of the National Academy of Sciences of the United States of America *105*, 4301–4305.

Padlan, E.A. (1994). Anatomy of the antibody molecule. Molecular Immunology *31*, 169–217.

Padlan, E.A., Abergel, C., and Tipper, J.P. (1995). Identification of specificity-determining residues in antibodies. FASEB Journal : Official Publication of the Federation of American Societies for Experimental Biology *9*, 133–139.

Pasini, E.M., Kirkegaard, M., Mortensen, P., Lutz, H.U., Thomas, A.W., and Mann, M. (2006). In-depth analysis of the membrane and cytosolic proteome of red blood cells. Blood *108*, 791–801.

Perkins, M.E., and Rocco, L.J. (1988). Sialic acid-dependent binding of Plasmodium falciparum merozoite surface antigen, Pf200, to human erythrocytes. Journal of Immunology (Baltimore, Md. : 1950) *141*, 3190–3196.

Peterson, N.C. (2005). Advances in monoclonal antibody technology: genetic engineering of mice, cells, and immunoglobulins. ILAR Journal / National Research Council, Institute of Laboratory Animal Resources *46*, 314–319.

Phyo, A.P., Nkhoma, S., Stepniewska, K., Ashley, E. a, Nair, S., McGready, R., ler Moo, C., Al-Saai, S., Dondorp, A.M., Lwin, K.M., et al. (2012). Emergence of artemisinin-resistant malaria on the western border of Thailand: a longitudinal study. Lancet *379*, 1960–1966.

Pinder, J., Fowler, R., Bannister, L., Dluzewski, A., and Mitchell, G.H. (2000). Motile systems in malaria merozoites: how is the red blood cell invaded? Parasitology Today *16*, 240–245.

Plassmeyer, M.L., Reiter, K., Shimp, R.L., Kotova, S., Smith, P.D., Hurt, D.E., House, B., Zou, X., Zhang, Y., Hickman, M., et al. (2009). Structure of the Plasmodium falciparum circumsporozoite protein, a leading malaria vaccine candidate. The Journal of Biological Chemistry *284*, 26951–26963.

Pleschka, S., Wolff, T., Ehrhardt, C., Hobom, G., Planz, O., Rapp, U.R., and Ludwig, S. (2001). Influenza virus propagation is impaired by inhibition of the Raf/MEK/ERK signalling cascade. Nature Cell Biology *3*, 301–305.

Prudêncio, M., Rodriguez, A., and Mota, M.M. (2006). The silent path to thousands of merozoites: the Plasmodium liver stage. Nature Reviews. Microbiology *4*, 849–856.

Prussia, A., Thepchatri, P., Snyder, J.P., and Plemper, R.K. (2011). Systematic Approaches towards the Development of Host-Directed Antiviral Therapeutics. International Journal of Molecular Sciences *12*, 4027–4052.

Puig, O., Caspary, F., Rigaut, G., Rutz, B., Bouveret, E., Bragado-Nilsson, E., Wilm, M., and Séraphin, B. (2001). The tandem affinity purification (TAP) method: a general procedure of protein complex purification. Methods (San Diego, Calif.) *24*, 218–229.

Qu, Z., Griffiths, G.L., Wegener, W.A., Chang, C.-H., Govindan, S. V, Horak, I.D., Hansen, H.J., and Goldenberg, D.M. (2005). Development of humanized antibodies as cancer therapeutics. Methods (San Diego, Calif.) *36*, 84–95.

Rasmussen, S.K., Næsted, H., Müller, C., Tolstrup, A.B., and Frandsen, T.P. (2012). Recombinant antibody mixtures: production strategies and cost considerations. Archives of Biochemistry and Biophysics *526*, 139–145.

Rayner, J.C., Huber, C.S., and Barnwell, J.W. (2004). Conservation and divergence in erythrocyte invasion ligands: Plasmodium reichenowi EBL genes. Molecular and Biochemical Parasitology *138*, 243–247.

Rayner, J.C., Liu, W., Peeters, M., Sharp, P.M., and Hahn, B.H. (2011). A plethora of Plasmodium species in wild apes: a source of human infection? Trends in Parasitology *27*, 222–229.

Rayner, J.C., Vargas-Serrato, E., Huber, C.S., Galinski, M.R., and Barnwell, J.W. (2001). A Plasmodium falciparum homologue of Plasmodium vivax reticulocyte binding protein (PvRBP1) defines a trypsin-resistant erythrocyte invasion pathway. The Journal of Experimental Medicine *194*, 1571–1581.

Reddy, K.S., Pandey, A.K., Singh, H., Sahar, T., Emmanuel, A., Chitnis, C.E., Chauhan, V.S., and Gaur, D. (2013). A bacterially expressed full-length recombinant Plasmodium falciparum RH5 protein binds erythrocytes and elicits potent strain-transcending parasite neutralizing antibodies. Infection and Immunity.

Reeves, P.M., Bommarius, B., Lebeis, S., McNulty, S., Christensen, J., Swimm, A., Chahroudi, A., Chavan, R., Feinberg, M.B., Veach, D., et al. (2005). Disabling poxvirus pathogenesis by inhibition of Abl-family tyrosine kinases. Nature Medicine *11*, 731–739.

Regules, J.A., Cummings, J.F., and Ockenhouse, C.F. (2011). The RTS,S vaccine candidate for malaria. Expert Review of Vaccines *10*, 589–599.

Reichert, J.M. (2010). Metrics for antibody therapeutics development. mAbs *2*, 695–700.

Reichert, J.M., Rosensweig, C.J., Faden, L.B., and Dewitz, M.C. (2005). Monoclonal antibody successes in the clinic. Nature Biotechnology *23*, 1073–1078.

Richard, D., MacRaild, C.A., Riglar, D.T., Chan, J.-A., Foley, M., Baum, J., Ralph, S. a, Norton, R.S., and Cowman, A.F. (2010). Interaction between Plasmodium falciparum apical membrane antigen 1 and the rhoptry neck protein complex defines a key step in the erythrocyte invasion process of malaria parasites. The Journal of Biological Chemistry *285*, 14815–14822.

Richards, J.S., and Beeson, J.G. (2009). The future for blood-stage vaccines against malaria. Immunology and Cell Biology *87*, 377–390.

Riechmann, L., Clark, M., Waldmann, H., and Winter, G. (1988). Reshaping human antibodies for therapy. Nature *332*, 323–327.

Rigaut, G., Shevchenko, A., Rutz, B., Wilm, M., Mann, M., and Séraphin, B. (1999). A generic protein purification method for protein complex characterization and proteome exploration. Nature Biotechnology *17*, 1030–1032.

Riglar, D.T., Richard, D., Wilson, D.W., Boyle, M.J., Dekiwadia, C., Turnbull, L., Angrisano, F., Marapana, D.S., Rogers, K.L., Whitchurch, C.B., et al. (2011). Super-

resolution dissection of coordinated events during malaria parasite invasion of the human erythrocyte. Cell Host & Microbe *9*, 9–20.

Riley, E.M., and Stewart, V.A. (2013). Immune mechanisms in malaria: new insights in vaccine development. Nature Medicine *19*, 168–178.

Rodriguez, M., Lustigman, S., Montero, E., Oksov, Y., and Lobo, C.A. (2008). PfRH5: a novel reticulocyte-binding family homolog of plasmodium falciparum that binds to the erythrocyte, and an investigation of its receptor. PloS One *3*, e3300.

Roestenberg, M., McCall, M., Hopman, J., Wiersma, J., Luty, A.J.F., Van Gemert, G.J., Van de Vegte-Bolmer, M., Van Schaijk, B., Teelen, K., Arens, T., et al. (2009). Protection against a malaria challenge by sporozoite inoculation. The New England Journal of Medicine *361*, 468–477.

Ruecker, A., Shea, M., Hackett, F., Suarez, C., Hirst, E.M. a, Milutinovic, K., Withers-Martinez, C., and Blackman, M.J. (2012). Proteolytic Activation of the Essential Parasitophorous Vacuole Cysteine Protease SERA6 Accompanies Malaria Parasite Egress from Its Host Erythrocyte. The Journal of Biological Chemistry *287*, 37949–37963.

Rycyzyn, M.A., Reilly, S.C., O'Malley, K., and Clevenger, C. V (2000). Role of cyclophilin B in prolactin signal transduction and nuclear retrotranslocation. Molecular Endocrinology (Baltimore, Md.) *14*, 1175–1186.

Sabchareon, a, Burnouf, T., Ouattara, D., Attanath, P., Bouharoun-Tayoun, H., Chantavanich, P., Foucault, C., Chongsuphajaisiddhi, T., and Druilhe, P. (1991). Parasitologic and clinical human response to immunoglobulin administration in falciparum malaria. The American Journal of Tropical Medicine and Hygiene *45*, 297–308.

Sakamoto, H., Takeo, S., Maier, A.G., Sattabongkot, J., Cowman, A.F., and Tsuboi, T. (2012). Antibodies against a Plasmodium falciparum antigen PfMSPDBL1 inhibit merozoite invasion into human erythrocytes. Vaccine *30*, 1972–1980.

Sanders, P.R., Gilson, P.R., Cantin, G.T., Greenbaum, D.C., Nebl, T., Carucci, D.J., McConville, M.J., Schofield, L., Hodder, A.N., Yates, J.R., et al. (2005). Distinct protein classes including novel merozoite surface antigens in Raft-like membranes of Plasmodium falciparum. The Journal of Biological Chemistry *280*, 40169–40176.

Saul, A. (1987). Kinetic constraints on the development of a malaria vaccine. Parasite Immunology *9*, 1–9.

Schaefer, W., Regula, J.T., Bähner, M., Schanzer, J., Croasdale, R., Dürr, H., Gassner, C., Georges, G., Kettenberger, H., Imhof-Jung, S., et al. (2011). Immunoglobulin domain crossover as a generic approach for the production of bispecific IgG antibodies. Proceedings of the National Academy of Sciences of the United States of America *108*, 11187–11192.

Schasfoort, R.B.M., and Tudos, A.J. (2008). Handbook of Surface Plasmon Resonance (Cambridge: Royal Society of Chemistry).

Schlegel, J., Redzic, J.S., Porter, C.C., Yurchenko, V., Bukrinsky, M., Labeikovsky, W., Armstrong, G.S., Zhang, F., Isern, N.G., DeGregori, J., et al. (2009). Solution characterization of the extracellular region of CD147 and its interaction with its enzyme ligand cyclophilin A. Journal of Molecular Biology *391*, 518–535.

Schwartz, L., Brown, G. V, Genton, B., and Moorthy, V.S. (2012). A review of malaria vaccine clinical projects based on the WHO rainbow table. Malaria Journal *11*, 11.

Seder, R. a, Chang, L.-J., Enama, M.E., Zephir, K.L., Sarwar, U.N., Gordon, I.J., Holman, L. a, James, E.R., Billingsley, P.F., Gunasekera, A., et al. (2013). Protection Against Malaria by Intravenous Immunization with a Nonreplicating Sporozoite Vaccine. Science (New York, N.Y.) 1–12.

Sergeeva, A., Kolonin, M.G., Molldrem, J.J., Pasqualini, R., and Arap, W. (2006). Display technologies: application for the discovery of drug and gene delivery agents. Advanced Drug Delivery Reviews *58*, 1622–1654.

Sharkey, R.M., Juweid, M., Shevitz, J., Behr, T., Dunn, R., Swayne, L.C., Wong, G.Y., Blumenthal, R.D., Griffiths, G.L., and Siegel, J. a (1995). Evaluation of a complementarity-determining region-grafted (humanized) anti-carcinoembryonic antigen monoclonal antibody in preclinical and clinical studies. Cancer Research *55*, 5935s–5945s.

Shields, R.L., Namenuk, a K., Hong, K., Meng, Y.G., Rae, J., Briggs, J., Xie, D., Lai, J., Stadlen, a, Li, B., et al. (2001). High resolution mapping of the binding site on human IgG1 for Fc gamma RI, Fc gamma RII, Fc gamma RIII, and FcRn and design of IgG1 variants with improved binding to the Fc gamma R. The Journal of Biological Chemistry *276*, 6591–6604.

Shimomura, T., Ochiai, M., Kondo, J., and Morimoto, Y. (1992). A novel protease obtained from FBS-containing culture supernatant, that processes single chain form hepatocyte growth factor to two chain form in serum-free culture. Cytotechnology *8*, 219–229.

Sim, B.K., Chitnis, C.E., Wasniowska, K., Hadley, T.J., and Miller, L.H. (1994). Receptor and ligand domains for invasion of erythrocytes by Plasmodium falciparum. Science (New York, N.Y.) *264*, 1941–1944.

Sinden, R.E. (2010). A biologist's perspective on malaria vaccine development. Human Vaccines *6*, 3–11.

Singh, B., Kim Sung, L., Matusop, A., Radhakrishnan, A., Shamsul, S.S.G., Cox-Singh, J., Thomas, A., and Conway, D.J. (2004). A large focus of naturally acquired Plasmodium knowlesi infections in human beings. Lancet *363*, 1017–1024.

Singh, S., Alam, M.M., Pal-Bhowmick, I., Brzostowski, J. a, and Chitnis, C.E. (2010). Distinct external signals trigger sequential release of apical organelles during erythrocyte invasion by malaria parasites. PLoS Pathogens *6*, e1000746.

Singh, S., Plassmeyer, M., Gaur, D., and Miller, L.H. (2007). Mononeme: a new secretory organelle in Plasmodium falciparum merozoites identified by localization of rhomboid-1 protease. Proceedings of the National Academy of Sciences of the United States of America *104*, 20043–20048.

Singh, S., Soe, S., Weisman, S., Barnwell, J.W., Pérignon, J.L., and Druilhe, P. (2009). A conserved multi-gene family induces cross-reactive antibodies effective in defense against Plasmodium falciparum. PloS One *4*, e5410.

Smith, S.L. (1996). Ten years of Orthoclone OKT3 (muromonab-CD3): a review. Journal of Transplant Coordination : Official Publication of the North American Transplant Coordinators Organization (NATCO) *6*, 109–19; quiz 120–1.

Sparrow, R.L., Healey, G., Patton, K. a, and Veale, M.F. (2006). Red blood cell age determines the impact of storage and leukocyte burden on cell adhesion molecules, glycophorin A and the release of annexin V. Transfusion and Apheresis Science : Official Journal of the World Apheresis Association : Official Journal of the European Society for Haemapheresis *34*, 15–23.

Srinivasan, P., Beatty, W.L., Diouf, a., Herrera, R., Ambroggio, X., Moch, J.K., Tyler, J.S., Narum, D.L., Pierce, S.K., Boothroyd, J.C., et al. (2011). Binding of Plasmodium merozoite proteins RON2 and AMA1 triggers commitment to invasion. Proceedings of the National Academy of Sciences *108*, 13275–13280.

Strohal, R., Kroemer, G., Wick, G., and Kofler, R. (1987). Complete variable region sequence of a nonfunctionally rearranged kappa light chain transcribed in the nonsecretor P3-X63-Ag8.653 myeloma cell line. Nucleic Acids Research *15*, 2771.

Stubbs, J., Simpson, K.M., Triglia, T., Plouffe, D., Tonkin, C.J., Duraisingh, M.T., Maier, A.G., Winzeler, E. a, and Cowman, A.F. (2005). Molecular mechanism for switching of P. falciparum invasion pathways into human erythrocytes. Science (New York, N.Y.) *309*, 1384–1387.

Su, X., Hayton, K., and Wellems, T.E. (2007). Genetic linkage and association analyses for trait mapping in Plasmodium falciparum. Nature Reviews. Genetics *8*, 497–506.

Sutherland, C.J., Tanomsing, N., Nolder, D., Oguike, M., Jennison, C., Pukrittayakamee, S., Dolecek, C., Hien, T.T., Do Rosário, V.E., Arez, A.P., et al. (2010). Two nonrecombining sympatric forms of the human malaria parasite Plasmodium ovale occur globally. The Journal of Infectious Diseases *201*, 1544–1550.

Taechalertpaisarn, T., Crosnier, C., Bartholdson, S.J., Hodder, A.N., Thompson, J., Bustamante, L.Y., Wilson, D.W., Sanders, P.R., Wright, G.J., Rayner, J.C., et al.

(2012). Biochemical and functional analysis of two Plasmodium falciparum blood-stage 6-cys proteins: P12 and P41. PloS One *7*, e41937.

Tamura, M., Milenic, D.E., Iwahashi, M., Padlan, E., Schlom, J., and Kashmiri, S. V (2000). Structural correlates of an anticarcinoma antibody: identification of specificity-determining residues (SDRs) and development of a minimally immunogenic antibody variant by retention of SDRs only. Journal of Immunology (Baltimore, Md. : 1950) *164*, 1432–1441.

Tan, S.-L., Ganji, G., Paeper, B., Proll, S., and Katze, M.G. (2007). Systems biology and the host response to viral infection. Nature Biotechnology *25*, 1383–1389.

Taylor, H.M., Triglia, T., Thompson, J., Sajid, M., Fowler, R., Wickham, M.E., Cowman, A.F., and Holder, A.A. (2001). Plasmodium falciparum homologue of the genes for Plasmodium vivax and Plasmodium yoelii adhesive proteins, which is transcribed but not translated. Infection and Immunity *69*, 3635–3645.

Taylor, T.E., Molyneux, M.E., Wirima, J.J., Borgstein, a, Goldring, J.D., and Hommel, M. (1992). Intravenous immunoglobulin in the treatment of paediatric cerebral malaria. Clinical and Experimental Immunology *90*, 357–362.

Teilum, K., Hoch, J.C., Goffin, V., Kinet, S., Martial, J.A., and Kragelund, B.B. (2005). Solution structure of human prolactin. Journal of Molecular Biology *351*, 810–823.

Tham, W.-H., Healer, J., and Cowman, A.F. (2012). Erythrocyte and reticulocyte binding-like proteins of Plasmodium falciparum. Trends in Parasitology *28*, 23–30.

Tham, W.-H., Wilson, D.W., Lopaticki, S., Schmidt, C.Q., Tetteh-Quarcoo, P.B., Barlow, P.N., Richard, D., Corbin, J.E., Beeson, J.G., and Cowman, A.F. (2010). Complement receptor 1 is the host erythrocyte receptor for Plasmodium falciparum PfRh4 invasion ligand. Proceedings of the National Academy of Sciences of the United States of America *107*, 17327–17332.

Theisen, M., Vuust, J., Gottschau, a, Jepsen, S., and Høgh, B. (1995). Antigenicity and immunogenicity of recombinant glutamate-rich protein of Plasmodium falciparum expressed in Escherichia coli. Clinical and Diagnostic Laboratory Immunology *2*, 30–34.

Thera, M. a, Doumbo, O.K., Coulibaly, D., Laurens, M.B., Ouattara, A., Kone, A.K., Guindo, A.B., Traore, K., Traore, I., Kouriba, B., et al. (2011). A field trial to assess a blood-stage malaria vaccine. The New England Journal of Medicine *365*, 1004–1013.

Thera, M.A., Doumbo, O.K., Coulibaly, D., Laurens, M.B., Kone, A.K., Guindo, A.B., Traore, K., Sissoko, M., Diallo, D.A., Diarra, I., et al. (2010). Safety and immunogenicity of an AMA1 malaria vaccine in Malian children: results of a phase 1 randomized controlled trial. PloS One *5*, e9041.

Theron, M., Hesketh, R.L., Subramanian, S., and Rayner, J.C. (2010). An adaptable two-color flow cytometric assay to quantitate the invasion of erythrocytes by

Plasmodium falciparum parasites. Cytometry. Part A : the Journal of the International Society for Analytical Cytology *77*, 1067–1074.

Thomas, P., and Smart, T.G. (2005). HEK293 cell line: a vehicle for the expression of recombinant proteins. Journal of Pharmacological and Toxicological Methods *51*, 187–200.

Tom, R., Bisson, L., and Durocher, Y. (2008). Transfection of HEK293-EBNA1 Cells in Suspension with Linear PEI for Production of Recombinant Proteins. CSH Protocols *2008*, pdb.prot4977.

Tomschy, a, Fauser, C., Landwehr, R., and Engel, J. (1996). Homophilic adhesion of E-cadherin occurs by a co-operative two-step interaction of N-terminal domains. The EMBO Journal *15*, 3507–3514.

Topolska, A.E., Lidgett, A., Truman, D., Fujioka, H., and Coppel, R.L. (2004). Characterization of a membrane-associated rhoptry protein of Plasmodium falciparum. The Journal of Biological Chemistry *279*, 4648–4656.

Tramontano, A., Chothia, C., and Lesk, A.M. (1990). Framework residue 71 is a major determinant of the position and conformation of the second hypervariable region in the VH domains of immunoglobulins. Journal of Molecular Biology *215*, 175–182.

Tran, T.M., Ongoiba, A., Coursen, J., Crosnier, C., Diouf, A., Huang, C.-Y., Li, S., Doumbo, S., Doumtabe, D., Kone, Y., et al. (2013). Naturally Acquired Antibodies Specific for Plasmodium falciparum Reticulocyte-Binding Protein Homologue 5 Inhibit Parasite Growth and Predict Protection From Malaria. The Journal of Infectious Diseases 1–10.

Treeck, M., Zacherl, S., Herrmann, S., Cabrera, A., Kono, M., Struck, N.S., Engelberg, K., Haase, S., Frischknecht, F., Miura, K., et al. (2009). Functional analysis of the leading malaria vaccine candidate AMA-1 reveals an essential role for the cytoplasmic domain in the invasion process. PLoS Pathogens *5*, e1000322.

Triglia, T., Chen, L., Lopaticki, S., Dekiwadia, C., Riglar, D.T., Hodder, A.N., Ralph, S. a, Baum, J., and Cowman, A.F. (2011). Plasmodium falciparum Merozoite Invasion Is Inhibited by Antibodies that Target the PfRh2a and b Binding Domains. PLoS Pathogens *7*, e1002075.

Triglia, T., Duraisingh, M.T., Good, R.T., and Cowman, A.F. (2005). Reticulocyte-binding protein homologue 1 is required for sialic acid-dependent invasion into human erythrocytes by Plasmodium falciparum. Molecular Microbiology *55*, 162–174.

Triglia, T., Thompson, J.K., and Cowman, A.F. (2001). An EBA175 homologue which is transcribed but not translated in erythrocytic stages of Plasmodium falciparum. Molecular and Biochemical Parasitology *116*, 55–63.

Tsuboi, T., Takeo, S., Iriko, H., Jin, L., Tsuchimochi, M., Matsuda, S., Han, E.-T., Otsuki, H., Kaneko, O., Sattabongkot, J., et al. (2008). Wheat germ cell-free system-based production of malaria proteins for discovery of novel vaccine candidates. Infection and Immunity *76*, 1702–1708.

Tsurushita, N., Hinton, P.R., and Kumar, S. (2005). Design of humanized antibodies: from anti-Tac to Zenapax. Methods (San Diego, Calif.) *36*, 69–83.

Uhlemann, a C., Oguariri, R.M., McColl, D.J., Coppel, R.L., Kremsner, P.G., Anders, R.F., and Kun, J.F. (2001). Properties of the Plasmodium falciparum homologue of a protective vaccine candidate of Plasmodium yoelii. Molecular and Biochemical Parasitology *118*, 41–48.

Vaccaro, C., Zhou, J., Ober, R.J., and Ward, E.S. (2005). Engineering the Fc region of immunoglobulin G to modulate in vivo antibody levels. Nature Biotechnology *23*, 1283–1288.

Varki, A. (2001). Loss of N-glycolylneuraminic acid in humans: Mechanisms, consequences, and implications for hominid evolution. American Journal of Physical Anthropology *69*, 54–69.

Vaughan, A.M., and Kappe, S.H.I. (2012). Malaria vaccine development: persistent challenges. Current Opinion in Immunology *24*, 324–331.

Verdrager, J. (1986). Epidemiology of the emergence and spread of drug-resistant falciparum malaria in South-East Asia and Australasia. The Journal of Tropical Medicine and Hygiene *89*, 277–289.

Wanaguru, M., Crosnier, C., Johnson, S., Rayner, J.C., and Wright, G.J. (2013). Biochemical Analysis of the Plasmodium falciparum Erythrocyte-binding Antigen-175 (EBA175)-Glycophorin-A Interaction: IMPLICATIONS FOR VACCINE DESIGN. The Journal of Biological Chemistry *288*, 32106–32117.

Weidle, U.H., Scheuer, W., Eggle, D., Klostermann, S., and Stockinger, H. (2010). Cancer-related issues of CD147. Cancer Genomics & Proteomics *7*, 157–169.

Wickramarachchi, T., Cabrera, A.L., Sinha, D., Dhawan, S., Chandran, T., Devi, Y.S., Kono, M., Spielmann, T., Gilberger, T.W., Chauhan, V.S., et al. (2009). A novel Plasmodium falciparum erythrocyte binding protein associated with the merozoite surface, PfDBLMSP. International Journal for Parasitology *39*, 763–773.

Wilkinson, B., and Gilbert, H.F. (2004). Protein disulfide isomerase. Biochimica Et Biophysica Acta *1699*, 35–44.

Williams, A.R., Douglas, A.D., Miura, K., Illingworth, J.J., Choudhary, P., Murungi, L.M., Furze, J.M., Diouf, A., Miotto, O., Crosnier, C., et al. (2012). Enhancing Blockade of Plasmodium falciparum Erythrocyte Invasion: Assessing Combinations of Antibodies against PfRH5 and Other Merozoite Antigens. PLoS Pathogens *8*, e1002991.

Woof, J.M., and Burton, D.R. (2004). Human antibody-Fc receptor interactions illuminated by crystal structures. Nature Reviews. Immunology *4*, 89–99.

World Health Organization (2008). THE GLOBAL MALARIA MALARIA ACTION PLAN.

World Health Organization (2012). World Malaria Report 2012 (Geneva, Switzerland).

Wranik, B.J., Christensen, E.L., Schaefer, G., Jackman, J.K., Vendel, A.C., and Eaton, D. (2012). LUZ-Y, a novel platform for the mammalian cell production of full-length IgG-bispecific antibodies. The Journal of Biological Chemistry *287*, 43331–43339.

Wright, G.J. (2009). Signal initiation in biological systems: the properties and detection of transient extracellular protein interactions. Molecular bioSystems *5*, 1405–1412.

Wu, C., Ying, H., Grinnell, C., Bryant, S., Miller, R., Clabbers, A., Bose, S., McCarthy, D., Zhu, R.-R., Santora, L., et al. (2007). Simultaneous targeting of multiple disease mediators by a dual-variable-domain immunoglobulin. Nature Biotechnology *25*, 1290–1297.

Wu, Y., Ellis, R.D., Shaffer, D., Fontes, E., Malkin, E.M., Mahanty, S., Fay, M.P., Narum, D., Rausch, K., Miles, A.P., et al. (2008). Phase 1 trial of malaria transmission blocking vaccine candidates Pfs25 and Pvs25 formulated with montanide ISA 51. PloS One *3*, e2636.

Yan, B., Boyd, D., Kaschak, T., Tsukuda, J., Shen, A., Lin, Y., Chung, S., Gupta, P., Kamath, A., Wong, A., et al. (2011). Engineering upper hinge improves stability and effector function of a human IgG1. The Journal of Biological Chemistry 1–14.

Yeoh, S., O'Donnell, R. a, Koussis, K., Dluzewski, A.R., Ansell, K.H., Osborne, S. a, Hackett, F., Withers-Martinez, C., Mitchell, G.H., Bannister, L.H., et al. (2007). Subcellular discharge of a serine protease mediates release of invasive malaria parasites from host erythrocytes. Cell *131*, 1072–1083.

Young, K.H. (1998). Yeast two-hybrid: so many interactions, (in) so little time... Biology of Reproduction *58*, 302–311.

Yu, X.-L., Hu, T., Du, J.-M., Ding, J.-P., Yang, X.-M., Zhang, J., Yang, B., Shen, X., Zhang, Z., Zhong, W.-D., et al. (2008). Crystal structure of HAb18G/CD147: implications for immunoglobulin superfamily homophilic adhesion. The Journal of Biological Chemistry *283*, 18056–18065.

Yu, Y., Lee, P., Ke, Y., Zhang, Y., Yu, Q., Lee, J., Li, M., Song, J., Chen, J., Dai, J., et al. (2010). A humanized anti-VEGF rabbit monoclonal antibody inhibits angiogenesis and blocks tumor growth in xenograft models. PloS One *5*, e9072.

Von Zons, P., Crowley-Nowick, P., Friberg, D., Bell, M., Koldovsky, U., and Whiteside, T.L. (1997). Comparison of europium and chromium release assays: cytotoxicity in healthy individuals and patients with cervical carcinoma. Clinical and Diagnostic Laboratory Immunology *4*, 202–207.

Zuccala, E.S., Gout, A.M., Dekiwadia, C., Marapana, D.S., Angrisano, F., Turnbull, L., Riglar, D.T., Rogers, K.L., Whitchurch, C.B., Ralph, S.A., et al. (2012). Subcompartmentalisation of proteins in the rhoptries correlates with ordered events of erythrocyte invasion by the blood stage malaria parasite. PloS One *7*, e46160.